**AMRL-TR-73-11** 



# ADVANCED HELMET SIGHT RETICLE ASSEMBLY (AHRA)

HONEYWELL INC.
SYSTEM AND RESEARCH DIVISION
2600 RIDGWAY PARKWAY
MINNEAPOLIS, MINNESOTA 55413

**JULY 1976** 

MAY 6 1917

Approved for public release; distribution unlimited

DOC FILE COPY

AEROSPACE MEDICAL RESEARCH LABORATORY AEROSPACE MEDICAL DIVISION AIR FORCE SYSTEMS COMMAND WRIGHT-PATTERSON AIR FORCE BASE, OHIO 45433

#### **NOTICES**

When US Government drawings, specifications, or other data are used for any purpose other than a definitely related Government procurement operation, the Government thereby incurs no responsibility nor any obligation whatsoever, and the fact that the Government may have formulated, furnished, or in any way supplied the said drawings, specifications, or other data, is not to be regarded by implication or otherwise, as in any manner licensing the holder or any other person or corporation, or conveying any rights or permission to manufacture, use, or sell any patented invention that may in any way be related thereto.

Please do not request copies of this report from Aerospace Medical Research Laboratory. Additional copies may be purchased from:

National Technical Information Service 5285 Port Royal Road Springfield, Virginia 22161

Federal Government agencies and their contractors registered with Defense Documentation Center should direct requests for copies of this report to:

Defense Documentation Center Cameron Station Alexandria, Virginia 22314

#### **TECHNICAL REVIEW AND APPROVAL**

AMRL-TR-73-11

This report has been reviewed by the Information Office (OI) and is releasable to the National Technical Information Service (NTIS). At NTIS, it will be available to the general public, including foreign nations.

This technical report has been reviewed and is approved for publication.

FOR THE COMMANDER

CHARLES BATES, J

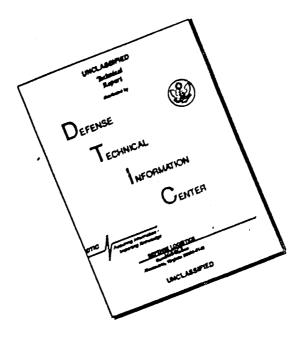
Chief

Human Engineering Division

Aerospace Medical Research Laboratory

AIR FORCE - 30 MARCH 77 - 100

# DISCLAIMER NOTICE



THIS DOCUMENT IS BEST QUALITY AVAILABLE. THE COPY FURNISHED TO DTIC CONTAINED A SIGNIFICANT NUMBER OF PAGES WHICH DO NOT REPRODUCE LEGIBLY.

REPORT DOCUMENTATION PAGE	READ INSTRUCTIONS BEFORE COMPLETING FORM
REPORT NUMBER 2. GOVT ACCESSION	
AMRLHTR-73-11	(4)
LITLE (and Substitle)	TYPE OF ASCORT & PERIOD COVERED
ADVANCED HELMET SIGHT RETICLE ASSEMBLY	Final Report.
	May 1970 - February 1972
(AHRA),	BERFORMING ORG. REPORT NUMBER
	Z9507-3016
7. AUTHOR(s)	8. CONTRACT OR GRANT NUMBER(s)
Patrick D./Pratt /	5 F33615-70-C-1655 new
	10010 1100 1100
PERFORMING ORGANIZATION NAME AND ADDRESS	10. PROGRAM ELEMENT, PROJECT, TASK AREA & WORK UNIT NUMBERS
Honeywell Inc., System and Research Division	AREA & WORK UNIT NUMBERS
2600 Ridgway Parkway	62202F, 7184-04
Minneapolis, Minnesota 55413	LDF
1. CONTROLLING OFFICE NAME AND ADDRESS	12. REPORT DATE
Aerospace Medical Research Laboratory	// Jul 2976
Aerospace Medical Division, AFSC	19: NUMBER OF PAGES
Wright-Patterson AFB, Ohio 45433  4. MONITORING AGENCY NAME & ADDRESS(if different from Controlling Office)	362 ce) 15. SECURITY CLASS. (of this report)
MONITORING AGENCY NAME & ADDRESS IT WITHOUT HOME COMMISSION OF	is. secont i ceass to ma report
(1) M1841 (17) 1041	Unclassified
16/1-01	15a. DECLASSIFICATION/DOWNGRADING SCHEDULE
The street of th	SCHEDULE
6. DISTRIBUTION STATEMENT (of this Report)	(10)
Approved for public release; distribution v	mlimited 36 4
77. DISTRIBUTION STATEMENT (of the abstract entered in Block 20, if differen	nt from Report)
7. DISTRIBUTION STATEMENT (of the abstract entered in Block 20, if differen	nt from Report)
7. DISTRIBUTION STATEMENT (of the abstract entered in Block 20, if differen	nt from Report)
	nt from Report)
8. SUPPLEMENTARY NOTES	
18. Supplementary notes  Supported in part by Air Force Avionics Laborato	
18. SUPPLEMENTARY NOTES Supported in part by Air Force Avionics Laborato	ry, Wright-Patterson AFB, OH
18. SUPPLEMENTARY NOTES Supported in part by Air Force Avionics Laborato	ry, Wright-Patterson AFB, OH
8. SUPPLEMENTARY NOTES Supported in part by Air Force Avionics Laborato 9. KEY WORDS (Continue on reverse side if necessary and identify by block nu	ry, Wright-Patterson AFB, OH
8. SUPPLEMENTARY NOTES  Supported in part by Air Force Avionics Laborato  9. KEY WORDS (Continue on reverse side if necessary and identity by block numbers)  Display Reticle	ry, Wright-Patterson AFB, OH
8. SUPPLEMENTARY NOTES  Supported in part by Air Force Avionics Laborato  9. KEY WORDS (Continue on reverse side if necessary and identity by block numbers)  Display Reticle  Helmet Imagery	ry, Wright-Patterson AFB, OH
Supported in part by Air Force Avionics Laborato  9. KEY WORDS (Continue on reverse side if necessary and identity by block numbers)  Display Reticle  Helmet Imagery  Visor Parabolic	ry, Wright-Patterson AFB, OH
Supported in part by Air Force Avionics Laborato  9. KEY WORDS (Continue on reverse side if necessary and identify by block number of the second state of the second s	ry, Wright-Patterson AFB, OH
Supported in part by Air Force Avionics Laborato  19. KEY WORDS (Continue on reverse side if necessary and identify by block num Display Reticle Helmet Imagery Visor Parabolic  20. ABSTRACT (Continue on reverse side if necessary and identify by block num This report describes the research and development	ry, Wright-Patterson AFB, OH  mber) of a 19-month program to develop
Supported in part by Air Force Avionics Laborato  19. KEY WORDS (Continue on reverse side if necessary and identity by block number Display Reticle Helmet Imagery Visor Parabolic  20. ABSTRACT (Continue on reverse side if necessary and identity by block number Display Parabolic a helmet display technique that uses the helmet visor	ry, Wright-Patterson AFB, OH  mber)  of a 19-month program to develop as the last optical element in the
Supported in part by Air Force Avionics Laborato  9. KEY WORDS (Continue on reverse side if necessary and identity by block number of the state of t	ry, Wright-Patterson AFB, OH  mber) of a 19-month program to develop r as the last optical element in the ng reticle and video imagery withou
8. SUPPLEMENTARY NOTES Supported in part by Air Force Avionics Laborato  9. KEY WORDS (Continue on reverse side if necessary and identity by block number Display Reticle Helmet Imagery Visor Parabolic  0. ABSTRACT (Continue on reverse side if necessary and identity by block number Display Parabolic a helmet display technique that uses the helmet visor	ry, Wright-Patterson AFB, OH  mber) of a 19-month program to develop r as the last optical element in the ng reticle and video imagery without isor. The single reflecting para-

470 184 SECURITY CLASSIFICATION OF THIS PAGE (When Date Entered)

EDITION OF 1 NOV 65 IS OBSOLETE

DD 1 JAN 73 1473

#### 20. Abstract (Cont'd)

cont.

projection assembly. To complete this design it was necessary to develop parabolic visor fabrication techniques, a miniature lamp, and a thin film dielectric coating for plexiglas visors. It was also recognized early in the program that the double-reflecting symmetrical parabolic visor was the best approach for video projection. The special optical conditions obtained with the symmetrical parabolic approach are the reduction of astigmatism and cancellation of coma. This permits the use of a simple triplet design for the collimation optics which projects collimated light to the parabolic visor. This permits a compact helmet mounted assembly. A fiber optic bundle and relay optics are used to relay video information from a 1-inch CRT mounted at the back of the helmet to the collimation optics. This design approach resulted in a reliable prototype that was assembled and delivered on February 15, 1972.



#### PREFACE

This program was conducted under Air Force Systems Command contract number F-33615-70-C-1655, "Advanced Helmet Sight Reticle Assembly (AHRA)." This program was administered under the direction of the Air Force Aerospace Medical Research Laboratory; Captain Dean F. Kocian was the project monitor.

Both Phase I and Phase II design concept studies as well as hardware fabrication were completed during the period from May 1970 through 24 February 1972. This one volume final report contains four appendixes and covers the period from May 1970 through 27 November 1972.

This report was prepared by the Advanced Development Group of the Systems and Research Center, Honeywell, Inc., 2600 Ridgway Parkway, Minneapolis, Minnesota 55413. The Systems Project Engineer was I.W. Metzger, and Principal Investigator was P.D. Pratt. Principal contributors to the effort were Dr. R.A. Woodson, I. (Irv) Abel, and R.R. LeChevalier.

The manuscript was released by the author in November 1972 for publication as a technical report. The report number assigned to this report by Honeywell is Z9507-3016.

Supported in part by the Laboratory Director's Fund

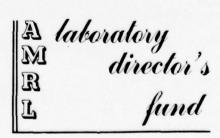


## TABLE OF CONTENTS

		Page
SECTION I	INTRODUCTION	1
	Phase I Design Concept Study Phase II Design Concept Study and Breadboard Demonstrations	1 1
	Prototype Fabrication	2
SECTION II	PHASE I DESIGN CONCEPT STUDY	6
SECTION III	PHASE II DESIGN CONCEPT STUDY	13
	Reticle Generator Selection of Design Concept Selection of Parabolic Visor Focal Length Visor, Bearing Detent and Mating to Tracks Reticle Generator Subassembly Layout Video Display Summary Design Concept Review Video Display Design Iterations Holographic Projection Technique	13 13 13 16 20 32 33 54 89
SECTION IV	BREADBOARDS AND BRASSBOARDS	92
	Reticle Generator Spherical Visor Reticle Breadboard Reticle Parabolic Visor Breadboard Holographic Breadboard Parabolic Visor Display Breadboard Parabolic Visor Display Brassboard	92 92 92 104 108 115
SECTION V	PARABOLIC VISOR DEVELOPMENT AND FABRICATION	119
	Development Recommendations	119 123
SECTION VI	VISOR COATING DEVELOPMENT	124
	Reticle Generator Requirements Development of Coating for Reticle Generator Video Display Coatings Requirements Vendor Selection and Development Program Plan to Develop Hard Dielectric Coatings for Plexiglas by Research of S&RC	124 124 124 130 130 131 131
	Evaluation and Test	134

## TABLE OF CONTENTS -- CONCLUDED

		Page
SECTION VII	RETICLE GENERATOR PROTOTYPE	135
	Design and Fabrication	135
	Helmet Mounted Assembly	135
	Reticle Generator Assembly	135
	Either-Eye Position Assembly	144
	Sensor Electronics Subassembly	146
	Visor	148
	Boresight Optics	150
	Reticle Generator and Either-Eye Position	152
	Adjustments	150
	Acceptance Tests	152
	Reticle Generator Evaluation and	155
	Recommendation	
	Visor Housing Evaluation and	156
	Recommendations	
SECTION VIII	VIDEO DISPLAY	157
	Design and Specification	159
	Requirements of AMRL Contract	160
	Layout of Helmet Mounted Display	
		160
	Optical Design by HRC	169
	Optics	169
	Flexible Sheath and End Tips	176
	Fiber Optic Bundle	176
	Fabrication, Assembly, Alignment, and Test	178
	Helmet Modification	182
	Visor	185
	Central Mirror Assembly	196
	Visor Assembly	196
	Collimator Lens	209
	Relay Lens	214
	Fiber Optic Bundle (FOB)	214
	Collimator Lens Assembly	214
	Preliminary Assembly	227
	Final Assembly and Test	227
	Assembly of Visor to Helmet	227
	Wearing of Helmet With All Parts in Place, Including Dummy CRT	236
	Acceptance Test	236
APPENDIX I	HOLOLENS DESIGN CONCEPT STUDY (PHASE II)	
APPENDIX II	RELAY LENS DESIGN DATA	
APPENDIX III	VIDEO VISOR PROJECTION FINAL REPORT HELMET MOUNTED DISPLAY DESIGN IRV/ABEL HONEYWELL RADIATION CENTER	
APPENDIX IV	DEVELOPMENT OF A HELMET-MOUNTED VISOR DISPLAY	

# LIST OF ILLUSTRATIONS

Figure		Page
1	Visor Reticle Projection Helmet Mounted Assembly	4
2	Visor Video Projection Helmet Mounted Assembly	5
3	Ray Trace of Parabolic Visor Reticle Projection	14
4	Prism Cutting Layout	15
5	Comparison of Range of Paraboloids with Bearing Track Offset 8.0 in.	17
6	Parabolid Visor Reticle Projection	18
7	Vision Locating and Locking Mechanism	19
8	AHRA Reticle Housing Assembly	21
9	Preliminary Reticle Projection Layout	22
10	Helmet Mounted Sight	23
11	Reticle Generator HMD	24
12	Reticle Projection with White Light Source	27
13	Composite Example of Technique to Reduce Aberration and Distortion of Off-Axis Curved Reflective Element	34
14	Exit Pupil Formed on Image of Aperture Stop by Combiner	36
15	Exit Pupil at Iris and Center of Eye Rotation	37
16	Optical Layout of HMD Optics and CRT	38
17	Three HMD Design Concepts	40
18	Two HMD Design Concetps	41
19	Double Reflecting Parabolic Combiner HMD	43
20	Double Reflecting Spherical Combiner HMD	45
21	Elliptical Combiner HMD Approach	47

Figure		Page
22	Symmetrical Elliptical Combiner	49
23	Schmidt Corrector - Spherical HMD	49
24	Tilted Spherical Combiner	52
25	10-Deg FOV, Symmetrical, 2 in. ft-L (Three Mirrors)	53
26	10-Deg FOV, Beam Splitter and Three Central Mirror Display Design	58
27	10-Deg FOV, Split Visor and Single Central Mirror Display Design	58
28	10-Deg FOV, with 0.25 in. Diameter FOB Display Design	61
29	10-Deg FOV with 0.25 in. FOB Display Design	62
30	10-Deg FOV, 2.25 in. F.L. Display Design	63
31	10-Deg FOV, 2.25 in. F.L. Display Design	64
32	10-Deg FOV, 2 in. F.L. Display Design	65
33	10-Deg FOV, 1.5 in. F.L. Display Design	66
34	15-Deg FOV, 2.25 in. F.L. Display Design	69
35	15-Deg FOV, 2.25 in. F.L. Display Design	70
36	15-Deg FOV, 2.0 in. F.L. Display Design	71
37	20-Deg FOV, 2.0 in. F.L. Display Design	72
38	20-Deg FOV, 2.25 in. F.L. Display Design	73
39	20-Deg FOV, 2.25 in. F.L. Display Design	74
40	20-Deg FOV, 2.25 in. F.L. Display Design	75
41	Parabolic Distortion	77
42	Parabolic Distortion and Skewed Exit Pupil	78

Figure		Page
43	Correction of Parabolic Distortion	80
44	Parabolic Distortion and Ray Interference with Multiple Central Mirror Design	82
45	20-Deg FOV with 2 in. F.L. Display Design	83
46	20-Deg FOV with 2 in. F.L. Display Design	84
47	20-Deg FOV with 1.75 in. F.L. <b>P</b> arabola Display Design	85
48	20-Deg FOV with F.L. Display Design	86
49	20-Deg FOV with 2.25 in. F.L. Display Design	87
50	20-Deg FOV with 1.5 in. F.L. Display Design	88
51	First Computer Design with Principal Plane Inside Collimator Lens Assembly	90
52	Second Computer Design with Principal Plane Outside Collimation Lens Assembly	91
53	Spherical Visor Breadboard	93
54	Spherical Visor Breadboard	94
55	Breadboard of Parabolic Reticle Generator	95
56	Breadboard of Parabolic Reticle Generator	96
57	Breadboard of Parabolic Reticle Generator	97
58	Collimation of Reticle Generator Breadboard	99
59	Reduced Aperture of Collimation Telescope	100
60	Comparison of Standard GE Lamp with Honeywell Designs	101
61	Reticle Breadboard Power Supply	102
62	Coated Sample of Plexiglass for Ghose Image Suppression	103
62	Coometry of Hololong Franciscs and Reconstruction	1.05

Figure		Page
64	Geometry of Hololene Encoding and Reconstruction	106
65	Hololens Spectrograph Plot	107
66	Hololens Breadboard	109
67	Video Display Breadboard	111
68	Video Display Breadboard	112
69	Video Display Breadboard, Focus of Collimation Lens	113
70	Video Display Breadboard, Collimation Adjustment	114
71	Central Mirror Retracting Mechanism	117
72	Central Mirror Assembly	118
73	Visor Reticle Projection Helmet Mounted Assembly	136
74	Visor Reticle Projection HMA with Visor Retracted	137
75	Inside-the-Helmet View of the Visor Reticle Generator Assembly	138
76	Visor Reticle Projection HMA, Rear View	139
77	Attachment of Boresight Alignment Optics to Right-Hand Sensor Bar of Visor Reticle HMA	140
78	Reticle Generator, Helmet Mounted Assembly	141
79	Reticle Generator, 1.5 FL Paraboloid	142
80	Either-Eye Position Assembly	143
81	Visor Reticle Projection Tungsten Lamp	145
82	Sensor Electronics Assembly	147
83	Boresight Alignment Optics	151
84	Visor Video Projection HMA	158

Figure		Page
85	CRT Display Configuration - 2 FL Paraboloid	161
86	Video Display FOB, and Second Mirror	165
87	Video Display, First Visor Dogleg Design	166
88	Video Display Visor, Two-Ball Detent Design	167
89	Video Display, Last Dogleg Design Iteration	168
90	Developmental Helmet Mounted Display Prototype Delivered to AMRL in February 1972	170
91	Photograph of Front of HMD as Worn with Oxygen Mask, Visor in Operational Position	171
92	Photograph of Right Side of HMD as Worn with Oxygen Mask, Visor in Operational Position	172
93	Photograph of Left Side of HMD as Worn with Oxygen Mask, Visor Retracted	173
94	Photograph of Left Side of HMD as Worn with Oxygen Mask, Visor in Operational Position	174
95	Crt with Final Stages of Electronics and Cable	179
96	General View of HMU with Visor Retracted	180
97	Close-up of Helmet Mounted on Alignment Jig with Both Camera and Lorgnette Mounted in Place Behind the Aperture Plate	181
98	Side View of Standard XL Air Force HGU - 2A/P Helmet from Gentex, with Web Suspension and Communications Equipment	183
99	Front View of Standard XL Air Force HGU-2A/P Helmet with Accessory Pads of Various Thicknesses to Fit Helmet to Pilot so That His Eye can be Located to the Exit Pupil of the HMD When it Has been Installed	184

Figure		Page
100	Hardened Template Comprising 0.016 Thickness Gage Constrained between Opposing Aluminum Templates to Assume Parabolic Contour for Both the Constrained Area and the Exposed Area	186
101	Vacuum Formed Acrylic Paraboloid Resting in Concave Metal Mold in which such a Paraboloid had been Previously Epoxied and Optically Machined from a Parabolic Template	187
102	Concave Metal Mould Containing Paraboloidal Visor Shell Epoxied to the Mating Surface	188
103	Test Visor Located in Concave Wood Form in Position Occupied by Paraboloidal Visor when Cemented in Place Prior to Optical Centering and Perimeter Machining Operations	189
104	Concave Wood Form and Its Removed Tilt Plate	190
105	Oblique View of Concave Wood Form	191
106	Vacuum Formed Plexiglass Acrylic Visor Material Drawn to Paraboloidal Shape from Square, Flat Sheet	192
107	Completed Paraboloidal Visor Located in its Concave Wood Form in Position it Occupied when its Parallel Sides were Milled True, before Visor Extender Plates were Cemented to it.	195
108	Trapezoidal First Surface Mirror for Miscellaneous Optical Uses, Optical Prism Assembly Producing Laterial Offset of Boresight, Optical Prism Assembly Producing Both a Lateral Displacement and a Reversal of Boreshight Equivalent to a Trihedral Cube Corner Prism, Three Plexiglass Plates used as Specimens for Inconel Reflective Coating Process at Time of Coating HMD Visor to 3% Transmittance, Dummy Central Mirror Frame for Preliminary Focus Setting at Visor Focal Point, Combination Type Magnifier for Close Examination of Small Parts, Collimator Reticle Focusing and Boresighting Pl Central Mirror, CRT/Relay Lens Folding Mirror, Focus-Finding and Center-Finding Stylus for Visor During Critical Alignment Procedures, Collimator Boresight Mirror	

Figure		Page
109	Checking Focus Setting of Collimator at Exit End of FOB	198
110	View of Concave Side of Visor with Central Mirror and its Mount Arm in Operational Position, with Visor Clamp Linkage Attached and Open to Show Clamp Knob and its T-Bolt in Place in its Secure Setting	199
111	View of Concave Side of Visor	200
112	View of Concave Side of Visor (Linkage Open)	201
113	Visor Has Been Mounted, Aligned, Set to Selected Height	203
114	Previously Set Visor Reflects in Its Concave Face an Out- of-Focus Image of the Stylus Which has been Moved Away from the Center of Curvature Longitudinally Toward the Visor and Laterially to the Height Gage Which has been Set to Read the Height of the Optical Axis as Referenced by the Tip of the Stylus	204
115	General View of Set-up Used to Check the Tilt Angle of the Central Mirror	205
116	Height Gage, Set to the Height of the Visor Optical Axis, is Here Shown Setting the Height of an Index to be Used in Adjusting the Tilt of the Central Mirror	206
117	Visor Mounted in Its Tracks to Helmet Support Jig for Adjustment of Central Mirror	208
118	Set-up Used to Focus the Central Mirror after the Central Mirror has been Aligned	209
119	Visor Mounted in Its Tracks to Helmet Support Jig for Adjustment of Central Mirror	210
120	Adjusting Collimator Boresight Mirror Using Special Tool That Clamps to Mirror Frame	211
121	Checking Alignment of Collimator Boresight Mirror	212
122	Measuring Field Curvature of Collimator Lens Using Focusing Adapter with Illuminated Reticle and Tilting Adapter to Explore the Image Across the Field	213

Figure		Page
123	Helmet with Dummy CRT Installed and with Exit End of Fiber Optic Bundle Accessible for Examination of its Trans- mitted Image After the Resolution Target Has Been Imaged by the Relay Lens Sharply Upon the Entrance End of the FOB	215
124	Photograph of the Dummy CRT as seen through the Fiber Optic Bundle	216
125	1-27-72, FOB with Diffuse Illumination, Film Strip No. 6, Photo 21, Frame 2A	217
126	1-27-72, FOB with Axial Illumination, Film Strip No. 6, Photo 22, Frame 5A	218
127	1-27-72, FOB with Off-Axis Illumination, Angle Left, Film Strip No. 6, Photo 23, Frame 11A	219
128	1-27-72, FOB with Off-Axis Illumination, Angle Right, Film Strip No. 6, Photo 24, Frame 11A	220
129	1-27-72, FOB with Off-Axis Illumination, Angle Bottom, Film Strip No. 6, Photo 25, Frame 18A	221
130	1-27-72, FOB with Off-Axis Illumination, Angle Top, Film Strip No. 6, Photo 26, Frame 20A	222
131	Photograph of the Dummy CRT Which Comprises a Tube with a Standard 1951 USAF Resolution Chart Slide Transparency at One End and a 28-volt Lamp at the Other End to Provide the Illumination	223
132	Set-up Used to Photograph the Boresight Reticle Pattern of the Collimator Boresight/Focusing Plug	224
133	Macrophotograph of Reticle Pattern of the HMD Collimator Boresight/Focusing Plug	224
134	With Helmet Mounted on Alignment Jig with Aperture Plate in Place, Inside Calipers are Used to Set and Check Paral- lelism of Collimator Mechanical Axis with Transverse Plane by Means of Nylon Rod Jig Mounted on Collimator Lens Mount	225
135	With Helmet Mounted on Alignment Jig with Aperture Plate in Place, Inside Calipers are Used to Check Parallelism of Collimator Mechanical Axis with Transverse Plane by Means of Nylon Rod Jig Mounted on Collimator Lens Mount	226

Figure		Page
136	After the Mechanical Axis of the Collimator Lens Has Been Made Parallel with the Transverse Plane, the Optical Axis of the Collimator with its Boresight Mirror is Made Perpendicular to the Transverse Plane, Thus Boresighting These Two Optical Components	228
137	General View of HMU Mounted on Alignment Jig	229
138	Helmet with Fiber Optic Bundle Attached at its Entrance End to the CRT/Relay Lens Housing at Rear of Helmet, Clamped at Midpoint to Helmet, Exit End Standing Free	230
139	Checking Focal Setting of Exit End of Fiber Optic Bundle, Using Autocollimator Which Illuminates the FOB	231
140	Helmet with Visor Mounted and in Retracted Position, with Visor Cover Removed and Visible, with Visor Clamp Knob and Linkage Attached to Visor, with Fiber Optic Bundle Attached	232
141	View of Visor Mounted on Helmet, in Retracted Position, with Visor Cover Removed and Visible	233
142	Helmet with Visor Mounted and in Operational Position, with Visor Cover Removed and Visible, with Visor Clamp Linkage Attached and Folded to Operational Form, with Visor Clamp Knob Removed From Linkage and Placed in its Slot in Visor Cover, with Fiber Optic Bundle Attached at Both Ends and at Midpoint	234
143	View of Visor Mounted on Helmet, in Operational Position, with Visor Cover Removed and Visible, with its Image Seen Reflected by Convex Side of Visor	235
144	Helmet with All Optical Parts of HMD Mounted Except the Visor and its Central Mirror	237
145	View of CRT Images as Seen Looking into Boresight Mirror or Collimator with Helmet Mounted on Alignment Jib, Level, with Visor Up; Electronic Paraboloidal Distortion Compensation OFF	238
146	View of CRT Image as Seen Looking into Boresight Mirror of Collimator with Helmet Mounted on Alignment Jib, Level, with Visor Up; Electronic Paraboloidal Distortion Compensation ON	239

Figure		Page
147	Image of Retna Resolution Chart from TV Camera and Modified Display Electronics with Parabolic Sweep Distortion Correction OFF. The Video is Fed to the HMD CRT, Relayed to the FOB Where it is Conducted to the Exit End of the FOB, Collimated by the Collimator Lens, and Reflected Forward by the Boresight Mirror. The Visor is UP, so This Collimated Image is Recorded by a Pentax Camera which is "Looking" at the Boresight Mirror and which is Focused for Infinity. Note Dust On, and Flaws in the FOB.	240
148	Image of Retna Resolution Chart From TV Camera and Modified Display Electronics with Parabolic Sweep Dis- tortion Correction ON	241
149	Green CRT (new) Retna Resolution Chart, Parabolic Compensation OFF	242
150	Green CRT (new) Retna Resolution Chart, Parabolic Compensation ON	243
151	White CRT Retna Resolution Chart, Parabolic Compensation OFF	244
152	White CRT (old) Retna Resolution Chart, Parabolic Compensation ON	245
153	Close-up of Auxiliary Lens as Mounted on HMD to By-pass CRT	246
154	Here the Complete Set-up is Shown for Photographing with a Minox Camera - the Distortion Test Grid as Seen by the Entire HMD Optical System	247
155	When Helmet is Held at This Angle and an Aixiliary Lens Focuses an Image of a Rectantular Distortion Test Grid Pattern on the Object Plane of the Relay Lens the Aspect Angles Match and the Full Field Can Be Photographed with the Minox Camera	248
156	With the Helmet Removed From Its Alignment Jib, the Complex Supporting Means and the Position of the Photog- rapher's Hand are Visible	249
157	Minox Film Cassette After Film has been Removed for Processing	250

Figure		Page
158	Helmet Alignment Jig with Lorgnette in Place Showing Where the HMD Exit Pupil will be when the Helmet with HMD is Mounted on the Alignment Jip	251
159	Close-up of Helmet Mounted on Alignment Jig with Camera Tripod Mount Mounted in Place Behind Lorgnette	252
160	Close-up of Helmet Mounted on Alignment Jip with Camera Mounted in Place Behind the Lorgnette	253

#### LIST OF TABLES

Table		Page
1	Special Requirements of Phase I Design Concept Study	7
II	Overall Requirement of Phase I Design Concept Study	7
III	Visor Reticle Technique Weighting by Design Criteria	9
IV	Summary Phase I Design Concept Study	11
V	Video Display Optical Requirements	12
VI	Early Design Concept Review Approaches (10 deg FOV)	60
VII	Design Concept Study Approaches (15 deg and 20 deg FOV)	68
VIII	Final Design Approaches (20 deg FOV)	81
IX	Approaches Considered for Parabolic Mold Fabrication	120
X	Approaches Considered for Fabrication of Paraboloids	121
XI	M&DE Thin Film Laboratory AHRA Participation	126
XII	Acceptance Test Results (24 August 1971)	154

#### SECTION I INTRODUCTION

The objective of the Advanced Helmet-Sight Reticle Assembly (AHRA) project is to develop reticle and video projection assemblies to supplement or replace current concepts and helmet sight equipment for tactical aircraft. Specifically, the program seeks a means of projecting imagery to the observer's line of sight without requiring optical elements between the eye and the helmet visor. Appendix IV contains a summary report of the AHRA project presented as a paper by Captain D.F. Kocian on 9 November 1972 at the VCS Symposium at Brooks AFB, Texas. This paper not only highlights technical achievements of the AHRA program, but also includes recent design developments in the area of integrated helmet mounted sight/displays.

#### PHASE I DESIGN CONCEPT STUDY

The AHRA programs initially consisted of a design concept study phase (Phase I) to explore five techniques for projecting reticle and video imagery on the helmet visor as a part of the optical system. These visor projection techniques are the parabolic visor, the spherical visor, the visor coated with a hologram, a polaroid diffraction element inserted in the visor, and a visor embossed with a relief-phase hologram.

As a consequence of this study effort, it was recommended that additional breadboards be fabricated for projection of both reticle and video information on the helmet visor. Additional funding was obtained for an expanded Phase II effort to fabricate breadboards of the parabolic, holographic, and spherical approaches for evaluation of both discrete and video visor projection techniques. These evaluations were to be followed by fabrication of two flyable prototypes of the best techniques for projection of reticle and video information.

# PHASE II DESIGN CONCEPT STUDY AND BREADBOARD DEMONSTRATIONS

The Phase II effort started with a second design concept review (based on the Phase I design concept study) to definitely substantiate the ability of each technique to display both discrete and video information.

This review showed that the approach of the single reflecting parabolic visor for discrete reticle projection allows a much more compact design than the spherical visor approach. The Phase II design concept study resulted in several reticle generator feasibility designs that employed the General Electric lamp No. 1874. However, the lamp envelope was too large and it was proposed that Honeywell develop a special miniature lamp design. In addition, breadboard demonstrations showed that the holographic technique was not well enough advanced to be included in the AHRA program for either reticle or video display projection.

It was recognized early in the Phase II design concept study that the double reflecting parabolic visor was the best approach to video projection, not the single reflection spherical technique recommended in the Phase I design concept study. The special optical conditions obtained with the symmetrical parabolic approach are the reduction of astigmatism and cancellation of coma. This permits the use of a simple, triplet design for the collimation optics, which in turn results in a compact design for the double bounce parabolic visor display.

Subsequent breadboard evaluation of the parabolic approach confirmed that the symmetrical approach does substantially reduce the aberrations even with a paraboloid of poor optical quality. Consequently, the spherical approach was rejected on the assumptions that the refractive corrective optics for the spherical visor approach would be too large and that a parabolic visor of adequate quality could be fabricated.

The Phase II design concept review resulted in 25 designs for establishing the feasibility of the parabolic visor display. These design interactions were necessary since many tradeoffs must be made between optical parameters and spatial and mechanical constraints for a large number of optimization parameters.

A hololens was received from Naval Weapons Laboratory in the spring of 1971, but it was not satisfactory because of a blurred image reconstruction, coma, ghost images, and a reflected, defocussed image reticle pattern. Both Honeywell and the contract monitor agreed that a holographic approach would not be used for either the reticle generation or the video display projection techniques.

#### PROTOTYPE FABRICATION

By early 1971, after completion of the Phase II design concept study and breadboard evaluation, it became evident that additional funds were needed to continue the program. These funds were obtained in May 1971 for paraboloid fabrication, video display relay optics design, reticle projection condenser design, miniature lamp development, field alignment of ics, video display redesign to improve weight, and balance and multi-layer visor coatings for reticle projection. The primary emphasis in the spring of 1971 was to complete the parabolic visor fabrication, to develop annealing techniques, to complete fabrication of the miniature lamp, the reticle generator projection assembly and holographic breadboard.

Many techniques for parabolic visor fabrication were studied but only two approaches were tried -- vacuum forming over a parabolic mold and shaping on an aspheric numerical generation machine. The first approach was unsatisfactory due to surface blemishes and expense of mold fabrication. The second technique produced paraboloids of satisfactory quality for reticle projection and demonstration of the double reflection parabolic concept for the video display.

The Advanced Development Laboratory of Honeywell developed a lens end lamp for the reticle generator, which eliminates the need for a special condenser design and diffuser. Satisfactory multi-layered anti-reflectance and reflectance coatings were developed for the reticle generator visor by the Honeywell Thin Film Laboratory. Finally, the remaining mechanical assemblies were completed and the reticle visor projection assembly (Figure 1) was delivered in August 1971.

While the reticle generator assembly was nearing completion, emphasis was placed on video display fabrication. The collimation and relay lenses were designed by Honeywell Radiation Center and Optical Research Associates Both sets of optics were fabricated by Rogers and Clark. Hoeger Optical Co. provided a 2-in., focal-length parabolic section, and Evaporative Coatings Company coated the visor with a 3% transmittance reflected surface. The visor display (Figure 2) was assembled and delivered on February 15, 1972.



Figure 1. Visor Reticle Projection Helmet Mounted Assembly

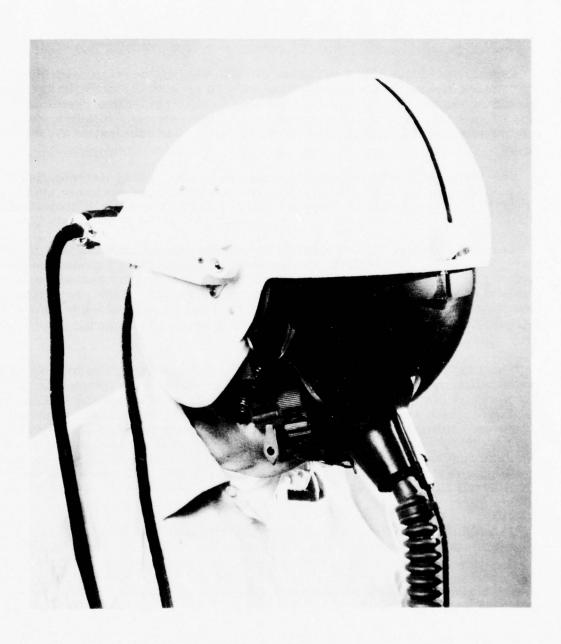


Figure 2. Visor Video Projection Helmet Mounted Assembly

# SECTION II PHASE I DESIGN CONCEPT STUDY

Objectives of the AHRA program were to design, develop, and fabricate an Advanced Helmet Sight Reticle Assembly to project a reticle image from the helmet visor. The program scope was first to perform a systematic study of several techniques for reticle projection; second, to fabricate one or more breadboard models; and third, to design and fabricate a flyable prototype.

The initial task was to perform a design concept study (later called Phase I) to perform the tradeoff study of five techniques for the optimum approach to reticle visor projection. Tables I and II list the five reticle projection techniques and the requirements to be considered in the detailed study.

This study effort did not identify any single projection technique that was clearly superior. Consequently, construction of laboratory models of the parabolic and holographic techniques was recommended for evaluation of their reticle projection characteristics. Also, the spherical visor projection technique was recommended for application to helmet display of video information, although display of video information was not originally intended to be included in the study.

The Phase I study conducted a tradeoff analysis of a large matrix of performance characteristics of the various approaches. The intent was that the total score or merit to be calculated form the various weighting factors was to indicate which reticle projection technique should be breadboarded for later evaluation. However, the total score of the various systems shown in Table III did not vary significantly, and the final decision of which approach to be breadboarded was made on the basis of advantages, disadvantages, cost, and growth potential for each system shown in Table IV. The reader is referred to Honeywell Document 14327-TR4 for detailed results of the Phase I Design Concept Study.

The first extension to the basic contract was awarded on 26 October 1971, to increase the number of breadboards from one to three. This allowed investigation of the feasibility of the parabolic, holographic, and spherical visor approaches for displaying both discrete and video information. This extension also increased the number of flyable prototypes from one to two optimized prototypes for reticle and display video projection. In addition, the contract required that the results of the Phase I design concept study be reviewed (Phase II) to definitely substantiate the ability of each of the most promising design approaches to display discrete and video information on the helmet visor. Section III then describes the Phase II design concept study and tradeoff analysis that resulted in the selection of the parabolic visor technique for displaying both discrete and video information on the visor.

Table I. Special Requirements of Phase I Design Concept Study

Concept study	
Technique for Systematic Study	
Parabolic visor, spherical visor, or combination of shapes	None
Relief and phase holograms of reticle on visor	<ul> <li>Brightness</li> <li>Resolution</li> <li>No interference with light source</li> <li>No undesired reconstruction</li> </ul>
Polarized light interaction with diffraction grating	<ul> <li>Use external light for image generation</li> <li>Eliminate expensive geometrically shaped visors</li> <li>Reduce AHRA weight</li> <li>Capability at low ambient light levels</li> <li>No undesired interactions</li> </ul>

Table II. Overall Requirement of Phase I Design Concept Study

Reticle Generator	Mounted within helmet-visor envelope
Alignment	<±2.5 deg
Exit Pupil	> 10 mm
Image	Infinity collimation Orange color Visible against 10,000 ft-L background
Vision	±120 deg with no distortion
Weight	>15 oz
Visor	Clear

Table III. Visor Reticle Technique Wei

Design Criteria/ Parameter	Must <sup>1</sup>	Go/	Want	Want Weight	Scale of Performance <sup>2</sup>	Perf. Weight	Parabolic	Perf. WT SC		Spheric
r ur ameter	must.	No Go		Factor	scare of refformance	Factor				
Visibility Against Clearly visible 15,000 FL with prightness level. 15 visor. Clearly visible at 20 K and Barely visible at 25 K FL Clearly visible at 15 K and Barely visible at 15 K and Barely visible at 10 Clearly visible at 15 K and Barely visible at 15 K and Barely visible at 15,000 Barely visible at 15,000					rly visible   Clearly visible   10   Clearly visible at 20K and   Barely visible at 25K FL   Clearly visible at 15K and   Barely visible at 15K and   Barely visible at 20K FL   Clearly visible at 20K FL   Clearly visible at 10,000					
Image Collimation	Collimated at optical infinity		Collimation over entire reticle field of view of reticle Collimated over center half view of reticle image  Collimated over center half of reticle Collimated at center of reticle					10	100	Need opti
Reticle Illumina- tion Uniformity					10	90				
Undistorted Vision						8	72	Same		
Sensitivity to nominal mechani- cal deflection or environment (humidity temp)	stivity to situity situity to situity si				Design must isolate visor from helmet flex	8	64	Same		
Visor transmit- tance (assume one visor)	ansmit- >10% Clear visor 8 Clear 10 T = 67% ssume 7				7	56	T = 67%			
No undesired reconstruction or interaction, with other light sources or reflections	5			7	None Faintly visible Visible but not objectionable Visible and objectionable	10 6 4 2	Primary to ghost image 120:1 R <sub>1</sub> = 30% T = 67% R <sub>2</sub> = 0.5%	6	42	Same
Exit Pupil	≥ 10 mm		≥20 mm	7	20-15 mm 10-15 mm	10 5		10	70	
Image distortion				6	Subjectively none Subjectively good Subjectively fair Subjectively poor	10 7 5 2	None	10	60	Need Opt Correction
Sharp Image					10	50	Need opt rection			
Reticle Generation	On visor		Use present visor	3	Current visor with no major modification New Visor	10	Need new visor	5	15	Same
Reticle Visibility against low ambient levels				3	At night 10 FL 30 FL 100 FL	10 4 2 1		10	30	
Reticle Intensity Adjustment				2	Panel adjustment Switch or mech, change Varies with background	10 5 0	Tungsten Lamp Source	10	20	Tungsten Source
Reticle Color				1	Orange Yellow green Red	10 8 5	Orange filter	10	10	Orange 1
				11	ements to be considered for		Total Score or Merit		779	Total Sc

<sup>1 -</sup> Each reticle projection assembly must satisfy "Must" requirements to be considered for breadboard fabrication.

 $<sup>2\,</sup>$  ~ The merit of each reticle projection assembly shall be calculated from the above parameters (14) by:  $\,$ 

Merit =  $\sum_{i}^{14}$  (want weight factor)<sub>i</sub> X (scoring weight factor)<sub>i</sub>

# eticle Technique Weighting by Design Criteria

bolic	Pe		Spherical	-	rf.	Holographic Dichromate Gelatine	Pe		Polaroid		rf.	Relief Phase Hologram Embossed on Visor	-	erf.
		100	<b>-</b>	WT 10	100		WT	_	Visible against any	1	SC -	Requires 6-foot optic bundle	10	100
							10	100	detectable background brightness			to couple 1 to 6 mw laser		100
Field of view	10	100	Need optical correction	10	100	Zone plate similar to high quality lens (angle of bisection only)	10	100	Inherent to formation of diffraction pattern	10	100	Zone plate similar to good quality lens	10	100
	10	90		10	90		10	90	Rings are uniform but transmission varies	10	90	Requires optics to spread laser beam to fill exit pupil	10	90
visor and ween para- tic sections med for tortion	8	72	Same	8	72	Gelatine coat introduces no distortion	10	90	Some distortion around edges where attached to visor	9	81		10	90
isolate visor Nex	8	64	Same	8	64	Require humidity seal and isolation from helmet flex.	8	64	Same as geometrical optical systems	8	64	Effect of visor deflection unknown at this time, but assume same as geometrical-optical	8	64
	7	56	T = 67%	7	56	T = 60-70%	7	56	T = 35%	4	32	Needreflective coat or higher powered laser T = 60-70≸	7	56
host image 67% R <sub>2</sub> = 0.5%	6	42	Same	6	42	Diffraction Eff ≥ 40% T = 60-70%, R <sub>2</sub> = 0.5% Primary/Ghost = 160:1 Two images at angle of bisection	4	28	None	10	70	Chromatic aberration colors see through imagery and some haze in plastic	4	28
	10	70		10	70		10	70		10	70		10	70
	10	60	Need Optical Correction	10	60	Zone plate forms high quality imagery (angle of bisection only)	10	60		10	60	Zone plate forms good image	8	48
	10	50	Need optical cor- rection	10	50	Angle of bisection only	10	50	Diffraction rings are fuzzy	2	10	Relief hologram may lack resolution of volume hologram	7	35
or	5	15	Same	5	15	Coat visor with gelatin	5	15	Insert element in visor	5	15	Emboss visor with hologram	5	15
	10	30		10	30		10	30	Ring brightness dependent upon ambient light	s 0	0		10	30
np	10	20	Tungsten Lamp Source	10	20	Tungsten Lamp Source	10	20	Transmittance cannot be varied	0	0	Panel adjustment for con- tinuous brightness control requires servo or stepmotor	5	10
	10	10	Orange filter	10	10	Shift wave length of reconstructed imagery by swelling gelatine	10	10	Neutral Grey	0	0	Krypton/Argon Laser (Yellow Green)	8	8
r Merit		779	Total Score or Merit		779	Total Score or Merit		783	Total Score or Merit		692	Total Score or Merit		744

Table IV. Summary Phase I Design Concept Study

Technique (State of Art)	Disadvantages	Advantages	Cost	Growth
Parabolic Visor (Advanced)	Difficult surface to fabricate     Limited to 3-deg FOV without correction	No correction required for 3-deg FOV	≥ \$10,000 for injection mold     Low production cost	Possible application to CRT displays
Spherical Visor (Advanced)	Requires refractive optics for correction     Additional mass of refractive optics	Easy surface to fabricate and check	• #10,000 for injection mold • Low production costs	<ul> <li>Possible application to CRT displays</li> </ul>
Dichromated Gel Hologram (Under Develop- ment)	Dichromated gelatine sensitive to temperature and humidity and not durable     Laser required for encoding each hologram     Low efficiency     Severe astigmatism except at angle of bisection     Direct reflection of reticle at angle of bisection     Adhesion problem between gelatin and plastic	Dichromated gel hologram     can be used with white light     source     High quality imagery     No optical correction     required	High initial cost     Medium to low production     costs	Possible application to CRT displays     Recent research by Kodak indicates humidity and swelling problems of dichromated gel hologram may be solved     New bleached holographic technique (Kodak) may allow encoding at angles (Kodak) may allow encoding at angles (Kodak) may allow encoding at angles to orange lasers
Relief Hologram (Developed)	Laser required for reconstruction of imagery     Chromatic aberration colors seethrough imagery     Scattering of laser light produces haze in plastic     Orange lasers not available now (6-12 months)     Low diffraction efficiency repurses a reflectance cost or more powerful laser.	High-quality imagery     Embossing relief hologram     on plastic is simple and     cheap     No optical correction     required	Low production cost     High initial cost for relief master	• Laser available in orange part of spectrum in 6 to 12 months

11

The Phase II design objectives for the reticle assembly were essentially the same as the Phase I effort except that the exit pupil requirements were increased to 15 mm, and reticle color would be orange and visible against 15,000 ft-L rather than 10,000 ft-L. The Phase II design requirements for the visor display assembly are included in Table V.

Table V. Video Display Optical Requirements

Horizontal Resolution	500 TV lines at 50% response output with 750 TV lines at 50% input from CRT
Grey Scale	Eight shades
Contrast	20% contrast ratio against 10,000 ft-L
Brightness Uniformity	3% image uniformity with 1% CRT uniformity
FOV	20 deg minimum
Exit Pupil	10 mm at surface of eye
Collimation	18 in. to infinity
Linearity	3%

# SECTION III PHASE II DESIGN CONCEPT STUDY

#### RETICLE GENERATOR

#### Selection of Design Concept

Three techniques were considered during the Phase II study for the approach to reticle projection on the helmet visor. These were a hololens encoated on the visor, a spherical-shaped visor, and a parabolic shaped visor. The holographic approach was discarded during the design concept study on the basis of the predicted low image brightness, difficulties in fabrication, and poor image quality of the holographic breadboard. The parabolic visor approach was selected and spherical approach rejected on the basis that refractive optics are not required for the parabolic approach but are required for the spherical visor. The Phase II design concept study also developed several designs of the parabolic approach using the standard, large GE lamp.

The superiority of the parabolic visor approach can be seen by comparing the ray trace drawings of the 3-deg reticle projection for a parabolic shown in Figure 3 and a spherical surface shown in Figure 4. The focal plane of a parabolic surface is very nearly flat for collimated rays entering the visor over a 3-deg field of view (FOV). In addition, the focal plane is very nearly perpendicular to the central ray. This indicates that the reticle image will be very well collimated in the center with slight decolimation at the edge of the field. This proved true in practice.

On the other hand, the spherical visor approach does not have a flat focal plane and requires a relatively complex refractive optics for correction of distortion, and chromatic and spherical aberrations. Figure 4 shows one approach, providing this correction with a simple prism.

The corrective prism is quite large and the focal plane is tilted. Not only must the reticle pattern have an elliptical shape to form a round virtual image, but the system is corrected for only one wavelength. Both the breadboard and helmet mounted versions were considered unacceptable in comparison to the compactness and superior image quality of the parabolic approach.

#### Selection of Parabolic Visor Focal Length

After the parabolic shape was selected for the reticle projection technique, a 1.5-in. focal length paraboloid was selected as the best compromise

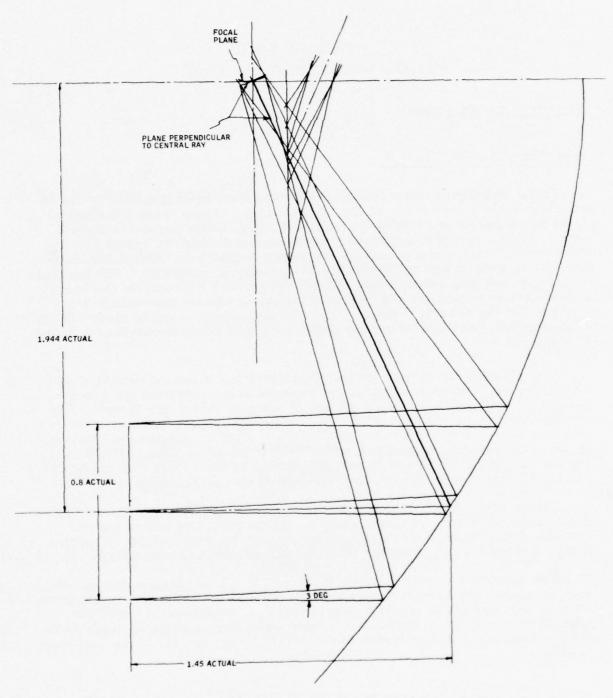


Figure 3. Ray Trace of Parabolic Visor Reticle Projection

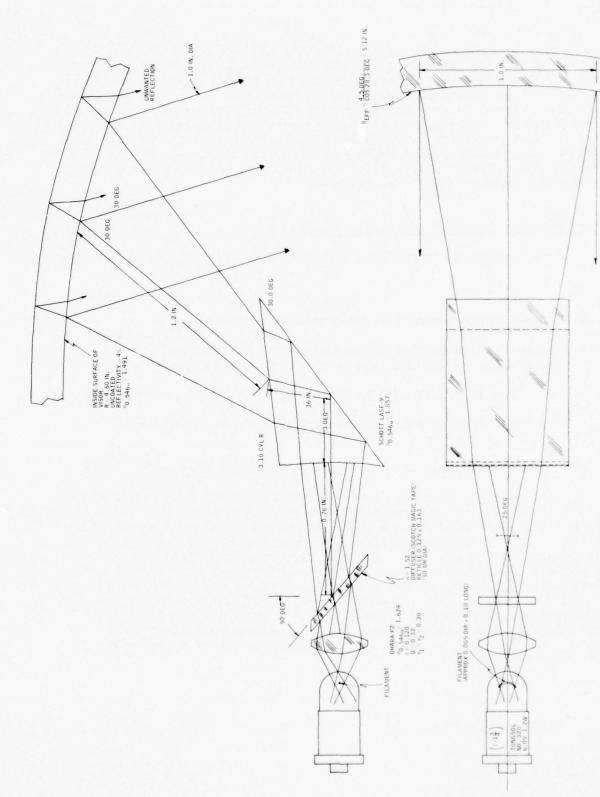


Figure 4. Prism Cutting Layout

among many design considerations. The primary advantage of the 1.5-in, focal length is a near perfect match with the existing visor bearing tracks of the Air Force helmet. This focal length also allows enough room between the visor and the helmet shell and pilot's forehead for the reticle generator assembly. Figure 5 shows the range of parabolic focal lengths considered during the study, and Figure 6 shows the final focal length of 1.5-in. selected for the reticle projection technique. Also, Figure 6 shows an early reticle generator design with a small 44 L type lamp without a condenser lens. It should also be noted that the 1.5-in. focal length paraboloid extends only 0.4 in. beyond a standard visor configuration.

#### Visor, Bearing Detent and Mating to Tracks

The requirements for attaching the visor to the helmet are as follows:

- Ease of part fabrication
- Visor tracks conform to the curvature of the helmet
- Ease of adjustment of tracks to ensure both planes of revolution are parallel and perpendicular to the line of sight
- Freedom of motion with no binding between bearings and tracks
- Bearings must provide attachment for both the visor and detent mechanism
- Accurate positioning of the visor in the active position

One early design shown in Figure 7 has a two-piece design for the track for ease of fabrication and assembly. The bearing is fabricated in one piece and has a hole detent for lower ball plunger which provides an accurate location of the visor in the lower position for boresighting. The upper ball plunger engages in a slot which provides horizontal or lateral registration. The ball plunger engages only at the bottom of the visor travel and thereby provides freedom of motion for storing the visor. The difficulty with this design is that no provision is made for vertical alignment of the visor. The detent approach was later abandoned in favor of securing the visor in the active position by tightening the visor knob. However, this approach requires that the visor be brought down firmly against the stops before tightening the visor knob.

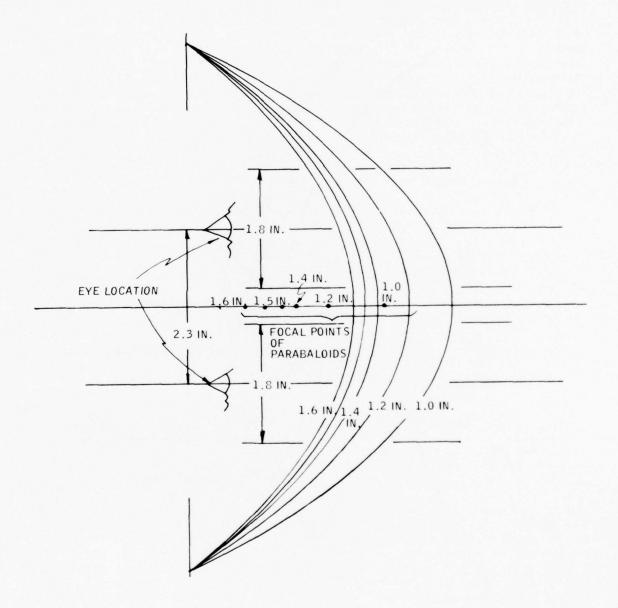


Figure 5. Comparison of Range of Paraboloids with Bearing Track Offset 8.0 in.

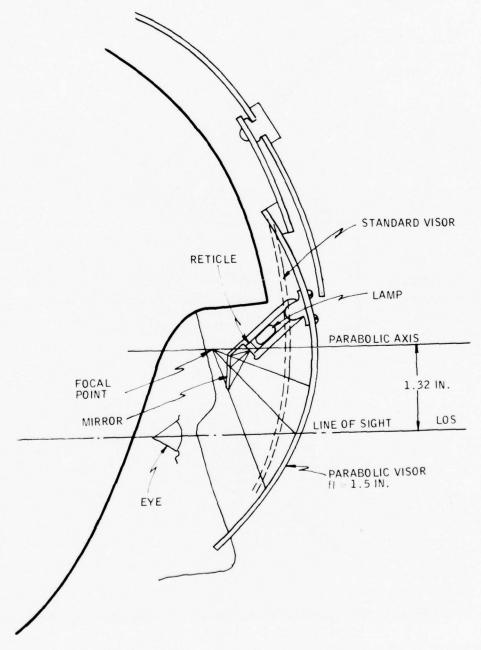


Figure 6. Parabolid Visor Reticle Projection

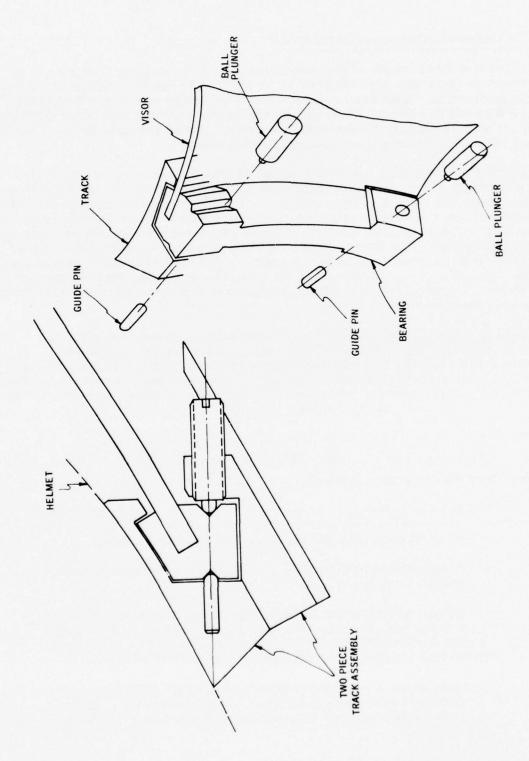


Figure 7. Vision Locating and Locking Mechanism

# Reticle Generator Subassembly Layout

After the focal length of the paraboloid had been selected, it was then necessary to generate several layouts to determine the feasibility of the visor reticle projection. The requirements for this design are described below. Figure 8 shows the first reticle generator layout utilizing the large GE lamp 1874. It was necessary to use this lamp since it was the only lamp available at that time with the required filament dimensions.

Figure 9 shows a preliminary layout of this design mounted on a visor with a retraction mechanism to allow the generator assembly to fit between the visor and the helmet. This design does not have the either-eye-switching mechanism and it uses two mirrors. It also does not allow enough room for a practical condensor lens design. Figure 10 shows another reticle generator design. However, this design requires the retraction mechanism to pivot about the filament coil axes which presents a difficult alignment requirement for the lamp filament. It also does not have the switching mechanism for either eye. Figure 11 was the final design layout conducted under the Phase II design concept study.

This layout utilizes a small lamp (with same filament as in the GE lamp) designed by the Advanced Development Laboratory of Honeywell. The small lamp design allows the eigher-eye-switching mechanism to be mounted on the visor of the helmet display. The last task performed under the Phase II design concept study was the definition of the design objectives for reticle projection. Design objectives are:

- Refer to Table 2-7 of Honeywell document 14327-TR4
- Low weight and minimum helmet envelope
- Reticle Generator assembly:
  - Reticle generator assembly shall be mounted to the visor with a retraction mechanism which shall allow the assembly to be stowed with the visor under the visor cover.
  - Clearance before forehead and reticle generator housing should be at least 0.25 in.
  - Either eye actuator is required and shall be mounted on a visor with its axis of rotation along the optical axis of the paraboloid to allow the reticle pattern to be located on and rotated about the optical axis of the paraboloid.
  - Operation of actuator knob for either eye operation is required with one gloved hand. Mechanism shall include adjustable stops for interpupilary distance adjustment.

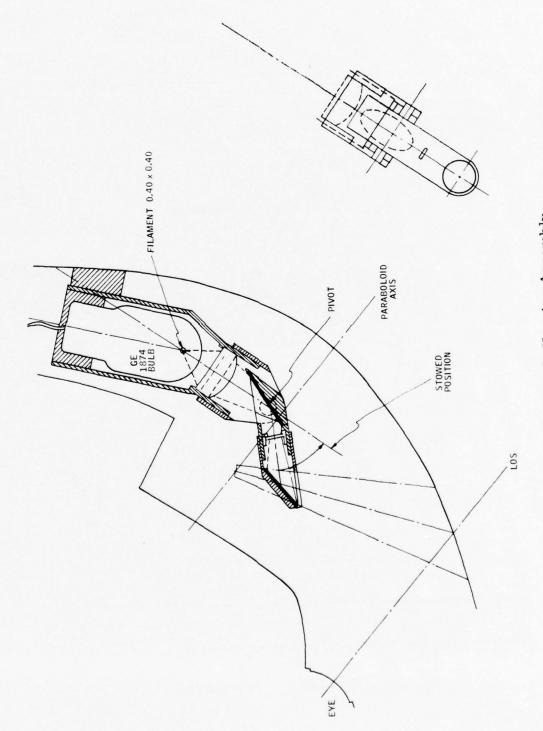


Figure 8. AHRA Reticle Housing Assembly

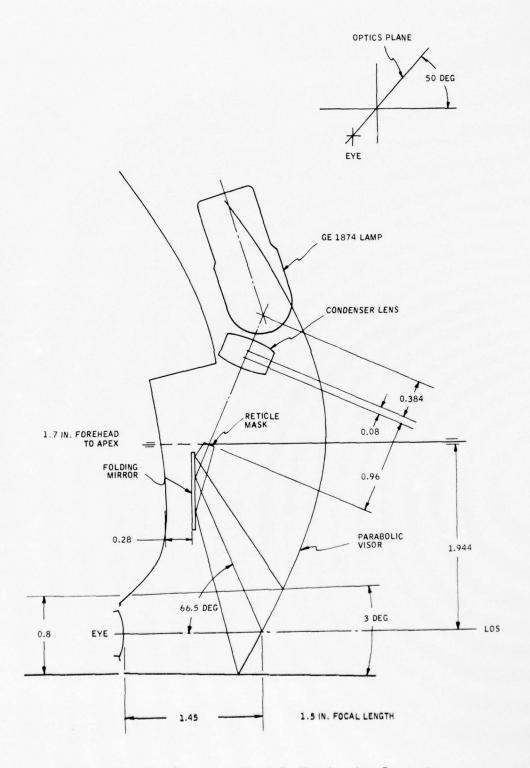
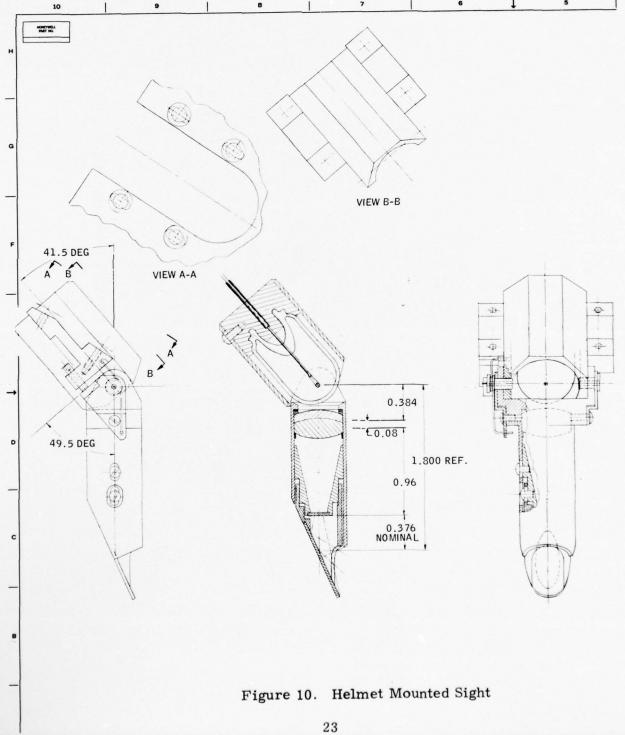


Figure 9. Preliminary Reticle Projection Layout



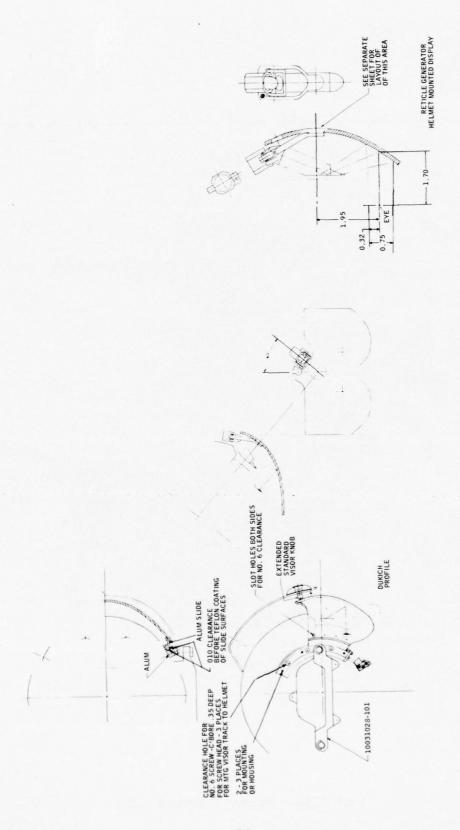


Figure 11. Reticle Generator HMD

- Tungsten lamp heat sink or radiator may be used to avoid melting plastic visor.
- The plane of the reticle shall be perpendicular to the line between the center of the reticle pattern and the center of the exit pupil projected upon the parabolic visor.

#### • Reticle Pattern

- 0.1 in. diameter
- Circular shape can be modified to present nearly circular imagery.

#### • Reticle Imagery

- 50 mr field of view (0.1-in. diameter reticle with EFL of 2 in.).
- Good image quality on a relative basis, i.e., acceptable to the observer without objectionable line splitting or waviness.
- Primary to secondary image ratio of greater than 190:1.
- 20% contrast of reticle pattern image against 20,000 ft-L background; i.e., reticle of brightness of 2800 foot lamberts with orange filter. (See Honeywell document 14327-TR4 for calculation.)

#### Reticle Generator Optics

- Exit pupil, 20 mm
- Overall distance between reticle pattern and tungsten lamp filament shall be 1.4 in. Illumination exit angle from reticle pattern should be approximately 22 deg to illuminate an 0.8-in. exit pupil at an effective focal length of approximately 2 in. Focal length of condenser lens is approximately 0.3 in. with a diameter of 0.5 in. and F number of 0.8. Objective of condenser lens design will be to provide a uniform illumination of the reticle pattern as well as uniform illumination of the exit pupil.

- Tungsten lamp with 100 hr life or longer, square 0.04-in. filament, and 4 watt power consumption. Lamp envelope should be 0.4 in. in diameter, 1.0-in. (maximum) inches long and tungsten coil should be 0.10 in. from end of glass envelope. (See Honeywell document 14327-TR4 for detailed brightness specifications.)
- Reticle Generator Adjustments
   (Longitudinal adjustments are along optical axis)
  - Longitudinal and rotary motion of plane mirror
  - Longitudinal adjustment of reticle pattern
  - Longitudinal adjustment of condenser lens
  - Adjustable stop for retraction mechanism
  - Longitudinal, lateral and angular adjustment of tungsten lamp in lamp housing assembly
  - Provision should be made to allow reticle pattern to be moved along the optical axis of the paraboloid for focus.

#### Boresight Adjustment

- Adjustable visor track stops will be incorporated in the visor track and bearing assembly. This allows the alignment of the visor assembly optical axis to be parallel to the horizontal plane of the boresight axis of the helmet.
- Contribution to boresight errors due to misalignment of visor tracks and bearings to be less than 7 mr. Therefore, visor bearings and tracks should be mated to within 0.007 in. and adjustable stops for visor bearings should be repeatable within 0.01 in.
- Sensor bar assembly shall be adjusted to provide boresight in horizontal plane by placing shims under the sensor bar mounting feet.
- Visor thickness ideally should be 0.1 in. to reduce seethrough distortion. However, actual visor fabrication may require a thickness of 0.15 in. to allow for error of centering inside parabolic surface with the outside surface of revolution.

## • Parabolic Visor

- Optical quality of outside surface of visor is determined by the original surface finish of the plexiglass sheet drawn over the male mold during vacuum forming. Consequently, care should be taken in handling parabolic sections to ensure no scratches formed on outside surface.
- Effective center of rotation of visor can be lowered if this will result in a reduction of the helmet envelope.
- Parabolic sections shall be annealed before plastic parabolic sections are rough cut to parabolic shape.
- Plexiglass parabolic visors shall be cleaned with ivory dishwater soap, isoproponal alcohol, and dried with Kay Dry paper.
- Surface finish of plastic paraboloid should produce no detectable lines splotting or waviness of imagery.

Analysis of Requirements for Parabolic Visor with Reticle Projection

Assembly -- The helmet sight reticle projection assembly which will be used with the parabolic visor HMS is shown in Figure 12. The major component parts are a square filament light source, condenser lens assembly, diffuser, color filter, reticle pattern, mirrors, and parabolic visor optical element.

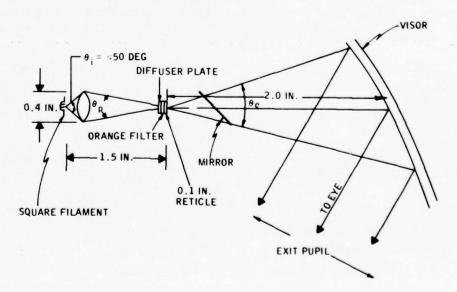


Figure 12. Reticle Projection with White Light Source

The key element of the reticle projection assembly is the condenser lens. This condenser performs two functions - first, it images the filament onto the diffuser behind the reticle pattern and allows the observer to view the filament image directly. It is this function of the condenser which allows the reticle to be viewed against backgrounds with a high brightness level. The second function of the condenser is to illuminate the desired exit pupil with light. The exit angle from the reticle pattern must be 20 deg to illuminate a 20-mm exit pupil at an effective focal length of 2 in. This places the requirement on the condenser exit angle to be 20 deg.

Uniform reticle illumination is obtained at the expense of the brightness of the imagery. Brightness is reduced because the diffuser (which fills in the dark areas between the image of the bright filament coils scatters and/or attenuates light. Uniform reticle illumination is also obtained by slightly defocusing the image of the filament on the reticle pattern, which again reduces reticle image brightness.

A square filament shape is necessary for the light source to conserve filament power and minimize heat generation. If the filament shape had an aspect ratio of 4 to 1, for example, then the narrow portion of the filament image is focused over a circular reticle pattern. Four times the power is needed for this tungsten lamp than one with a square filament. The actual size of the filament is determined by the magnification of the condenser systems; therefore, increasing the condenser magnification will reduce filament area and power. However, the magnification is partly a function of the condenser entrance angle which must be limited to reduce design complexity and allow space for the glass envelope of the tungsten lamp. The other limitation of condenser magnification is the condenser exit angle which is determined by the requirement to fill the exit pupil.

Figure 12 shows the length of the projection system from the filament to the visor to be approximately 3.5 in. and the diameter of the condenser housing to be less than 0.4 in. The entire reticle illuminator assembly is mounted to the upper edge of the visor and will be retracted with the visor under the visor cover.

Design Parameters -- The design parameters of the helmet sight reticle projection assembly are as follows:

- Image brightness 2800 ft-L (60-70% visor transmittance)
- Ghost image Minimum 120:1 ratio for primary to ghost image brightness
- Contrast 20% against 20,000 ft-L background brightness
- Visor with minimum scene brightness attenuation Inside 30% reflectance

- Transmittance 60-70%
- Outside 0.5% reflectance HEA minimum
- Reticle pattern 50-mr FOV. 0.1-in. diameter with EFL of 2.0 in. and orange filter
- Exit Pupil 20 mm
- Tungsten light source
  - Life not less than 100 hr
  - Square filament 0.04 in.
  - 2.0-w power consumption (design goal)
- Diffuser ground glass
- Condenser lens diameter 0.30 in. with two elements

One of the most important requirements noted is that the ghost image must have a low brightness level compared to the brightness of the reticle image. Experience has indicated that the ratio of the primary-to-ghost-image brightness should be a minimum of a 120:1. To realize this ratio with the 60-70% visor, it is necessary to use a dielectric, multilayer, 30% reflective coating on the inside surface (R<sub>1</sub>) and a 0.5% reflective coating on the outside surface (R<sub>2</sub>). However, both of these coatings are expensive. This visor (70% transmittance) reduces the background brightness from 20,000 ft-L to 14,000 ft-L. Therefore, a differential contrast ratio of 20% against a background brightness of 14,000 ft-L requires that the virtual image brightness should be 2000 ft-L.

<sup>1</sup>Primary/ghost brightness ratio =  $\frac{m^{R_1}}{T^2 R_2}$ 

<sup>2</sup>Differential contrast = total image brightness-background brightness x 100 background brightness

where

total image brightness = virtual image brightness + background brightness, for example:

Total image brightness = 2,800 + 14,000 = 16,000 ft-L

<sup>3</sup>HUD specification, MIL-D-81641, 1 Jan. 1970; F-4 HUD proposal CAA-3907, 26 May 1969, Conductron; F-14A weapon system, VDiG, AN/AVA-12, 2 March 1970.

Selection of Reticle Illuminator Design -- The reticle projection assembly power requirements is another critical design parameter of the reticle projection assembly. If the light source is in excess of 2 w, then the lamp becomes not only an objectionable source of heat to the pilot but it may melt the visor or visor cover. Therefore, not only must an efficient reticle projection design be selected for the helmet reticle assembly, but also the design must provide a uniform reticle illumination.

One method to obtain this uniformity is to focus the filament image on one end of a special noncoherent and scrambled fiber optic bundle. The other end of the fiber optic bundle will uniformly illuminate the reticle pattern. The other method of producing a uniform illumination across the reticle pattern is to use a diffuser plate between the reticle pattern and the condenser. Although the fiber optic bundle has lower losses than the ground glass diffuser, it is not recommended for this application since the lamp power requirement is less than 2 w for the glass plate diffuser.

Reticle Projection Technique Efficiencies -- The efficiency of the projection assembly is defined as the image brightness presented to the observer divided by the surface brightness of the tungsten coil of the light source. It is calculated from the product of the visor reflectance; the filament coil packing fraction; the luminous transmittance of the orange-color filter; the transmittance of the condenser; and transmittance of the fiber optic bundle or diffuser plate.

The average brightness of the filament coil over its length is reduced by the voids or empty spaces between the filament coils. This reduction of source brightness from the surface brightness or luminance of the tungsten wire is referred to as the filament coil packing fraction and is assumed to be 50%.

The luminous transmittance of the orange-color filter is assumed to be 65%. The combined transmittance of the condenser and fiber optic bundle is considered to be 35%, which assumes that the 2-element condenser optics has a transmittance of 80%, the fiber optic bundle combined end loss and transmittance reduces the image brightness by 30% and that there is a 40% brightness loss when the filament image is slightly defocused on the end of the fiber optic bundle. It is assumed that the combined defocusing and light scattering of the glass plate diffuser will result in a 90% loss of light or an effective transmittance of 10%. The total efficiencies for the various techniques are calculated from the products of the optical component efficiencies. The projection assembly with the 65% visor reflectance and FOB diffuser has the highest efficiency (7.4%), while the assembly with the 30% reflectance visor and glass diffuser has the lowest efficiency (0.98%).

Filament Dimensions -- The critical design parameter of power consumption of the light source can now be calculated. It is important to identify the variables that specify the filament area such as the exit pupil and field of view since lamp power consumption is proportional to the area of the tungsten filament. The filament diameter can be determined from the relationship below for the case of the fiber optic bundle diffuser (assuming condenser entrance angle of approximately 50%).

Filament diameter = 
$$\frac{\text{FOV x Exit Pupil}}{2 \text{ x sin}(25 \text{ deg})}$$

where

FOV - is the reticle pattern angular field of view (valid for small angles)

This equation shows that the size of the filament, used with a fiber optic bundle diffuser, is a function of the reticle field of view (50 mr) and exit pupil (20 mm).

The primary difference between the fiber optic bundle diffuser and the ground glass diffuser plate is that a smaller condenser exit angle  $(\theta_p)$  (see Figure 12) is needed with diffuser plate. The function of the diffuser plate is primarily to diffuse the image of the filament, but it also spreads the light out over a larger exit-pupil angle  $(\theta_e)$  than the condenser exit angle  $(\theta_p)$ . This increase in dispersion allows the condenser lens to be designed for a smaller exit angle  $(\theta_p)$  and higher magnification. The filament diameter then becomes

Filament diameter = 
$$\frac{D \tan (\theta'/2)}{\sin (25 \text{ deg})}$$

for the ground glass diffuser case.

where

$$\theta_{\rm p}^{\prime} < \theta_{\rm p}$$

D - reticle pattern diameter (0.1 in.)

 $\theta_n'$  - condenser exit angle for diffuser plate (= 14 deg)

 $\theta_{\rm p}$  - condenser exit angle for fiber optic bundle diffuser (20 deg)

The filament dimensions are 0.04 x 0.04 in. for the fiber optic bundle diffuser and 0.025 x 0.025 in. for the glass diffuser.

Power Requirements and Life Expectancy -- The prediction of power, average luminance, and life of the nonstandard, square filament, tungsten lamps is a function of many variables such as shape of the tungsten coil, diameter of coil, thickness of tungsten wire, spacing of coils, current and potential, envelope dimension and material, lead-in wires, and gas mixture and pressure. To avoid the complexity of theoretical prediction with such a large number of variables, it is standard procedure to pick an existing lamp with the same filament area and extrapolate from known operating conditions. Graphs and equations are available for extrapolation, and it is assumed that lamps with the same area require the same power for corresponding levels of luminance.

To make these extrapolations it is first necessary to calculate the required tungsten surface brightness by dividing the image brightness by system efficiency. Tungsten surface brightness (luminance) levels are also correlated to the tungstens urface color temperatures<sup>4</sup>. The next step in the power calculation is to select a catalog lamp with known power consumption and color temperature, which has approximately the same filament area as the lamps required by the reticle projector designs. Nomographs<sup>5</sup> are then available that allow estimation of power requirements at difference luminance levels. Power requirements for lamps with different filament dimensions can be found from the ratio of the filament areas since it is generally accepted that power requirements of lamps with the same color temperature and packing fraction vary as the projected area. Finally, the rated life of a known lamp is determined and is extrapolated to the life at other luminance levels by the equation<sup>6</sup>.

$$Life_1 = Life_2 \left( \frac{Lumens_2}{Lumens_1} \right)^{3.67}$$

#### VIDEO DISPLAY SUMMARY

The recommendation for the AHRA video display prototype at the end of the Phase I design concept study was to reflect video imagery once off a spherical visor with two mirrors and corrective refractive optics. However, at the conclusion of the Phase II design concept review it became evident that the parabolic visor was the only feasible approach to video display projection.

<sup>&</sup>lt;sup>4</sup>L. Levi, "Applied Optics: A Guide to Modern Optical System Design." Table 26, page 554.

<sup>&</sup>lt;sup>5</sup>Kingslake, "Applied Optics and Optical Engineering." Figure 16, page 60, Volume 1.

<sup>&</sup>lt;sup>6</sup>Kingslake, "Applied Optics and Optical Engineering." Table, page 61.

The parabolic visor not only allows much simpler and smaller refractive optics, but it may also be self correcting for larger fields of view, such as 40 deg. The additional advantage of the parabolic visor approach is that off-the-shelf optics could be used to adequately demonstrate the design concept. This allowed a timely demonstration of the video display breadboard. The most difficult problem associated with the spherical visor approach is that the refractive optics must have a diameter of 1.25 in. Optics of this diameter cannot be fitted to the helmet without significantly increasing the helmet envelope.

The development of the above parabolic approach to the video display was accomplished in six major steps. First, a design concept review was made to examine many geometrical approaches to the video display, and those approaches which appeared to be most promising were selected for further examination. Secondly, layouts were made of the optical components of these approaches on the helmet to determine optical constraints. Third, computerized automatic optical design programs were run based upon those layouts which best satisfied the design requirements. Fourth, the optimized optical computer design data were used to produce detailed drawings of the optical elements. Fifth, additional computer programming was required, since the first computer designs did not satisfy the 0.4-in. exit pupil requirements. Sixth, final detailed design layouts were made of the optical elements and the means for mounting them on the helmet.

This subsection discusses the design concept study which consists of the design concept review, preliminary layouts, and computer programming that were necessary before the sixth and final design step of component helmet layout (refer to Section VIII).

## Design Concept Review

General Approach -- The objective of the design concept review was to select a geometric-optical technique for displaying video information that can be conveniently mounted on an Air Force helmet. Although the use of the curved visor eliminates any optical elements between the observer's eye and visor, it does require correction of the aberrations and distortions generated by the curved combiner. The problem to be solved by the design concept review is to select a system of curved combiner/mirrors that will require a minimum of corrective techniques for the aberrations and distortions generated by the off-axis reflective curved combiner.

elehin no

The corrective techniques that can be used can be grouped into the following basic categories:

- Symmetrical arrangement of combiners
- Aspheric refractive elements
- Collimation or relay lenses
- Aspheric fiber optic bundle
- Nonlinear generation of CRT sweep voltages

A composite illustration of these techniques for optical correction is shown in Figure 13. This illustration is not to scale nor will all the optical elements be found simultaneously in any one design approach.

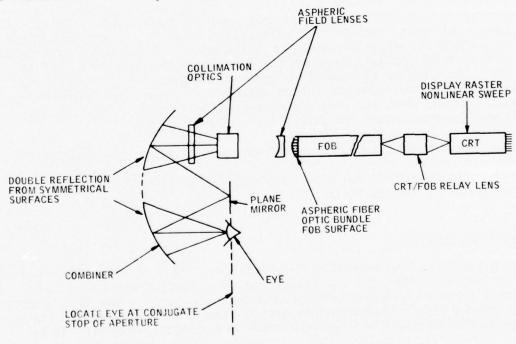


Figure 13. Composite Example of Technique to Reduce Aberration and Distortion of Off-Axis Curved Reflective Element

Because of its effect on image quality, astigmatism is the most important aberration that must be compensated for in a wide field of view system with off-axis reflective combiners. If astigmatism cannot be adequately corrected, image quality will be unsatisfactory. The symmetrical arrangement of parareflective surfaces shown in Figure 13 removes both astigmatism and coma

when the aperture stop and its image, the exit pupil, are located at a distance equal to the focal length of the combiner from the vertex.

Asymmetrical aberrations including astigmatism, distortion, and field curvature may be compensated for by use of decentered aspheric multi-lement field lenses placed in front of the fiber optic bundle (FOB) and/or between the collimation optics and combiner as shown in Figure 13. However, if design constraints on the optical system require the use of two field lenses in the same optical system, they tend to cancel each other's corrections. In this situation, additional correction can be obtained by generation of nonlinear sweep voltages for the CRT raster (Figure 13).

The problem may also be attacked by providing an aspheric surface on the end of the FOB (Figure 13) to compensate for field curvature. A single multi-element aspheric lens may then be used to correct for the remaining asymmetrical aberration which is principally astigmatism. In addition, the collimation lens (Figure 13) can be designed to include toric elements which will compensate for astigmatism, provided that other surfaces are shaped to correct for coma and spherical aberrations.

In addition to the techniques illustrated, the FOB and collimation or relay optics can be tilted to align the FOB image with the focal surface of the combiner. Generally, the requirement for tilting optical elements must satisfy the Schiemphlug condition which requires that the intersection of the image and object planes lies on the principal plane of the collimation or relay lens.

F-Number of Optical System -- The optical system with the largest F number, other considerations being equal, will have the highest image quality and resolution, and will require the least difficult optical design.

In an HMD design an increase in exit pupil decreases the F number of the system. The exit pupil is the image of the aperture stop of the collimation or relay optics; therefore, the aperture stop is equal to the exit pupil times the magnification of the optical system. To achieve an operationally useful exit pupil, some of the following design approaches require the F number of the collimation or relay optics to be quite small and present difficult design problems.

The exit pupil and the aperture stop of the relay lens for the elliptical combiner approach shown in Figure 14 are located at the foci of the ellipse, and, therefore, must be located near the top of the ellipse in order to view the display. Consequently, the object distance is approximately three times the image distance, and the magnification is 0.3. Therefore, if an exit pupil of 10 mm is used, the aperture stop must be 30 mm or 1.2 in. In most helmet applications, an aperture stop of this size would present a serious design problem because of the physical size and weight of the relay optics.

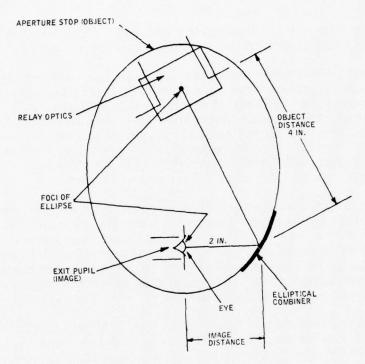


Figure 14. Exit Pupil Formed as Image of Aperture Stop by Combiner

Exit Pupil -- The exit pupil is a critical design consideration for a curved combiner HMD design approach and must be minimized to obtain the best image quality and resolution. Therefore, it is necessary to consider the effect of the exit pupil location and size upon the observer's vision. At a minimum, the exit pupil should equal the 5-mm diameter of the eye's iris. If an exit pupil of 5 mm, for example, is located 9 mm behind the iris of the eye to coincide with the axis of rotation of the eyeball (Figure 15a), then a full field coverage can be attained with the limited eye freedom of  $\pm 2.5$  mm. Although full foveal vision is obtained, the peripheral vision is restricted, resulting in tunnel vision.

Full peripheral vision can be obtained if the exit pupil is located at the iris, but only in the center of the field as shown in Figure 15b. Therefore, for an optical system with limited eye freedom area, it is not possible to have both peripheral vision and a full field of view. An exit pupil of 10 mm diameter or more will allow peripheral vision over the entire field.

Full foveal vision, of course, is necessary over the entire field coverage; but peripheral vision is not essential since the eye scans the field.

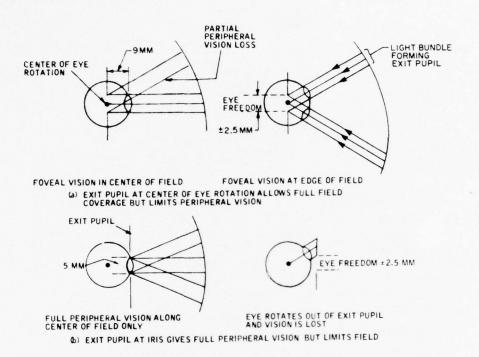


Figure 15. Exit Pupil at Iris and Center of Eye Rotation

The price for full coverage of the format field along any line of sight is a larger exit pupil with consequently larger optics working at a smaller F number and a reduction of image quality.

Design Mounting Constraints -- Honeywell experience with HMDs shows that the CRT should be remotely mounted at the back of the helmet (for lowest cg) and that relay optics and an FOB should be used to convey the imagery to the front of the helmet. It is also Honeywell's experience that the eye relief should be approximately 2 in.

The basic design problem of video projection on a curved visor is that a real image must be formed in the vicinity of the center of the forehead at the focal point of the eye combiner. Obviously, the CRT itself cannot be located at this position and some form of relay optics must be used. The present design approach is to use an FOB with relay lens to transfer imagery from the CRT mounted at the back of the helmet. This design approach relays the CRT imagery to the top of the helmet above and to one side of the forehead as shown in Figure 16. Collimation optics, relay optics, and curved mirrors can all be used to form a real image at the focal point of the eye combiner near the center of the forehead.

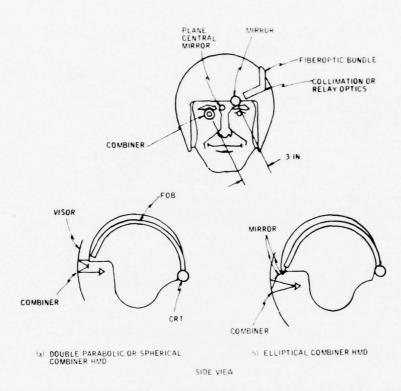


Figure 16. Optical Layout of HMD Optics and CRT

Honeywell experience with HMD design shows that approximately a 2-in. eye relief provides an excellent compromise for helmet-mounted optical systems, minimizes expansion over the basic helmet envelope, and allows a 20-deg field of view. The eye relief of 2 in. establishes the focal length of the eye combiner to be either 1 or 2 in., depending upon the design approach.

In the case of the symmetric parabolic and Schmidt corrector combiner approaches, the eye is located in the focal plane, and the focal length and eye relief are equal. In the case of the symmetrical spherical and tilted spherical combiner approaches, the eye is located near the radius of curvature which is twice the focal length of the combiner. The elliptical combiner approach, selected as an example for the purposes of this proposal, has a focal length of 1.4 in. as derived from the eye relief distance.

A spacing of approximately 3 in. is needed between the collimation or relay optics and HMD wearer's line of sight. This spacing stems primarily from the requirement to accommodate the full envelope of light rays reflected from the 2-in. focal length mirrors and combiners to provide the full 20-deg field of view as shown in Figure 16. The active area of the curved combiners and mirrors is approximately 1.5-in. in diameter. Therefore, the 3-in.

spacing also allows the central mirror, in the example of the symmetrical designs, to be mounted between the combiner and curved mirror without an overlay.

Design Concepts -- The 20-oz weight and spatial limitations of visor projection of video information preclue the use of large, heavy refractive optics to correct for off-axis aberrations introduced by a curved visor. The curved visor is needed to provide optical power and project collimated light from the image of the end of the fiber otpic bundle towards the eye to form a virtual image at infinity. Two objections to the use of a single curved reflective element to provide the required magnification of the image are: first, all curved surfaces introduce image aberrations; and, secondly, the short combiner focal length of 1.4 in. (required to form a virtual image with an angular subtend of 20 deg from a 0.5-in. FOB image) is not long enough to provide a satisfactory mounting location for the FOB.

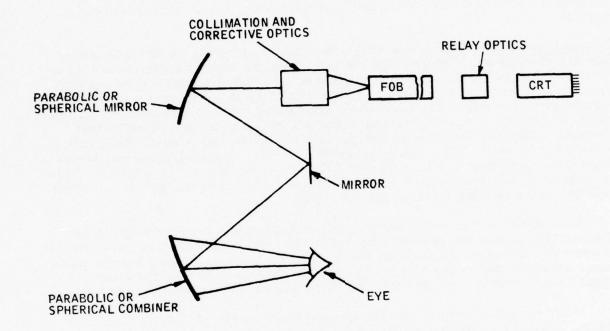
Therefore, either relay and/or collimation optics must be used in the HMD design to provide corrections for the aberrations of the curved combiner. In addition, these optics must be combined with plane mirrors, curved mirrors, an FOB, and relay optics to relay the FOB imagery over a longer separation distance than that allowed by a short focal length of 1.4 in.

Many design concepts have been considered by Mr. Irv Abel, senior optical designer at Honeywell Radiation Center, and Mr. John Miles, consulting optical designer of Chicago. As a result, six approaches have been selected as candidate systems for subsequent analysis. Such analysis must show which ones can provide the required optical performance and simultaneously permit convenient mounting of the FOB and optics on an Air Force helmet.

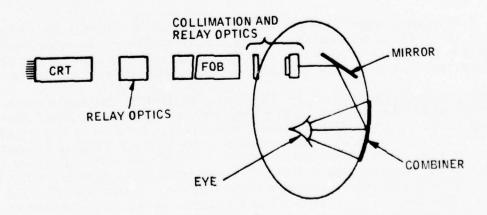
The six design concepts are shown in Figure 17a and 17b, and Figure 18a and 18b. These approaches are the double reflecting parabolic combiner, double reflecting spherical combiner, elliptical combiner, Schmidt corrector spherical combiner, the tilted spherical, and parabolic combiner.

Helmet Mounted Displays -- The double reflecting parabolic combiner helmet mounted display employs a symmetrical arrangement of a parabolic combiner and mirror about a common central mirror, as shown in Figure 17a. This symmetry is extended to the location of the eye and collimation optics on either side of the central plane mirror. The symmetrical arrangement of the parabolic combiner and mirror projects collimated light from the FOB via the optics to the eye. Therefore, this design concept satisfies the requirement for correction of aberrations and increased separation distance to provide for a convenient mounting of one end of the FOB near the top of the helmet.

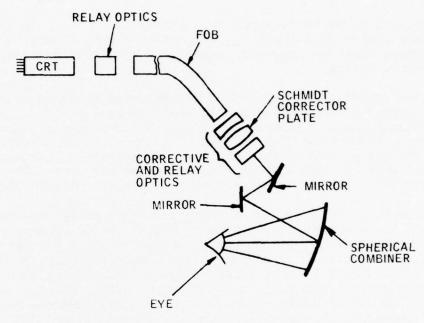
The double reflecting spherical combiner design concept utilizes the same principle of symmetry as the parabolic combiner approach. The major difference is that spherical aberrations are not the same as parabolic aberrations;



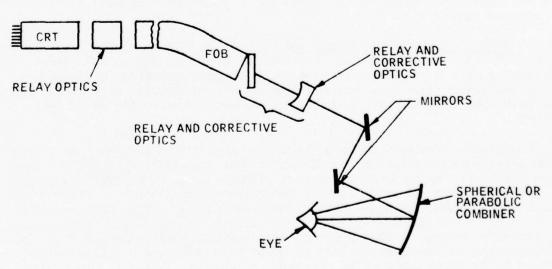
a) Double Reflection Parabolic Combiner



b) Elliptical Combiner Figure 17. Three HMD Design Concepts



a) SCHMIDT CORRECTOR SPHERICAL COMBINER



b) TILTED SPHERICAL OR PARABOLIC COMBINER

Figure 18. Two HMD Design Concepts

consequently, the corrective optics are not the same. The same illustration (Figure 17a) is used to portray both design concepts, however. The double reflecting spherical approach requires larger and more complex refraction corrective optics.

The elliptical combiner HMD design concept, shown in Figure 17b, requires one reflection off of an elliptically shaped combiner, and one or more reflections off plane mirrors to provide the required increased separation distance between the FOB and eye. This provides the potential for satisfactory mounting of the FOB near the top of the helmet. Corrective optics and a relay lens are both employed to correct for combiner aberrations and to project collimated FOB imagery off the combiner towards the eye.

The Schmidt corrector spherical combiner design approach shown in Figure 18A utilizes an arrangement of two or more plane mirrors and three optical elements to provide optical correction and to provide increased separation between the FOB and eye. The name of this design approach is derived from the type of spherical combiner used to project collimated light towards the eye, and the Schmidt corrector plate, which is used to provide part of the optical corrections. The two optical elements located on either side of the Schmidt corrector plate not only act as the relay to increase the separation distance, but provide additional optical correction.

The tilted spherical and parabolic combiner approaches shown in Figure 18b are another arrangement of spherical or parabolic combiner and relay or collimation optics.

Double Reflecting Parabolic Combiner HMD -- Reflective systems normally cover only a very small field of view with adequate image quality. However, the special optical conditions obtained with a symmetrical design based on double reflection from a paraboloid (Figure 19) can provide high image quality over a 20-deg field and still meet the constraints of mounting on a flight helmet.

Principal advantages of the parabolic approach are derived from symmetrical arrangement of the eye, collimation lens, parabolic mirror, and parabolic combiner about a central mirror. This arrangement, shown in Figure 19, places the eye, central mirror, and collimation optics in a single plane which also contains the focal point of both paraboloids. The FOB is at the focal length of the collimation optics which projects collimated light toward the parabolic mirror. This collimated radiation is then reflected from the parabolic mirror towards the central plane mirror where a real image is formed in the focal plane of the parabolic combiner. Reflection from the central mirror causes the parabolic combiner to project collimated radiation towards the eye. The parabolic reflective surfaces act as a relay element which accepts collimated light from the FOB and projects collimated light towards the eye, thus forming a virtual image with unity magnification. The

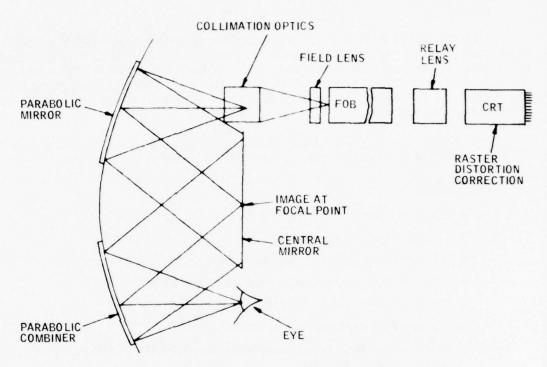


Figure 19. Double Reflecting Parabolic Combiner HMD

exit pupil which is the real image of the aperture stop is also formed by the parabolic reflective surfaces acting as relay elements with unity magnification.

The unity magnification of the equivalent relay system results in two advantages. First, the collimation optics are small and lightweight since the aperture stop need only be approximately 0.45 in. to form an exit pupil of 0.4 in. at the eye. Second, the collimation optics F number if relatively high because of its small aperture. For the AHRA program, the F number is 3.1 for an aperture of 0.45 in. and a focal length of 1.4 in. This combination allows a virtual image with an angular subtend of 20 deg from the format of a 0.5-in. FOB with good resolution.

The special optical conditions obtained with a symmetrical parabolic approach are the reduction of astignatism and cancellation of coma which allows the design of optical system with highly corrected imagery over the field. Astigmatism is removed when the aperture stop and its image (exit pupil) are located at a distance equal to the focal length of the parabolic mirror and the parabolic combiner are confocal or equivalent to a single paraboloid, and the combination represents an afocal system.

A 20-deg field with highly corrected imagery is now possible since the moderate field curvature can easily be compensated by a properly designed collimation lens and distortion can be corrected by a special function generator for the CRT raster sweep voltages. Any see-through distortion of the parabolic (or any other combiner) can be removed by varying the combiner thickness over the field.

This elegant design approach to the wide field of view reflective combiner HMD is a prime candidate system for design development.

## Advantages

- Highly corrected imagery over wide field
- Small lightweight optics
- Moderately large F-number system
- Easily mounted on helmet and under visor
- Easily fabricated refractive optics
- Lack of asymmetrical aberrations
- Cancellation of coma and reduction of astigmatism due to symmetrical design
- No aspheric refractive optics required
- Short collimation lens focal length

## Disadvantages

Difficulty of parabolic mirror and combiner fabrication

Double Reflecting Spherical Combiner HMD -- The double reflecting spherical combiner HMD approach will require more complex optical correction and will have less satisfactory image quality than the parabolic approach; however, the spherical optical system will be somewhat less expensive to fabricate in production quantities. The double refelecting spherical combiner approach has very nearly the same optical layout as the parabolic approach except that spherical rather than parabolic reflecting surfaces are used. Furthermore, in the limiting case of a single ray, the optical performance also becomes very nearly the same.

If the eye relief is 2 in. for this design approach (Figure 20), then the radius of curvature of the spherical surfaces are 4 in. and the focal lengths are 2 in. The location of the FOB and corrector elements in the focal plane of the collimation optics projects collimated light toward the spherical mirror to be reflected towards the central plane mirror, forming a real image in the focal plane. The reflected light of the real image is then directed towards the spherical combiner which in turn projects collimated imagery toward the

eye. Therefore, the spherical reflective surfaces act as a relay element that accepts collimated radiation of the FOB and projects collimated light toward the eye which forms a virtual image with unity magnification.

The exit pupil or real image of the aperture stop is also formed by the spherical reflective surfaces acting as a relay element. This time, collimated radiation is transferred by the central mirror. Collimated light is transferred by the spherical elements since the eye and collimation optics are located near the foci of the two surfaces. Although the common spherical surface has a focal point near the center, the foci of the mirror and combiner may be considered as having their own separate locations closer to the exit pupil and aperture stop as shown in Figure 20. Consequently, the exit pupil and collimation lens may have to be placed slightly back of the plane containing the central mirror.

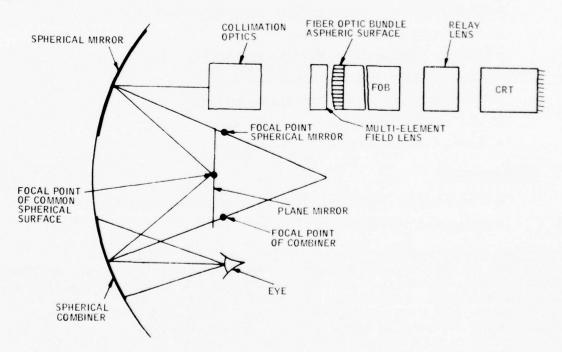


Figure 20. Double Reflecting Spherical Combiner HMD

One advantage of the spherical approach is that the aperture stop of the collimation optics needs to be moderately larger than the exit pupil. This aperture when combined with a focal length of approximately 1.4 in. may allow a relative high F number which in turn may satisfy the primary design objective to minimize aberrations. Also, the symmetrical approach of the two spherical surfaces tends to cancel coma. Astigmatism, field curvature distortion, and spherical aberration of the pupil are the most significant remaining aberrations.

Astigmatism would tend to be uniform across the field because of the symmetrical arrangement of the two spherical mirrors. On-axis astigmatism may be corrected by a toric surface in the collimation lens array. Off-axis residual astigmatism correction requires an aspheric multi-element field lens as shown in Figure 20. This field lens may also be required to compensate for spherical aberration of the pupil. Distortion may be corrected by raster sweep correction on the CRT, and symmetrical field curvature may be compensated by an aspheric surface FOB. The requirements for coma, symmetrical field curvature, and spherical aberration correction are relatively modest and would be included in the corrective design of the collimation optics.

# Advantages

- Ease of spherical combiner and mirror fabrication
- Cancellation of coma by symmetrical reflection
- Relatively high F-number
- Small, lightweight refractive optics
- Modest symmetrical aberrations
- East of mounting components on helmet
- Uniform astigmatism across the field
- Short collimation lens focal length

# Disadvantages

- Fabrication of aspheric field lens and fiber optic bundle surface
- Spherical aberration of all rays

Single and Double Reflection Elliptical Combiner -- The elliptical combiner design concept has the disadvantages of asymmetrical astigmatism, decentered aspheric multi-element field lenses, large relay aperture, and requirement for telephoto design of relay lens with small F number. The elliptical mirror design approach is shown in Figure 21 without folding mirrors required to mount system components on the helmet. A separation distance of 3 in. between the line of sight and the FOB mirror allows use of an ellipse with reasonable foci separation and eccentricity. One advantage of the elliptical combiner approach is that, by locating the exit pupil and aperture stop at the two foci, imaging of the exit pupil is accomplished without spherical aberration of the pupil. However, this advantage is reduced by exit pupil distortion caused by variable magnification across the field. Such distortion may be corrected by designing the aperture stop for the smallest magnification which occurs at the limit of downward vision or at the lower portion of the field.

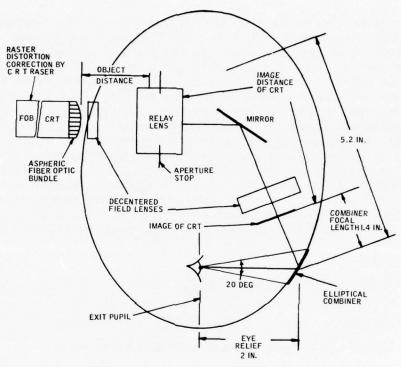


Figure 21. Elliptical Combiner HMD Approach

The example shown in Figure 21 has a separation distance between the center of the eye combiner and one focus of 5.2 in. The image of the FOB must be formed at an effective combiner focal length of 1.45 in. as determined by the 5.2-in. object distance of the aperture stop and its 2.0-in. image (exit pupil) distance or eye relief. This in turn establishes the image distance of the relay lens for the FOB image to be 3.75 in.

The image height is approximately the same as the 0.5-in. format of the FOB for an image angular subtend of 20 deg. Therefore, a relay lens focal length of approximately 1.87 in. is needed for an object or image distance of 3.75 in. The relay stop of 1.02 in. is established by the combiner magnification (aperture stop-image/object distance) of 0.39 and the requirement for a 0.4-in. exit pupil. Therefore, the F number for the relay lens is quite low, approximately 1.8.

From this analysis it can be seen that not only must the small F number relay lens correct for the off-axis aberrations of the single reflective elliptical combiner, but it may require a telephoto design to reduce the 3.75-in. back focal length to a value compatible with helmet mounting. This clearly will be a very difficult design problem, and this approach was rejected for the AHRA program.

Another objection to the elliptical design concept is a high degree of asymmetrical astigmatism resulting from the single reflection. This aberration is difficult to compensate and requires the use of a decentered asymmetrical multi-element field lens located in front of the CRT or possibly near the real image of the CRT. In addition, the elliptical mirror does not provide good imagery for a wide field of view because of symmetrical astigmatism and off-axis coma, and field curvature along with residual distortions. These off-axis aberrations could be corrected by another decentered aspheric multi-element field lens while the main part of the relay lens corrects for spherical aberration. A cylindrical or toric surface would be required in the relay lens assembly to correct for symmetrical astigmatism. Considerable difficulty can be expected with adapting this design to an HMD due to the large refractive optics. Many techniques for correction and compensation of aberrations must be used in this difficult design, including aspheric FOB field curvature correction raster sweep distortion correction, relay lens, and CRT tilting.

## Advantages

• None for 20-deg field of view

# Disadvantages

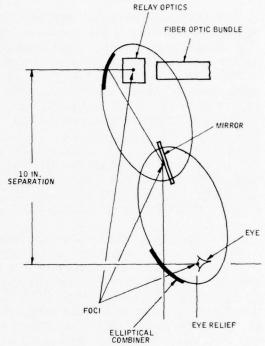
- Large optics and difficult mounting problem
- Difficult optical design
- Long relay lens focal length

The symmetrical elliptical combiner approach was considered as shown in Figure 22, but was rejected due to the large 10.4-in. separation between the elliptical combiner and elliptical mirror.

Schmidt Corrector-Spherical Combiner -- The Schmidt corrector-spherical combiner design concept is not feasible for a 20-deg field of view HMD because of its small F number. The Schmidt corrector-spherical combiner design concept has the well known advantage of well corrected imagery. This approach only has merit for small fields of view, however, since the F number of the optics becomes very low for wider field-of-view systems. The general application of the Schmidt system is to correct collimated light for spherical aberration and to form a real image at the focal length of a spherical mirror.

However, the modification for an HMD application requires the formation of a real image before reflection off the spherical mirror/combiner. This introduces two additional sets of optics (see Figure 23), one to project collimated light from the FOB into the corrector element and another to form a real image at the focal length of the combiner. The combiner then projects collimated imagery toward the eye.

Figure 22. Symmetrical Elliptical Combiner



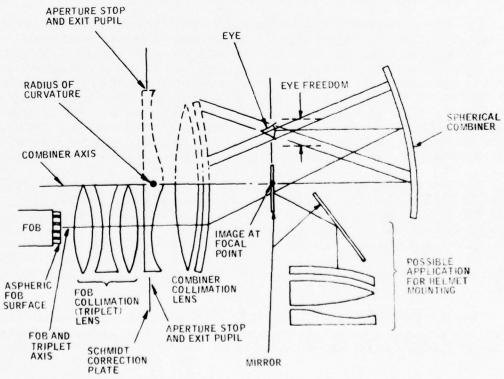


Figure 23. Schmidt Corrector - Spherical HMD

Figure 23 shows the optical elements required for the modified Schmidt approach to correct for the aberrations created by a spherical combiner. The Schmidt corrector field lens is designed to compensate for the large amount of aberration produced when a spherical mirror is used at a low F number with large field angles. This corrector, which is also the aperture stop and exit pupil, must be located at the center of cirvature of the combiner in order to preserve the concentric character of the spherical surface and correct for spherical aberrations. The remaining aberrations can be corrected by other techniques.

A decentered aspheric field lens can correct for residual asymmetrical astigmatism; the CRT sweep raster generator can correct for distortion; and the aspheric FOB can correct for asymmetrical field curvature. The combiner collimation lens is designed to correct for the remaining aberrations.

To assist in understanding this design, Figure 23 shows not only the approximate arrangement of the refractive optics mounted on a helmet, but also the optical components laid out in a straight line (less mirrors) along the axis of the mirror. The refractive optics consist of two groups. The first, an "off-axis" triplet, projects collimated light into the second, an "on-axis" combiner collimation optic assembly which includes the aspheric corrector plate. The term "off-axis" for the triplet refers to location of the triplet axis off the axis of the spherical combiner.

The axis of the combiner collimation optics is located on the axis of the spherical combiner (Figure 23) and, therefore, it is referred to as "on-axis" even though only one half is used. The axis of the combiner collimation lens lies on the axis of the spherical mirror and forms a real image at the focal point of the spherical/combiner. The purpose of the shift in axes is to project the collimated light from the triplet through the decentered combiner collimation optics, hence to the spherical visor and into the eye. Since only one half of the combiner collimation otpics will be illuminated with collimated light from the triplet, the other half of the visor collimation is not needed (see dotted portion of optics Figure 23) and is omitted in the actual design.

The two sets of optics act as a relay lens with the Schmidt Corrector Plate in the middle of the assembly in the area of collimated light. The FOB is in the focal plane of the triplet, and therefore collimated light is projected through the corrector plate into the second set of optics. Since collimated light is received by the visor collimation otpics, a real image is formed at its focal length. This real image is also positioned at the focal length of the spherical visor; consequently, collimated light is projected back toward the eye.

The aperture stop of the system is located at the radius of curvature of the spherical combiner and is located in the corrector plate. Its image, which is the exit pupil, is located directly on the opposite side of the combiner axis.

Therefore, the eye should also be located in the same area to minimize the requirement for exit pupil, aperture stop, and clear aperture of the combiner collimation lens. This increases the F number of the system and reduces the design difficulty for the optical system. However, for a wide field of view and helmet installation, the eye must be placed forward of the optimum exit pupil to allow mirrors to be placed in the desired optical angle away from the eye and out of the working field of view. This forces a nonoptimum eye location.

The optical layout shown in Figure 23 shows the F number of the large corrector plate and combiner collimation lens to be approximately 0.5 since the focal length (one half radius of curvature) is approximately one half of the aperture stop. Not only will the refractive optics be quite large and difficult to mount, but the F number of the system is at the theoretical limit. Therefore, this design approach was rejected.

#### Advantages

- Well-corrected imagery
- Minimal off-axis aberrations
- Basic design approach has been proven
- Ease of spherical combiner fabrication

#### Disadvantages

- Small F number
- Difficulty of mounting large optics on helmet
- Fabrication of aspheric field lens and fiber optic faceplate

Tilted Spherical and Parabolic Combiner HMD -- The tilted spherical and parabolic combiner design concepts have asymmetric astagmatism which will result in poor image quality and resolution. The basic problem of the tilted spherical or parabolic combiner design is asymmetrical astigmatism caused by a single reflection from a curved surface which is difficult to compensate. The problem is aggravated by the requirement that the stop and its image both lie near the center of curvature or focus in order to obtain unity magnification (Figure 24).

For an eye relief of 2 in., the radius of curvature of the spherical visor is also 2 in. Therefore, the single spherical combiner approach is undesirable on two counts. First, the 2-in. radius of curvature increases the asymmetrical astigmatism. Second, the use of a single spherical reflective surface prevents reduction of the asymmetrical astigmatism through the symmetry of two reflections.

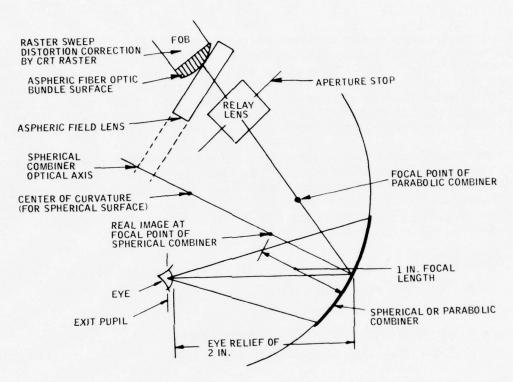


Figure 24. Tilted Spherical Combiner

With this concept, the best approach to the correction of asymmetrical aberrations is the use of an aspheric multi-element field lens centered and normal to the combiner axis (Figure 24). Consequently, the field lens must have a low optical power to ensure a reasonable F number. Therefore, its primary function will be similar to the Schmidt corrector plate described previously.

The relay lens which forms a real image at the focal length of the combiner provides correction for symmetrical aberrations and field curvature. Asymmetrical field curvature is corrected by the aspheric FOB surface, and distortion is corrected by the raster sweep generator circuits (Figure 24).

Evaluation of the design concept for system F number, relay focal length, FOB image and object distances, and variation of the image and optic distance of the stop in its image was not completed. The probability of correcting for asymmetrical astigmatism, while retaining adequate image quality and resolution, is low. The decision to discontinue the evaluation was reinforced by the difficulty of mounting the relay-lens on the helmet. Figure 25 shows a design iteration for one possible location of the relay optics for the parabolic visor approach.

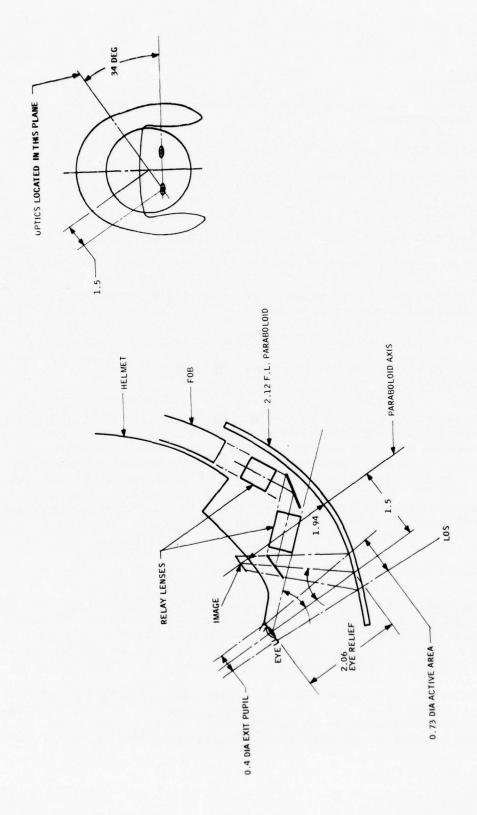


Figure 25. 10-Deg FOV, Nonsymmetrical Parabolic Vision, 2.12 in. ft-L

## Advantages

- Ease of spherical combiner fabrication (spherical combiner approach)
- Relatively large F number of relay optics
- Small diameter optics at radius

# Disadvantages

- Aspheric field lens and fiber optic bundle faceplate
- Poor image quality and resolution
- Asymmetrical astigmatism caused by single combiner with short radius of curvature
- Difficult problem of mounting large relay optics on helmet
- Difficulty of parabolic combiner fabrication (parabolic combiner approach)

This design concept review showed that the symmetrical optical path onto a parabolic visor offers the most likelihood of success. In this approach, the image is reflected from the parabolic surface twice, once immediately in front of the eye (parabolic combiner) and the second time at a point on the other side of the parabolic surface (parabolic mirror) and equidistant from the focal point. By reflecting twice from the shaped surface, the effect of coma is removed by cancellation. Astigmatism is minimized by locating the collimation lens and the eye in the focal planes.

## Video Display Design Iterations

The next phase of the design concept study was to determine the location and spacing of the parabolic visor and other optical components. Sketches of these design layouts were required before the optical computer designs could proceed. These designs were performed on an iterative basis, with each change in the optical approach causing changes in the physical layout.

These layouts were oriented along the plane containing the optical axes of the optical components. This portion of the optical design was relatively complex and time consuming since the optical parameters were traded off against mechanical constraints for helmet mounting. The parameters varied

and the factors optimized are shown in the following listing. Optimization was facilitated by first-order ray tracing between the various elements as indicated:

# Parameter to Vary

- Distance between visor optical axis and observer line of sight
- Angle between vertical plane containing the line of sight (LOS) and the plane containing the LOS and optical axis of the visor
- Location and alignment of FOB
- Mirror locations, separations, and angles
- Optical elements locations and dimensions
- Angle of vision obscuration by mirrors
- Location of real image and extreme optical rays between optical components
- Locations of exit pupil and aperture stop (entrance pupil)
- Sections of helmet required to be removed
- Active areas and focal length of paraboloid
- Cross sectional of plane containing the observer line of sight and visor axis
- Front view showing outline eye location and optical element location

#### To Optimize the Following

- Field of view
   20 deg as design goal
- Exit pupil 0.4 in (10 mm) design goal
- Forehead clearance 0.25 in. minimum
- Upward vision 40 deg without obscuration
- Visor mounting
   Clearance for collimation optics,
   FOB, and mirrors between visor and helmet

- Inclination angle of optical axis
- > 30 deg for minimum interference with visor tracks
- Optics mounting
- Optical components must be mounted between visor and helmet shell with minimum removal of helmet shell
- Visor retraction
- Components below brim of helmet must retract with visor

# By Ray Tracing Between the Following

- Center of eye rotation
- Curved mirror

• Eye pupil

- Aperture stop

Combiner

- FOB
- Central mirror
- Focal surfaces

The difficulty inherent in these design iterations results from the complex interaction between the many variables and the large number of factors to be optimized. The three-dimensional aspects of the problem were visualized through the use of head models and actual helmets together with mock-ups of optical elements. A feeling for the trend of an iteration or series of iterations was a valuable asset to the design engineers, but even then the effort was time consuming. Any effort to take short cuts would have lead to excessive use of expensive computerized optical designs which would have proved useless because the mechanical constraints would not have been properly established.

A total of 25 design iterations was required to produce a suitable design for the prototype model. These design iterations were divided into four phases. The first phase was to select the basic approach to the symmetrical parabolic display. The second and third phases of the design iterations of the design iterations (summarized in Tables VI and VII) started with a narrow 10 deg field of view, then a 15 deg field of view, and ended with a 20 deg field of view.

In the beginning it was not fully appreciated that the double-bounce parabolic approach would be self correcting and would cancel aberrations. Therefore, initially only narrow fields of view were attempted. When it became evident that a simple triplet lens only would be required for the collimation optics, efforts were directed towards obtaining the full 20 deg field of view. However, all of the first three phases were carried out with preliminary ray tracing techniques which indicated that three central mirrors could be used, which allows closer visor fit to the helmet.

Once a reasonable component layout was obtained at the conclusion of phase three, the optical design constraints were established for the subsequent programming of automatic optical design routines. The optical programming at the Honeywell Radiation Center consisted of the large-scale CDC-6600 central processor with an in-house terminal facility. The software consisted of ACCOS automatic design program, GOALS optical evaluation program, and WOE wave optics modulation transfer function. The HRC facility included plotting routines for lens shape, image shape, and evaluation data plus the mechanical design programs of STARDYD and EASE.

After the automatic design programming had established the optical design parameters, the optical evaluation routines were programmed to determine optical performance data. Several iterations between the automatic design and performance evaluation programs were required. When the final optical design was completed, it became evident (from rigorous rays trace drawings) that the three central mirror design was not feasible. Therefore, the fourth phase (Table VIII) was devoted to obtain a 20 deg field of view with a single central mirror. However, at the conclusion of this effort another computer run was made to obtain the full 0.4-in. exit pupil. To obtain this exit pupil the entrance pupil had to be moved out beyond the last vertex of the collimation lens assembly. The earlier runs located the principal plane near the next-to-last vertex of the collimation lens assembly.

## Analysis of Design Layout Iterations --

Selection of the Basic Approach to the Symmetrical Parabolic Design -- The first phase of the design layout iterations established the basic approach to the symmetrical parabolic design. Figures 26 and 27 show two attempts to solve the difficult problem of mounting the mirror which reflects the light rays from the FOB at the top of the helmet down into the pilot's vision.

The primary design problem of the parabolic visor display is that the paraboloid and its focal plane should be as close to the helmet as possible to minimize the envelope of the display. Some of the design iterations place the focal plane within the observer's forehead or very close to it. Therefore, this introduces the problem of mounting the central mirror, which must be located in the parabolic focal plane as required by the symmetrical parabolic design.

This problem can be solved by using three central mirrors as shown in Figure 26; however, Figure 27 shows another approach with one central mirror. It can be seen in Figure 27 that translating the upper mirror portion of the paraboloid moves the focal plane of the paraboloid away from the forehead. Therefore, only one central mirror is needed rather than three. However, this approach was rejected due to the difficulty of fabricating a split paraboloid.

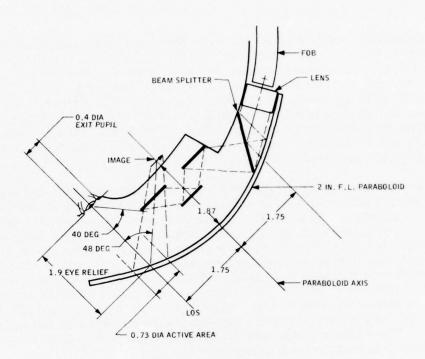


Figure 26. 10-Deg FOV, Beam Splitter and Three Central Mirror Display Design

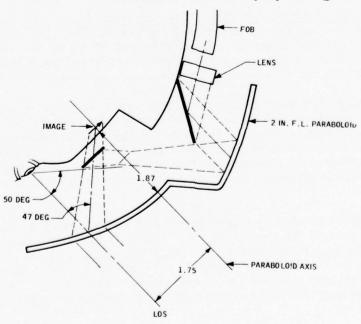


Figure 27. 10-Deg FOV, Split Visor and Single Central Mirror Display Design

The approach in Figure 26 also solves the problem of reflecting light from the FOB to the parabolic mirror with a beamsplitter next to the collimation lens. Although this approach does allow only one mirror to be used by the combiner, it does reduce the brightness of the display and thereby this approach was rejected. This phase of the design concept study concluded with the decision to follow the three-central and two-folding mirror approach shown in Figures 28 through 40.

Design Layouts for 10 Deg Field of View (Table VI) -- The second phase of the design iteration for the design concept study is summarized in Table VI for the layouts shown in Figures 28 through 33. This effort was devoted primarily to developing a 10-deg field of view with a 0.4-in. diameter exit pupil. The first two designs in Figures 28 and 29 were for use with a 0.25-in. diameter FOB. This was a fused bundle with small, 7-micron fibers to obtain the desired resolution. However, after several contacts with American Optical, the FOB vendor, it was determined that the percentage of blemishes would be too high with a 12-in. fused FOB. Therefore, the 0.25-in. fused FOB design approach was rejected, and the flexible 0.5-in. FOB was used.

During this phase of the design iteration it was assumed that the diameter of the collimation triplet would be approximately equal to the required exit pupil, i.e., the double reflective parabolic visor acts as a relay element with unity magnification. Therefore, the exit pupil which is the image of the entrance pupil has approximately the same dimensions as the aperture stop. It should also be noted that the 0.5-in. FOB requires a relatively long focal length for the narrow 10-deg field of view and presents a severe mounting problem. The first design with the 0.5-in. FOB (Figure 30) was rejected since the forehead clearance was 0.5 in., greater than the required 0.25 in. This results in a rather large eye relief of 2.34 in. and an unnecessary increase in the helmet envelope.

Figure 31 shows a variation of the same design as Figure 30, except that the visor is moved closer to the forehead. However, this design lacks the clearance to fit the folding mirror (next to the FOB) under the visor.

Two other design iterations were tried for the 10-deg field of view and are shown in Figures 32 and 33. The first design uitlized a 2 in. focal length paraboloid and had satisfactory upward vision and forehead clearance, but a problem still exists in fitting the folding mirror between the visor and the helmet. The second design approach in Figure 33 used a much shorter focal point paraboloid of 1.5 in. Again this design does not allow the folding mirror and bundle to be fitted between the visor and helmet. However, this design uses only one central mirror instead of three and reduces the difficulty of retracting the central mirrors. This design also has a good upward vision clearance of 56 deg. However, the included angle between the incident and reflective ray off the visor combiner (in front of the eye) is 54 deg where in previous designs the included angle is between 48 and 36 deg. Consequently, the 1.5-in. focal length paraboloid approach was rejected on the basis of high

Table VI. Early Design Concept Review Approaches (10 deg FOV)

The state of the s

	e l							
Three, Central Mirrors	Figure	28	29	30	31	32	33	
	Comments	Ease of mounting collimation lens with short focal length and small diameter FOB	Same as Figure 28 except visor moved out 0.31 in.	Forehead clearance larger than needed	Close fit between visor and first collimation lens mirror	Close fit between visor and first collimation mirror	Only one central mirror required	Collimation mirror cannot be fitted under visor
	Eye Relief	2.06	2.34	2.34	2.06	6.1	1.96	
	Forehead Clearance (in.)	0.4	0, 5	0.45	0.38	0.35	0.5	
	Incline Angle (deg)	34	34	34	34	45	1	
	Forehead to Apex	1, 94	2.25	2.25	1.94	1.87	2.1	
	LOS to Axis	1, 5	1.5	1,5	1.5	1.75	1.5	
	Visor Focal Length (in.)	2.25	2.25	2.25	2.25	2.0	1.5	
	Clear Vision (deg)	40	40	40	40	40	99	
	FOB Diameter (in.)	0.25	0.25	0.5	0.5	0.5	0,5	

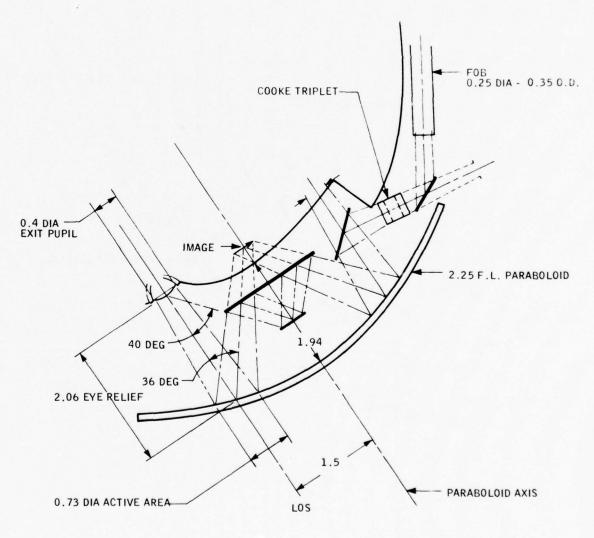


Figure 28. 10-Deg FOV, with 0.25 in. Diameter FOB Display Design

A CONTRACTOR OF THE PARTY OF TH

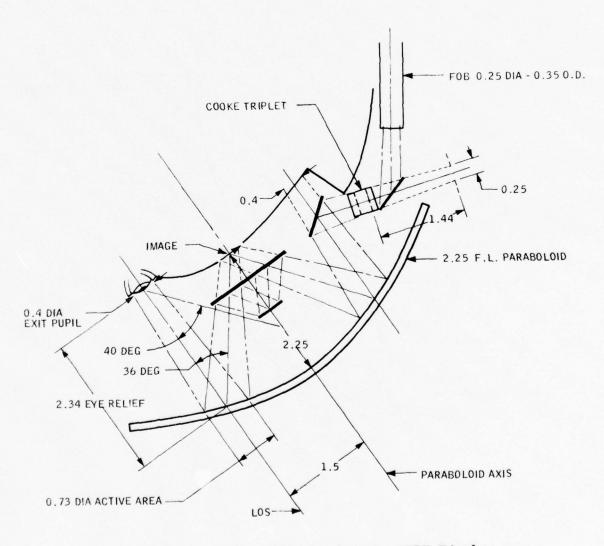


Figure 29. 10-Deg FOV with 0.25 in. FOB Display Design

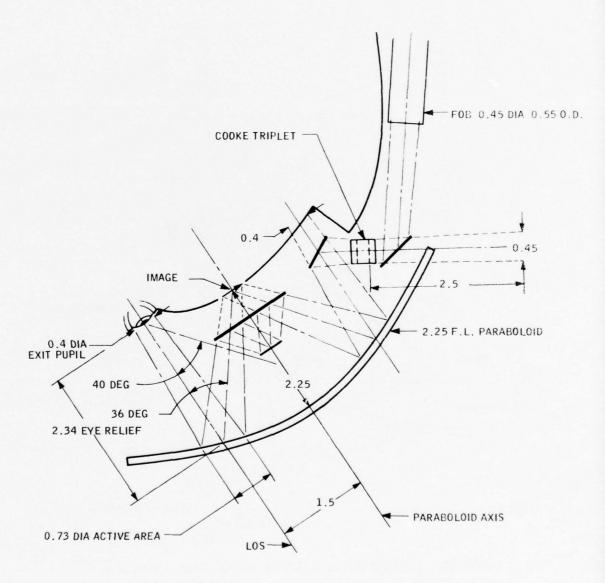


Figure 30. 10-Deg FOV, 2.25 in. F.L. Display Design

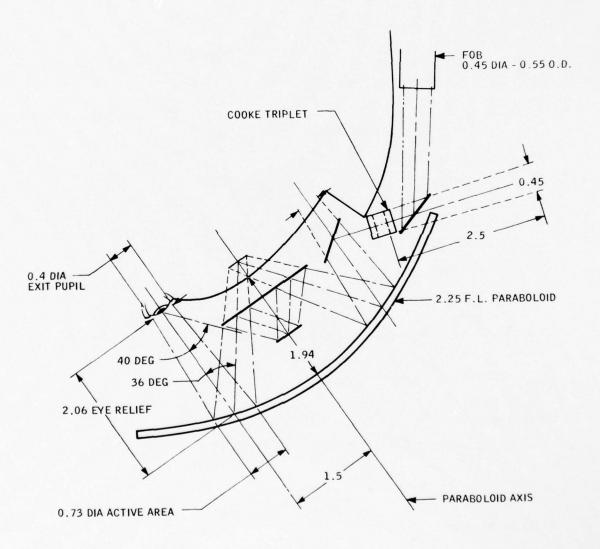


Figure 31. 10-Deg FOV, 2.25 in. F.L. Display Design

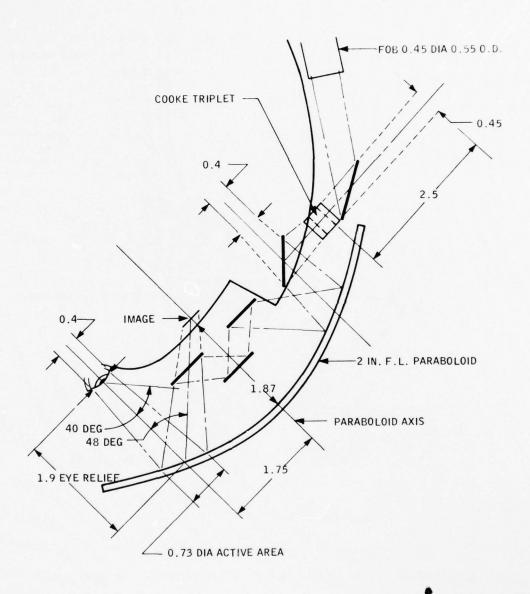


Figure 32. 10-Deg FOV, 2 in. F.L. Display Design

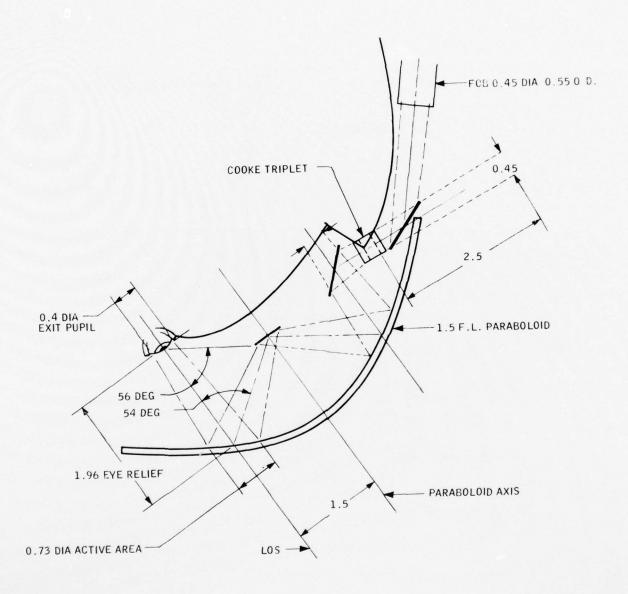


Figure 33. 10-Deg FOV, 1.5 in. F.L. Display Design

aberrations generated by the large incidence angle and the close fit for optical components. It was believed that a wider field of view could be obtained from the experience of these design iterations, since it was learned at this time that the double bounce parabolic approach did cancel aberrations.

Design Layouts with 15 deg and 20 deg Fields of View -- The third phase of the design iterations (Table VII) for the design concept studies increased the field of view to 20 deg as required by the design program. The first design shown in Figure 34 was acceptable and met all the design requirements, but other iterations were made to increase the forehead clearance. However, the second approach shown in Figure 35 had too large a forehead clearance and unnecessarily increased the helmet envelope and eye relief. This design used a long focal length paraboloid of 2.25 in. and had a restricted upward vision of 30 deg. The next design iteration (Figure 36) used a shorter focal length paraboloid of 2 in. and had an acceptable eye relief and upward vision. However, this design may have a difficult problem for mounting the collimation folding mirror. Another problem of the design shown in Figure 36 is that too much of the helmet would have to be removed to mount the folding mirror which is located on the optical path between the collimation lens and parabolic mirror.

The next four designs were concerned with obtaining a full 20-deg field of view and 0.4 in. pupil. It should be noted that the focal length of the collimation lens for the last four designs (Figures 37 through 40) was shorter, with the wider 20-deg field of view which minimizes the FOB mounting problem. The first design approach (Figure 37) had a limited upward vision of 33 deg, which indicated that a longer focal length paraboloid or a larger separation distance between the optical axes and the eye line or sight could be used. However, the next design iteration (Figure 38), with a longer parabolic focal length but a reduced separation distance of 1.5 in., reduced the upward vision from 33 deg to 27 deg, which was considered unacceptable. This design also had an inclination angle of 34 deg, which was also considered to be objectionable at that time.

The next design iteration (Figure 39) utilized the 2.25-in. focal length paraboloid and separation distance of 1.5 in., but with the visor mounted further out from the helmet. However, this was a design iteration in the wrong direction since the upward vision angle was reduced from 27 deg to 22 deg. On the other hand, there was adequate room for mounting the FOB and folding mirrors. Finally, Figure 40 shows a relatively good design with an upward vision clearance of 32 deg, with a 2.25-in. focal length paraboloid and a 1.75-in. separation.

The end result of these series of design iterations was that it became apparent that the original upward vision goal of 40-deg could not be met and that a 32-deg upward vision clearance was necessary. However, the design shown in Figure 40 had a forehead clearance which was somewhat longer than necessary, and either a shorter focal length paraboloid could be used or the visor could be moved closer to the head.

Table VII. Design Concept Study Approaches (15 deg and 20 deg FOV)

_											-				
	Figure	34	35		36	37		38			39			40	
Three Central Mirrors and 0, 5-in. FOB	Comments	Acceptable design	Forehead clearance larger than necessary. Move visor closer to forehead.	Clear visor angle too small	May have tight fit between visor and collimation mirror	Reduced clear vision	Try longer FL or separation	Reduced clear vision	Low incline angle	Increase separation distance	Visor out too far	Reduced clear vision	Low incline angle	Reduced clear vision	Longer forehead clearance than necessary. Try 2.0-in. FL.
	Forehead Clearance (in.)	0.25	9.0		0.3	0.35		0.33			0.65			9.0	
	Incline Angle (deg)	34	34		45	45		34			34			45	
	Forehead to Apex	1.94	2.25		1.87	1.87		1,94			2,25			2.25	
	LOS to Axis	1.5	1.5		1.75	1.75		1.5			1.5			1,75	
	Visor Focal Length (in.)	2.25	2.25		2.0	2.0		2.25			2.25			2,25	
	Clear Vision (deg)	40	30		40	33		27			22			32	
	FOV (deg)	15	15		15	20		20			20			20	
	Eye Relief	2.06	2.3		1.84	1.84		2.06			2.3			2.3	

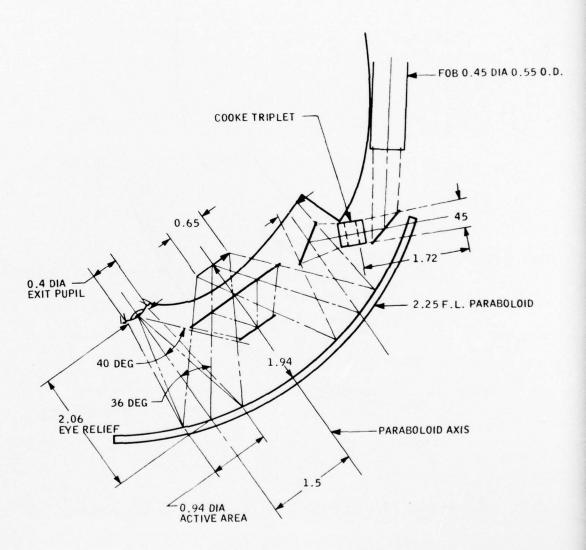


Figure 34. 15-Deg FOV, 2.25 in. F.L. Display Design

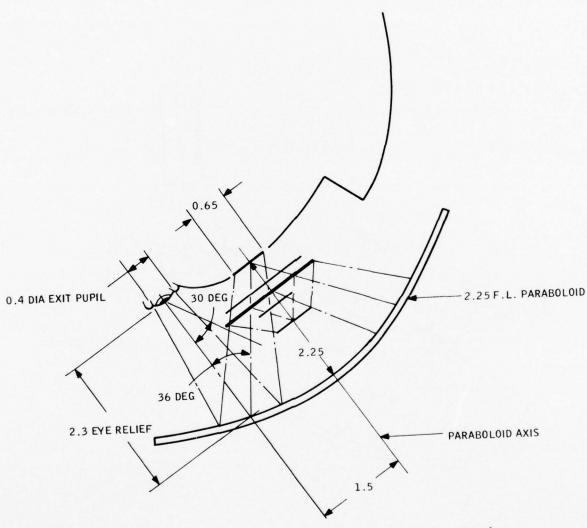


Figure 35. 15-Deg FOV, 2.25 in. F.L. Display Design

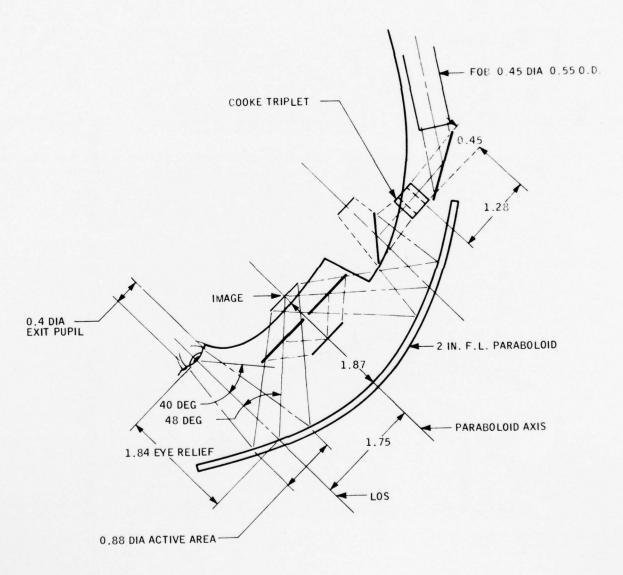
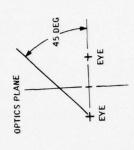


Figure 36. 15-Deg FOV, 2.0 in. F.L. Display Design



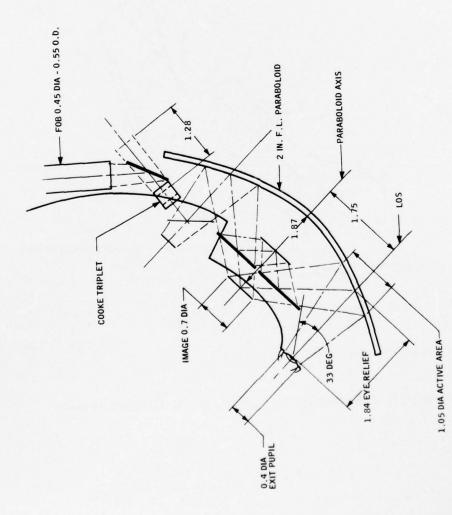
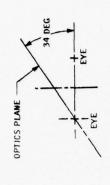


Figure 37. 20-Deg FOV, 2.0 in. F.L. Display Design



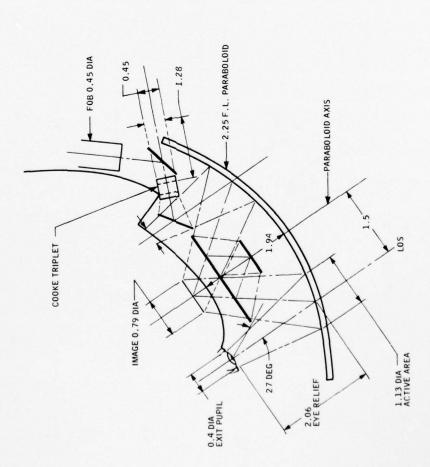


Figure 38. 20-Deg FOV, 2.25 in. F. L. Display Design

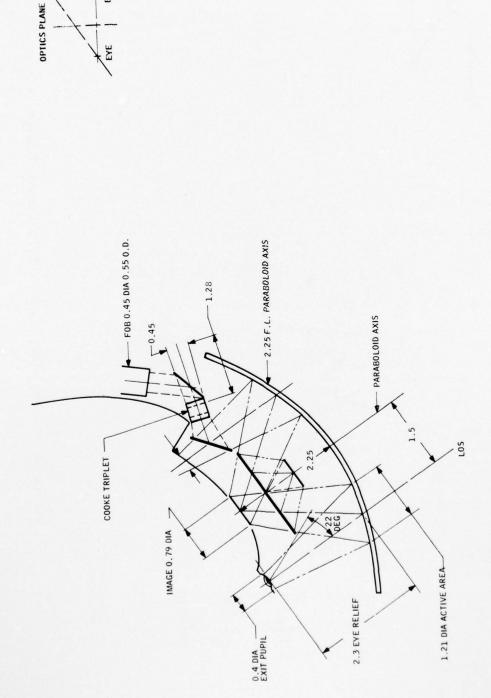


Figure 39. 20-Deg FOV, 2.25 in. F.L. Display Design

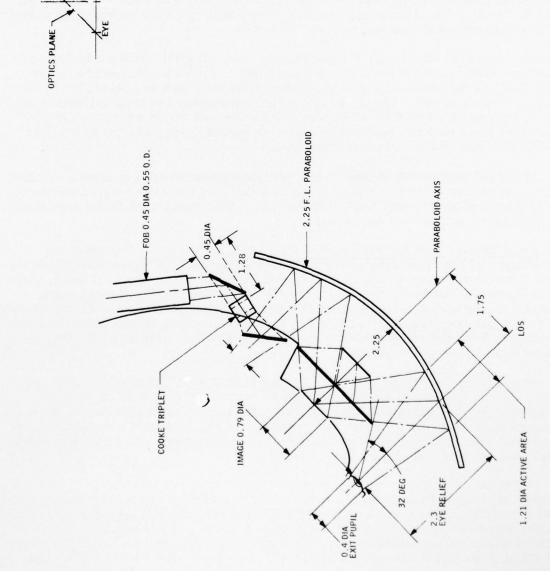


Figure 40. 20-Deg FOV, 2.25 in. F.L. Display Design

First Optical Computer Designs -- At this point in the design concept study several computer runs were conducted. The first run was made with a 2-in. focal length paraboloid, 1.75-in. separation, and a 25-deg field of view. The second computer run was made with a 2.25-in. focal length paraboloid, and 1.75-in. separation but with a 20-deg field of view. These computer runs showed through rigorous ray tracing that the three central mirror approach could not be used. Parabolic distortion was also present which reduced the exit pupil from 0.4 to 0.3 in. Consequently, another computer run was made with six elements to increase (at Contract Monitor's request) the exit pupil from 0.3 to 0.6 in. However, six elements could not be conveniently mounted under the visor, and this design was rejected.

At the same time another preliminary computer run was made for the spherical visor case with a 2-in. focal length. This run was made in the event that the double-reflection parabolic approach was not feasible. This computer run showed a large amount of astigmatism, but that uniform and optical correction would be possible. However, as the work progressed it became evident that the parabolic approach would be satisfactory, and the spherical visor design was not continued.

The final and fourth phase of the design concept study consisted of six designs based on rigorous ray tracing and the correct relationship between the aperture stop and exit pupil dimensions. The results of these six trials are discussed in the next subsection.

Final Design and Layouts for 20-deg Field of View -- The primary importance of the first optical computer designs was the discovery of parabolic distortion shown in the design layout in Figure 41. For example, rays A and B, which form 10-deg angles above and below the horizontal axes, form 11.5-deg and 8.5-deg angles (Figure 44) with a horizontal as they enter the exit pupil area (rays A' and B'). This produces an image distortion or curvature along the plane which contains the observer line of sight and the optical axis of the paraboloid.

Not only is the image distorted by the double reflection of the parabolic visor, but the exit pupil (image formed by the entrance pupil) is skewed. Consequently, the exit pupil is smaller, and the entrance pupil and collimation optics must be larger than originally planned. All of the earlier design layouts showed that the collimation optics diameter would be approximately equal to the exit pupil, i.e., 0.4 in.

It should be noted from Figure 42 that the image of points 1, 2, and 3 in the entrance pupil is formed at points 1', 2', and 3' along a line which makes an angle of 38 deg with the horizontal. Therefore, the exit pupil volume is skewed whose cross section has a shape of a tilted parallelogram. The vertical distance between two parallel rays at the top and the bottom of this exit pupil area has a dimension of 0.3 in. However, the vertical distance between 1' and 3' is 0.4 in., which would be equal to the height of the exit pupil if the exit pupil area were not skewed; i.e., if 3' was directly under 1'.

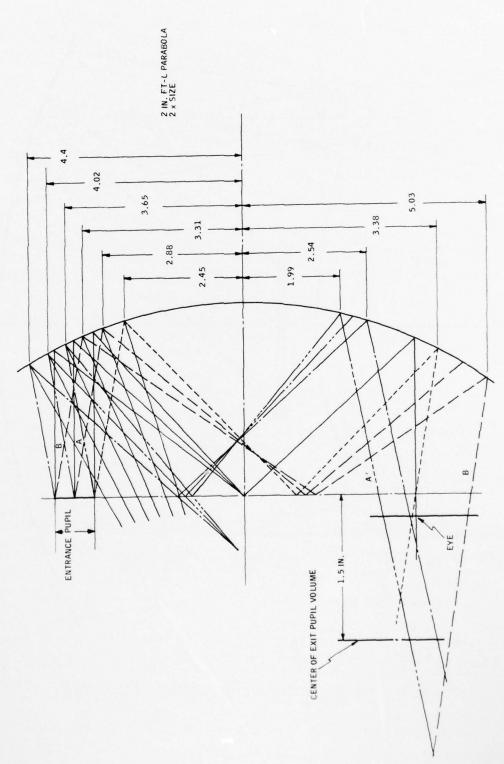
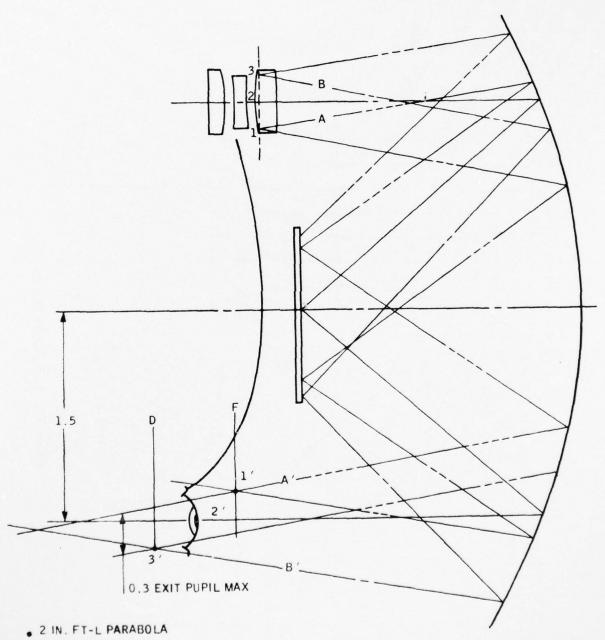


Figure 41. Parabolic Distortion



. 2 x SIZE SCALE

Figure 42. Parabolic Distortion and Skewed Exit Pupil

One advantage, however, of the skewed exit pupil is that the exit pupil has a vertical height of 0.3 in. over the entire area between the vertical planes D and E (Figure 42). If the exit pupil volume were not skewed, then the exit pupil would decrease immediately on either side of its maximum dimension.

To correct for the image distortion created by the double reflecting parabolic visor combiner, it is necessary to distort the ray trace passing through the entrance pupil as shown in Figure 43. This corrective ray trace was generated by initiating an undistorted ray trace at the eye. It can be seen if rays A and B leave the exit pupil at a 10-deg angle with a horizontal; these rays then will form 11-deg and 9-deg angles with a horizontal at the top of the paraboloid as they enter the entrance pupil. This distortion correction can be provided by introducing a parabolic distortion in the horizontal and vertical sweeps of the CRT electronics. It should also be noted that the image of points 1 through 5 in the exit pupil are imaged along a curved slanted line (points 1' through 5').

It was decided that the most optimum location for the entrance pupil would be approximately at the center of the line formed by 1' through 5' (Figure 43) at the top of the parabolic ray trace. The eye location relative to the forehead shown in Figures 41, 42, and 43 was determined by a survey of a number of subjects at Honeywell which showed the average distance of eye pupil behind the forehead to be 0.5 in. A clearance of 0.25 in. is required between the central mirror and the forehead; consequently, the total distance then between the focal plane of the parabolic visor and the eye pupil is approximately 0.75 in. This is the relationship which is shown in Figures 42 and 43.

Consequently, the primary design objective of the layouts shown in Figures 44 through 50 and summarized in Table VIII is to determine the location and size of the entrance pupil required for a 0.4-in. exit pupil. Another design consideration is that a folding mirror must be mounted in the optical path between the parabolic mirror and the entrance pupil to allow a satisfactory mounting for the FOB.

The first design iteration (Figure 44) shows why the three central mirror concept is not feasible. These mirrors could not be mounted without blocking some of the rays. The design iteration shown in Figure 42 was one of the early attempts to relate the exit pupil and entrance pupil. It can be seen that not only is the exit pupil skewed but also that the center of the exit pupil is approximately 1.5 in. behind the parabolic focal plane rather than the desired 0.75 in. (Figure 41).

The ray traces in the next design iteration shown in Figure 45 are drawn such that the image of the exit pupil is formed at the top of the visor where the collimation aperture stop must be located. However, this design iteration was incorrect because the eye was only set back 0.5 in. rather than 0.75 in.

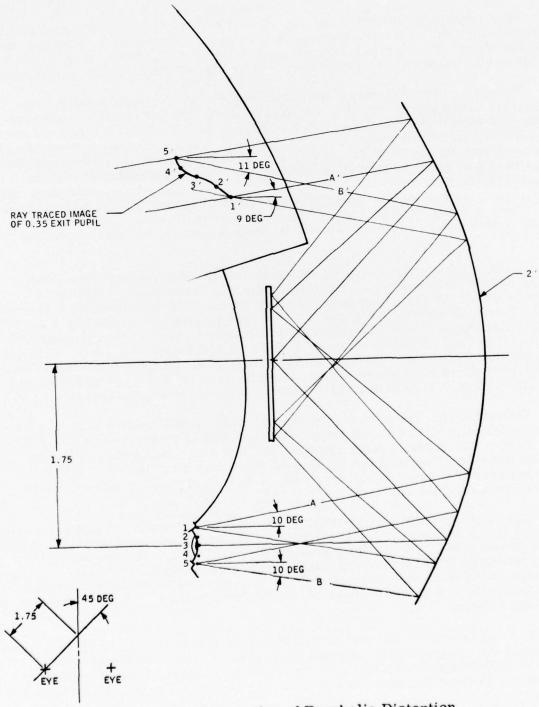


Figure 43. Correction of Parabolic Distortion

Table VIII. Final Design Approaches (20 deg FOV)

Eye Relief Entranc Pupil		Visor Focal Length (in.)	Separation of LOS to Axis	Incline Angle (deg)	Comments	Figure
		2.0	1.75	Three central mirror concept not possible  Exit pupil should be 0.75 in, behind focal plane rather than 1.5 in.  Skewed exit pupil  Parabolic distortion		
2.12		2.0	1.75	45	Exit pupil needs to be 0.75 in. behind focal plane rather than 0.5 in.	45
2.36	0.5	2.0	1.75	45	Folding mirror can be fitted	46
2.06	0.55	1.75	1.75		Folding mirror can be fitted	47
2.46	0.52	2,00	1.50	33.5	Folding mirror can be fitted	48
2.76	0.47	2,25	1.50	34	May not be able to fit folding mirror	49
1.88	0.56	1,5	1.50		Not enough room for FOB and folding mirror	50

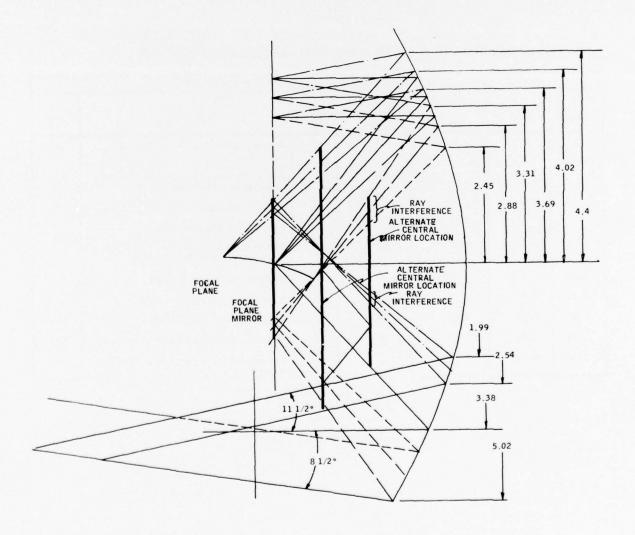


Figure 44. Parabolic Distortion and Ray Interference with Multiple Central Mirror Design

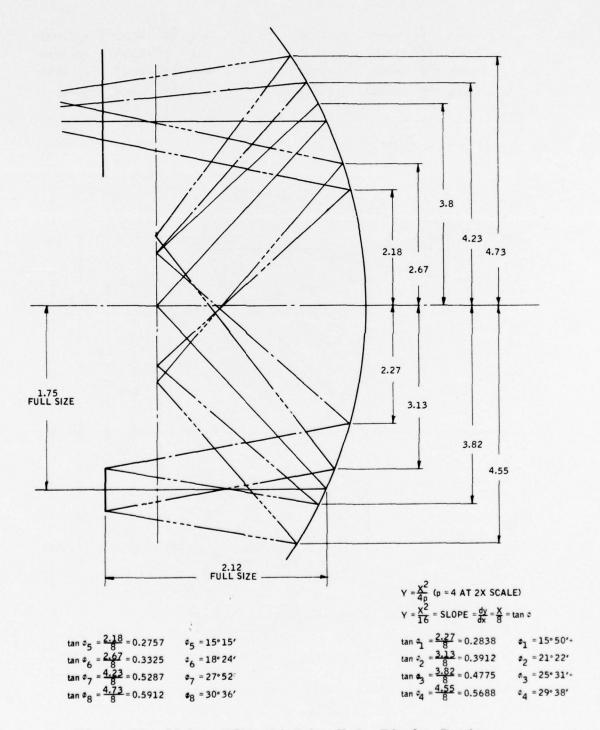


Figure 45. 20 Deg FOV with 2 in. F. L. Display Design

	$\tan \phi_5 = \frac{2.22}{8} = 0.2775$	ø <sub>5</sub> = 15° 30′	$\tan \phi_1 = \frac{2.20}{8} = 0.2750$	\$1 = 15° 23'
	$\tan \frac{x}{6} = \frac{2.80}{8} = 0.3500$	¢6 = 19°18′	$\tan \phi_2 = \frac{3.06}{8} = 0.3825$	¢2 = 20°56'
	$\tan \frac{3.72}{8} = 0.4650$	φ <sub>7</sub> = 29°57′	$\tan \varphi_3 \approx \frac{3.72}{8} = 0.4650$	\$3 = 24°57'
	$\tan \alpha_{\rm B} = \frac{4.67}{8} = 0.5838$	ø <sub>8</sub> = 30°17′	$\tan \phi_4 \approx \frac{4.66}{8} = 0.5825$	\$4 = 30° 13'

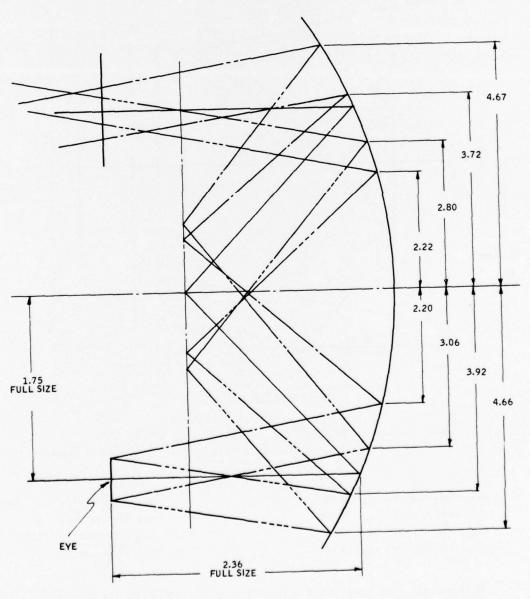


Figure 46. 20-Deg FOV with 2 in. F.L. Display Design

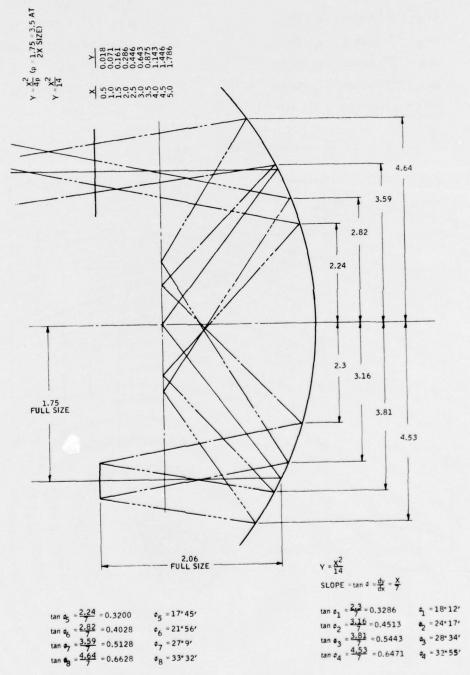


Figure 47. 20 Deg FOV with 1.75 in. F.L. Parabola Display Design

$$\tan c = \frac{x}{8} = m_1$$

$$\tan c = \frac{x}{8} = m_1$$

$$\tan c = \frac{x}{8} = 0.20625 \quad c_1 = 11^{\circ} 39'$$

$$\tan c = \frac{2.4}{8} = 0.3000 \quad c_6 = 16^{\circ} 42'$$

$$\tan c = \frac{2.49}{8} = 0.31125 \quad c_2 = 17^{\circ} 17'$$

$$\tan c = \frac{3.10}{8} = 0.3875 \quad c_7 = 21^{\circ} 11'$$

$$\tan c = \frac{3.44}{8} = 0.4250 \quad c_3 = 23^{\circ} 2'$$

$$\tan c = \frac{4.02}{8} = 0.5025 \quad c_8 = 26^{\circ} 41'$$

$$\tan c = \frac{4.17}{8} = 0.52125 \quad c_4 = 27^{\circ} 32'$$

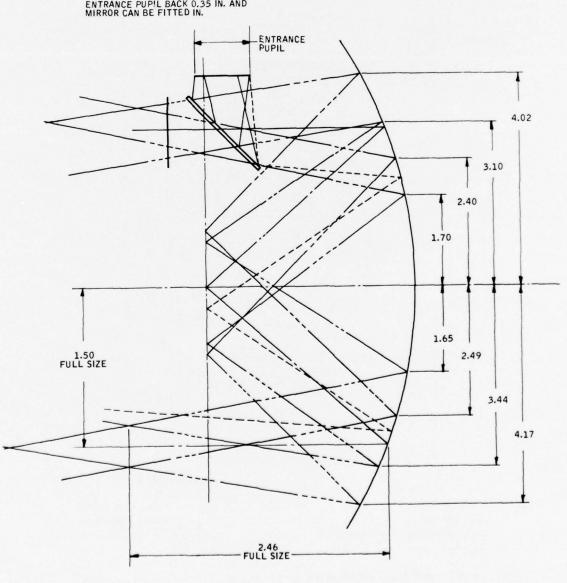


Figure 48. 20 Deg FOV with F. L. Display Design

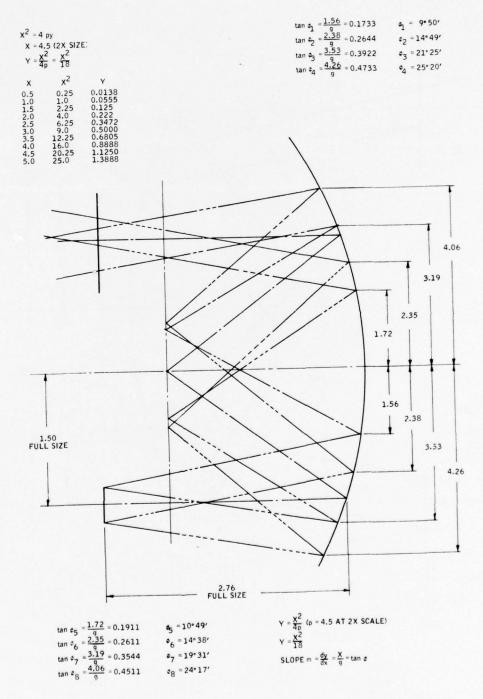


Figure 49. 20 Deg FOV with 2.25 in. F.L. Display Design

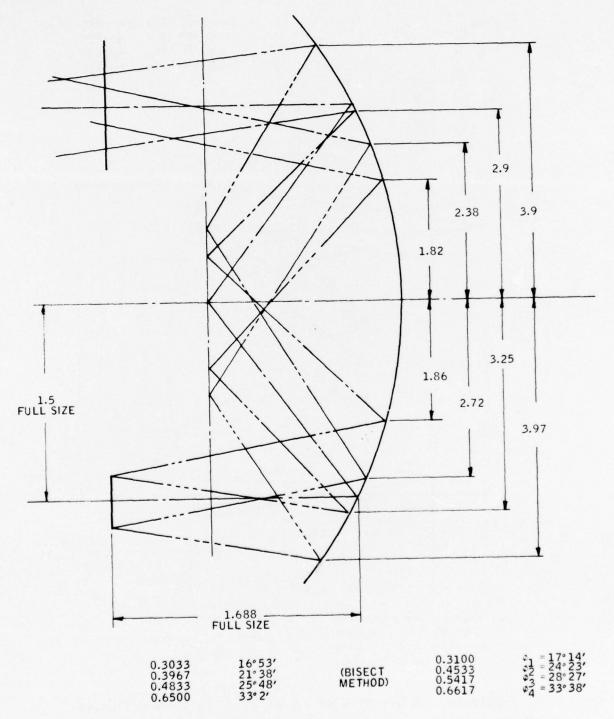


Figure 50. 20 Deg FOV with 1.5 in. F.L. Display Design

The layouts shown in Figures 46, 47, and 48 all provide adequate space for mounting the folding mirror. The layout shown in Figure 47 used a 1.75-in. focal length paraboloid. This approach was rejected primarily on the basis of not having the tooling to make the paraboloid. However, tooling existed for the 2.0-in. focal length paraboloids for the layouts shown in Figures 46 and 48. The layout shown in Figure 48 utilized a 1.5-in. separation between the optical axes and the paraboloid, and this design was selected for the final design on the basis of existing tooling and smaller separation to reduce parabolic distortion.

The layout shown in Figure 49 was rejected since the folding mirror interferes with the extreme ray trace on top of the paraboloid. The layout shown in Figure 50 was rejected since the short focal length of 1.5 in. would not allow enough room for mounting the FOB onto the visor. Also, both designs required new tooling.

Final Optical Design Computer Runs -- Figure 51 shows the helmet layout of the 1.5-in. separation with 2-in. focal length parabolic case shown in Figure 48. The first computer design for the 1.5-in. separation and 2.0-in. focal length positioned the first lens element too close to the upper ray trace at the top of the paraboloid. The principal plane or aperture stop was placed within the first lens element as shown in Figure 51. This arrangement allowed only a 0.3-in. exit pupil.

This problem was solved by moving the principal plane in front of the first surface of the first element of the collimation lens assembly (see Figure 52). This allows the lens to be moved further away from the upper ray trace and allowed the full 0.4-in. exit pupil. This helmet layout (Figure 52) shows that a 0.6-in. diameter entrance pupil is required to form a 0.4-in. exit pupil image which was used for the final optical computer design for the video display.

## HOLOGRAPHIC PROJECTION TECHNIQUE

The holographic projection technique was examined as part of the Phase I design concept study, and the results are summarized in Honeywell Document 14327-TR4, November 1970. This study was continued as part of the Phase II design concept review at the Honeywell Corporate Research Center. The results of this study are contained in a memorandum included in Appendix 1H. The objectives of the study were to develop holographic phototechnology and investigate suitable alternate materials for encoding hololenses. The effort concluded with the fabrication of two hololenses from 649-F photographic film and dichromated gelatin.

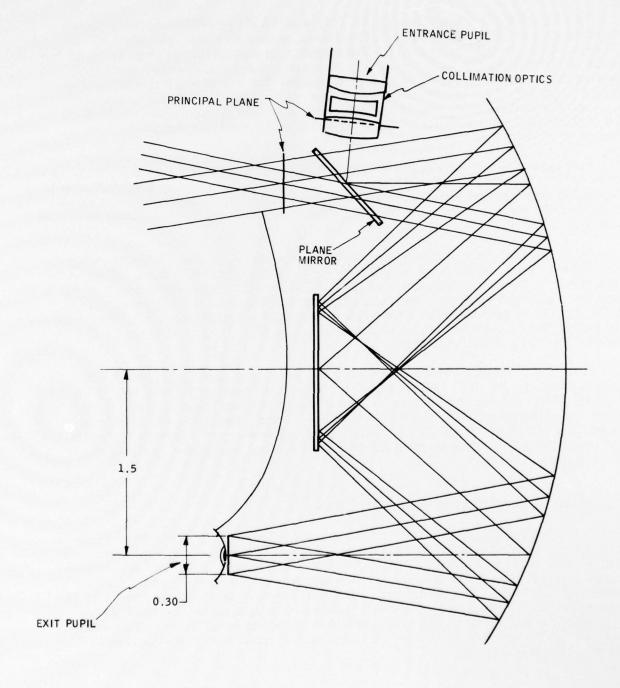


Figure 51. First Computer Design with Principal Plane Inside Collimator Lens Assembly

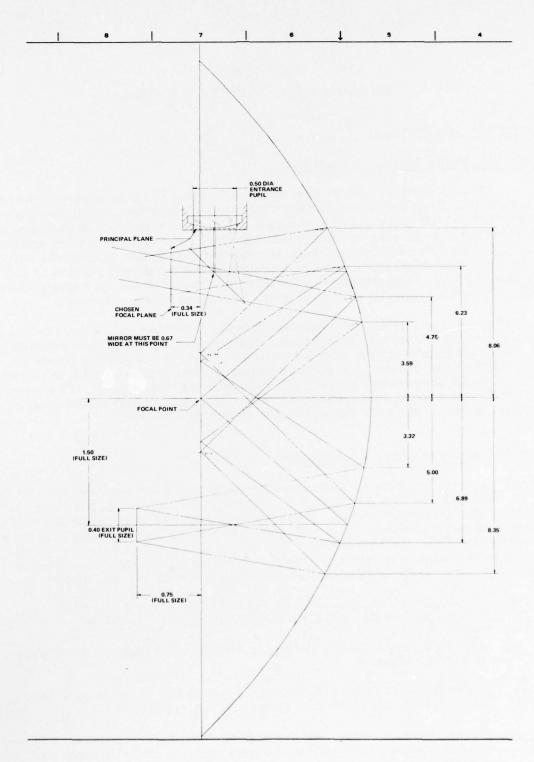


Figure 52. Second Computer Design with Principal Plane Outside Collimation Lens Assembly

## SECTION IV BREADBOARDS AND BRASSBOARDS

### RETICLE GENERATOR

## Spherical Visor Reticle Breadboard

Figure 53 shows a photograph of the spherical visor breadboard which consists of a filament transformer, reticle, reticle lamp, cylindrical singlet prism, and spherical mirror. A noncircular reticle pattern is mounted at an angle to the optical axis of the system as shown in a drawing in Figure 54. The light from the illuminated reticle passes through the cylindrical prism and off the spherical mirror which duplicates the combiner portion of the spherical visor. The purpose of the aperture mask shown in Figure 53 is to limit the eye location to ensure proper correction of aberrations.

The basic problem of the spherical visor technique is the correction of chromatic and spherical aberrations. Spherical abberation is corrected by the tilted plane and curved surface prism. However, a doublet prism is required to fully correct for chromatic aberration, and a red filter had to be used with the breadboard (Figure 53) to obtain sharp imagery. The spherical approach was rejected as a candidate since it requires refractive optics (doublet prism), whereas the parabolic approach does not.

### Reticle Parabolic Visor Breadboard

Objectives -- The primary objectives of the parabolic visor breadboard were (1) to establish the feasibility of this reticle projection technique, and (2) to optimize the prototype design. Design feasibility was decided on the basis of image quality, resolution, and collimated imagery, and the reticle generator was optimized for uniform illumination of the exit pupil and reticle pattern. To accomplish these objectives, the following requirements were placed on the design of the reticle breadboard shown in Figures 55, 56, and 57.

- Allow paraboloids to be mounted with focal lengths of from 1.5 in. to 2.5 in. and diameters of from 4 in. to 10 in.
- Allow alignment of the parabolic section axis to the optical axis
  of the breadboard.
- Allow adjustment of the included angle at the paraboloid between the incident and reflected light from the reticle.
- Allow adjustment and interchange of condenser lenses and tungsten lamps to obtain uniform illumination of the exit pupil and reticle.

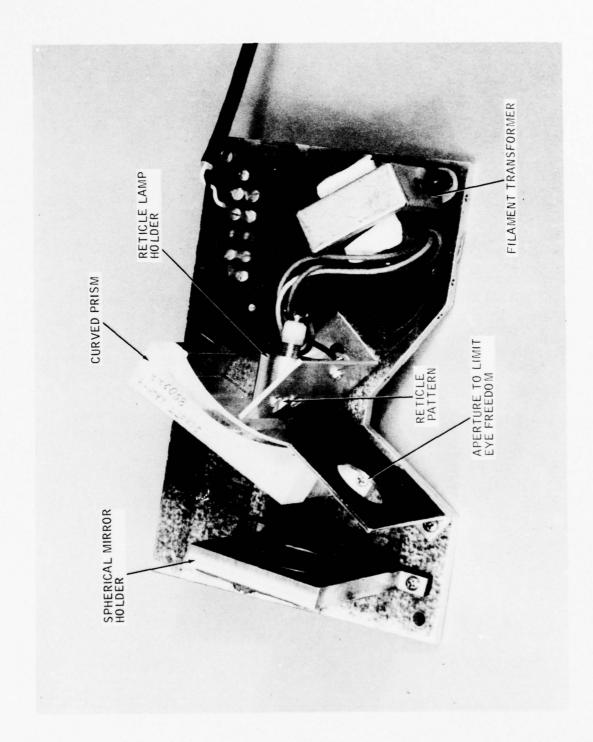


Figure 53. Spherical Visor Breadboard

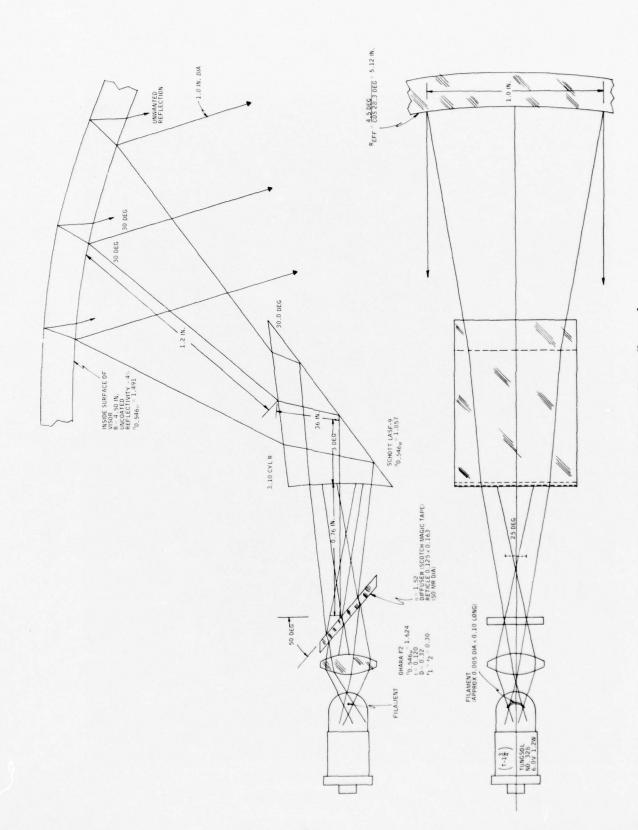


Figure 54. Spherical Visor Breadboard

THE PROPERTY OF THE PARTY OF TH

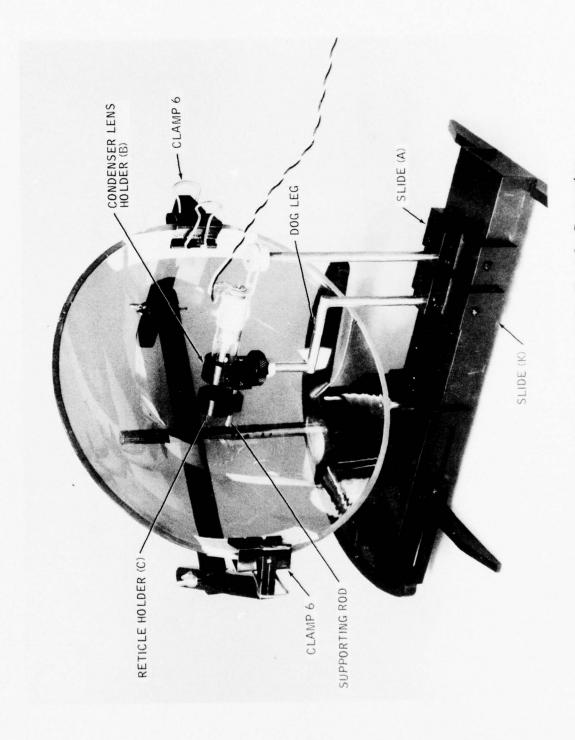


Figure 55. Breadboard of Parabolic Reticle Generator

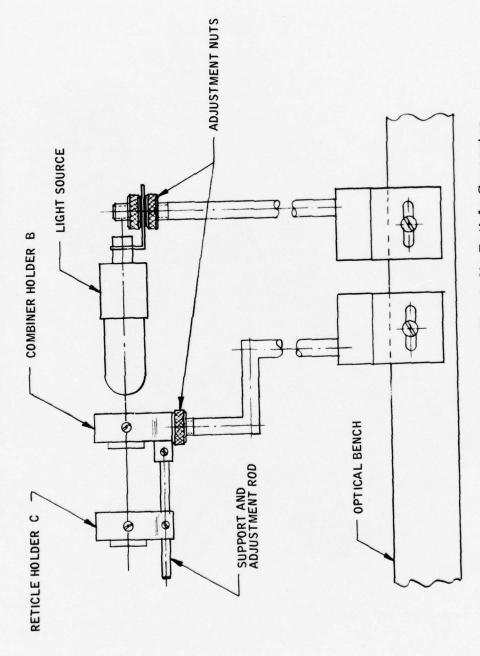


Figure 56. Breadboard of Parabolic Reticle Generator

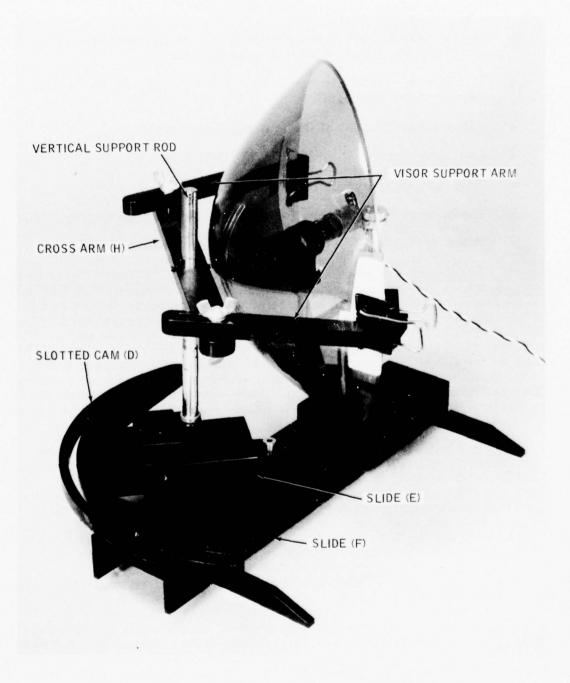


Figure 57. Breadboard of Parabolic Reticle Generator

- Allow focus adjustment of the condenser lenses to project the filament image on the reticle pattern.
- Allow collimation adjustment (with boresight telescope) of reticle at the focal point of the paraboloid.
- Position the reticle to be perpendicular to central ray to the center of the exit pupil.
- Allow measurement of the exit pupil diameter.
- Evaluate uniform illumination of the exit pupil.
- Evaluate uniform illumination of reticle.
- Evaluate reticle imagery for distortion and image quality.
- Allow evaluation of surface finish quality of paraboloid.

Reticle Breadboard Tungsten Lamps, Power Supply, Diffuser Ghost Image Suppression -- The reticle breadboard is shown in Figures 58 and 59 with the standard GE 1874 tungsten lamp used during the early phases of the AHRA program. Figure 60 presents a comparison of the standard 1874 lamp with the various lamps designed by Honeywell. The final design (used in the prototype model) was a lens end version which has the same filament dimensions as the GE 1874 lamp, but consumes less power. The lens end design of the lamp allows the filament to be positioned much closer to the condenser lens system than with the 1874 lamp. This allows a large entrance angle to the condenser system and provides the large exit pupil required by the AHRA program.

The original design for reticle generator incorporated a low-loss randomized FOB to diffuse the image of the filament on the reticle and allow remote location of the large GE 1874 lamp at the back of the helmet. How-ever, the FOB received from the manufacturer did not have the required degree of random fiber arrangement, and this approach was not used. Instead, the lens end lamp design was used with reduced dimensions which allowed the lamp to be mounted under the visor. The lens end lamp design also provided some diffusion of the filament image.

Figure 61 shows a photograph of a variable tungsten lamp power supply for experimentation of image brightness versus power consumption.

Figure 62 shows a coated square piece of plastic supplied by Optical Coating Laboratories, Inc., for the demonstration of ghost image suppression generated by the parabolic visor. This plastic substrate has a high efficiency antireflective coating of between 0.5% and 0.75%, and the other side has a multilayer dielectric reflective coating of between 30% and 40%. These coatings eliminate ghost imagery when viewed against a 1000 to 2000 ft-L background. The brightness ratio between the primary and secondary image was approximately 150 to 1.

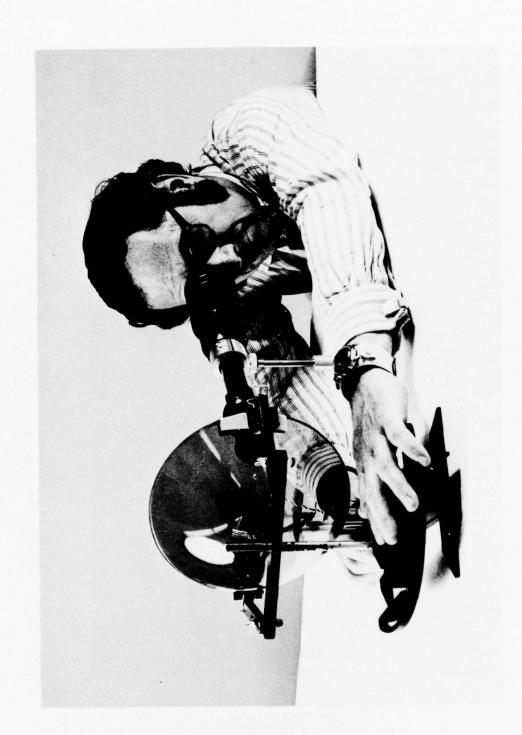


Figure 58. Collimation of Reticle Generator Breadboard

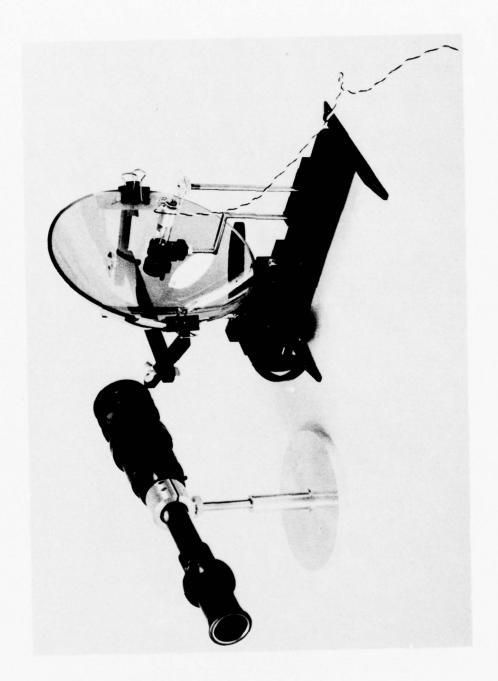


Figure 59. Reduced Aperture of Collimation Telescope

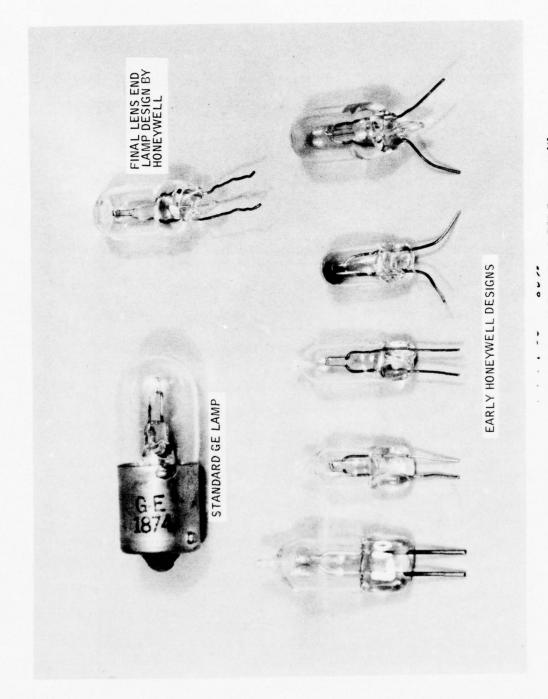


Figure 60. Comparison of Standard GE Lamp with Honeywell Designs



Figure 61. Reticle Breadboard Power Supply

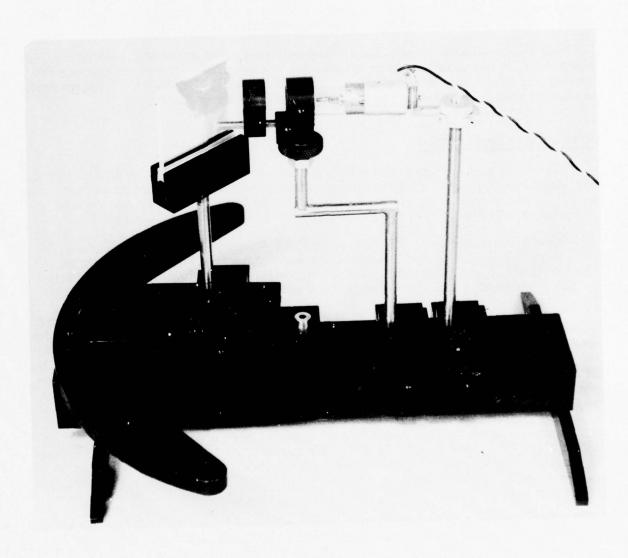


Figure 62. Coated Sample of Plexiglass for Ghost Image Suppression

Evaluation of Reticle Breadboard -- The imagery of the reticle breadboard was evaluated with and without the collimation telescope (4X power, Figure 58). Some waviness and fine line splitting was observed by either moving the collimation telescope or eye across the exit pupil of the paraboloid. Also, the effective focal length increases as the observer views the image toward the outside of the parabolic section which decreases the magnification.

All three effects of waviness, line splitting, and parabolic distortion were considered second-order effects for the purposes of demonstrating the concept of projection of a reticle image with a parabolic visor. Consequently, the breadboard demonstration was considered to be satisfactory.

### Holographic Breadboard

The primary purpose of the holographic breadboard was to determine if the state of the art of hololens development would allow its use used for reticle visor projection. If the hololens would be satisfactory for reticle projection, then it could also be considered for video visor projection.

Two hololenses were fabricated for the AHRA program. First, a 0.8-in.-diameter dichromated gel hololens was fabricated by Naval Weapons Center (NWC), and, secondly, a 0.25-in.-diameter hololens was fabricated by the Honeywell Corporate Research Center (CRC).

The first hololens fabricated by NWC was made from specially hardened gelatin-coated glass squares from Kodak. The dichromated gelatin hololens was constructed at 5145 angstroms with a shear angle of 114 deg and a focal length of 2.7 in. The hologram was not encoded at the angle of bisection, but at an incident angle of 30 deg and a reflection angle of 36 deg. The best reconstruction geometry for sharpest virtual image was found (by NWC) to be at 29 deg incident and 39 deg reflection angle at a focal point of 2.44 in. Unfortunately, the virtual image at infinity has zero horizontal parallax at 2.54 in. and zero vertical parallax at 2.66 in. so the sharpest image is not at infinity. Figures 63 and 64 show the geometry of construction and reconstruction. Figure 65 is a spectrograph plot (NWC) for the hololens and is a measure of how much light is diffracted from the incident beam as a function of wavelength.

The hololens is protected by a cover plate epoxy to the gelatin-covered glass and cut to a 0.8-in. diameter. This sandwich has light rose tint.

Two CRC hololenses were fabricated from bleached 694 spectroscoptic plates, one fixed with isopropanol and one not. The selection of the reversal bleach process for producing phase holograms from Kodak spectroscoptic plates type 649-F was chosen as an alternate to the procedures used at NWC. This is a new technique for producing phase holograms developed by Kodak and eliminates most of the flare light formed with holograms bleached by other

Principle Control of the Principle of th

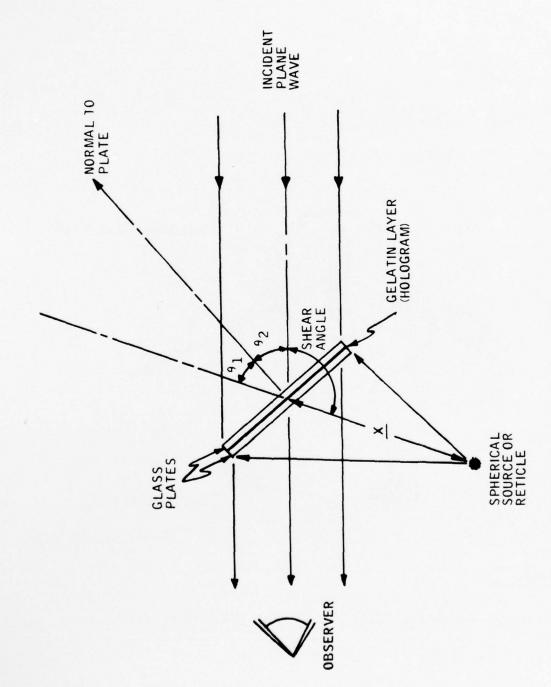


Figure 63. Geometry of Hololens Encoding and Reconstruction

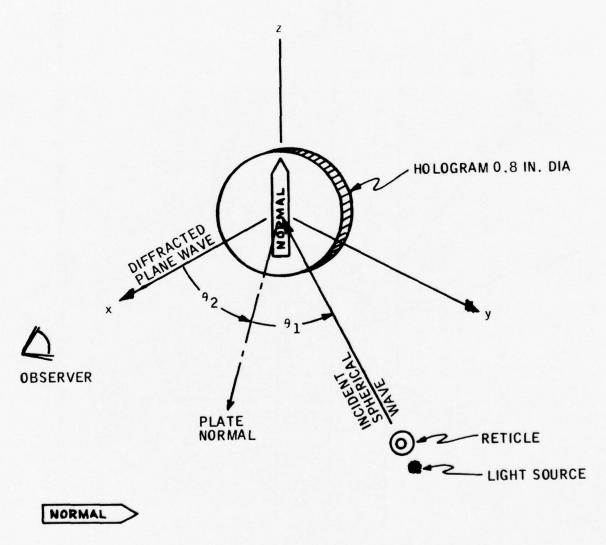


Figure 64. Geometry of Hololens Encoding and Reconstruction

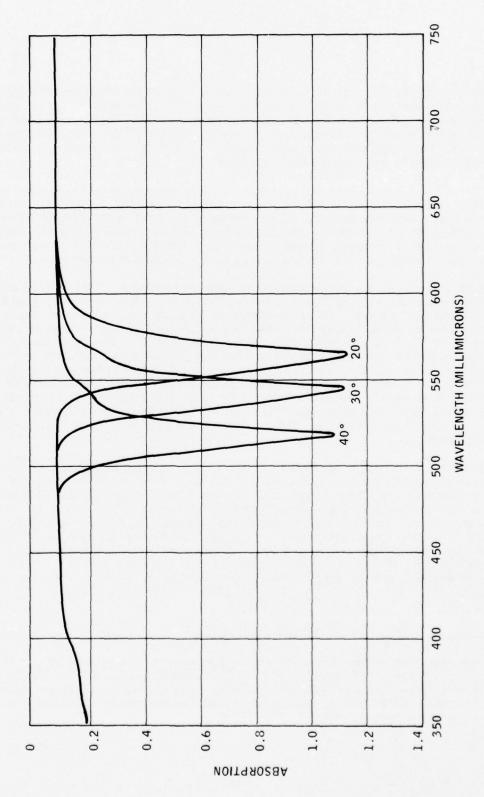


Figure 65. Hololens Spectrograph Plot

processes. It also should be able to produce a virtually transparent phase hololens with a diffraction efficiency as high as 40% and yield a high signal-to-noise ratio. The primary advantage of the reversal bleach technique is the ease by which phase holograms can be made. On the other hand, dichromated gelatin is a very difficult material to work with and there are many difficulties to be overcome to get reproducible results.

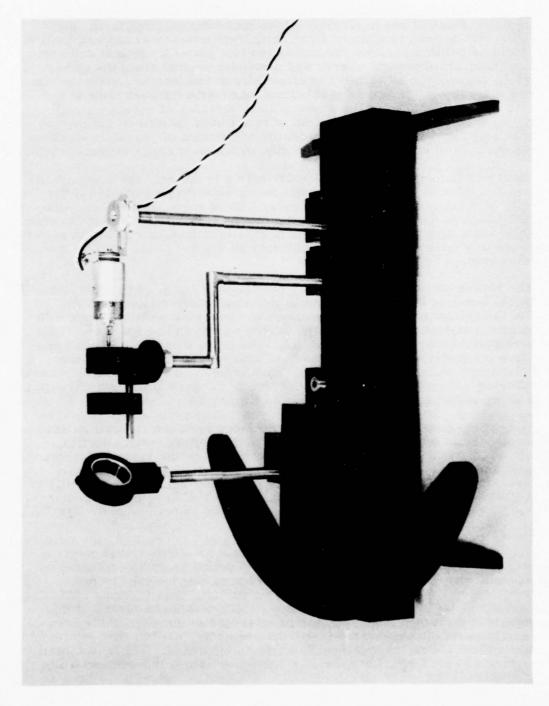
The NWC hololens was set up on the reticle breadboard (Figure 66) with a reticle pattern located at its focal point and its imagery evaluated at various incident and reflection angles. Three types of imagery were identified -- real, reflected, and virtual. The real image and smallest was to the left, the virtual image was largest and to the right, and the reflected image was in the center (illuminated reticle pattern is to the right of the observer).

Both the real and virtual images had several orders. Two orders could be detected for the virtual image while an infinite number of orders could be seen for the real image. The increasing orders for the real image decreased in size and converged to a point to the left of the field of view of the observer. On the other hand, the virtual image orders increased in size and extended to the right of the observer. Therefore, the images became very dim and difficult to see. The direct reflected image had at least two reflected images due to multiple reflections within the hololens sandwich. It was also noted that, when the hololens was rotated counter clockwise (looking down), all three types of imagery were aligned at the extreme left edge of the hololens. However, all three images are spread out across its aperture when the hololens is used properly.

The CRC hololens was evaluated on a separate optical bench but showed the same types of real and reflected and vertical images. Both the NWC and CRC hololenses had fuzzy images and showed a broken line effect. However, the CRC hololenses had the poorest imagery and showed signs of waviness which may be due to the wedge of the glass used for mounting. In addition, the CRC hololens was much noisier than the NWC hololens, probably because it was under developed and techniques for processing the hololens had not yet been perfected. However, neither hololens was satisfactory for use in the AHRA program, and the single reflection parabolic visor approach was selected.

#### PARABOLIC VISOR DISPLAY BREADBOARD

The objective of the parabolic visor display breadboard was to demonstrate the feasibility and image quality of the symmetrical parabolic visor video projection technique. The breadboard includes a resolution test pattern (to simulate the end of the FOB), an off-the-shelf collimation lens, a parabolic plastic section, and a single mirror.



The video display breadboard (Figures 67 and 68) allows the following adjustments: vertical and horizontal alignment of the tungsten lamp, the resolution test pattern (simulated fiber optic bundle imagery) and collimation lens; focus of collimating lens and resolution test pattern; vertical and horizontal adjustment of central mirror and parabolic section along the optical axis of the paraboloid; adjustment to align mirror and lens in a common plane perpendicular to optical axis of paraboloid; separation between mirror and collimation lens to duplicate the interpupillary distance of observer; collimation focus adjustment for paraboloid of real image formed on the mirror by the collimation lens; lateral and vertical adjustment of parabolic section; and adjustments to allow use of paraboloids with a wide range of focal lengths.

Figure 67 includes the CRT and relay optics in the original design; however, this portion of the breadboard was never used (Figure 68) due to the difficulty of obtaining an off-the-shelf relay lens of adequate quality. Also, the CRT image is not necessary to determine the feasibility of the symmetrical parabolic visor approach. Instead, the tungsten lamp and a resolution pattern were used to simulate the real image formed on the end of the FOB by the CRT and relay lens.

The reticle pattern, illuminated by the tungsten lamp, is positioned along the optical bench to be at the focal point of the collimation lens. Infinity focus of the collimation lens is determined by observing a sharp image with a collimation telescope prefocussed at infinity as shown in Figure 69. This was accomplished without the paraboloid. The adjustment for collimation of the entire parabolic visor breadboard is to position the focal point of the parabolic visor on the central mirror. This adjustment is verified by viewing the reflected imagery from the left-hand side of the parabolic visor through a prefocussed collimation telescope shown in Figure 70.

The optical bench was fabricated so the reticle pattern and optical axes of the collimation lens are along the center of the optical bench. Height, lateral, and interpupilary adjustments are provided by the various support rods and threaded blocks shown in Figure 67. The FOB simulator was a standard Air Force line-bar target illuminated by a tungsten lamp and cut to the FOB diameter. This pattern provides not only the field of view requirements, but also allows an estimate of the resolution capability of the system.

Since the symmetrical parabolic approach is self correcting, the requirements on the collimation lens are not severe, and an off-the-shelf camera lens was used. The two folding mirrors in the actual prototype collimation lens assembly were not included in the breadboard since these are not required for demonstration of the concept feasibility. One inherent difficulty in breadboard configuration is that the eye pupil could not be placed at the exit pupil of the system because of the interference of the edge of the parabolic section with the observer's face. Consequently, the full exit pupil could not be obtained; but the system quality could be evaluated. The breadboard did not include correction for parabolic distortion, since this correction is provided by the CRT drive electronics.

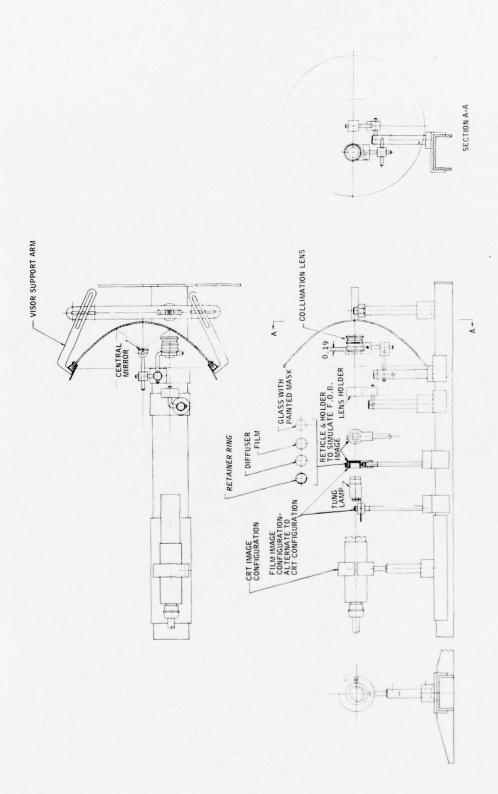


Figure 67. Video Display Breadboard

The state of the s

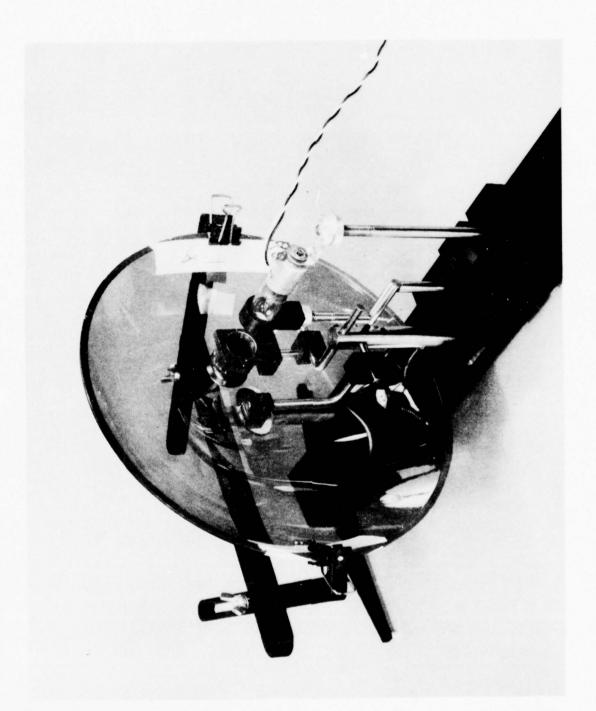


Figure 68. Video Display Breadboard



Figure 69. Video Display Breadboard, Focus of Collimation Lens



Figure 70. Video Display Breadboard, Collimation Adjustment

The first evaluation of the symmetrical approach was with a paraboloid of poor quality with surface waviness. However, the resolution target was positioned such that the image appeared with good resolution; consequently, feasibility of the symmetrical parabolic approach was demonstrated.

### PARABOLIC VISOR DISPLAY BRASSBOARD

One of the important steps in the development of the parabolic visor display was the fabrication of a brassboard which allowed various optical components to be laid out on an inexpensive helmet shell. The following design parameters were verified during component layouts on the brassboard.

- The 12-in. length of the FOB was shown to be correct to convey the CRT real image from the relay lens focal plane to the focal plane of the collimation lens
- Capability of the flexible FOB to follow the curvature of the helmet
- Clearance between the visor and the FOB
- Clearance between the collimation lens assembly and visor
- Clearance between the central mirror and forehead
- Helmet cutouts for mounting the collimation optics
- Alignment of the collimation optics assembly, central mirror, and visor
- Visor track alignment on helmet for ease of visor movement
- Visor cover fit over the visor and mate with visor tracks
- Location of the CRT/relay optics housing at the back of the helmet
- Noninterference between the collimation lens assembly and saddle for the CRT/relay optics housing with the observer's head
- Ease of operation of the central mirror retraction mechanism

Two other important display design problems were discovered during experimentation with the brassboard. First, the use of four mirrors in the optical path between the CRT and the observer's eye reduced the image

brightness dramatically when standard reflective mirror coatings were used. Therefore, highly efficient front-surface reflective coatings were needed to reduce brightness loss. Secondly, the design of the central mirror retraction mechanism (Figure 71) failed to project the pilot from injury in the event the helmet is rotated downward. A second pivot (Figure 72) was added to the design of the mirror retraction mechanism to prevent such an injury.

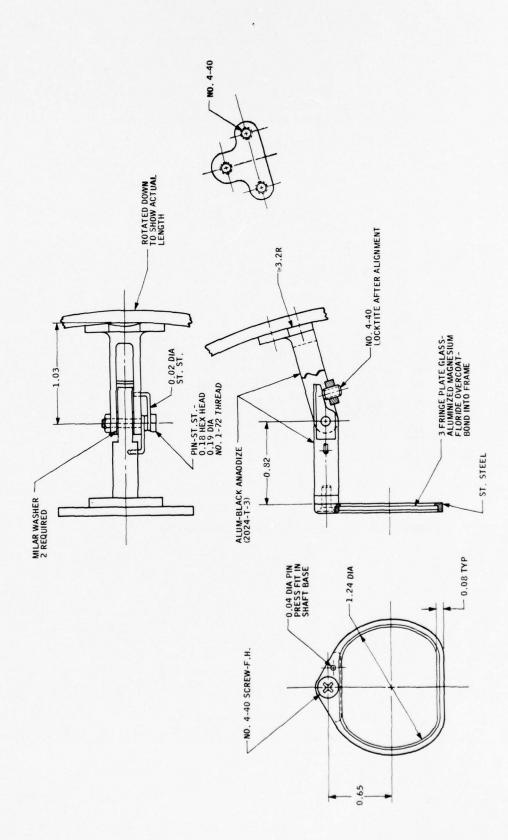


Figure 71. Central Mirror Retracting Mechanism

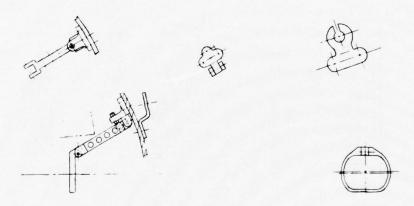


Figure 72. Central Mirror Assembly

# SECTION V PARABOLIC VISOR DEVELOPMENT AND FABRICATION

### DEVELOPMENT

The first evidence of the usefulness of the parabolic visor approach for reticle and video imagery projection was obtained after observing surprisingly good image quality over a 3 deg field of view from a search light quality parabolic mirror without corrective refractive optics. This evidence was reinforced when it was recognized that a double reflection parabolic mirror was self-correcting for larger fields of view and that the eye could be located in the exit pupil. These two relationships permit much smaller refractive optical corrective elements for video projection than with a spherical visor.

Many approaches were investigated for fabrication of paraboloids to take advantage of its inherent advantages. Table IX summarizes techniques for making molds, when required, and Table X lists techniques for forming plastic paraboloids. The techniques that show the greatest promise were compression molding, injection molding, aspheric blade generation, and fine cut and polishing of premolded parabolic blanks. The last technique was selected for the AHRA program on the basis of time and cost for fewer than 10 units. Compression molding becomes feasible for fabrication of more than 10 units and injection molding for fabrication of more than 100 units. However, both compression and injection molding require fabrication of molds with a satisfactory optical finish. Honeywell started the development of a mercury pool spin technique for fabricating molds without the high cost associated with the usual technique of cutting, grinding, and polishing molds. However, this effort was discontinued when a technique could not be developed for vacuum forming paraboloids with adequate optical finish.

Omnitech Corporation claimed that they had a proprietary technique for forming plastic paraboloids without degradation of the surface finish from direct contact with the mold surface. It was assumed that a parabolic glass mirror fabricated by Ferrand Optics (by the aspheric blade technique) could be used to form the male mold and that any residual waviness in the plastic parts either from the mold or in the molding process could be removed by optical polishing techniques. However, a good surface finish was not obtainable and a long-term waviness could not be removed without changing the parabolic shape. Therefore, other techniques to fabricate parabolic sections had to be considered.

The difficulty of fabricating a short focal length paraboloid by the above technique is that the parabolic surface must be tested for its accuracy and surface figure. The usual testing methods are useful for paraboloids with much longer focal lengths. For example, a Ronchi tester can be used to

Table IX. Approaches Considered for Parabolic Mold Fabrication

		Reason for Rejection
Vendor and Date	Technique	or Action
Honeywell Inc., January 1970	Two layers of DC 200 silicone and epoxy 7777-A over a mercury pool spun a constant RPM until epoxy is cured. Mold is electroformed nickle replica.	Irregularities in molded concave surface and limited funds prevented continuation of experimentation.
John Ransom Laboratory July 1970 (Telecon)	Technique was not specified.	Not convinced J.R.L. can fabricate molds to desired quality.
Ferrand Optics and Formost Manufacturing Co.	Quartz mirror to be used to electro form a nickle replica by Formost Manufacturing Co.	Quartz mirror had zone of waviness. Accuracy is suspect since formed by blade technique and reticle image quality not as good as other paraboloids.
American Optical, November 1970	Rough cut and grind male and female injection molds with tape-controlled mill followed by hand polishing	Technique for optical testing was not described. Minimum of 10,000 molded parts required and mold does not belong to customer. Quality of surface finish can not be predicted.

Table X. Approaches Considered for Fabrication of Paraboloids

Vendor and Date	Technique	Reason for Rejection or Action
Honeywell Inc., January 1970	Vacuum formed over male mold	Surface blemishes. Under stress and no correction for see through distortion.
Honeywell Inc., February 1970	Vacuum formed over male mold covered with felt	Could not avoid folds in felt. Under stress and correction not possible
Plastics Inc., September 1970	Vacuum formed over male mold	Surface bubbles, imperfections, under stress and no correction for distortion
Omnitech, October - December 1970	Proprietary technique to form over mold without contact	Some pits, considerable waviness, and no correction for distortion
American Optical, November 1970	Remove undulations from Omnitech Paraboloids	Finished piece is not round and deep undulations may not be removed. No test would be made to check surface; therefore, no guarantee that final surface will be a paraboloid. Prices very high, \$1800
American Optical, November 1970	Mill, grind, and polish from solid piece	Not set up to perform operation
Omnitech, November 1970	Free formed	Thickness uniformity is good, but no control over radius of curvature
Omnitech, November 1970	Injection molding with Poly- carbonate plastic. Recommend that visor be trimmed from large parabolic section to avoid stresses due to non-uniform flow at edges.	Good finish, but no technique or equipment to check for parabolic shape after polishing
American Optical, November 1970	Injection Molding with plexiglass	Very good optical finish with mini- mum stress. Low recurring costs but high mold costs.
Omnitech, December 1970	Use female mold to put undulations on outside of molded visor	Inside is surface of generation, not a paraboloid
American Optical, December 1970	Agreed to consider Ronchi ruling or knife test as means to hand polish rough paraboloids	American Optical never followed up on request to polish paraboloids
Honeywell Inc., January 1971	Fine cut pre-formed parabolic blanks on computer-controlled, high-quality lathe with hydrostatic spindle followed by optical polish.	Limited funds available
Aero Graphics, December 1970 - February 1971	Machine pre-molded parabolic blank on servo tracer lathe with special cutter. Object was to cut to true parabolic and polish without changing shape.	Long period waviness present in polished surface. Concluded to generated paraboloids on servo tracer lathe.
Honeywell Inc., March 1971	As above but used mechanical tracer lather	Not feasible with limited funds of AHRA Program
Hoeger Optical, April 1971	Supply vendor with machined pre- molded paraboloids. Sections to be fine cut on aspheric generation machine (with laser readout) and followed by optical polish.	Some waviness still present, but satisfactory for reticle projection and adequate to demonstrate the concept for video projection
Frank Cooke (Brookfield, Mass), May 1971	Use parabolic templet to rough out glass female blank with thin parabolic male blade. Blade will be shaped to true paraboloid against female blank in parallelogram aspheric generator. Glass female blank will then be replaced by plastic blank and shaped to true paraboloid.	This option never exercised since "Trueness" of paraboloid is a function of mechanical geometry and tolerances of parallelogram aspheric generator. Also, Frank Cooke has never polished plastic before. This technique could be used for mold fabrication.
Hoeger Optical, May 1971	Compression molding of preformed parabolic blanks with long temperature cycle to relieve stresses	High cost of molds and limited time

locate the low or high spots of a long focal length parabolic mirror and it can then be reground and corrected. However, this test requires that the Ronchi tester and eye be located at the focal point of the paraboloid. This is a difficult technique with a paraboloid with a 1.5- to 2.0-in. focal length and requires viewing optics with a Ronchi ruling of approximately 2000 lines/in.

Therefore, a method was found which used an absolute reference for the desired parabolic shape, rather than attempting to polish to an optically tested parabolic shape. Such an absolute reference was the Honeywell Inc. computer-controlled cam cutter which generates a parabolic templet to an accuracy of 50 µin. Parabolic visor sections were then formed by skinning plastic parabolic blanks on a tracer servo lathe with the parabolic cam. The basic assumption for this approach to visor fabrication was that machine tool marks are fine enough that optical polishing to remove them does not significantly change theparabolic shape formed with the parabolic templet. If the period of the fine tool marks is less than 0.05 in., then a flexible optical lap with an effective smoothing of 0.1 to 0.3 in. would remove the fine machine marks (50 µin. peak to peak) without significantly changing the parabolic surface.

Parabolic section fabrication was accomplished in the following steps:

- Cut a male parabolic cam and female surface of generation cam (0.016 in. from the parabolic cam) with an rms surface roughness of less than 50 μin.
- Use male cam to cut a male aluminum paraboloid mold and vacuum form parabolic blanks from plexiglass sheets.
- Anneal parabolic blanks per PC13044-01 while supported in concave mold.
- Cut a female aluminum paraboloid concave tool with female cam
- Cement plexiglass parabolic blanks in the female paraboloid tool
- Insert 0.016-in.-shim between male and female cams to smooth out short term cam surface roughness
- Fabricate precision plexiglass cutter tool with 15-deg rake,
   15-deg primary clearance, and 30-deg secondary clearance
- Chuck up female paraboloid with plastic blank on servo tracer lathe and skin out plastic paraboloid
- Mount female tool and skinned paraboloid on lapping table and polish

The basic problem in developing this technique was that a long-term waviness with a period of 0.25 in. was present in all paraboloids. The shim insert between cams was to eliminate the cam cutter as a source of waviness; the sharp precise cutting tool was to eliminate material flow as possible source, and very light polishing eliminates the lapping table as the source. Therefore, it was concluded that servo hunting of the tracer lathe was the most probable cause.

A mechanical tracer lathe was set up at Honeywell to eliminate servo hunting as the source of waviness. However, this approach was abandoned when Hoeger Optical Company was contracted to fabricate two paraboloids for the AHRA program at a much lower cost. It was pointed out at Hoeger Optical Company that the most probable cause of the long-term waviness was harmonics of the lathe spindle vibration. It was also determined that Hoeger Optical Company had a precision aspheric surface generation machine with better than 10-µin. accuracy and negligible spindle vibration. Therefore, paraboloids were finally formed by Hoeger Optical Company by skinning out and polishing the paraboloids. Although the paraboloids still has some long-term waviness, the image quality was acceptable for the reticle generator and adequate to demonstrate the concept of the double reflection paraboloid.

### RECOMMENDATIONS

The following action items are recommended for improvement of fabrication of the parabolic sections for helmet visors.

- Investigate compression molding, mercury pool, and blade generation techniques for mold fabrication.
- Develop methods for testing short focal length paraboloids for surface finish and accuracy.
- Use casting technique for fabricating pre-formed parabolic blanks rather than vacuum forming. Test for residual stresses with polaroid films.

## SECTION VI VISOR COATING DEVELOPMENT

### RETICLE GENERATOR

### Requirements

One of the key design parameters is the reduction of ghost images reflected off the outside surface of the parabolic visor. These images should have negligible brightness compared to the primary reticle image reflected from the inside surface. For background brightness of approximately 2000 ft-L, it has been determined that a ratio between the primary ghost image should be at least 120:1. To realize this ratio with a 60 to 70 percent transmittance visor, it is necessary to use a dielectric, multilayer, 30 percent reflective coating on the inside surface and a 0.5 percent reflective coating on the outside surface.

Both coatings should be quite durable to show no signs of abrasion with 50 rubs with a cheesecloth. Both the HEA and reflectance coating should be useful at incident angles of from 20 to 40 deg.

The coating should also show no evidence of pitting or corrosion when exposed to an atmosphere of  $120 \pm 4$  deg and from 95 to 100 relative humidity for a period of 24 hr.

### Development of Coating for Reticle Generator

Work performed in 1971 by the Honeywell Thin Film Laboratory (TFL) in support of the AHRA helmet sight project can be divided into three distinct areas of thin film activity:

- Development and evaluation of thin film deposition techniques required to deposit antireflective and beamsplitter coatings (funded by Materials and Process Engineering burden).
- Testing and evaluation of optical films and optical fabrication processes which showed promise for use on helmet sight devices (funded jointly by MPE burden and AHRA project).
- Deposition of optical thin films on helmet sight hardwareperformed on request for specific use by AHRA project (funded by AHRA project).

Table XI summarizes this information in chronological order and according to funding participation.

Deposition of Optical Films on Glass Elements -- The primary use of optical films on glass for helmet sight applications has been for first surface reflectors for mirrors, prisms, and combiner glasses. The primary materials system used for these elements has been Cr/Al/MgF2 deposited by thermal evaporation, sequentially, without breaking vacuum and on substrates heated to approximately 200°C. Resultant films are hard and durable, and exhibit reflectances in the range of 85-90 percent. A total of nine elements were coated for use on the AHRA program for bench, calibration, and acceptance testing of both test and deliverable hardware.

Antireflective (AR) films were not needed on glass.

Deposition of Optical Films on Plexiglas -- The primary use of optical films on plexiglas for helmet sight applications has been for metal filters and dielectric beamsplitters on the inside visor surface, and AR films on the outside surface.

Initially, tests were performed to determine whether an argon-ion glow discharge environment would by itself degrade plexiglas. The end goal was to determine whether ion sputtering could be used to deposit optical films on plexiglas.

Test results showed that an argon ion plasma by itself does not degrade plexiglas, nor does the presence of the presence of the plexiglas degrade or affect the plasma. There were legitimate concerns, however, with heat distortion of the plexiglas in the plasma. While most vendor and literature sources report 85°C (185°F) to be a maximum service temperature, a somewhat lower temperature limit should more reasonably be assumed for applications where the plexiglas constitutes a critical optical element. Using reduced power levels and shielding the plexiglas from direct exposure to the ion plasma, the Thin Film Laboratory was successful in ion sputter depositing metal filters of Cr, Cu, and Ni onto plexiglas without apparent optical distortion. The TFL also successfully sputtered thin films of teflon onto plexiglas for use as an antireflective coating.

In general, ion sputtering was an effective but slow and relatively difficult method of depositing optical thin films on plexiglas.

Electron beam evaporation techniques which rapidly deposited films on plexiglas without raising the substrate temperature were considered to be the best way of fabricating helmet sight visors. Work was then initiated using a Sloan e-gun mounted in a 10-in. oil diffusion-pumped vacuum system. A Sloan quartz crystal rate and thickness monitor was used to control multilayered film thicknesses. A Cary 14 spectrophotometer was used extensively to measure optical properties of the deposited films.

Table XI. M&DE Thin Film Laboratory -- AHRA Participation

September			Organic coating tests tests Ordered new E-beam system
August	cessfully coated with 40% T beamsplate with 40% T beamsplate with and <0.1% R AR film.  Coated visor deflivered to project til livered to project for bench, calibration, and customer acceptance testing	Durability of coated visors examined using cheese cloth and eraser tests. Eleven beamsplitter test depositions and 9 AR test depositions and 9 AR test depositions rates are visor in the coating first area visor.	Tested dip and spray techniques for applying organic contings to plexiglas Appropriations for new E-beam system Developed technique to hot press TiOp pellers for E-beam evaporation
July	Hard-coated 1 combiner glass with Cri All MgF2. Tested solvent resistance of plextglas to H2O, detergent, sisfopropyl alcohol, methyl alcohol, petroleum ether, petroleum ether, laysov cleaning I "visor cleaning I"visor cleaning I"visor cleaning instructions.	Total of 97 depositions made in Maylaly ownerd development of flat dielectric beamsplitters and high-efficiency AP films on plexiglas performed water absorption tests on plexiglas—determined time /temperaluter required for complete dry-out prior to coating Purchased R-830 ascrylic coating material	Tested R-830 acrylic coating as means of improving durability, solvent, and abra-sion resistance of plexiglas ston resistance of plexiglas the solvent of Schmidt lens in belmet sight system.  Submitted capital appropriations for new E-beam system.
June	Hard-coated 2 combiner glasses and 1 front sur- face mirror with Cr/Al/MgF2	Continued develop- ment of AR and beamsplitter films on plexiglas	High-efficiency AR films deposited (< 0.5 R) over 1 Prod 2 Bad Still using bor- rowed E. gun and power supply
May	Coated 3 lenses with Mar'2s for helmet sight test apparatus	Test deposited AR films on ALSI-Co glass, glass, plexiglas and "ABCITE" (17 depositions)	TFL requests additional second final; burden funds for "optical contings" "Anti-fog" and "bottochromic" burden activities started burden activities bear splated over the permitten of flat 4-layer beamsplitter collar reflection—eter attachment for Cary 14 - to frame measure—ment of % A
April	Coated two front surface mirrors with Cr/Al/MgF2	Examined interface and procured sample panels of ABCITE" (hard-coated plexiglas)	Update on S&R needs Evaluated TFL's capabilities Fourteen test depositions made to determine and AR status OCLI-versus- TFL costs and capabilities examined ARHA
March			Tested effort of on piece of pasma on piece; glas- nemo written- lon sputtered Cr. Cu and Ni filters onto plexiglas ion sputtered teffon onto plexi- glas for AR Borrowed two E-guns from SSEC
February			Test deposited 1/4 \ MgF2 AR on glass
Months (1971) Parameter	АНКА	TFL Burden + AHRA	TFL Burden

Dielectric Beamsplitters on Plexiglas -- An in-house cost/technical capabilities analysis of helmet sight optics requirements showed that it was both financially and technically advantageous to utilize in-house thin film facilities. One of the first tasks was to develop a multilayered, dielectric beamsplitter which exhibited the required optical characteristics at approximately 40 percent T over most of the visual wavelength region of 0.4 to 0.7  $\mu$ . A 4-layer  $1/4 \ \lambda \ TiO_2/MgF_2/TiO_2/MgF_2$  system was successfully developed after testing out various material systems and thickness combinations.

Antireflective (AR) Films on Plexiglas -- Because the index of refraction of plexiglas (1.48 to 1.49) is close to that of typical glass substrates (1.47 to 1.51), most of the materials systems used to deposit an AR film on glass are also applicable to plexiglas. The films cannot, of course, be deposited on a hot substrate, and therefore special care must be taken to select a first-layer material which has some intrinsic adhesion to the plexiglas.

Because of the need to eliminate ghosting effects of the projected image, a high-efficiency AR film is required on the outside visor surface. To attain the minimum 120:1 primary/ghost image ratio, an AR film which reduces the outside surface reflection to less than 0.5 percent R is required. This type of film is typically referred to as a "high-efficiency" coating and is always multilayered--a simple, single  $1/4~\lambda$  layer  ${\rm MgF}_2$  film which reduces the reflectivity to 1.25 percent is not adequate.

The AR system which was successfully devised by the Thin Film Laboratory for the AHRA visor application is a 2-layer coating of 1/4 "  $CeF_3/MgF_2$ . This system custs the reflectance of the front surface to less than 0.5 percent over most of the visible  $\lambda$  region.

Coating of the AHRA Visor -- The first AHRA visor was successfully coated with a 40 percent T beam splitter and < 0.5 percent R AR film during July 1971. Uniformity of the visor was excellent (±1 percent T eye-to-eye) and had more than sufficient reflectivity to obtain the required reticle brightness. Absorbtivity of this all-dielectric film system was less than 5 percent. As expected, durability of the films was such that they would pass a tape test-with abrasion resistance limited to acceptance with cheese cloth tests.

A "Visor Cleaning Kit" with associated "Cleaning and Handling Instructions" was also prepared and sent along with the coated visor for subsequent use by Honeywell and AFMRL personnel.

Peripheral Coatings Development Activities -- The development of a helmet sight system which utilizes the visor itself as a critical optical element required that more than typical consideration be given to the thin film coatings on this visor. The visor (or substrate) surface had to first be finished to final optical figure without flaws or internal stresses which might distort a projected or see-through image. Cleaning of this substrate prior to coating was given special attention. Adhesion of the coating would have to be

obtained through the select use of certain first-layer materials. Because of the severe temperature limitations imposed on plexiglas II acrylic as opposed to glass substrates, the usual method of heating the substrates to elevated temperatures during coating could not be used to obtain abrasion resistance and film durability. Uniformity of the film from eye-to-eye and even side-to-side was an important consideration that was solved by placing a crystal sensor for the depositions in the visor knob location (center forehead).

In all, a total of some 117 thin film depositions was made to test out the effects of various parameters and conditions on the end quality of the visor coatings. Examples of a few of the side tests performed are illustrated in the following paragraphs.

# Degradation of Plexiglas in an Ion Plasma-Detailed Previously --

Outside Coatings Vendor Survey -- Some preliminary investigations and inquiries were made to determine what outside vendors could do in the way of coating plexiglas with beamsplitter and AR thin films. Several companies have advertised these types of coatings capabilities, but most would not firmquote the visor coatings unless provided on "best-effort" or "previous development" basis. Uniformity, durability, and abrasion resistance were the unknown factors which clouded their abilities to firm-quote the jobs.

Several companies have "proprietary coatings" for protecting plexiglas from abrasion, but these were mainly organic overcoats, the likes of which are extremely difficult to apply uniformly enough so as to avoid subsequent difficulties with optical distortion and ripple effects.

Cost analysis of one large, optical coating house-versus-the Honeywell in-house coating showed outside costs to be significantly higher for volumes up to 100 units.

Improvement of Durability and Abrasion Resistance -- Several approaches to improving the durability of optical thin films on helmet sight visors were preliminarily examined.

The basic problem of durability involves getting good adhesion of the first-layer film to the base substrate. Included in the development activities were (1) measurement of percent of moisture absorbed by plexiglas and determination of bake-out techniques to eliminate same prior to coating, (2) testing of more than six different dielectric thin films to determine which had the better as-deposited adhesion to plexiglas, and (3) testing of various cleaning agents and techniques to determine the best manner of cleaning visors prior to coating.

The basic problem of abrasion resistance stems from the fact that most thin film coatings are only 1000-10,000 Angstroms thick and must be deposited on a substrate that is extremely "soft," compared to the hardness of the thin film materials.

Three basic techniques of improving the abrasion resistance of the coating were preliminarily investigated. The first is to change the substrate to a harder material. Some work was given to using "Abcite" (DuPont material) in place of plexiglas. Both beamsplitter and AR films were successfully deposited on Abcite. The biggest problem to be faced, however, is forming the visor from this laminate material.

The second technique to improve abrasion resistance is to overcoat the optical coating with a thicker, more abrasion resistant coating. Several lacquer, epoxies, urethanes, and proprietary coating materials (including Bee Chemical's R-830 coating) were tested. Most materials improved abrasion resistance, but only at an intolerable loss in visor clarity and distortion free visibility.

The third technique was to simply increase the number of layers of the thin film optics materials which were deposited on the visor. This technique was seen to improve the abrasive resistance, but not so significantly as to provide a final solution to the problem.

In summary, the durability of the beamsplitter film is such that it will pass all MIL specs for tape tests, and will pass some degree of cheese cloth rub tests. The films as-deposited cannot be expected to pass the same eraser rub tests which optical films on glass are expected to pass.

Solvent Resistance Tests -- Because plexiglas is somewhat affected by most common organic solvents, it is necessary to place some restrictions upon the environments that helmet sight visors are allowed to experience. Contrary to present flight usage and handling of ordinary helmet visors, helmet sight visors must be treated with the care and respect due any other high-quality optical surface. Cleaning of visors with most organic solvents such as most alcohols, chlorinated hydrocarton solvents, acetone, etc., will likely cause some degradation of the optical quality of the coated visors. Tests show the best way to clean these critical visors is to simply wash with a soft cloth in mild detergent solution and water.

Thin Film Coatings Summary -- Techniques to deposit beamsplitter and AR films on helmet sight visors were successfully demonstrated on the first AHRA helmet sight visor. As has been seen, the visor itself is now a critical element in the optics train and must be handled and used with some moderate degree of special consideration.

The coatings themselves must be functional from both the helmet sight systems operation standpoint and from a comfort/human-factors viewpoint for the pilot. Initial work has been aimed at verifying the functionality of the visor and its coatings. Work in the future will undoubtedly be aimed at improving both the versatility and ruggedness of this important optical element while at use in the flight environment. Future work is expected to include

improving the durability and abrasion resistance of the coatings, examining variable transmission visors for day-night applications, and reducing costs associated with fabrication of the finished helmet sight visor.

#### VIDEO DISPLAY COATINGS

#### Requirements

The requirement for the video display coating is to provide a 20 percent contrast with a 150 ft-L brightness CRT against a 10,000 ft-L background brightness. The calculations below show that if an absorption (A) of 10 percent is assumed, then a visor with a transmittance (T) of 3.3 percent and a reflectance of at least 87 percent will provide the required contrast. The coating must be provided on the inside and should pass the standard 50-rub cheesecloth abrasion test.

The image visibility specification of the AHRA program requires that the brightness of the CRT image shall have a 20 percent contrast as viewed against a 10,000 ft-L background through the visor. The relationship between the CRT brightness, background brightness, visor transmittance, and absorption is:

$$C = \frac{B_{CRT} \times R \times T_0}{B \times T}$$

where

C - is the contrast

 ${
m ^{B}}_{
m CRT}$  - is the brightness of the CRT, 150 ft-L

R - is the reflectance of the visor

T - is the transmittance of the visor

B - is the brightness of the background, 10,000 ft-L

T<sub>o</sub> - is the transmittance of the FOB and optics,  $\approx 0.5$ 

Solving for the ratio of visor reflectivity to transmittance.

$$\frac{R}{T} = \frac{CxB}{B_{CRT} \times T_{o}}$$
= 26.8

Since the sum of the transmittance, absorption, and reflectivity of the visor is equal to one, the relationship can be written as:

$$\frac{1-T-A}{T} = \frac{R}{T}$$

and

$$T = \frac{1-A}{27.8}$$

If, for example, absorption (A) = 0.1, then

$$T = 3.2\%$$
 and  $R = 86.8$ 

#### Vendor Selection and Development

Three sources for visor coating were considered: Honeywell Research Center to develop a hard dielectric material coating (described in the following subsection), a gold coating to be developed by Gentex, and an inconel coating to be developed by Evaporation Coatings Company. None of the coatings developed at Systems and Research were satisfactory. They either showed evidences of crazing or turning to powder in the presence of humidity. The gold coating developed by Gentex did not have the durability required by the program. However, Evaporated Coatings Inc. did provide a satisfactory inconel coating which was used.

#### Program Plan to Develop Hard Dielectric Coatings for Plexiglas by Research of S&RC

The objective of this program is to develop a Honeywell in-house capability to fabricate partially reflecting and antireflection coatings for plexiglas. These coatings utilized the hard, dielectric materials such as the oxide ceramics and would withstand the MIL-M-13508A hardness, adherence, and humidity tests.

Multilayer coatings will be designed with the aid of the optical coatings computer code. The anticipated materials compatibility, durability, and optical performance will be the criteria used to select the coating materials. The selected materials will be used to fabricate reflecting and antireflecting coatings. Initial coatings will be deposited on flat squares of plexiglas. The best coating system(s) will be deposited on actual visors or parabolic shapes.

Program Plan -- The program consisted of four steps:

1) Coating Design -- The reflectivity of multilayer coatings at selected wavelengths will be computed for various material

combinations. Materials of interest include Al<sub>2</sub>O<sub>3</sub>, MgO, TiO<sub>2</sub>, Y<sub>2</sub>O<sub>3</sub>, Ta<sub>2</sub>O<sub>5</sub>, CdS, MgF<sub>2</sub>, ZnS, CaF<sub>2</sub>, AgCl, SiO<sub>2</sub>, SiO, ThO<sub>2</sub>, CeF<sub>3</sub>, CeO<sub>2</sub>, LaF<sub>3</sub>, GeO<sub>2</sub>, and As<sub>2</sub>S<sub>3</sub>. Material combinations which give lowest reflection over the widest waveband will be considered for antireflection coatings; those which give highest reflection over the widest waveband with the least number of layers will be considered for partially reflecting coatings. The anticipated compatibility and durability of the materials combinations giving the best optical performance will be used to select materials for evaluation.

- 2) Materials Evaluation -- Selected materials will be deposited onto plexiglas substrates, and the hardness and adhesion of the coating will be noted. Deposition conditions will be optimized to promote adhesion and prevent crazing. Coating thickness calibrations will be made for each material.
- 3) Coating Fabrication -- Antireflection and partially reflecting coatings will be fabricated from selected material combinations. Initially, the coatings will be deposited on flat plexiglas substrates. The best coating system(s) will be deposited on parabolic visors.
- 4) Coating Evaluation -- Transmission measurements over the visible wavelength spectrum will be made on coated and uncoated substrates to evaluate the optical performance of the coatings. The cheese cloth and tape tests will be used to evaluate hardness and adhesion. Exposure to 95 percent humidity will be used to evaluate humidity resistance.

Technical Discussion -- The theory of optical coatings is well established with excellent review articles in books such as the Physics of Thin Films. Volumes 1, 2, and 5. This program will utilize double-layer antireflection (AR) coatings. The advantages of a double-layer coating for plexiglas are numerous. The relatively low index of refraction of plexiglas ( $n \approx 1.5$ ) severely limits the materials that could be used for a single-layer AR coating. Few materials come close to satisfying the index of refraction requirement (the index of a single-layer coating must equal the square root of the index of plexiglas), and only  $MgF_2$  (n = 1.38) gives a somewhat durable coating. A double layer coating allows the use of many materials, including the hard, dielectric materials. In addition, the mathematics of a double layer system can be easily handled on a computer so that layer thickness can be computed for various material (i.e., index of refraction) combinations. For coatings of more than two layers the mathematics become much more complex; the usual design practice is to assume quarter-wave layer thicknesses, computer the index of refraction requirements, and search for materials that meet those requirements.

A computer code exists which handles the general equations describing a double layer coating. With this code material combinations (and the required layer thicknesses) which will give zero reflection loss at a specific wavelength can be computed. In addition, the reflection loss at adjacent wavelengths can be calculated so that the bandwidth about the reflection minimum can be obtained. Thus, the material combinations that yield the broadest bandwidth can be selected.

For fabricating partially reflecting coatings the standard technique of alternating quarter-wave layers of high and low index of refraction will be used. Two computer codes are available to handle the necessary computations. A simple code is used to calculate the reflectance at a specific wavelength as the number of layers is increased. A general code performs the same calculation as a function of wavelength. The general trend for quarter-wave reflective coatings is as follows. The larger the index of refraction ratio, i.e.,  $n_{\rm hi}/n_{\rm lo}$ , the fewer number of layers required to achieve a given reflectance. Large index ratios also yield broader bandwidths. Thus, on a plexiglas substrate a coating of quarter-wave layers of Ta<sub>2</sub>O<sub>5</sub> (n = 2.42) and MgF<sub>2</sub> (n = 1.38) would require 23 layers for nearly 100 percent reflection, while layers of Al<sub>2</sub>O<sub>3</sub> (n = 1.77) and SiO<sub>2</sub> (n = 1.46) would require 65 layers for the same reflection. In addition, the bandwidth of the Ta<sub>2</sub>O<sub>5</sub>/MgF<sub>2</sub> coating would be approximately three times broader than that of the Al<sub>2</sub>O<sub>3</sub>/SiO<sub>2</sub> coating.

Honeywell experience with the fabrication of optical coatings has been limited to substrate materials such as quartz, sapphire and glasses. Plastic substrates present a new materials compatibility problem. The main problem is caused by the low-temperature resistance of plastics. Materials and new deposition techniques must be found which do not require substrate heating in order to yield hard and well adhering films. The technique of heating a substrate to 300°C in order to obtain a hard and durable MgF2 coating is no longer possible. In fact, precautions must be taken to ensure that the radiation from the evaporating source does not heat the plastic substrate above its softening point. Hard ceramic oxides deposited on cooled plexiglas substrates may yield the hard and durable optical coatings that are required.

Related Experience and Facilities -- Honeywell S&RC has worked with optical coatings since the beginning of the laser gyro program. Extremely low-loss, low-scatter dielectric mirrors were developed for the laser gyro when it was found that such mirrors were not commercially available. Since then mirrors and antireflection elements are being routinely produced for internal (Honeywell) use in He-Ne and CO<sub>2</sub> laser optical systems. Recently, a program with the Air Force Avionics Laboratory (Contract No. F33615-70-C-1495, AFAL-TR-71-16) was successfully completed in which a hard and durable 8- to 14- $\mu$  antireflection coating was developed for Ge33Se55As12 glass.

The facilities available for fabricating and evaluating optical coatings include:

- Four oil diffusion pumped vacuum systems and one ion pumped system
- Sloan quartz crystal and Balzer optical thickness monitors
- Sloan interferometer
- Perkin-Elmer and Heathkit spectrophotometers

#### Evaluation and Test

The transmittance of the inconel-coated visor for the video display was measured to be 3 percent. However, prior to delivery of the visor coated by Evaporated Coatings, Inc., Honeywell provided a test visor of the correct material and form. Three flat plates of plexiglas acrylic were used to monitor the coating process. These flat samples were measured for both transmittance and reflectance, whereas the curved visor could be measured (with Honeywell's present equipment) only for transmittance. Since the flat samples were found to be within tolerance the test visor also had the specified transmittance, Honeywell then proceeded to have the final visor coated using the same technique.

If the initial coating were out of tolerance then another test visor would have been used. The final visor was not used during the initial coating, since it is not feasible to remove a poor coating from acrylic in order to recoat it correctly.

For the major future redesign, consideration should be given to developing a new coating technique which would greatly reduce the unwanted reflection of the pilot's face in the visor, particularly in those areas of the visor which are outside the critical area used by the display. This would provide a uniform transmittance so that the distant scene is seen uniformly well over the whole field; the periphery of the display area, however, has its transmittance reduced to the specified value, not by a reflecting coating but by an absorbing coating. The blending of reflecting and absorbing coatings at their interface can be gradual rather than abrupt if this makes fabrication easier for an acceptable visor.

# SECTION VII RETICLE GENERATOR PROTOTYPE

#### DESIGN AND FABRICATION

# Helmet Mounted Assembly

Figures 73, 74, 75, 76, and 77 show several views of the visor reticle projection prototype helmet mounted assembly. The helmet assembly (parabolic visor in the active position) is shown in Figure 73 with the sensor electronics assembly, visor, visor cover, visor knob, sensor bar, either-eye mechanism, and reticle generator. Figure 74 shows the same view of the helmet mounted assembly with the visor in the retracted position. Figure 75 shows a close-up photograph of the reticle generator taken from the inside of the helmet. The reticle generator assembly moves up with the visor in the retracted position since the reticle generator assembly is mounted to the visor. The helmet cutout (see Figure 75), makes contract with the reticle generator barrel and swings the barrel toward the visor, which allows it to be retracted with the visor under the visor cover. The spring-loaded reticle generator pivots rotate the reticle generator assembly away from the visor as the visor is moved down again.

Figure 76 shows the rear view of the helmet mounted assembly. This view shows the left sensor bar, cable, and "T" cable connection to the right sensor bar and connector. The small shielded cable to the reticle generator is also shown above the left sensor bar. This figure also shows the rear portion of the visor cover with the cutouts that allow free air movement under the visor cover. These cutouts are provided to prevent formation of a vacuum from high-velocity airflow over the top of the visor cover during bail-out. Vacuum thus formed may detach the visor cover from the helmet. Figure 77 shows the attachment of the boresight alignment optics to the right-hand sensor bar. This assembly is interchangeable and can be attached to the left-hand sensor bar to boresight its electrical axis to the optical line of sight of the reticle generator and parabolic visor.

Figure 78, which shows the installation drawing on a Gentex web suspension helmet, does not include the actual reticle generator assembly or either-eye position mechanism installed on the flyable prototype. These assemblies are shown in Figures 79 and 80.

# Reticle Generator Assembly

The reticle generator assembly consists of a folding mirror, reticle, condenser lenses, tungsten lamp, generator barrel support, and retraction



Figure 73. Visor Reticle Projection Helmet Mounted Assembly



Figure 74. Visor Reticle Projection HMA with Visor Retracted



Figure 75. Inside-the-Helmet View of the Visor Reticle Generator Assembly

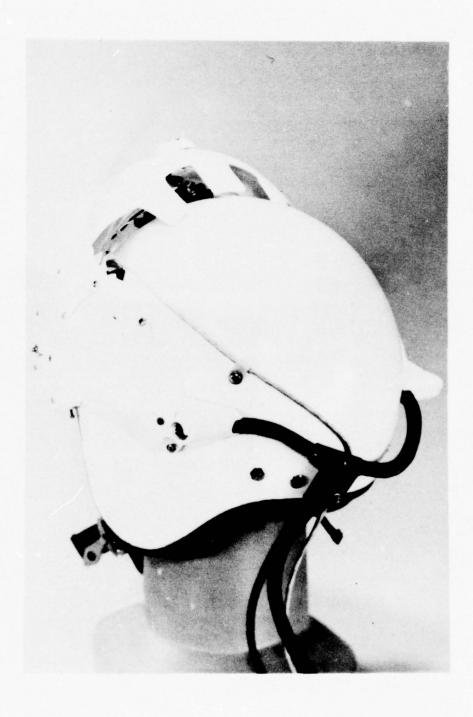


Figure 76. Visor Reticle Projection HMA, Rear View



Figure 77. Attachment of Boresight Alignment Optics to Right-Hand Sensor Bar of Visor Reticle HMA

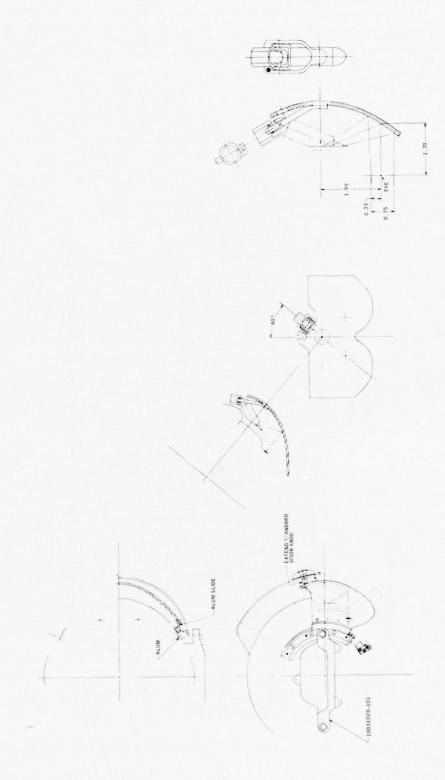


Figure 78, Reticle Generator, Helmet Mounted Assembly

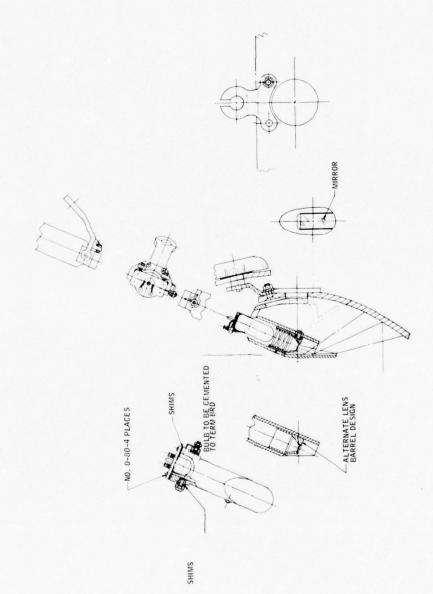
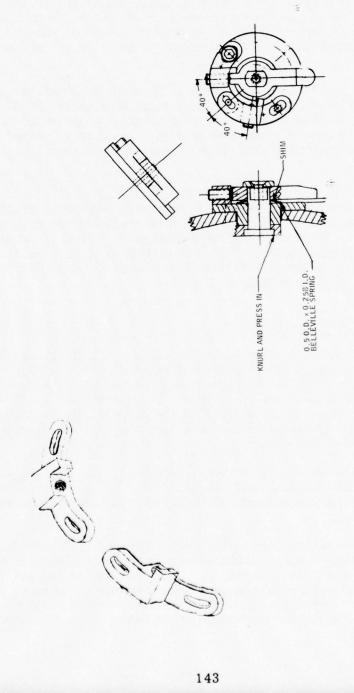


Figure 79. Reticle Generator, 1.5 FL Paraboloid



± 7° ADJUSTMENT

Figure 80. Either-Eye Position Assembly

pivots. The purpose of the tungsten lamp and condenser lenses in the reticle generator (Figure 79), is to provide the brightest possible image by focussing on the reticle. The folding mirror positions the (mirror) image of the illuminated reticle pattern at the focal point of the parabolic visor, and a collimated virtual image is thereby projected into the observer's vision. The effective focal length of a curved parabolic combiner is the distance from the reticle to the center of the combiner portion parabolic surface. This system acts as a simple magnifier and provides field of view as established by the reticle pattern dimension and effective focal length of the curved combiner.

One of the most difficult problems of the reticle generator design was the tungsten lamp. The filament of the lamp must be located quite close to the condenser lenses to obtain the desired exit pupil, or illuminated area of the parabolic visor. Also, the filament must be accurately located on the optical axis of the reticle generator and must be relatively large; i.e., 0.04 in. (Figure 81).

The lamp design shown in Figure 81 was the special type of lamp originally specified for fabrication by the Honeywell Advanced Development Laboratories, since no standard lamps were available for use in the reticle generator system. However, the final Honeywell design incorporated a lens at the end of the lamp housing. This effectively positions the filament much closer to the first condenser element (lamp lens) and satisfies the requirement for a large condenser entrance angle.

# Either-Eye Position Assembly

The eye-position assembly shown in Figure 78 allows the observer to project the virtual image of the reticle into the vision of either eye. This is accomplished by simply rotating a lever arm on the assembly from one spring-loaded detent position to another. The either-eye mechanism is designed to center the reticle pattern on the optical axis of the paraboloid. Rotating the either-eye mechanisms will therefore project a collimated virtual image into either eye.

This assembly consists of a central shaft pressed into the light source and reticle generator support arm (Figure 80). This central shaft rides in the bore of the mounting flange which is fastened to the parabolic visor by three screws (Figure 80).

The lever arm is attached to the end of the central shaft as it protrudes through the mounting flange. Lateral movement is loaded by a spring washer between the flange and the lever arm. The end positions of the lever arm are constrained by mechanical stops which are adjustable to  $\pm 7$  deg from the nominal position. These mechanical stops also contain a spring-loaded ball which engages a vee groove in the end of the lever arm, locking the assembly

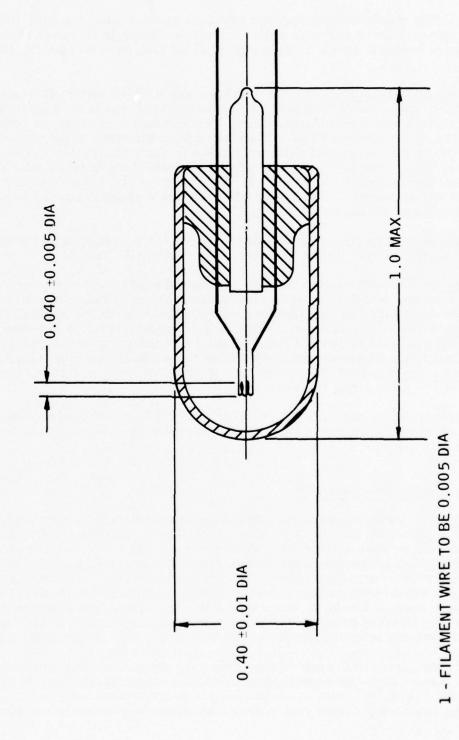


Figure 81. Visor Reticle Projection Tungsten Lamp

in position. The mechanical stops are adjusted by loosening the stop hold-down screw and rotating the lever arm until the reticle image is in the center of vision. The hold-down screw is then tightened to ensure the repeatability of position.

Visor Tracks and Sliders -- The visor tracks and sliders were fabricated from aluminum with teflon-coated sliders and nickel coated tracks to assure smooth operation. The tracks' mounting surface was machined as close as possible to the contour of the helmet shell. They were then mounted to the existing helmet mounting holes, coated with mold release, and aligned with spacer shims. The voids between the tracks and helmet shell were filled with epoxy. After curing, the tracks were removed, and the hardened epoxy was trimmed to the shape of the tracks. The epoxy fill provides a close fit to the helmet shell for alignment during assembling.

An adjustable stop and plate (Figures 73 and 78) is mounted at the bottom end of both tracks for vertical alignment of the parabolic visor.

Visor Cover -- The visor cover for the reticle generator assembly was fabricated with a large, standard, double-track visor cover. Extenders were used to allow both sides of the standard cover to mate with the special visor tracks (Figure 76). The extenders provide sufficient clearance between the housing and the helmet to permit full retraction of the parabolic visor and reticle generation. However, the addition of the extenders required a spacer to be added to the standard visor knob screw for additional clearance and free movement of the knob along the visor cover retraction slot.

The cutouts at the top rear of the visor cover (Figure 77) were extended to the helmet shell to provide protection for the reticle generator and to allow free air circulation.

# Sensor Electronics Subassembly

The molded, white lexan sensor housings are each fastened to the helmet shell at three points by No. 6-32 screws (Figure 82). Mounted within these housings, at two points, are the shielded sensor printed circuit card assemblies. These shielded sensor assemblies consist of a drawn aluminum can and cover tin plated for corrosion resistance and solderability. The lead sulphide photo sensors are oriented properly and cemented inplace on the shield cover. The cover and case are held together by three standoffs which also position and capture the flexible printed circuit tape and stiffener board assembly. Figure 82 shows the internal details of the shield can and cover assembly.

Each nylon-jacketed branch of the device connector/cable assembly is terminated inside its lexan sensor housing with a cable clamp, No. 6-32 screw and nut. The "T" joint of the cable is a polyurethane molding containing a metal reinforcing clamp ring around the cable bundle where it attaches

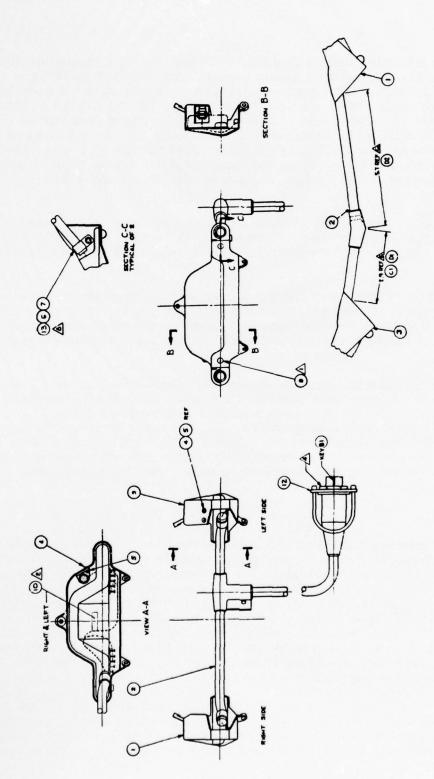


Figure 82. Sensor Electronics Assembly

to the back of the helmet shell with a No. 6-32 screw. The connector at the end of the cable is equipped with a loop lanyard consisting of a 1/8-in. - diameter, stainless-steel stranded cable whose ends are silver brazed into 1/4-in. diameter stainless-steel tips. The tips are retained in an anodized aluminum lanyard plate of 1/8-in. thickness. The primary lanyard for disconnecting the HMU in an emergency is located on the aircraft side of the connector interface. The HMU lanyard, described previously, is a secondary or convenience lanyard for securing the dangling HMU device cable to the pilot's torso harness. The configuration described is as requested by MCAIR engineering.

The primary consideration in choosing materials is weight, closely followed by corrosion resistance. Here again, the unique environment in which the HMU operates and the function it performs must be given special consideration.

Injection-molded lexan was chosen for the sensor housings because of their complex shape. Lexan exhibits toughness and impact resistance with light weight, and yet is softer than metal. This is important from the standpoint of canopy scratching which could occur during rapid movements of the pilot's head.

The aluminum cans and covers, drawn utilizing 0.016-in. stock, are necessary to protect the sensor amplifier circuitry from electromagnetic interference. An extensive test and evaluation program has defined a definite need for these shield assemblies. The extreme forming that takes place led to aluminum as the most suitable material for drawing. The assemblies, once formed, are quite rigid and have been integrated into the electronics and sensor support structure, yielding several advantages.

### Visor

The paraboloid fabrication procedure developed as a part of the AHRA program is as follows: First, a cam is generated to the true parabolic shape required for the inside of the parabola. From this cam a male mold is cut in an aluminum ingot. Acrylic blanks are then pulled using a vacumn forming approach using this male mold. These acrylic blanks are next annealed at approximately 195°F for a period of 16 hr. Next these blanks are potted into female molds machined from the same parabolic cam. This potting is performed using 6020A epoxy with an appropriate mold release. Then the potted assembly is rough machined by an outside vendor to remove the majority of the excess material and to approximate the parabolic shape required. These rough-machined parts are then delivered to Hoeger Optical Company, Chicago, Illinois, for finish machining. Hoeger Optical Company removes an additional 0.003 to 0.004 in. using a precise aspheric generator. Hoeger also laps and polishes the final configuration. At the completion of the finishing operation, the parabolas are referenced and cut to the proper configuration.

Difficulties in holding the finished thickness of the parabola were caused by variations in the potting thickness, which caused a loss in the reference location of the outside surface of the parabola which was not available to indication due to the potted condition of the assembly. The solution to this problem for future displays will be predetermine the final thickness and introduce a witness mark at the bottom of the parabola for the use in the finishing polishing operation.

The visor cutout configuration was matched to the standard Air Force oxygen mask. This configuration differs from the standard Air Force visor shape in that the nose area tends to be broader, and overall the visor tends to be shorter. This was to be expected since the Air Force visor is normally longer than necessary to permit the pilot to achieve a tight interface with the oxygen mask. In the visor reticle system, the visor must lock into a predetermined vision for elevation boresight alignment which precludes any interface of the visor with the oxygen mask.

In the final visor reticle configuration for operational use, the parabola must meet certain criteria as identified by the visor reticle performance requirements and by the Air Force visor specification. These performance criteria include:

- Sharp, well defined reticle image
- Maintenance of the reticle image quality over the entire exit pupil
- Undistorted see-through capability
- Parallelism of the see-through lines of sight for both eyes
- Stability of boresight alignment when moving the eye over the exit pupil
- Parallelism of the reticle axis when looking at the image with either eye

The last requirement for parallelism of the reticle line of sight when transferring the reticle from one eye to the next would be unnecessary should the either-eye requirement be eliminated. The remainder of the design requirements for an acceptable parabola must be satisfied for any visor reticle system.

Image quality, see-through distortion, prismatic deviation, (i.e., from one eye to the other) and boresight stability are all concerns based on the results of this program. However, based on the knowledge gained from this program, each of these problem areas can be solved with proper attention. The image quality problem resulted from ripples identified in the surface of

the parabola. These ripples are present in the early fabrication stages due to the molding process. Continued machining of the parabola did not remove the ripples from the surface, therefore, they were either inherent stress patterns in the material or the machining process does not lend itself to removal of the ripples. Testing is presently planned to identify the source of the ripples.

See-through distortion is a key concern for the future visor reticle system. Honeywell did not satisfy the existing Air Force visor specifications for seethrough distortion. Testing indicates that this see-through distortion is serious and is a cause of eyestrain. This distortion results from non-uniform figuring of the inside and outside surfaces of the parabola and may also result from stress patterns in the basic parabola material. Tests are planned to identify the sources of the distortion.

Prismatic effects in the parabola are the result of improper matching of the outside surface of the parabolas to the inside surface. Analysis has shown that the desired outside shape is a parabola somewhat larger than the inside parabola so as to cause a tapering of the parabola from the center to the outside edges. The outside edges should be approximately 0.025 in. thinner than the center section for the complete elimination of prismatic errors. As yet the only solution to this prismatic error is the finishing or characterizing of the outside surface in addition to the inside surface.

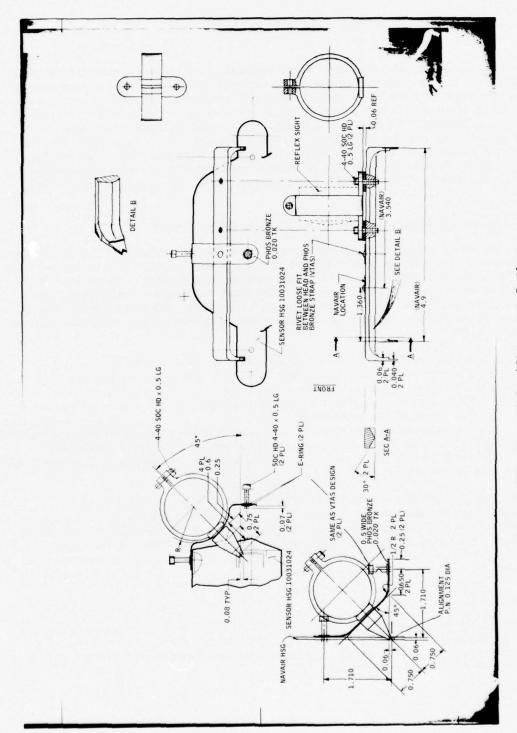
Boresight shifts when moving the eye about the exit pupil probably result from the same surface imperfections which cause distortion and prismatic errors. Once the distortion and prismatic errors are eliminated, the boresight instabilities will also be solved.

During the course of the parabola evaluation program several worthwhile test procedures are planned which will be used in future programs. These are

- Distortion-measuring tests using a projector and lantern slide
- Prismatic measurements using the same projector setup and/or a collimator telescope measuring setup
- A fast, simple easy-to-use surface figure evaluation system
- Focal length measuring test set-up capable of measuring focal length to 0.002 in.

# Boresight Optics

The boresight telescope shown in Figure 77 and in the print in Figure 83 can be mounted on either sight electronics assembly. The boresight assembly fits into the slots on the end and in the hole on the top of the sensor bar



A CONTRACTOR

Figure 83. Boresight Alignment Optics

assembly (Figure 76). The telescope consists of a bazooka reflex peepsight mounted on the reversible frame as shown in Figure 83. The bazooka peepsight projects a virtual collimated image of a reticle. A half-silvered reticle pattern is etched on a flat glass plate at the focal point of a half-silvered spherical mirror. Therefore, not only does ambient light illuminate the reticle pattern, but the assembly is very compact. This assembly serves the same function as a unity power telescope which forms an erect virtual image of the reticle pattern but has the advantage of light weight and compactness. The part number for the peepsight from A. Jaegers is 21A866.

# Reticle Generator and Either-Eye Position Adjustments

The best method of illuminating and aligning the reticle at the focal point of the parabolic axis is to use a lens end lamp with a precisely centered filament and three independent orthogonal reticle adjustments. However, the available lamps were not precisely assembled, and space limitations prevented independent reticle adjustments. Therefore, the final design shown in Figure 79 incorporated reticle and lamp adjustments, which to some degree cross couple.

The reticle and condenser subassembly can be adjusted inside the generator barrel; however, this adjustment not only changes the condenser focus of the tungsten filament on the reticle, but cross couples reticle alignment in two directions, parallel and perpendicular to the visor optical axis. The tilt adjustment of the generator barrel cannot resolve this cross coupling since this adjustment is required to align the folding mirror to be perpendicular to the optical axis of the parabaloid. Therefore, the reticle/condenser assembly must be adjusted inside the generator barrel to place the center of the reticle on the visor axis.

Focus or adjustment of the reticle along the visor optical axis is accomplished by shimming at the either-eye position assembly. Horizontal or lateral reticle adjustment is accomplished by shimming the barrel pivot screws. Focus of the tungsten lamp image on the reticle was adjusted by moving the lamp and cementing inside the barrel as a final alignment step.

#### Acceptance Tests

The helmet sight reticle assembly meets all the program requirements with the exception of weight, which has approximately 1 oz in excess of the requirements. On this basis, this assembly has been excepted by Capt. Dean Kocian for delivery on 24 August 1971.

The acceptance tests were divided into six categories, including:

- Optical design
- Reticle generation
- Ability to satisfy either-eye sighting capability
- Demonstration of visor slider motion
- · Alignment and stability capability
- Overall mechanical design

The results of these acceptance tests are presented in Table XII.

The acceptance test demonstrated the ability of the reticle generator to provide a collimated, sharp reticle image which was free of line splitting and distortion. The only defect observed by Capt. Dean Kocian, when viewed with a six power telescope was a prismatic effect of the reticle image. However, the prismatic effect was not noticeable with the naked eye.

Tests also demonstrated the capability of the visor coatings to eliminate ghost images formed by the front surface of the visor as viewed against the 1000 ft-L background. However, ghost images were slightly visible at maximum illumination against a dark background. These ghost images were eliminated by reducing the lamp power while retaining a visible image. Visor transmittance was measured to be 64%, which satisfies the requirement of minimum visor transmittance to eliminate ghost images. However, when the visor was tested in bright sunlight, some undesired reconstructions were observed. These images were from eyebrows and highly reflective metal glass rims which are close to the focal point of the parabola. This suggests that visor transmittance is not optimum. Additional reduction in visor transmittance may be desirable in the future design to eliminate these reconstructions.

Acceptance reticle generation tests were concerned with the visibility of the reticle, uniformity of the reticle illumination, exit pupil size, reticle color, and reticle field of view. The 20% visibility contrast requirement against the 15,000 ft-L background was easily satisfied, and a 53% contrast was achieved with an input lamp power of 4 w. Although the reticle illumination was uniform, some dark images of the lamp filament gaps were observed due to the inability to completely defocus the image of the lamp filament on the reticle. Future designs will consider the use of smaller filament wire, tighter filament windings, and improved filament alignment to the lens at the end of the light bulb. These improvements should greatly reduce dark areas of reticle illumination due to filament nonuniformities. The requirement of a 20 mm exit pupil size was exceeded and found to be 30 to 40 mm. The requirement for an orange reticle color was achieved by designing the lamp to operate at a reduced color temperature of 1900°K at 4 w. Measurement of the 3-deg reticle field of view was demonstrated by measuring the distance subtended by the reticle image at a known distance from the observer.

Table XII. Acceptance Test Results (24 August 1971)

Design Parameters	Test Criteria	Test Results
Optical Design	Image must be collimated, sharp, and distortion free	Noticeable prismatic effects, but sharp and collimated
	No ghost image against !000 ft-L background	Adequate
	3. Maximum visor transmittance	9600 ft-L transmittance @ 15,000 background
	No undesired reconstruction from other light sources	Internal reflection of glass rims and eyebrows
Reticle Generation	1. Visibility - 20% contrast against 15,000 ft-L background	50% contrast
	2. Reticle illumination uniformity	Some filament granularity
	3. Exit pupil > 20 mm	20-30 mm
	4. Reticle color - orange	Sufficiently orange
	5. Field of view > 3 deg	3 deg
Either-Eye Capability	Reticle to remain in focus and collimated	Collimated and focused - either eye
	2. Boresight error < 2.5 deg	1 deg
	3. Adjustable interpupilary distance	Additional adjustment needed
Slider Motion	Smooth sliding action, positive locking	No measurable alignment shifts
Alignment Capability and Stability	1. Boresight accuracy 2.5 deg	<2 mr - right side 1 deg - left side
Mechanical Design	Sliding mechanism to be operated freely and without excessive freedom	Insignificant (acceptable)
	Visor locking to be provided to ensure repeatable locking	Insignificant (acceptable)
	3. Added helmet weight, 15 oz	16 oz

The third category of tests was to determine capability of the assembly to present a focused and collimated image to either eye with a boresight tolerance of 2.5 deg. It was demonstrated that the reticle does remain collimated (focused image in 6x telescope) for either eye without any adjustments. The boresight error was approximately 1 deg for either eye, which is well within the 2.5-deg tolerance. However, the reticle was not uniformly illuminated for vision with both eyes. Insufficient interpupilary adjustment was found to be the cause, and modifications were made before delivery.

The alignment requirement of the optic axis to the sensor electronics assembly axes of 2.5 deg was satisfied. The right side alignment was approximately 2 mr, while the left side alignment was approximately 1 deg.

The visor slider assembly provided the necessary smooth sliding motion and positive locking while maintaining adequate boresight alignment. No measurable alignment shifts were observed when repeating engagement and disengagement of the visor.

The components of the advanced helmet reticle sight assembly were weighed individually, and it was determined that the weight added to the existing helmet will be approximately 16 oz. The requirement was for a total added weight not to exceed 15 oz. However, future designs will easily meet the necessary weight requirements since the track assemblies can be fabricated from lighter materials.

#### Reticle Generator Evaluation and Recommendation

Evaluation -- The condenser assembly consists of three plano convex lenses with individual focal lengths of 4 mm. The reticle was a reproduction on a photographic negative and was mounted between two cover glasses using 7228 silicon cement. The reticle was positioned at a distance of approximately 0.125 in. from the condenser lenses. The basic problem of the reticle generator assembly results from the imperfect lamps fabricated by ADL. Only two of the 10 lamps produced by ADL had filaments which were either grossly displaced off the axis of the lamp lens or too far away from the lens. These two tungsten lamps still had to be displaced from the center line of the reticle barrel and tilted to compensate for the off-axis filament. The image formed at the reticle had many dark spaces (gaps between filament coils) due to the inability to correctly defocus the condenser system. The large spacing between the filament and lens prevented defocusing the reticle image. The ADL lamps were also fabricated with tungsten wire feed-throughs which presented difficulty in handling and soldering. The high lamp current of 2 amps at 2 v requires heavy lead-in wires. Also, the reticle generatorhousing was complicated and difficult to machine.

Recommendations -- Future lamps must be fabricated to place the filaments on the optical axis of the lens and at the required spacing. Also, the lamp filament wire should be reduced in diameter to reduce the current and increase the number of coils.

The reticle generator housing should be redesigned as a two-piece construction, with the lens, reticle, and mirror mounted in one common barrel and the lamp on a separate mount. The barrel should be made from aluminum, and the lamp holder can be made from a dielectric material such as fiberglass.

# Visor Housing Evaluation and Recommendations

A standard visor cover was used to protect the visor while in a stored position. However, due to the increased distance of the visor from normal position, extenders were necessary to mate the visor cover to the track assembly. A three-piece aluminum assembly was fabricated, but proved to be quite heavy. Also, the standard visor cover did not entirely cover the visor tracks. Furthermore, the radius of the housing did not match the radius of the track assembly, and the locking mechanism attached to the visor rubbed the housing at mid-point of the visor travel. Consequently, future helmet mounted assemblies should have a custom visor cover to reduce weight and improve visor retraction mechanization.

# SECTION VIII VIDEO DISPLAY

The HMD (Figure 84) is considerably more complex than the HMS. Both use a paraboloidal visor as the "combining glass" for superimposing the generated image onto the distant scene, and both must meet certain operational and safety conditions. However, the field of view of the generated image is much larger in the HMD, and its method of generation is quite different.

Because of the larger field, the HMD uses a double-bounce optical system at the visor, while the HMS requires only a single bounce because of its small field angle. Moreover, the video display requires a CRT to generate its initial optical image at the helmet, while the reticle generator of the HMS uses a reticle and lamp with condensing lens for that purpose.

The HMD must be designed not only to place its exit pupil at the eye, but also to minimize the optical aberrations such as distortion, coma, etc.

The drawings for the fabrication of the HMD are furnished. These drawings for Mod 6 are value engineered to provide the necessary information for Honeywell's Tech Lab to build the HMD in close liaison with the responsible engineer. In many instances the assembly drawing provides enough information to fabricate parts without separate detailed part drawings.

New drawings would be required for use in fabricating parts in production quantities, since all the information must be on the drawing in detail in lieu of engineering liaison.

The following list identifies the working drawings which are not up-to-date. All bear the drawing number SK58185 and are distinguished by sheet numbers from 1 to 18. Note that sheet 9 has been included, though it is an obsolete preliminary layout that is superceded by the later sheet 10.

- 1) Original layout configuration -- not updated.
- 2) CRT mount -- obsolete. New design uses a longer tube with a central slot around which the clamping ring is centered. Because the FOB was shorter than expected, the CRT mount was raised about 0.4 in. to fit. This change led to a change in the strap bracket which was altered to suit.
- 3) Collimation optics
- 4) Collimation optics mount and spacers

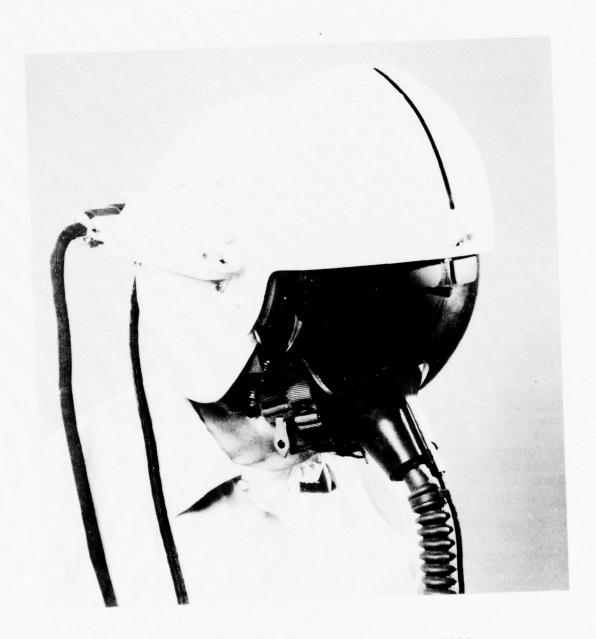


Figure 34. Visor Video Projection HMA

- 5) Central mirror assembly -- obsolete. New design modified the arm to provide both length and pivot adjustment. The clamping knob bracket was made into a double-jointed hinged linkage.
- 6) Visor cover -- obsolete. The double-jointed hinged linkage permitted lowering the upper portion of the visor cover.
- 7) CRT and relay lens assembly. A minor modification replaced the large thumb screw by a setscrew in the CRT clamp which is located near the center of the CRT mount.
- 8) Ray trace -- 2 in. FL design criterion
- 9) Preliminary relay lens mount and spacers
- 10) Final relay lens mount and spacers
- 11) Relay lens element No. 2. Assembled nearest the CRT face-plate which is considered to be Element No. 1.
- 12) Relay lens element No. 3
- 13) Relay lens element No. 4. Cemented to No. 5.
- 14) Relay lens element No. 5. Assembled adjacent to aperture stop in front subassembly.
- 15) Relay lens element No. 6. Cemented to No. 7.
- 16) Relay lens element No. 7
- 17) Relay lens element No. 8
- 18) Relay lens element No. 9. The last element to be assembled in the rear subassembly. This is the short conjugate end of the relay lens.

#### DESIGN AND SPECIFICATION

The design of the HMD is the result of a thorough consideration of the requirements for weight and balance, safety, interchangeable eye viewing, and optical performance as well as compatibility with the GFE display electronics which must be modified to incorporate distortion compensation in the vertical and horizontal sweep circuits.

The specification for the HMD is in the form of a Statement of Work (covering the HMS as well) which is dated 13 October 1970 and which was amended 7 April 1971.

# Requirements of AMRL Contract

In the Summary, the basic requirements of this contract are stated as objectives or design goals. The extent to which these requirements have been met was shown during the acceptance tests conducted in Honeywell's Optical Laboratory on 25 January 1972 in the presence of Mr. Tom Furness and Capt. Dean Kocian.

Breifly, the principal requirement of this contract may be excerpted from paragraph 4.1.3 of the Statement of Work. In part it states: ... The contractor shall design and fabricate a flyable sight assembly and display assembly using these approaches which meet the specifications of paragraph 4.2... Then paragraph 4.2.2 states the CRT Visor Display Specifications and paragraph 4.3 gives the Performance Specifications and paragraph 4.4 gives the Environmental Considerations.

# Layout of Helmet Mounted Display

To a great extent the layout of the HMD was decided not on the basis of optical system design considerations, but on the basis of the requirement to preserve balance and minimize displacement of the center of gravity. Thus, the CRT is located at the base of the rear of the helmet. This design decision led to another; namely, use a FOB to convey the image from the back of the helmet to the top front where it can be introduced to the double-bounce paraboloid. This led to another decision, since it was not feasible to use a FOB large enough to match the full CRT raster area.

Accordingly a relay lens was introduced between the CRT and the FOB to provide an image reduction factor of 0.667. A folding mirror was also introduced for obvious reasons. The FOB requires both focusing adjustments at each end.

The exit end of the FOB must be located in the focal plane of the collimator lens to produce the required collimated image and two folding mirrors are required at the collimator lens, the first to allow the collimator lens subassembly to fit into the limited space between the helmet shell and the visor in its retracted position. The second (collimator) folding mirror is used as a boresight mirror to direct the collimated image to the paraboloidal visor parallel to its optical axis and to the boresight direction defined by the SSU Sensor Bars. This direction is also the boresight direction of the HMD image as seen by the right eye (after the second bounce from the paraboloid).

This layout of the HMD is shown in Figure 85. Provision has been made to switch the display to the left eye. It is a factory operation to make this switch because of the equipment required to correctly boresight the system as well as to make the other critical optical adjustments associated with this switch.

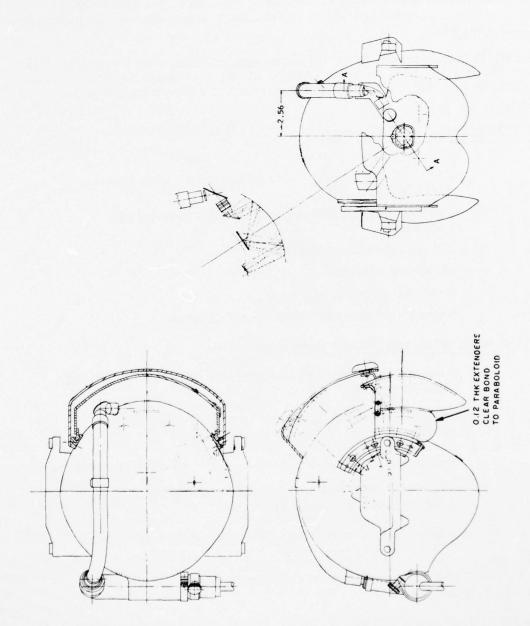


Figure 85. CRT Display Configuration - 2 FL Paraboloid

A recommendation for the improvement of the design is to provide for appropriate keys and focus stops at necessary places to facilitate interchangeability of subassemblies while maintaining alignments which have been preset at the factory.

This HMD design was a result of many compromises between the requirements for the system such as vision obscuration, minimum helmet envelope, helmet balance and ease of component mounting, as shown in the following listing:

# • CRT/Optics/FOB Housing

- CRT rotational and focus adjustments with locking mechanism
- Locate CRT on helmet with minimum envelope increase
- Corona discharge safety
- Minimum weight
- FOB nonmetallic clamp
- Lens moisture and shock proof mounts

# Visor Bearing and Detent Mechanism

- Repeatable alignment of visor optical axis to less than
   7 milliradians
- Positive detent to fix visor in active and STOW positions
- Bearing and track design to prevent binding or sticking
- Visor cover and bearings must not obscure line of sight between LSA and sensors
- Visor bearing and track design should result in a minimum extension of the helmet envelope
- Bearing and track design should be adaptable to any visor contour
- Bearing and track design should allow for the weight and loading of the optics and retraction mechanism attached to the upper edge of the visor

# • Fiber Optic, Visor Retraction Mechanism and Optics

- Mount, refractive optics, mirror and fiber optic bundle under visor
- Locate central mirror under visor and retraction mechanism beneath the helmet cut out over the forehead
- Focus adjustment mechanism from 15 inches to infinity
- Mechanism or mounting adjustment which will allow display to be projected in front of either eye

A flexible round cross section FOB was used for the display prototype instead of a semi-rigid flattened FOB to simplify fabrication and either eye operation. The flexible fiber optic bundle follows the contour of the helmet easily and allows a great deal of freedom in laying the bundle around the helmet. It allows rapid removal, reshaping, and reinstallation for use with the other eye. A semi-rigid flattened FOB would reduce the helmet envelope, but would have required two bundles for either eye operation. The tradeoff is between the disadvantage of more clearance required for a larger bundle and the advantage of a flexible bundle.

Another approach that was considered was the use of a fused tapered FOB. The tapered FOB would couple directly to the FOB faceplate of the CRT and then taper down to fit under the visor. However, this approach was dropped when it was learned that the blemish content is excessive for long fused FOBs.

One of the original design concepts was for the FOB to cross over from the lower right back side of the helmet to the left front top side over the forehead. The intent here was to counter balance the collimation optics located on the left side with the FOB. However, this requires a longer and heavier FOB than the noncrossover approach. In addition, the crossover FOB approach would not really improve the counter balance and may make it worse since the CRT cable would be attached to the helmet on the same side as the collimation lens.

The lightest weight, flexible sheathing for the FOB is stainless steel SL, Anaconda strip wrap. However, it is not moisture proof, nor has it a long life for repeated flexing. Therefore, white opaque shrink tubing was used for moisture proofing and a long flex life was not considered necessary for this application.

The various angles of the folding mirrors in a collimation optics assembly were selected to ensure that the FOB would lie in a plane parallel to the visor tracks. This prevents the FOB from interfering with either the visor bearing tracks or the helmet-mounted sensor electronics.

Two cutouts were made above the forehead to accommodate the mounting of the collimation optics assembly. This weakens the structure of the helmet to some degree, but later models will include a saddle underneath the collimation assembly to increase the strength. The collimation optics, mirrors, and FOB were all mounted within a common assembly for accurate subassembly alignment. The FOB and second mirror are adjustable for focus and alignment (Figure 86).

The visor track and bearing design was quite similar to that of the reticle prototype assembly to reduce fabrication costs. The visor tracks and bearings were fabricated from delron for minimum friction and weight. However, this material is somewhat hydroscopic and does flex which may cause some problem with binding in the tracks. Consequently, other materials will be considered in the future.

The vertical side extenders for the visor had a curved section or radii at along the bottom edge. This section was added to the extenders to prevent a discontinuity in visor transmittance, for peripheral vision.

Flat visor extenders were used to avoid the requirement for fabrication of new cams with a conic section that would curve inward and mate with the visor tracks. Another alternate that was considered is to extend the parabolic section beyond the tracks, and doglegging back towards the visor tracks. Figure 87 shows one of the first design dogleg design iterations with a single ball detent mechanization. Although this design allows unobscured side vision the visor dogleg and visor cover are difficult to fabricate. Figure 88 shows another design which incorporates a two ball detent design and with a slightly reduced dogleg. Figure 89 is the last dogleg design iteration, and does not include detent mechanism. All these approaches were rejected due to the requirement for new tooling for visor fabrication and obscuration of side vision.

Several locations for the CRT were considered, but these arrangements were rejected since they either raised the center of gravity or increased the danger of whiplash. The final configuration shown in Figure 85 lays the CRT in a horizontal position just above the nape of the neck. The CRT mount is fitted into a saddle cutout of the helmet, which partially moves the CRT forward and minimized the interference with the pilot's head rest. The position was also selected since the 3-in. track length of the relay optics positions the 12 in. FOB in the correct position over the forehead. The clamp with the nut or capscrew secures the CRT assembly to the helmet saddle mount while the kurled nut allows the CRT to be rotated to align the imagery to local horizon.

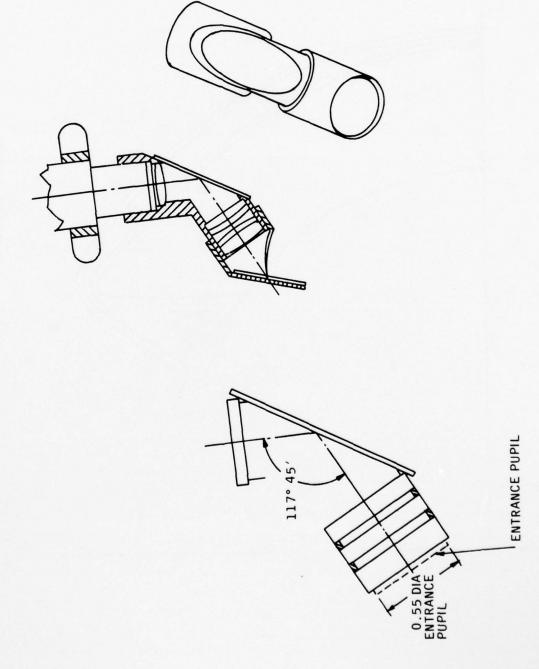


Figure 86. Video Display FOB, and Second Mirror

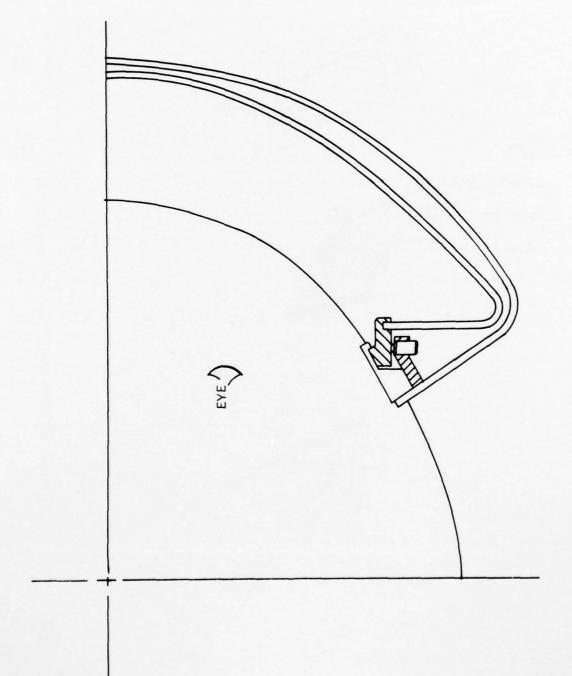


Figure 87. Video Display, First Visor Dogleg Design

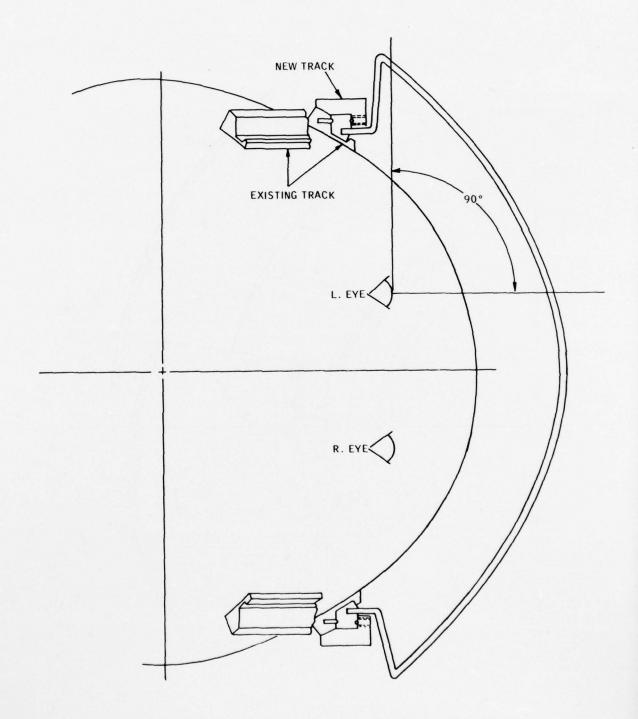


Figure 88. Video Display Visor, Two-Ball Detent Design

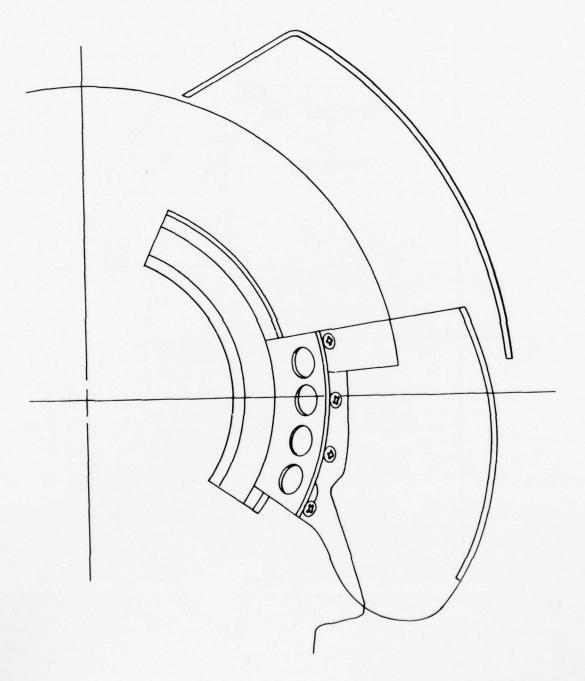


Figure 89. Video Display, Last Dogleg Design Iteration

The visor knob was mounted in the center of the visor cover in spite of the increase in helmet envelope. Other approaches to reduce helmet envelope are to mount the visor knob on the side or behind the visor cover. However, due to limited time and funds, the knob was placed in the most convenient location for ease of fabrication. The visor cover curvature does not precisely follow the point of knob attachment to the visor. Consequently, the distance between the visor cover and the visor increases as the visor is retracted and a double linkage coupling was used between the visor knob and visor.

The Gentex web suspension helmet was used, to isolate the outer shell from the flexing of the inner web suspension. It was estimated that boresight shift due to helmet flexure would be less than 5 mr with a web suspension helmet.

Photographs of the HMD are presented as Figures 90 through 94.

#### Optical Design by HRC

The computer design of the double bounce-paraboloid and collimation lens was completed at Honeywell Radiation Center in Lexington, Massachusetts, under the direction of Mr. Irving Abel. Details are given in Appendix III.

The double-bounce paraboloidal visor/combiner is a particularly useful optical system because it provides for filling the eye (located at the exit pupil of the double-bound paraboloidal) with a relatively wide field that is substantially free from coma and astigmatism. The image distortion, which it contributes, is substantially of first and second order type which is correctable by suitable compensation of the horizontal and vertical sweeps of the CRT. This electronic distortion compensation is fully described in Customer Engineering Letter to Captain Dean F. Kocian, CEL No. 12655-5, 20 April 1972.

#### Optics

An essential feature of the optical system design is the provision for a sufficiently large (0.4 in.) exit pupil at the eye so that the display image can be seen even if the helmet shifts slightly on the head. Note that the HMS sensors are attached to the helmet, not to the pilot's head. Therefore, boresight alignment is maintained in spite of any relative motion between the helmet and the head of the pilot.

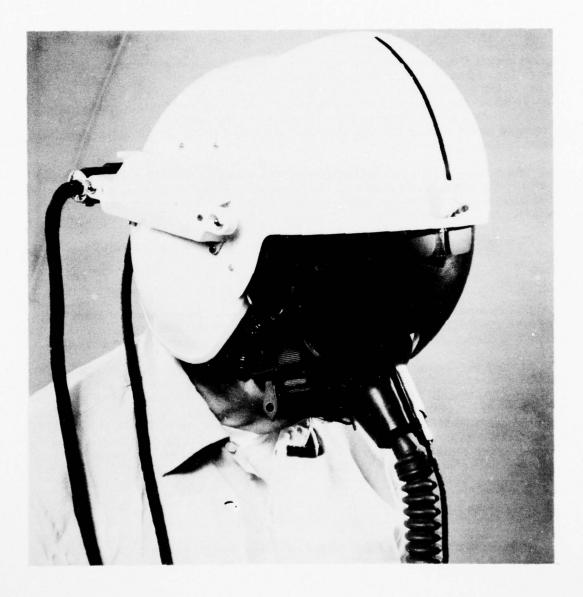


Figure 90. Developmental Helmet Mounted Display Prototype Delivered to AMRL in February 1972



Figure 91. Photograph of Front of HMD as Worn with Oxygen Mask, Visor in Operational Position (Note the two blackened areas near the brow of the visor cover. These areas are opaqued to prevent the phenomenon known as "white-out" which could otherwise obscure the display under certain adverse lighting conditions)

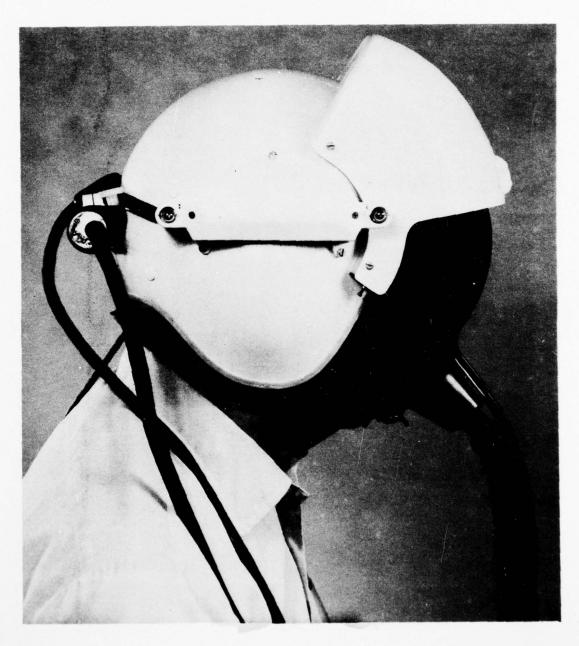


Figure 92. Photograph of Right Side of HMD as Worn with Oxygen Mask, Visor in Operational Position

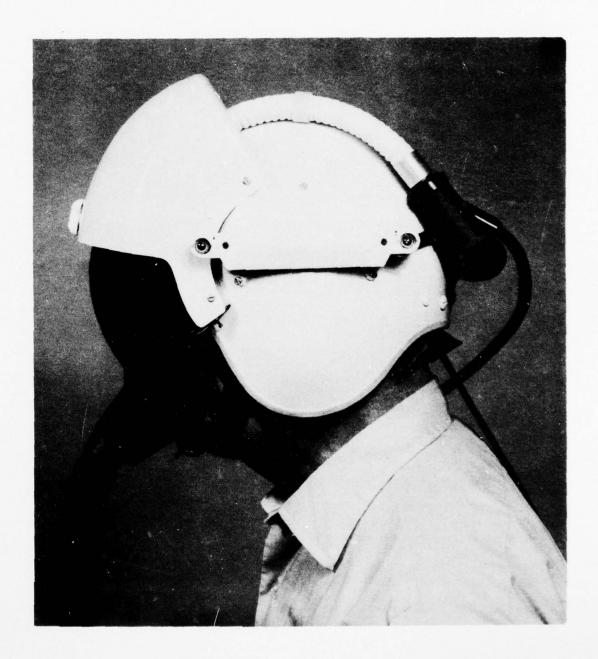


Figure 93. Photograph of Left Side of HMD as Worn with Oxygen Mask, Visor Retracted



Figure 94. Photograph of Left Side of HMD as Worn with Oxygen Mask, Visor in Operational Position

Display Electronics -- The GFE Display Electronics was designed for use with a Hughes HMD which has a plano combiner/mirror that reverses the image. Thus, it was necessary to provide for reversing one of the sweeps of the Display Electronics package to make it compatible with the Honeywell HMD which has an even (not odd) number of reflecting surfaces.

CRT -- The GFE CRT is the basic display image generator for the HMD. Its video quality naturally affects the display image quality with respect to brightness, brightness uniformity, resolution, contrast, distortion, focus, color, etc. Within size and electronic tolerance limits, the CRT is replaceable.

Lenses -- In order to produce acceptable display image quality, the relay lens and the collimator lens must be of excellent optical quality. This means that they must (a) be well designed, (b) have their elements made within close tolerances, (c) be assembled with current spacings and be well centered, (d) have efficient low reflectance coatings to minimize light loss and ghost images and flare, (e) have well designed mounts, and (f) be correctly positioned for magnification and focus. During subassembly and final assembly the surfaces of the lenses must be kept clean and free from scratches.

Fiber Optics Bundle (FOB) -- The nature of the FOB is such that flaws of various kinds are often found. The individual glass fibers are 0.0004 in. in diameter (including the cladding of lower index glass) in our FOB. In order to make a FOB having an image area of 0.3 x 0.4 with a diagonal of 0.5 in. from a CRT raster that is 0.45 x 0.60 with a diagonal of 0.75 in., the relay lens must produce a magnification of 0.667.

The FOB comprises approximately 750,000 individual fibers. These fibers are composed of about 20,875 multifibers, each multifiber being a fused fiber bundle containing 6 x 6 - 36 individual fibers with a cross section of about 0.0024 x 0.0024 in. With so many small fibers and multifibers, it is understandable that fiber breakage and multifiber breakage becomes a serious problem.

The fabrication technique, as made by the American Optical Co., Southridge, Massachusetts, calls for 125 rows of multifibers to be laid smoothly in place, each row containing 167 multifibers. As these rings of multifibers are assembled within the 0.60 in. wide channel, the probability of a row of these multifibers getting skewed increases as the top row is approached. Examination of our FOB revealed such row skewing (recorded in photographs). The effect of this skewing is to change the transmittance of that row of multifibers. Broken fibers and a few broken multifibers were noted also. The photographs show that there are various width gaps between multifibers, though this is not a serious problem.

The misregistration of multifibers results in dislocations in image detail with resulting loss in resolution. Since the size of the individual fibers is about optimum from a system MTF standpoint, the dislocation of multifibers is a factor in reducing MTF locally.

Suggestions for improving optical performance of the HMD must include (a) improved manufacturing techniques for the FOB, (b) improved means of specifying the optical performance of the FOB, (c) improved methods of inspecting the FOB, (d) consideration of lowering the profile of the FOB by using a ribbon-type cross-section between the potted rectangular entrance and exit ends; this ribbon form giving a much lower profile as it passes over the helmet.

For the long-range design, consideration should be given to eliminate the FOB entirely, if possible. Preliminary studies indicate that this may be achieved with new state-of-the-art video generators that are very compact and light weight. Honeywell is currently testing some promising proprietary techniques along this line.

The specification for the flexible FOB is as follows.

# Flexible Sheath and End Tips

SL Anaconda stainless steel, strip wound, sheathing covered with thin wall shrink tubing for moisture proofing. End tips shall be aluminum with approximate 0.65 diameter and extend 0.75 in. from end cap. OD of sheathing is approximately 0.75 and final OD with shrink tubing shall be 0.8 in. or less. OD of end cap over sheathing and shrink tubing shall be less than 0.88 in.

# Fiber Optic Bundle

- Fiber breakage -- less than one percent
- Blemish -- less than  $30 \times 10^{-6}$  (in.)
- End face flatness -- 7 wavelengths at 5890Å
- Numerical aperture -- not less than 0.56
- Fiber diameter -- 10 ±1 micron (including clad)
- Transmission -- total end losses less than 35 percent and internal losses less than 10 percent per foot
- Length -- 12.0 in.
- Cross section -- 0.29 in. x 0.39 in.

Mirrors -- Reference has been made to folding mirrors at the relay lens and at the collimator lens. Another very important mirror is the central mirror located normal to the axis of the paraboloidal visor and at its focal point; it is an essential part of the double-bounce visor subsystem. Thus, not counting the two partial reflections at the visor itself, the optical system has reflections at four plano mirrors. High reflectance mirrors are needed to keep the image brightness at the desired level.

Mounting the mirrors is critical, but uses standard optical fabrication and assembly techniques. Aligning the boresight mirror takes a special method described later.

Suggestion for a smaller central mirror: Since the size of the central mirror was made adequate for both right and left eye operation (by switching subassemblies to the other side), it could be made smaller if only the right eye is to be used. Replace it with a "left-hand" central mirror on those HMDs made for left eye'd pilots. The smaller central mirror will have several obvious benefits.

<u>Visor</u> -- The visor is designed to have a focal length of 2.0 in. The optical surface quality on the concave side is critical for the display image. Since the Mod 6 HMD was assembled, new techniques have been developed for making better quality visors. These techniques are being continually pursued both within Honeywell and at selected vendors.

In the early stages of this program it was assumed that the optical surface quality of both the convex and the concave sides of the visor would either be acceptably good in all azimuths, or (if not up to such standards) would be substantially equally good/bad in all azimuths. For this analysis it was assumed that the paraboloidal visor shell would be a surface of revolution within significant limits.

This did not prove to be the case for the Mod 6 visor, so area selection was used to optimize the performance of the HMD. This area selection is described in Figure 102.

If the visor shell had rotational symmetry, the perimeter could be cut with any arbitrary azimuth -- but it must be cut with the optical axis correctly boresighted and centered with respect to the collimator exit pupil and the HMD exit pupil (which is where the observer's eye belongs). This requires referencing procedures. The technique adopted was to make accurate reference cuts on the visor at suitable places on the perimeter.

It should be obvious now that the design must provide for mounting the visor so that (when in its operating position) the optical axis is correctly positioned. The reference cuts provide for alignment and alignment checking of the mounting.

The visor is a critical part of the optical system. We recommend that improved fabrication techniques be developed to produce better visors with respect to rotational symmetry and optical surface quality.

The see-through image quality would also benefit from improved fabrication techniques as well as by designing the convex face specified to minimize deviation of transmitted light from the distant scene to the eye.

Another improvement to the visor form would make the visor cover and the entire helmet-mounted display smaller. This change would eliminate the flat extender plates that attach the visor to the track sliders. These extender plates will not be needed if the outer area of the visor (beyond that area which must be paraboloidal for optical reflection of the video image) is curved around gradually to meet the visor track sliders. The machining technique which generates the paraboloidal surface can also generate a surface of revolution which has a smoothly curved contour of arbitrary design.

For the major future redesign, consideration should be given to developing a new coating technique which would greatly reduce the unwanted reflection of the pilot's face in the visor, particularly in those areas of the visor which are outside the critical area used by the display. This would provide a uniform transmittance so that the distant scene is seen uniformly well over the whole field; the periphery of the display area, however, has its transmittance reduced to the specified value, not by a reflecting coating but by an absorbing coating. The blending of reflecting and absorbing coatings at their interface can be gradual rather than abrupt if this makes fabrication easier for an acceptable visor.

The see-through image quality and boresight accuracy depend not only on the optical surface quality on the concave side, but also on the convex side. Optical homogeneity of the visor is important, but this does not constitute a real problem area. The mathematical formula for the convex surface has been studied to optimize it from a boresight standpoint. Debugging the computer program to solve this problem will be scheduled for early work.

The major area for future improvement of the visor is in the method of generating a good paraboloidal concave surface. We anticipate that present studies will result in a marked improvement in visor image quality.

FABRICATION, ASSEMBLY, ALIGNMENT, AND TEST (Figures 95 through 97)

The preceding description has dealt primarily with the concepts of system design and the design of components.

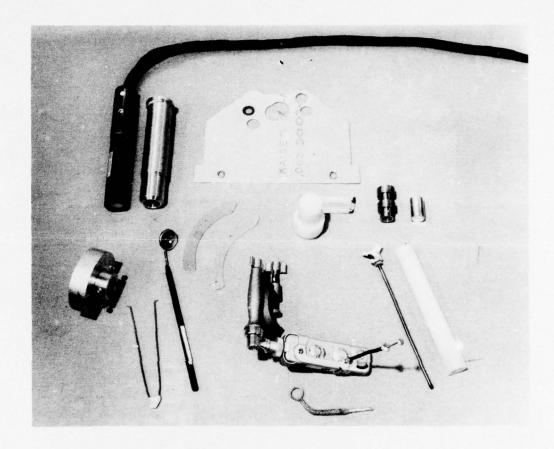


Figure 95. CRT with Final Stages of Electronics and Cable (Dummy CRT less resolution target, aperture plate, tilting adapter to explore field of collimator lens assembly, lens cell extractor tongs for Mod 5 HMD, dental mirror for visual inspection in cramped spaces, two shims used in mounting helmet onto its alignment fixture when the visor cover has been removed, nylon plug used in fabricating lens spacer rings, front surface mirror with three scribed reticle lines for measuring the field size of an optical system, calibrated reticle holder for measuring curvature of field of collimator lens, front surface mirror with special scribed reticle pattern mounted on tube forming collimator focussing plug, Minox camera with shutter release and mounting clamp used to photograph the actual display inside the helmet, lorgnette jig comprising an open ring on a bent post that fits helmet alignment fixture to define the exit pupil position of the HMD for properly locating the Minox camera, collimator boresight mirror adjusting tool, nylon rod jig for preliminary mechanical alignment of collimator assembly less collimator boresight mirror.)

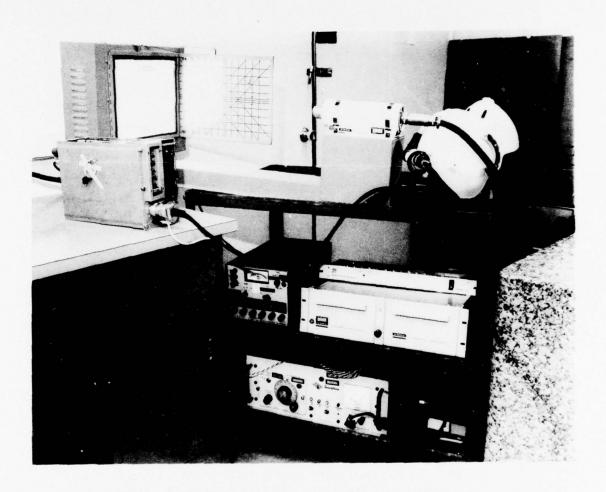


Figure 96. General View of HMU with Visor Retracted (Mounted on alignment jig, mounted CRT, closed-circuit TV system with power supply, COHU TV vidicon camera, camera electronics, modified GFE Hughes display electronics with modified circuit card inside, light box with various object target patterns)

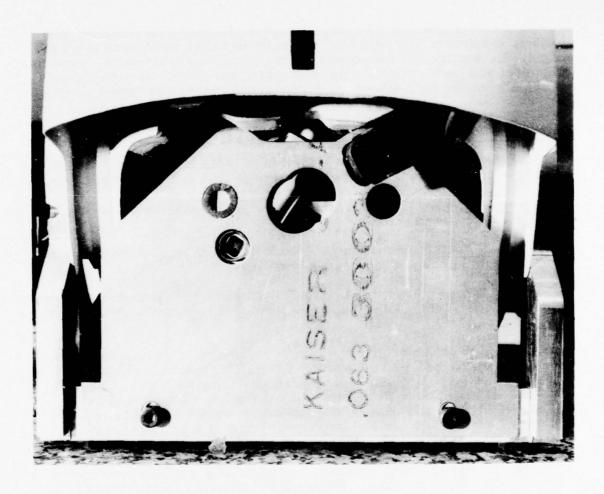


Figure 97. Close-up of Helmet Mounted on Alignment Jig with Both Camera and Lorgnette Mounted in Place Behind the Aperture Plate (This aperture plate defines the various optical aperture positions used in the alignment procedures. Note that the collimator boresight mirror is directly in front of its aperture, and the camera is directly behind its aperture. A pointer in the center of the central mirror aperture defines the optical axis of the paraboloidal visor when it is in its operational position. The bottom of the visor can just be seen below the brow of the visor cover. Note the brow of the helmet shell has been cut out on both right and left sides to accommodate the collimator assembly for either right or left eye viewing of the display.)

At the time when Dr. Woodson was engaged as a consultant on this project, the design was complete and parts had been fabricated to a great extent. He was made responsible for the remaining fabrication, assembly, alignment and test. Accordingly, the remainder of this section appears principally in the form of specifications and directives for these processes.

### Helmet Modification

Keep helmet modification at a minimum (AMRL directive). See Figures 98 and 99 for the standard XL Air Force HGU-2A/P helmet by Gentex.

<u>CRT Mounting</u> -- Encase the CRT in a fiberglass insulating sleeve to protect the high voltage leads.

Collimator Cutouts -- Accommodate the collimator lens assembly by providing cutouts in both sides of the helmet brow.

SSU Sensor Bars -- Adapt the helmet for standard SSU sensor bars by raising their locations slightly, while still preserving the required boresight direction.

In order to better control the position of the pilot's eye with respect to the position of the exit pupil of the HMD, serious consideration should be given to the advisability of providing each pilot using the HMD with a custom fit helmet using the polyurethane foam technique. This would ensure that the helmet would always be placed on the head in the same relative position with negligible variation in the exit pupil position with respect to the eye.

This suggestion has a corollary. Since pilots who have heads close enough alike to use the same size helmet do not, in general have their right (or left) eyes at the same position relative to the helmet they are wearing, it would appear to be highly desirable if the HMD helmets could be not only custom fit to the head but could concurrently be so positioned at the time of foam-fitting that the HMD exit pupil position does indeed coincide with the pilot's eye. Naturally this would mean that the foam padding would have different contours for different pilots -- some having thicker padding on top, some thicker on the sides, some thicker in front or back, than other pilots.

In this way the HMD could be designed to have a fixed exit pupil position with respect to the helmet with the assurance that each pilot who had the foam fitting padding would have his eye correctly placed to see the display superimposed on the scene.

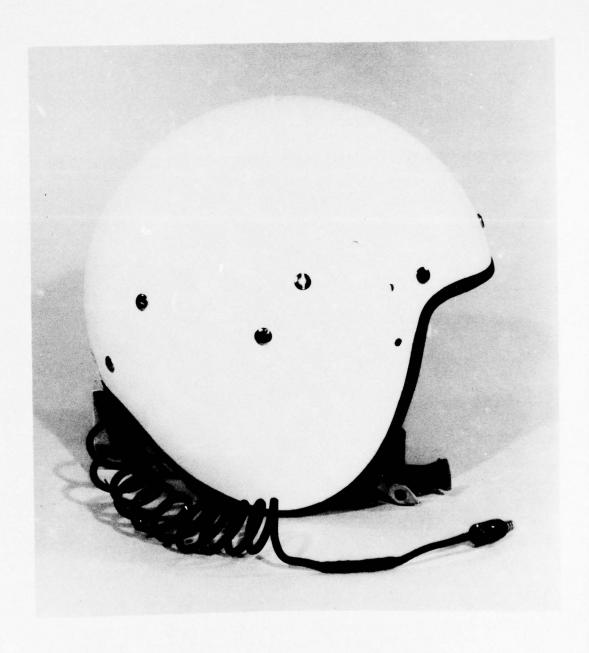


Figure 98. Side View of Standard XL Air Force HGU - 2A/P
Helmet from Gentex, with Web Suspension and Communications Equipment (The HMD has not been
installed on it)



Figure 99. Front View of Standard XL Air Force HGU-2AP Helmet with Accessory Pads of Various Thicknesses to Fit Helmet to Pilot so That His Eye can be Located to the Exit Pupil of the HMD When it Has Been Installed (Note web suspension which minimizes helmet flexure during use.)

This procedure appears to be the most feasible way to provide quantities of HMDs, all of which would have the imperative property of fitting the helmets assigned wearer.

A further corollary of this suggestion follows naturally. When (and if) HMDs are produced in quantity, it is necessary to consider stocking spares. It is unlikely that the Armed Services would wish to stock one or more spare HMD-equipped helmets for each pilot who has one. It is likely, however, that accidents could occur that would damage a sensor bar, a visor cover, a CRT, a relay lens, a Fiber Optic Bundle, a collimator lens assembly, a visor, or a visor track. If each of these eight subassemblies could be designed as interchangeable parts with provisions for assuring correct focus and orientation where appropriate, so that a service technician (suitably trained) could replace broken or damaged parts in a field maintenance base, then the stock-piling of spares and the making of repairs become attainable objectives. Such interchangeability would lead to economies in manufacture also.

### Visor

This subsection is limited to specific tooling and procedures.

Tooling -- Use the specially designed tooling to produce the paraboloidal visor

- Parabolic templates (see Figure 100)
- Paraboloidal molds (see Figure 100 and 101)
- Aperture mask, conical paper (see Figure 102)
- Paraboloidal support wooden form (see Figure 103)
- Tilt plate (see Figures 104 and 105)

Metal Mold Procedures -- Use both convex and concave aluminum molds for this process (see Figures 100 and 101).

- Place the acrylic sheet of Plexiglas over the convex paraboloid mold in the special vacuum forming mixture. Apply heat to soften the plastic. Lower the fixture over the mold for vacuum processing. Cool and remove the formed plastic (see Figure 101).
- Trim excess material and apply mold release agent.
- Epoxy the acrylic shell into the concave parabolid mold. (Figure 101).

It is very important that the epoxy cement film be thin and uniform all around the visor blank to avoid asymmetric strains (Figure 106). The epoxy cement's liquid when applied in the center of the

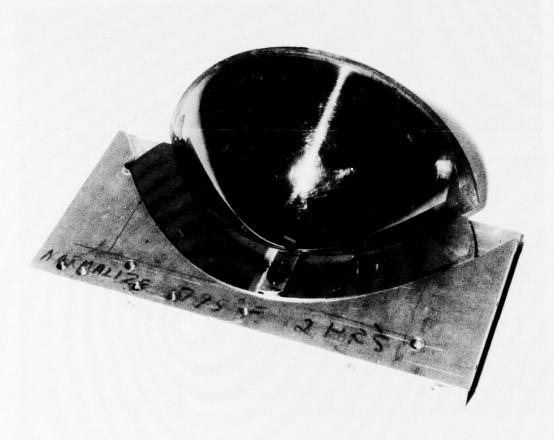


Figure 100. Hardened Template Comprising 0.016 Thickness Gage Constrained between Opposing Aluminum Templates to Assume Parabolic Contour for Both the Constrained Area and the Exposed Area (Focal length is a meridianal half section of a 1.5-in. paraboloid shell made of a different template)

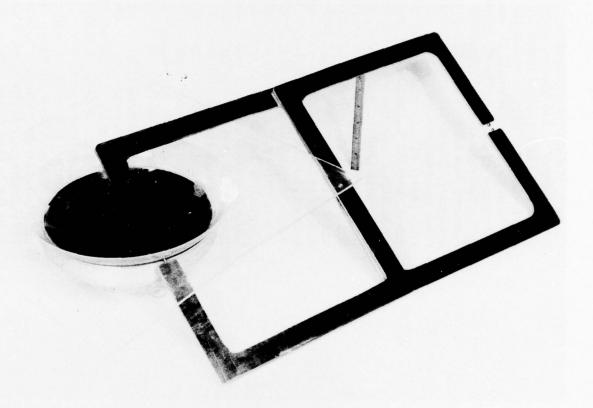


Figure 101. Vacuum Formed Acrylic Paraboloid Resting in Concave Metal Mold in which such a Paraboloid had been Previously Epoxied and Optically Machined from a Parabolic Template (Caliper is shown in position to measure shell thickness. Six-inch rule reveals the scale of the photo)

Figure 102. Concave I

which is undesirable. If the paraboloid were accurately it by changing its focus and/or direction, as observable lathe and centered so that the paraboloid's optical axis appear at infinity on axis except as aberrations distort mask was conceived, made, and used. If a point light This reveals, by flickering, such image motion seen because the apertures are seen at a frequency of the paraboloid had uniformly good surface contour and smoothness over the whole aperture zone. The avail-40 flashes per sec, appreciably above the flicker freapertures as close to the visor shell as practicable to runs true. The aperture mask would not be needed if important to select the best areas within the aperture of the mold is a conical paper mask having 4 circular Shell Epoxied to the Mating Surface. (Fitting the rim minimize vignetting of light after reflection from the assembly, minus the aperture mask, is mounted on a able paraboloid did not have such quality, and it was zone for use in the HMD. Accordingly, the aperture formed and true running, negligible flicker would be apertures positioned to define the 4 critical areas of in a telescope mounted to the lathe bed with its axis lathe is turned about 10 revolutions per sec, or 600 parallel to the lathe axis and displaced 1.5 in. The Concave Metal Mould Containing Paraboloidal Visor the visor. The cone angle is computed to place the source is located at the focal point, its image will concave face of the visor shell. In operation this quency. The procedure for finding the optimum

tedious. Examine the star image in the telescope while tedious. Examine the star image in the telescope while the lathe is spinning. Between spins, rotate the aperture mask in about 5-deg increments and note the star image quality/steadiness at each new mask setting. After rotating the mask through 36 such 5-deg increments, the results will repeat. Referring to image quality notations vs angle, select promising settings for retesting. Narrow down the candidate settings until the best is found. Mark the rim of the visor shell to locate aperture azimuths.)

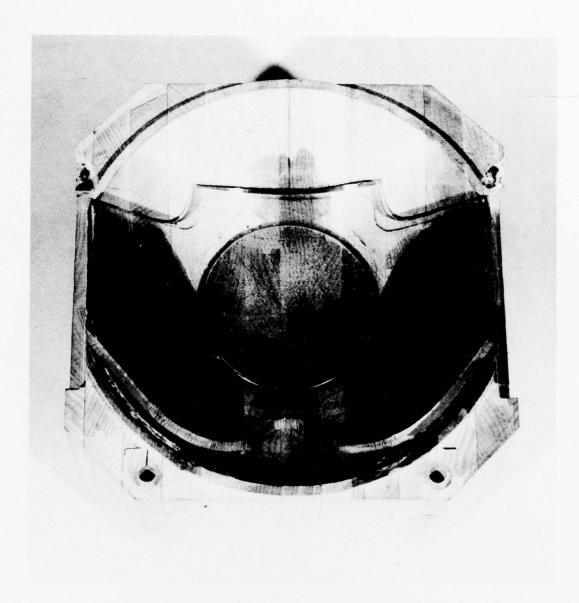


Figure 103. Test Visor Located in Concave Wood Form in Position Occupied by Paraboloidal Visor when Cemented in Place Prior to Optical Centering and Perimeter Machining Operations (Visor is first cleaned, coated with a parting material, and carefully floated on three epoxy "ponds," the outer two being confined with clay dams, the central pond being centered for gravity. Distributed forces are required to counteract flotation forces)

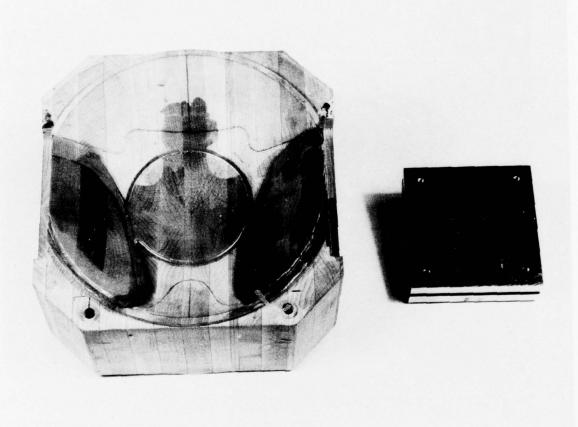


Figure 104. Concave Wood Form and Its Removed Tilt Plate (For mounting form in a lathe with 4-jaw chuck to provide two tilt axis adjustments and two transitional entering adjustments for a paraboloidal visor which may be removably cemented into the wood form)

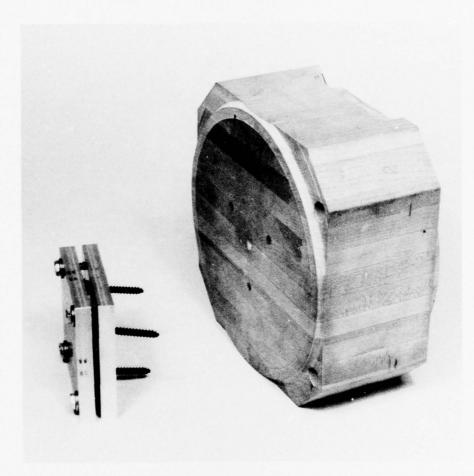


Figure 105. Oblique View of Concave Wood Form (Showing the rear surface on which is mounted the tilt plate, here shown removed. Note marks made on back member of tilt plate by 4-jaw chuck of centering lathe. Note the front and back true zonal surfaces which were turned on the lathe after optical alignment had been achieved)

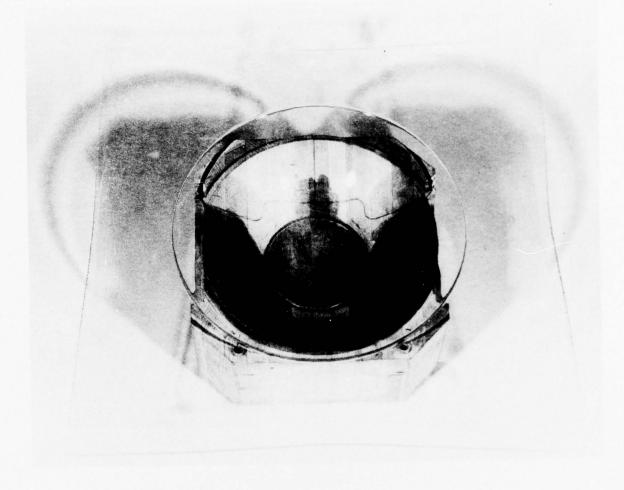


Figure 106. Vacuum Formed Plexiglass Acrylic Visor Material Drawn to Paraboloidal Shape from Square, Flat Sheet (Note how four sides are drawn in from edges. Formed shape is resting in a concave wood form which has been used in subsequent visor alignment and perimeter machining operations)

concave-up mold, forming a kind of lake on which the visor blank floats like a boat. It is necessary to press the visor blank down into the "lake bed," forcing the epoxy to rise around the "sinking boat" which is the visor blank. The "loading" of the visor blank must be uniform around its rim (as done by a local vendor: Roy Mattson of Aero Graphics) to produce a true fit between the visor blank and the mold as indicated by a uniformly thick epoxy cement layer. A height gage can be used to check the levelness of the visor blank before the epoxy cement sets.

R. A. Woodson suggests an alternative method of "sinking the boat" (which is the visor blank) in the epoxy lake in the mold. The idea is to use a distributed force that neutralized epoxy hydrostatic pressure down on the concave face of the visor blank. This can be done by placing a clean impervious flexible plastic sheet (such as Saran wrap) inside the visor blank to form a protective liner; fill this liner with a suitable liquid having about the same specific gravity as the epoxy liquid it must counterbalance. The height of liquid inside the visor blank should be the same as the height that the epoxy cement liquid should rise around the outside of the visor blank. A set of position-trim screws around the rim of the visor blank can be used for centering purposes. The epoxy film can be made dark by an additive to provide a very sensitive indication of that cement's film thickness.

#### Machine and Polish Visor

As stated previously, the concave paraboloidal aluminum mold with the paraboloidal visor blank accurately cemented to its concave surface, was machined and polished by John Hoeger, Chicago. Because a temperature below 32°F may cause uncementing of the visor blank from the aluminum mold, the assembly requires shipment in a controlled ambient temperature container. John Hoeger used proprietary procedures for machining and testing the concave paraboloidal surface. He has indicated that he can produce more accurate surfaces than that of the AHRA Mod 6 visor is required. Appropriate specification is required.

#### Finish contour and polish visor concave surface

Since Hoeger's procedures are proprietary, they are not discussed here. However, when he was questioned about non-paraboloidal zones which are observed, John Hoeger indicated that he polished more in certain areas than in other areas in

order to remove some deeper grinding marks (scratches), since no tolerance had been applied to control image quality (as influenced, e.g., by "low zones" of extra polishing). Refer to Figure 107, which shows evidence of zonal ripples in the concave surface of the visor.

- Return assembly to Honeywell
  - Note: Temperature control for return shipment is as critical as for shipment to John Hoeger.
- Mount on lathe and put aperture mask in place (Figure 102)
- Select best aperture areas of visor (Figure 102)
- Apply reference marks for perimeter shaping
- Spray with stripping film and remove visor from mold
- Rough cut its perimeter per reference marks (Figure 106)

### Wood Support Form Procedures --

- Accurately epoxy visor blank in wood support form (Figure 106)
- Mount wood support form with tilt plate in lathe (Figure 105)
- Adjust 4-jaw chuck and tilt plate to center paraboloid
- Turn two zonal surfaces on wood form true to paraboloid
- Remove from lathe and mount on mill true to zonal cuts
- Cut true four square sides on wood form
- Mill critical visor perimeter for visor extenders (Figure 107)
- Drill three mounting holes for central mirror mount
- Attach visor extenders to visor track sliders
- Mount visor tracks with sliders and extenders to jig
- Bring jig and extenders into registration with visor
- Bond extenders to visor while blocked in registration (Figure 107)
- Disassemble extenders from visor track sliders
- Remove visor and its cemented extenders from support

#### Concave Surface Coating --

- Clean visor, pack, ship to Evaporated Coatings, Inc.
- Apply inconel to transmit 3 percent visible light and inspect
- Ship to Honeywell and inspect again

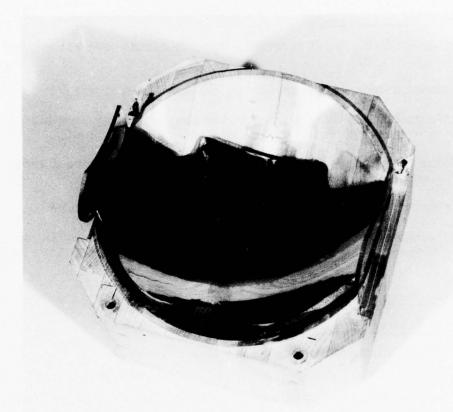


Figure 107. Completed Paraboloidal Visor Located in Its Concave Wood Form in Position It Occupied when Its Parallel Sides were Milled True, before Visor Extender Plates were Cemented to It. (Note that mill cut wood as well as plastic visor. Wood form was mounted on mill using as reference surface the two true zonal surfaces which had been turned on a lathe after the tilt plate and 4-jaw chuck had been adjusted for optical alignment of the visor which had been cemented in place. Note that this photograph of the final visor clearly shows a rippled surface in the outer zone. Appropriate analysis could reveal the depth of the ripples as well as their spatial periodicity. The ripples seen in the lower area of the visor are reflections of smooth, unrippled, edges bordering the wood image from the upper area of the wood form)

# Central Mirror Assembly

- Cement 2-in. focal reference cone to dummy central mirror (Figure 108)
- Mount above alignment unit in frame of central mirror
- Mount central mirror support bracket with alignment unit on visor and test its length and angle adjustment range
- Remove central mirror support bracket and remove dummy mirror
- Cement central mirror in its frame on support bracket
- Mount central mirror support bracket and the visor clamp linkage on appropriate sides of visor (Figures 109, 110, 111)

# Visor Assembly

# Tooling and Accessories Requirements --

- Adjustable height surface plate with septum
- Aperture plate with 5 apertures -- aluminum (Figures 95, 97)
- Reference jig to hold visor track in registration (Figure 97)
- Height gage and adjustable stylus gage
- Adjustable spot light
- Two autocollimators, boresighted to bases (Figure 112)
- When in correct alignment, the above parts form the "Visor Optical Bench" (VOB) on granite block (Figures 112, 137)

#### Procedures --

- Mount helmet on reference jig at correct tilt angle (Figure 120)
- Assemble visor on helmet in jig
- Make preliminary tests of visor tracking and its stops
- Remove helmet from jig
- Remove visor from tracks and tracks from helmet
- Set visor track stops by these substeps

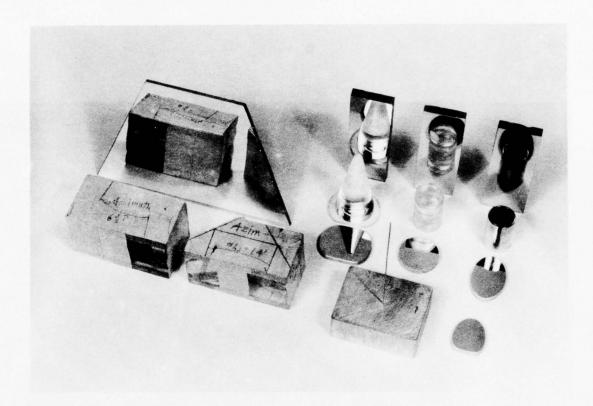


Figure 108. Trapesoidal First Surface Mirror for Miscellaneous Optical Uses, Optical Prism Assembly Producing Lateral Offset of Boresight, Optical Prism Assembly Producing Both a Lateral Displacement and a Reversal of Boresight Equivalent to a Trihedral Cube Corner Prism, Three Plexiglass Plates used as Specimens for Inconel Reflective Coating Process at Time of Coating HMD Visor to 3% Transmittance, Dummy Central Mirror Frame for Preliminary Focus Setting at Visor Focal Point, Combination Type Magnifier for Close Examination of Small Parts, Collimator Reticle Focusing and Boresighting Plug, Central Mirror, CRT/Relay Lens Folding Mirror, Focus-Finding and Center-Finding Stylus for Visor During Critical Alignment Procedures, Collimator Boresight Mirror.

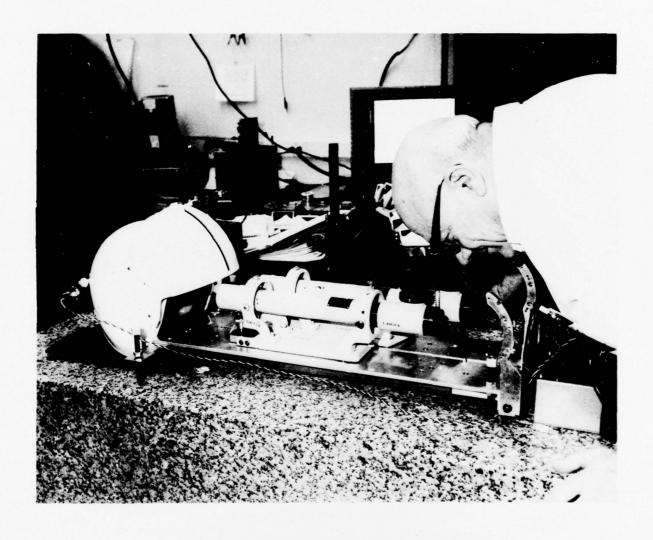


Figure 109. Checking Focus Setting of Collimator at Exit End of FOB



Figure 110. View of Concave Side of Visor with Central Mirror and Its Mount Arm in Operational Position, with Visor Clamp Linkage Attached and Open to Show Clamp Knob and Its T-Bolt in Place in Its Secure Setting. (The useful side of the central mirror faces the visor, not the forehead of the wearer. Note the visor slides attached to the visor extender plates. Retouched Photo)



Figure 111. View of Concave Side of Visor (With central mirror mount and clamp linkage attached, with linkage clamp T-bolt in place as inserted, with central mirror mount arm depressed to show stowing action. Note enlarged reflected image of central mirror at its left, not seen there when in use)



Figure 112. View of Concave Side of Visor (With central mirror mount, with visor clamp linkage open to show its construction, with central mirror mount arm in its operational position, with central mirror depressed to show its safety folding feature which protects wearer's forehead in the event of an accident)

- Mount visor tracks on jig
- Mount visor in tracks
- Align VOB with jig facing concave side of visor (Figure 118)
- Set stylus gage tip at center of curvature of the vertex area of visor and illuminate with spot light (Figure 113)
- Test level setting of visor with height gage at top true-milled edge (Figure 114)
- Adjust visor track stops as necessary to bring center of curvature at correct height relative to visor top
- Lock visor track stops when optical axis is level
- Align central mirror assembly on VOB by these substeps:
  - Mount aperture plate on jig with horizontal knife edge mounted in center of center aperture (Figure 115)
  - Set height gage at optical axis height and center on VOB at about 30 in. from aperture plate (Figure 134)
  - Illuminate height gage with spot light (Figure 114)
  - View image of height gage in central mirror (Figure 116)
  - Adjust tilt angle of central mirror to center image of height gage with horizontal knife edge; this reflection from the back face of the central mirror is a necessary preliminary adjustment (Figure 117)
  - The left autocollimator of the VOB serves as test collimator; the right autocollimator serves as test telescope for this test of the optical quality of the double bounce portion of the optical system. Light from the collimator is incident through the left aperture onto the concave side of the visor, then reflected (Figure 118) to a focus at the central mirror, thence diverging to its second reflection at the visor, thence, as collimated light, passing out through the right aperture to the telescope. The preliminary setting of the central mirror permits the image to be found in the telescope.

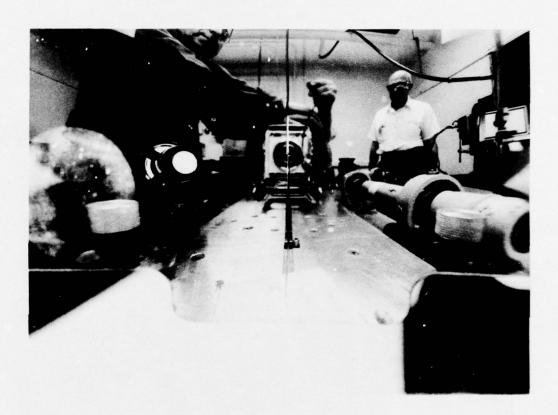


Figure 113. Visor Has Been Mounted, Aligned, Set to Selected Height. (Its optical axis passes horizontally, through the focal point and the center of curvature, of the polar zone. The height of the optical axis above the horizontal reference surface plate can be found by measuring the height of the center of curvature with a height gage. If the height gage will not reach the center of curvature, an auxiliary stylus can be used. In this photo the stylus is set with its top at the center of curvature as evidenced by the inverted stylus image touching it at the center. The stylus can be identified because its top half inch is seen to be illuminated by a spotlight. The stylus image is seen to be illuminated from behind by the spotlight whose inverted image is seen at the right. The height of the stylus tip can be measured by sliding it to within reach of a height gage - not shown in this photo)

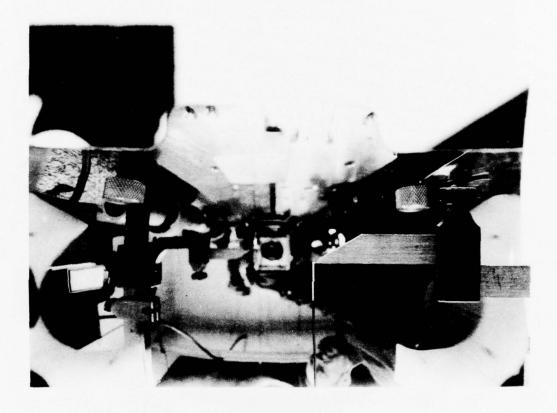


Figure 114. Previously Set Visor Reflects in Its Concave Face an Out-of-Focus Image of (among other items) the Stylus Which has been Moved Away from the Center of Curvature (of the Polar Zone) Longitudinally toward the Visor and Laterally to the Height Gage Which has been Set to Read the Height of the Optical Axis as Referenced by the Tip of the Stylus. (Note also the inverted, out-of-focus image of the height gage at the left with its index pointer set on the - blurred - tip of the stylus image. The height gage may now be repositioned along the optical axis for further alignment settings)

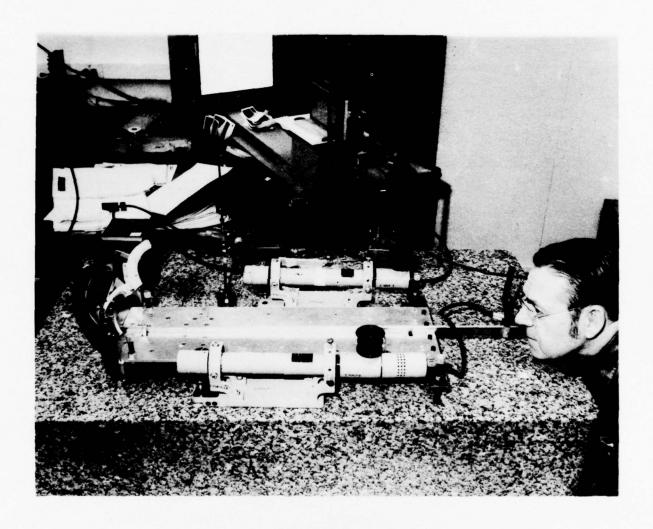


Figure 115. General View of Set-up Used to Check the Tilt Angle of the Central Mirror. (The spotlight, to the right of the height gage, is illuminating the eye which can see its own image formed by the central mirror. When that image is boresighted true, the central mirror is normal to the boresight line.

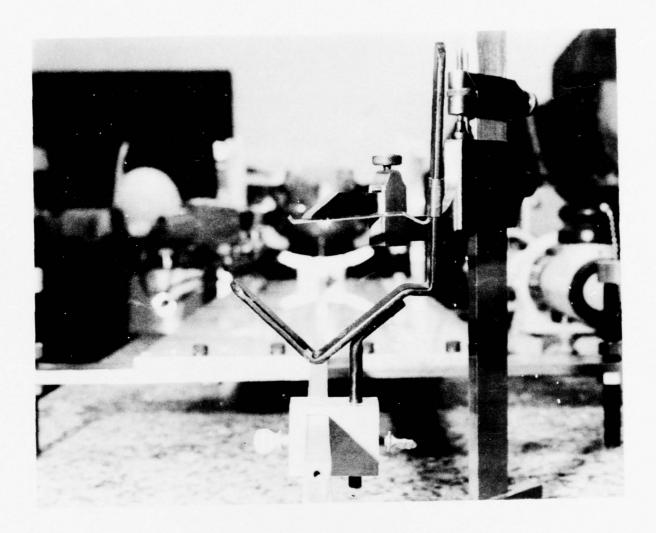


Figure 116. Height Gage, Set to the Height of the Visor Optical Axis, is Here Shown Setting the Height of an Index to be Used in Adjusting the Tilt of the Central Mirror. (The bright, starlike image directly above the horizontal central alignment bar shows that the starlike image formed by the central mirror is at the same height as the star source, so the mirror is aligned in tilt.)

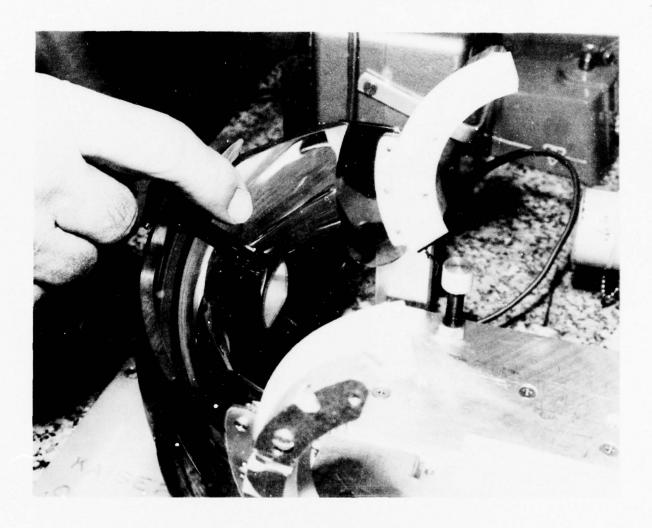


Figure 117. Visor Mounted in Its Tracks to Helmet Support Jig for Adjustment of Central Mirror. (Allen wrench in eccentric screw to adjust tilt angle of central mirror with clamping screws loosened.

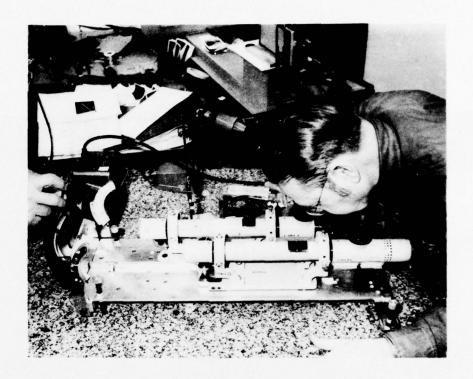


Figure 118. Set-up Used to Focus the Central Mirror after the Central Mirror has been Aligned. (Light from the collimator is directed axially to the visor's reflection aperture center, thence coming to focus at the focal point of the parabola. If the central mirror is located at this focal point, the collimator reticle image, formed by the central mirror, also is formed at this same focal point. Thence the light diverges to the complementary reflection aperture of the paraboloid which collimates the light, directing it to the aligned telescope. If, however, the central mirror is not located at the focal point of the paraboloid, but is displaced by 0.002 in., 0.1% of the 2-in. focal length, the collimator's reticle image, after two reflections, will be 0.004 in. out of focus or out by 0.002 times the focal length. The image formed by the third reflection of this system will not be located at infinity, but at a distance of  $f^2/x = 2^2/0.004 = 1000$  in. This is readily detected by the 20X telescope. It is as if the observer were noting that an object point 9 in. from his eye is closer than a similar point 11.5 in. from his eye. Another, easier, clue that the central mirror is out of focus is: not only is the collimator reticle out of focus, it is also displaced from the axis. not centered in the telescope field of view. This procedure is so sensitive that the central mirror must first be set nearly right)

- Adjust the length of the central mirror arm to correct for focus as required (Figure 119)
- Adjust the tilt of the central mirror to correct for aperture stop imaging as required (Figure 120)
- Adjust the tilt of the central mirror arm and its azimuth to avoid vignetting of the HMD as required
- Repeat the above three adjustments as necessary because they are not mutually independent. It will be necessary to repeat them as successive approximations that converge to the correct central mirror setting. Note that this procedure tests the visor using apertures (Figure 121) that are in the correct zone of the paraboloid, but whose centers are in a horizontal plane rather than in an inclined plane, as in the HMD.
- Mount helmet and visor tracks on reference jig

#### Collimator Lens

- Fabricate mount with spacers
- Procure lens elements from Rogers & Clark Manufacturing Co.
- Procure lens proof gages from Rogers & Clark
- Verify proof gages and lens elements
- Coat lens elements for antireflection (Honeywell Thin Film Lab)
- Assemble collimator lens elements in mount with temporary spring retainers; cement would be premature now.
- Provide special test tooling for collimator lens
  - Focal surface micrometer gage
  - Adjustable tilt adapter for test telescope
  - Spot light illuminator

#### Test Procedure --

- Measure curvature of field (Figure 122)
- Measure focal length
- Test resolution

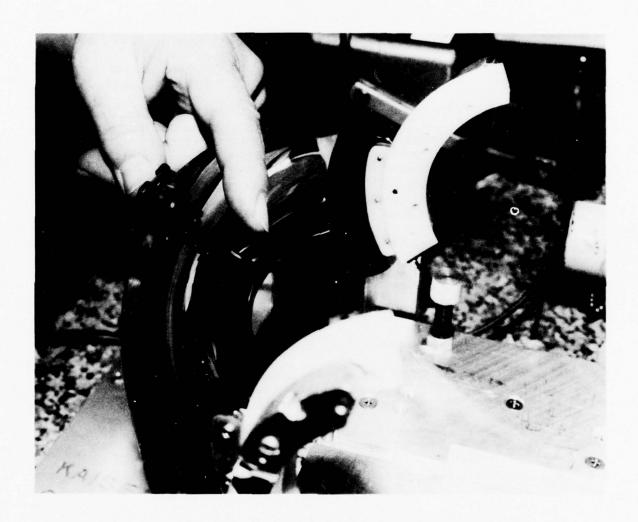


Figure 119. Visor Mounted in Its Tracks to Helmet Support Jig for Adjustment of Central Mirror (Allen wrench in eccentric screw to adjust length of central mirror arm with clamping screws loosened)

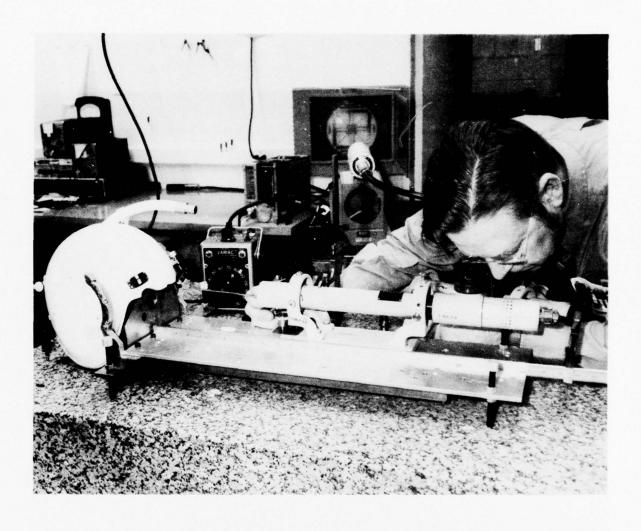


Figure 120. Adjusting Collimator Boresight Mirror Using Special Tool That Clamps to Mirror Frame

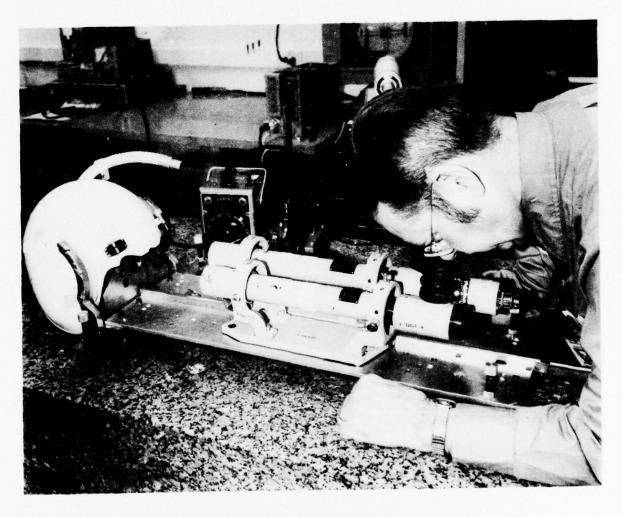


Figure 121. Checking Alignment of Collimator Boresight Mirror



Figure 122. Measuring Field Curvature of Collimator Lens Using Focusing Adapter with Illuminated Reticle and Tilting Adapter to Explore the Image Across the Field (The 20X telescope provides critical focus.)

## Relay Lens

- Optical design by Optical Research Associates
- Glass fabrication by Rogers & Clarke
- Mount fabrication, optical coating, cementing and assembly by Herron Optical Co., Division of Bausch & Lomb, Inc.
- Inspection lens elements prior to cementing and assembly at Herron Optical by David Fridge of Instrument Development Engineering Associates
- Functional test of relay lens at Honeywell

### Fiber Optic Bundle (FOB)

- Procure from American Optical Company
- Visually inspect image quality (Figure 123)
  - Voids
  - Misregistration of image (Figure 124)
  - Multifiber rows skewed with resultant tilt of illumination, causing nonuniform image brightness (Figures 125 through 130)
- Make photographic recording of image quality (Figure 131)

# Collimator Lens Assembly

### Tooling --

- Focusing reticle plug (Figures 132 and 133)
- Nylon extension arm (Figures 95, 134)
- Adjustment arm for folding mirror and collimator (Figures 95, 120, 136)

#### Procedure --

- Assemble collimator lens with focusing reticle plug on helmet (on alignment jig with aperture plate
- Coarse-align collimator using nylon rod jig and caliper (Figures 95, 134, and 135)

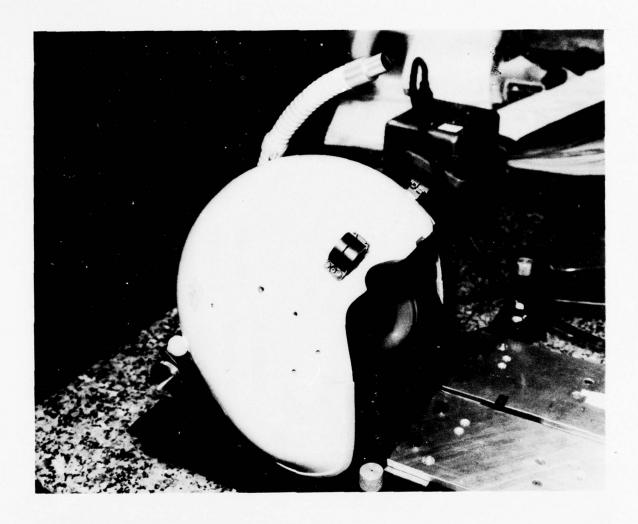


Figure 123. Helmet with Dummy CRT Installed and with Exit End of Fiber Optic Bundle Accessible for Examination of its Transmitted Image After the Resolution Target Has Been Imaged by the Relay Lens Sharply Upon the Entrance End of the FOB (Brightness of dummy CRT resolution target is controlled by variac shown in the background. Lamp is not in place here.)

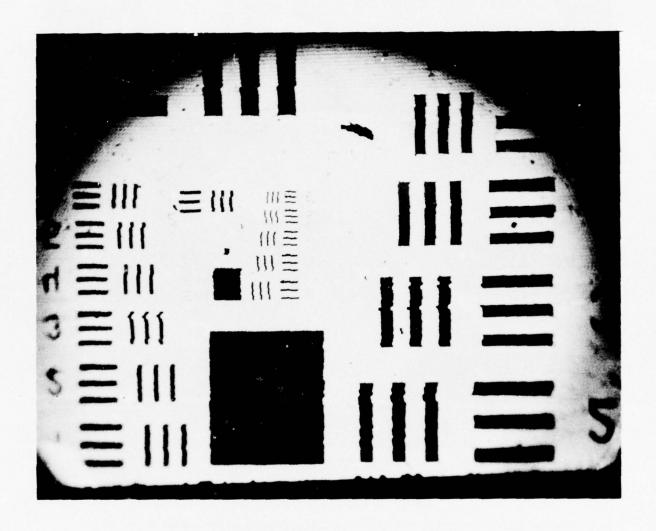


Figure 124. Photograph of the Dummy CRT as seen through the Fiber Optic Bundle (Though this photo is somewhat out of focus and overexposed, it clearly shows the dislocations of rows of multifibers in the FOB. This causes image misregistration in the horizontal direction.)

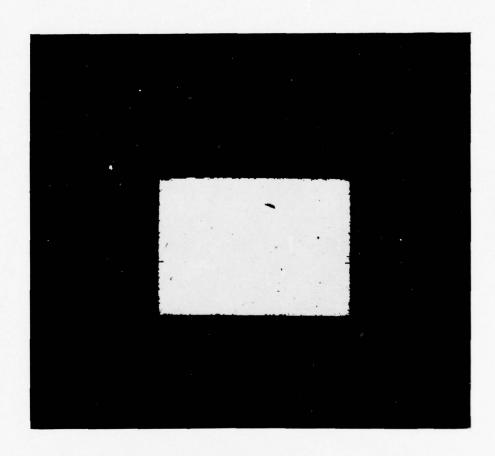


Figure 125. 1-27-72, FOB with Diffuse Illumination, Film Strip No. 6, Photo 21, Frame 2A

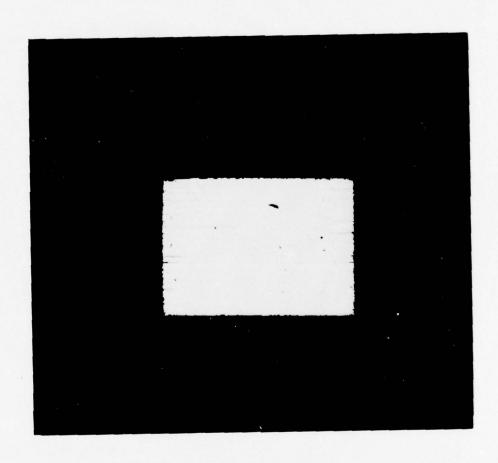


Figure 126. 1-27-72, FOB with Axial Illumination, Film Strip No. 6, Photo 22, Frame 5A

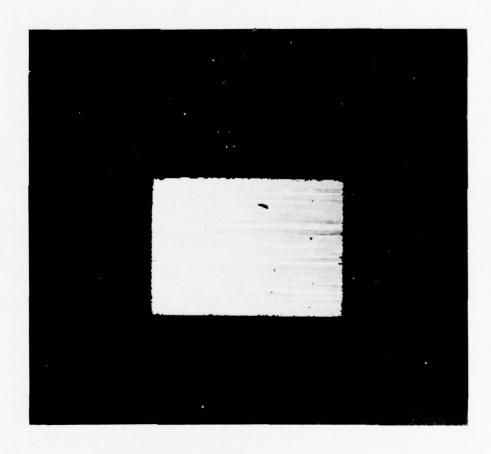


Figure 127. 1-27-72, FOB with Off-Axis Illumination, Angle Left, Film Strip No. 6, Photo 23, Frame 11A

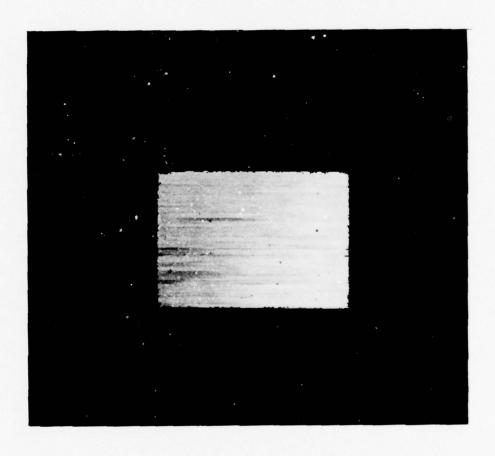


Figure 128. 1-27-72, FOB with Off-Axis Illumination, Angle Right, Film Strip No. 6, Photo 24, Frame 11A

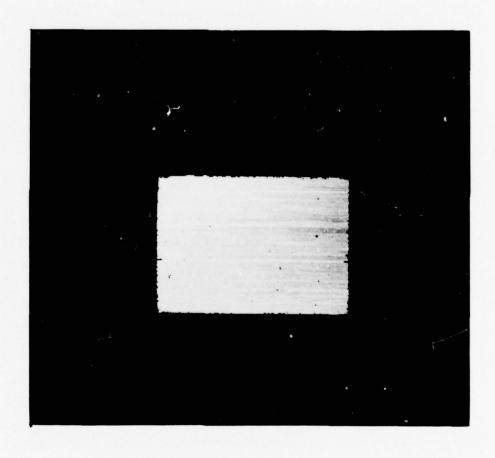


Figure 129. 1-27-72, FOB with Off-Axis Illumination, Angle Bottom, Film Strip No. 6, Photo 25, Frame 18A

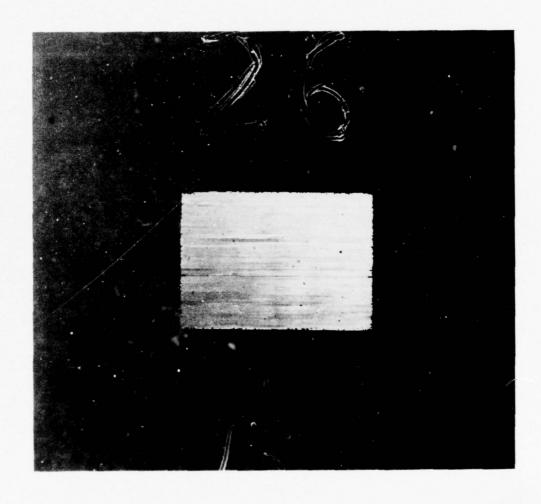


Figure 130. 1-27-72, FOB with Off-Axis Illumination, Angle Top, Film Strip No. 6, Photo 26, Frame 20A

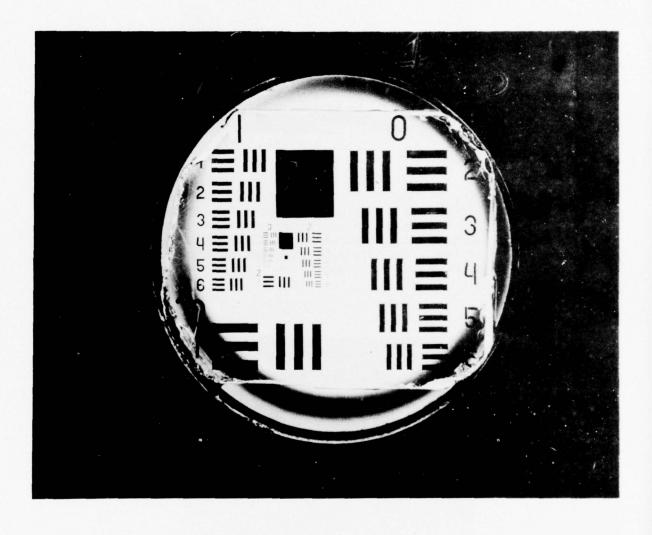


Figure 131. Photograph of the Dummy CRT Which Comprises a Tube with a Standard 1951 USAF Resolution Chart Slide Transparency at One End (in Place of the CRT Faceplate and its Video-written Image) and a 28-volt Lamp at the Other End to Provide the Illumination.

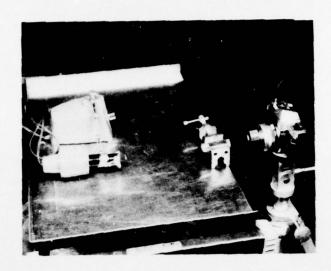


Figure 132. Set-up Used to Photograph the Boresight Reticle
Pattern of the Collimator Boresight/Focusing Plug
(This plug and an accessory collimator lens are
held in the drill/press vise. Illumination source is
at left. The camera is focused, at infinity, on the
reticle pattern image.)

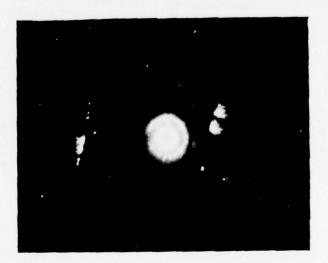


Figure 133. Macrophotograph of Reticle Pattern of the HMD Collimator Boresight/Focusing Plug (The preceding photograph shows the set-up used to take this photo. The circular image defines the boresight direction when used with the HMD collimator in place of the Fiber Optic Bundle.)

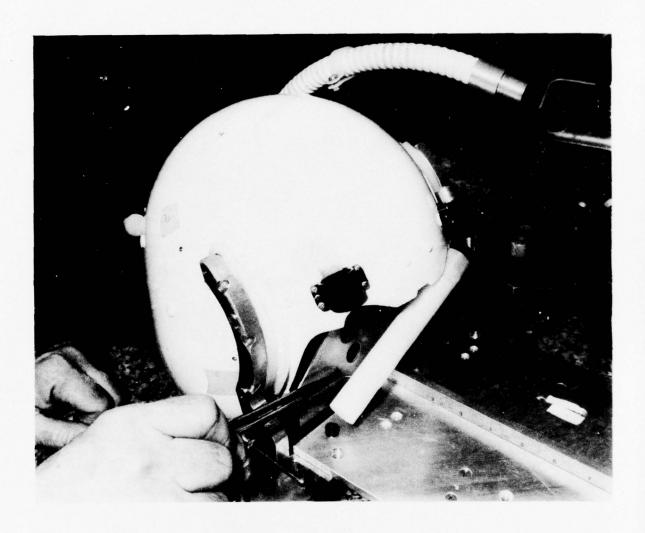


Figure 134. With Helmet Mounted on Alignment Jig with Aperture Plate in Place, Inside Calipers are Used to Set and Check Parallelism of Collimator Mechanical Axis with Transverse Plane by Means of Nylon Rod Jig Mounted on Collimator Lens Mount.



Figure 135. With Helmet Mounted on Alignment Jig with Aperture Plate in Place, Inside Calipers are Used to Check Parallelism of Collimator Mechanical Axis with Transverse Plane by Means of Nylon Rod Jig Mounted on Collimator Lens Mount. In This Photo the FOB is Mounted at Focal Plane of Collimator Lens, Though Normally This Parallelism Alignment and Test is Done Before Such FOB Assembly.

- Assemble folding mirror and adjustment arm
- Adjust VOB to nominal height of collimator aperture
- Illuminate reticle plug from rear, sight with telescope
- Aim collimated beam with adjustment arm using telescope (Figure 136)
- Clamp collimator in its saddle mount
- Clamp folding mirror, making sure that the aperture is correctly located with respect to the aperture plate (Figure 136)
- Check boresight with telescope; realign if necessary and reclamp; recheck boresight

# Preliminary Assembly (Figure 137)

- Assemble relay lens and its folding mirror
- Assemble FOB at relay end and at collimator end, attach clamp (Figure 138)
- Orient the FOB for correct aspect of rectangular format
- Focus relay end of FOB with dummy CRT installed
- Focus collimator end of FOB and check aspect angle (Figure 139)
- Check image of dummy CRT as seen from collimator folding mirror using the telescope on the VOB
- Make needed adjustments as are apparent and recheck image
- Remove from alignment jig

#### FINAL ASSEMBLY AND TEST

### Assembly of Visor to Helmet

- Assemble visor cover (Figures 140 through 143)
- Attach visor clamp and test its function
- Check clearances of visor and other parts during visor motion

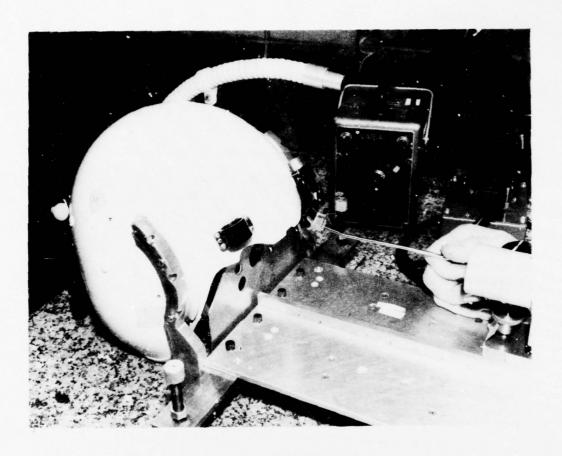


Figure 136. After the Mechanical Axis of the Collimator Lens Has Been Made Parallel with the Transverse Plane, the Optical Axis of the Collimator with its Boresight Mirror is Made Perpendicular to the Transverse Plane, Thus Boresighting These Two Optical Components. Using the Special Tool That Clamps to the Boresight Mirror Frame (to Get Increased Leverage and Thus Increased Directional Control), the Autocollimator Sets the Boresight Direction for Light Reflected From the Collimator's Focal Plane Mirror Plug, so That Boresighting Can Be Achieved. The Collimator and the Boresight Mirror are Then Clamped.



Figure 137. General View of HMU Mounted on Alignment Jig
(Mounted CRT and spare CRT with its cable coiled and without its fiberglass insulating sleeve, dummy CRT with 1951 USAF resolution target and with illuminator lamp and 28-v power supply, COHU TV vidicon camera, camera electronics, modified GFE Hughes display electronics with modified circuit card raised on extender card for access, light box with various object target patterns. On the granite block are special alignment instruments including the adjustable height surface plate with septum, two autocollimators, either or both of which may be used as boresight collimator on telescope.)

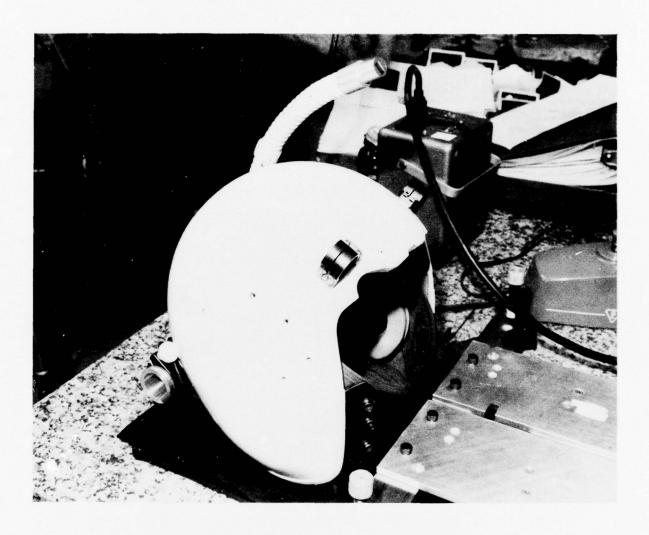


Figure 138. Helmet with Fiber Optic Bundle Attached at its Entrance End to the CRT/Relay Lens Housing at Rear of Helmet, Clamped at Midpoint to Helmet, Exit End Standing Free

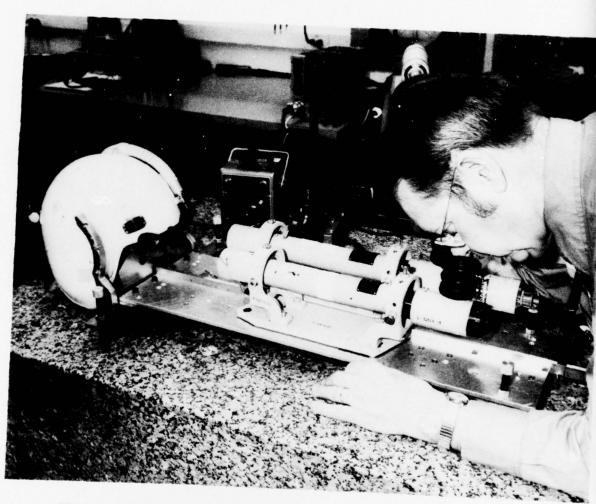


Figure 139. Checking Focal Setting of Exit End of Fiber Optic Bundle, Using Autocollimator Which Illuminates the FOB (The telescope on the left of autocollimator is not in use.)



Figure 140. Helmet with Visor Mounted and in Retracted Position, with Visor Cover Removed and Visible, with Visor Clamp Knob and Linkage Attached to Visor, with Fiber Optic Bundle Attached

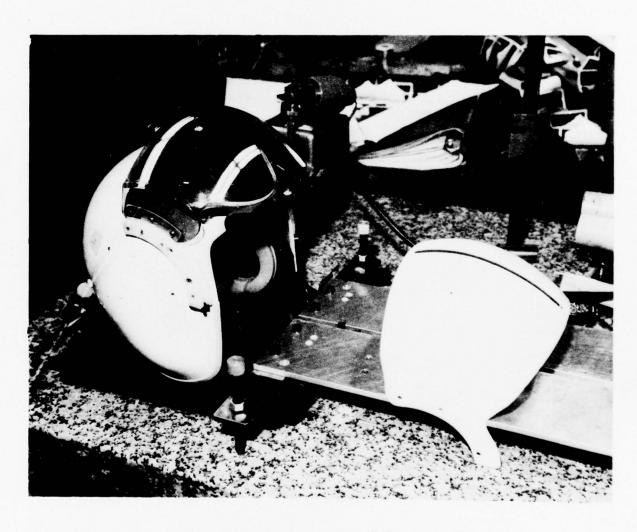


Figure 141. View of Visor Mounted on Helmet, in Retracted Position, with Visor Cover Removed and Visible



Figure 142. Helmet with Visor Mounted and in Operational Position, with Visor Cover Removed and Visible, with Visor Clamp Linkage Attached and Folded to Operational Form, with Visor Clamp Knob Removed From Linkage and Placed in its Slot in Visor Cover, with Fiber Optic Bundle Attached at Both Ends and at Midpoint

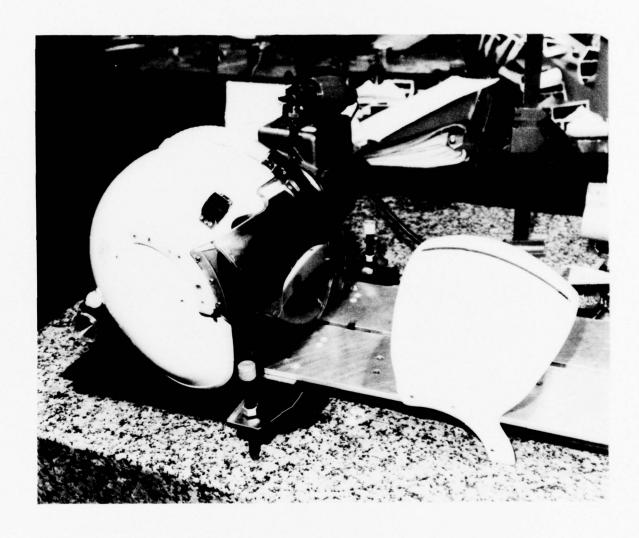


Figure 143. View of Visor Mounted on Helmet, in Operational Position, with Visor Cover Removed and Visible, with its Image Seen Reflected by Convex Side of Visor

# Wearing of Helmet With All Parts in Place, Including Dummy CRT

- Adjust focus of dummy CRT as necessary
- Check aspect angle of FOB format and adjust at collimator end as necessary
- Check focus of FOB at collimator end and adjust there as necessary
- Replace dummy CRT with functional CRT having distortion sweep compensation (Figure 144)
- Focus CRT in its mount and rotate format as required
- Test visor retraction and clamping
- Test location of exit pupil relative to eye position
- Test sense of distortion sweep compensation and correct if necessary (Figures 145 through 152)
- Test for white-out condition, correcting visor opaque areas if necessary
- Clean up HMD for Acceptance Test by Customer

# Acceptance Test

- Repeat procedure for the critical portions of the testing done during assembly and adjustment operations
- Demonstrate performance in operation by using test targets and standard TV camera system (Figures 153 through 156)
- Following formal Acceptance Test take documentary photographs to verify quantative measurements and to provide a permanent record of the HMD to supplement photographs taken during various steps in the assembly and alignment of the subassemblies and the final assembly (Figures 157 through 160).



Figure 144. Helmet with All Optical Parts of HMD Mounted Except the Visor and its Central Mirror (Here shown removed from helmet. The dummy CRT is in place of the CRT.)

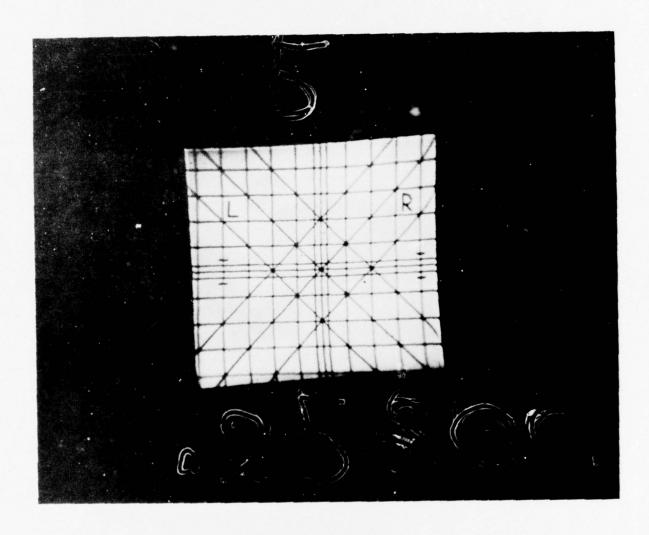


Figure 145. View of CRT Images as Seen Looking into Boresight Mirror or Collimator with Helmet Mounted on Alignment Jig, Level, with Visor Up; Electronic Paraboloidal Distortion Compensation OFF

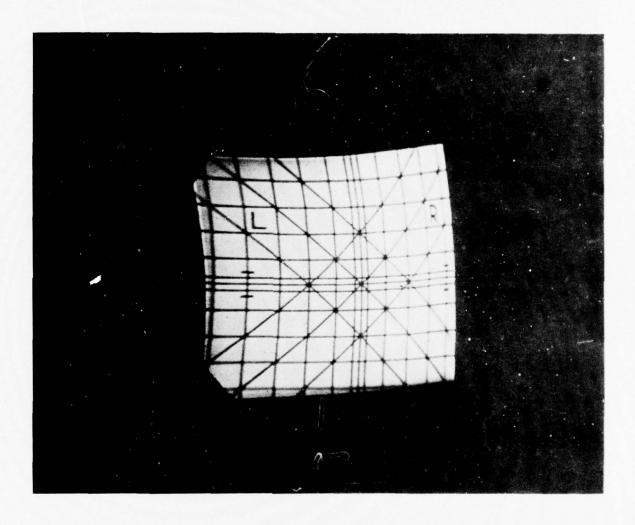


Figure 146. View of CRT Image as Seen Looking into Boresight Mirror of Collimator with Helmet Mounted on Alignment Jig, Level, with Visor Up; Electronic Paraboloidal Distortion Compensation ON

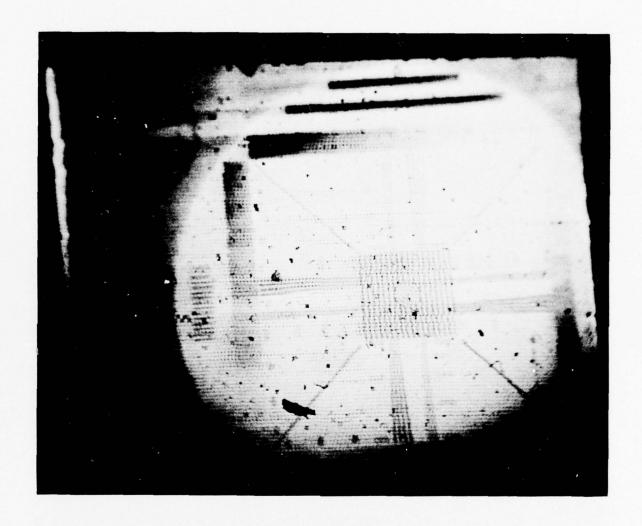


Figure 147. Image of Retna Resolution Chart from TV Camera and Modified Display Electronics with Parabolic Sweep Distortion Correction OFF. The Video Is Fed to the HMD CRT, Relayed to the FOB Where it is Conducted to the Exit End of the FOB, Collimated By the Collimator Lens, and Reflected Forward by the Boresight Mirror. The Visor is UP, so This Collimated Image is Recorded by a Pentax Camera Which is "Looking" at the Boresight Mirror and Which is Focused for Infinity. Note Dust On, and Flaws in the FOB.

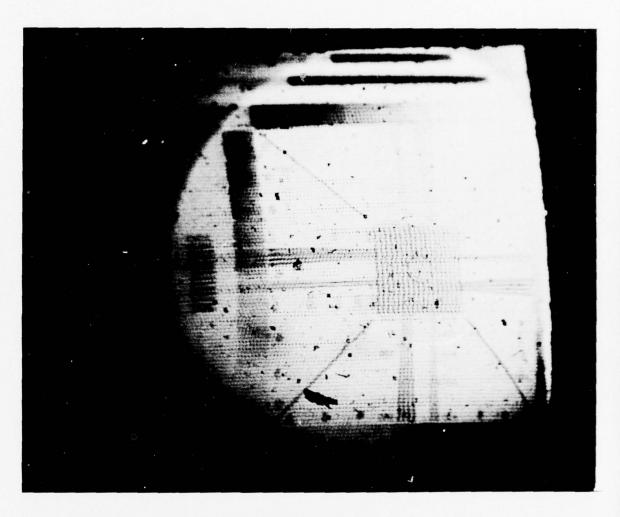


Figure 148. Image of Retna Resolution Chart From TV Camera and Modified Display Electronics with Parabolic Sweep Distortion Correction ON. (The conditions for this photo are the same as for the preceding photo except for the electronics setting with parabolic distortion correction selection. Note that the image shows curved image lines which would have been seen as straight lines by a pilot wearing this HMD with the visor DOWN, since the distortion produced electronically compensated that produced optically by the visor. Without the visor down, the camera sees only the electronically produced distortion.)

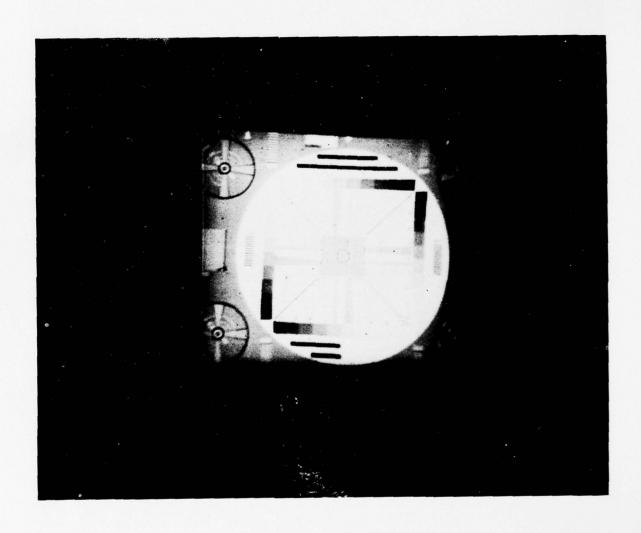


Figure 149. Green CRT (new) Retna Resolution Chart, Parabolic Compensation OFF

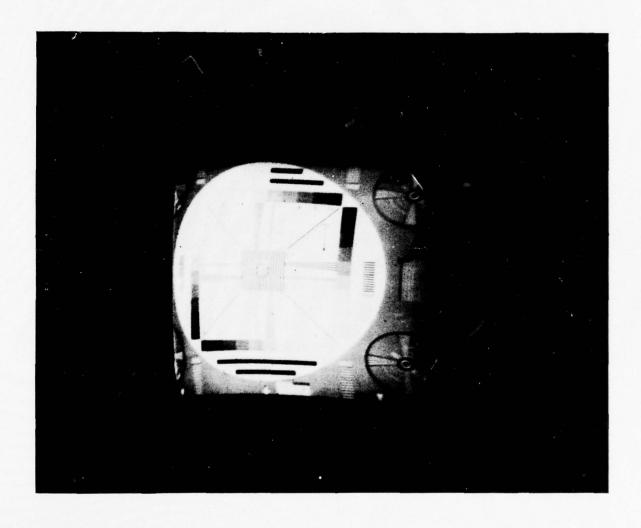


Figure 150. Green CRT (new) Retna Resolution Chart, Parabolic Compensation ON

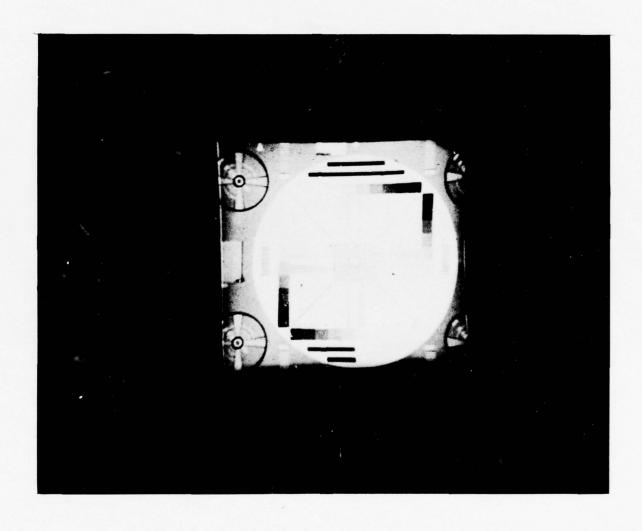


Figure 151. White CRT Retna Resolution Chart, Parabolic Compensation OFF

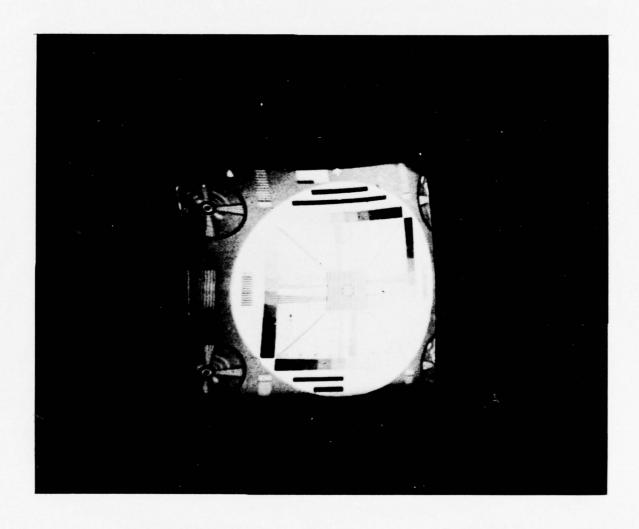


Figure 152. White CRT (old) Retna Resolution Chart, Parabolic Compensation ON

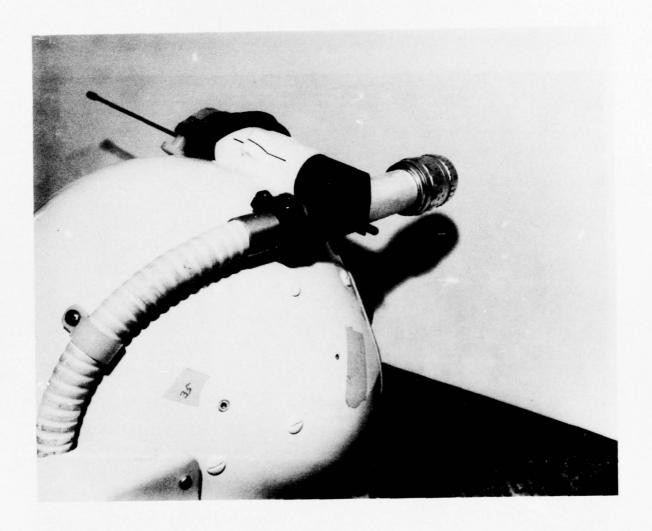


Figure 153. Close-up of Auxiliary Lens as Mounted on HMD to By-pass CRT (This mount required removal of CRT/relay lens folding mirror. Only this mirror was removed; the rest of the HMD optical system is in place. The object is focused on the object plane of the relay lens, as if it were the CRT raster.)

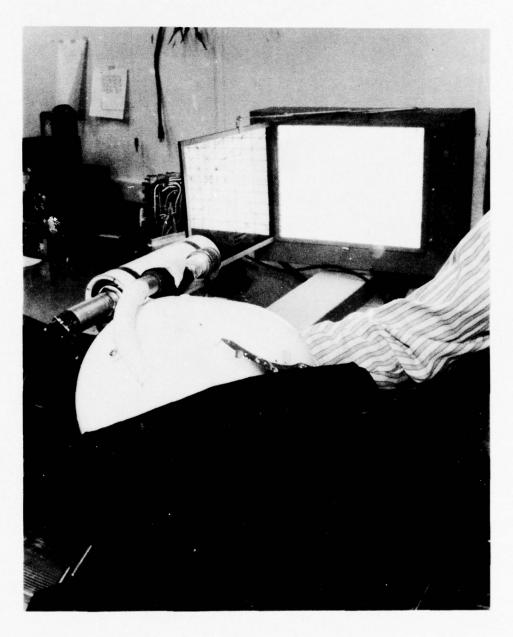


Figure 154. Here the Complete Set-up is Shown for Photographing with a Minox Camera the Distortion Test Grid as Seen by the Entire HMD Optical System (Minus the CRT and its Electronic Distortion Compensation Circuitry) (The black cloth prevents the camera from looking through the visor at irrelevant objects.)



Figure 155. When Helmet is Held at This Angle and an Auxiliary Lens Focuses an Image of a Rectangular Distortion Test Grid Pattern on the Object Plane of the Relay Lens (with CRT/Relay Lens Folding Mirror Removed) the Aspect Angles Match and the Full Field Can Be Photographed with the Minox Camera. The Final Image Reveals the Distortion of the Entire HMD Optical System (Minus the CRT and its Electronic Distortion Compensation Circuitry). Note That the Visor is in its Operating Position. The Camera can be Exposed in the Manner Shown. In Order to Avoid Undesired Imagery Being Photographed Through the Visor, an Opaque Cloth is First Placed Over the Visor.



Figure 156. With the Helmet Removed From Its Alignment Jig, the Complex Supporting Means and the Position of the Photographer's Hand Are Visible. (Note the parallel clamp in the lower left corner and the locating tapes around the ball-joint clamp. The rectangular distortion test grid image is visible as reflected from the hinged side plate. In this photo the grid appears overexposed. At its left, above the TV camera, is visible the display electronics card (raised on an extender card for access). This is the card carrying Honeywell's electronic paraboloidal distortion correction circuitry.)

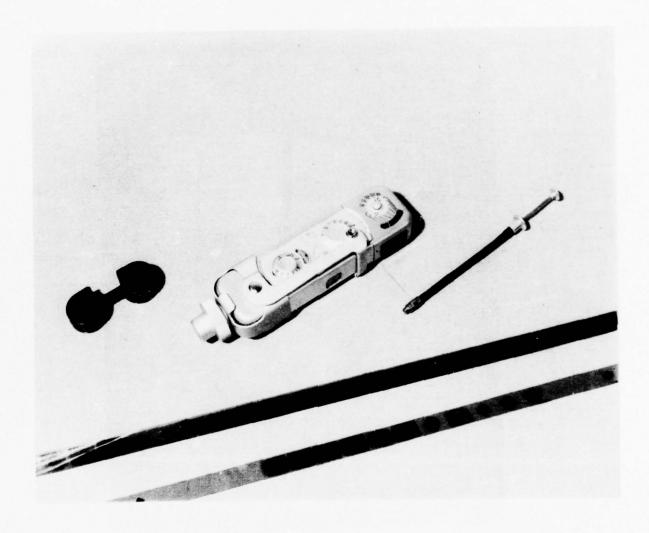


Figure 157. Minox Film Cassette After Film Has Been Removed for Processing (Minox camera in its tripod mount with shutter cable release removed and placed nearby, two lengths of processed Minox film negatives.)

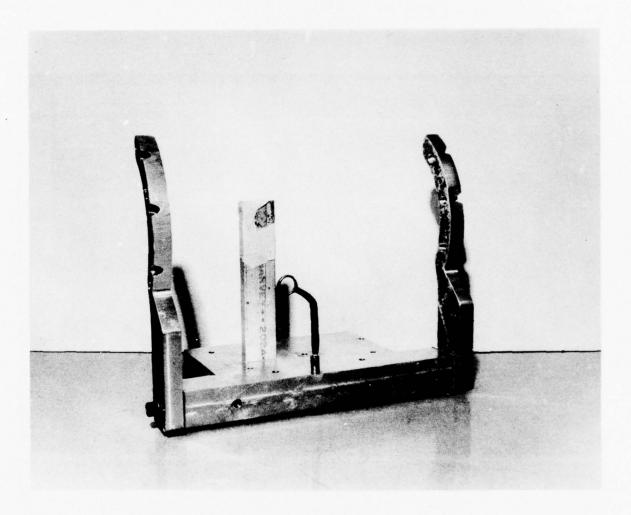


Figure 158. Helmet Alignment Jig with Lorgnette in Place Showing Where the HMD Exit Pupil Will Be When the Helmet With HMD is Mounted on the Alignment Jig (The rectangular post behind the lorgnette is a custom camera clamp support with the clamp position defined by the edge of tape.)

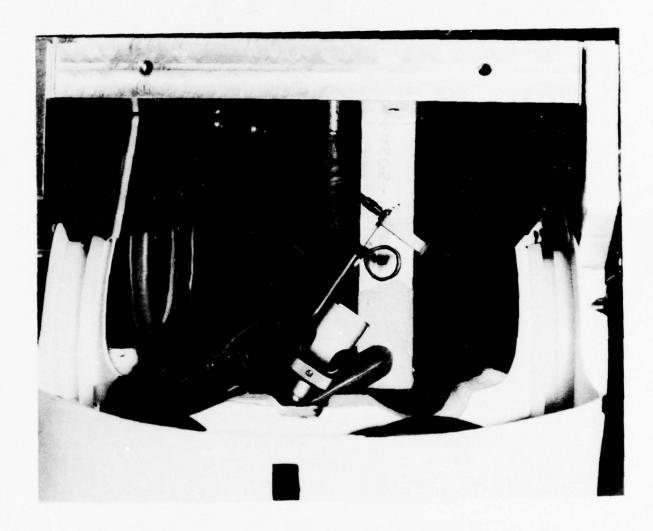


Figure 159. Close-up of Helmet Mounted on Alignment Jig With Camera Tripod Mount (Less Camera) Mounted in Place Behind Lorgnette (Camera can be removed for reloading and then replaced without changing preset alignment. Note camera shutter cable release attached to camera tripod mount.)

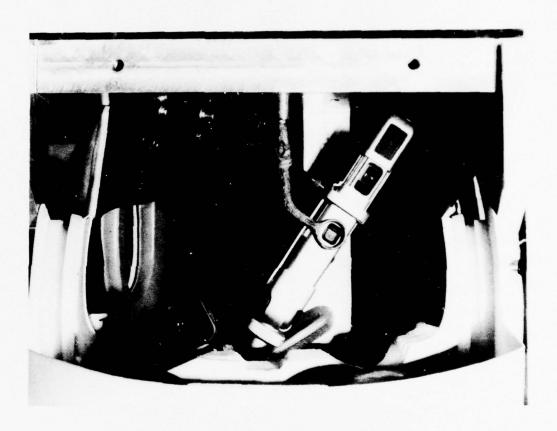


Figure 160. Close-up of Helmet Mounted on Alignment Jig with Camera Mounted in Place Behind the Lorgnette (Camera viewfinder and exposure meter are not used in this set-up. HMD collimator assembly with boresight mirror are visible three inches from lorgnettedefined exit pupil. When visor is lowered, the central mirror will be positioned midway between the exit pupil and the collimator boresight mirror. Note shutter cable release below collimator assembly. Film is advanced between exposures by closing and reopening Minox camera. Other photos of Minox camera show it closed.)

# APPENDIX I HOLOLENS DESIGN CONCEPT STUDY (PHASE II)

## INTRODUCTION

Work on holographic display was originally undertaken in response to a request from Honeywell's Systems and Research Division. Their interest is in projection of a reticle pattern to the eye of a pilot wearing a helmet sight. The reticle projection is currently accomplished by means of a geometrically shaped visor projection in front of the pilot's eye. Other methods of reticle projection are desirable.

One other method is to coat the face plate of the helmet sight with a material in which a hologram would be encoded. The hologram would serve as an optical element in the projection system.

The holographic display project was begun in order to investigate this idea. Work to date has involved the specific task of reticle projection. However, holographic display has greater scope than this one application. Alterable holographic displays offer many important possibilities for effective presentation of information. Visually-coupled control systems in aircraft can use more sophisticated holographic displays. The flexibility of holographic systems for information display and processing provides attractive methods for interfacing with computer input and output.

Because of these possibilities, the work has been materials-oriented. In addition to the specific task of reticle projection, this project has the aim of developing phototechnology and investigating suitable alterable materials for real-time displays that are of interest in a variety of applications. Although the emphasis in this appendix is on the specific application of the helmet sight reticle, it is important to remember that there are other potentially useful applications.

#### THEORY

In reticle projection, the hologram simply acts as a curved mirror; that is, an optical element in the projection train. The image of the reticle itself is not stored in the hologram.

To understand how the hologram can act as a curved mirror, consider Figure 161. This shows a similarity between zone plates and holograms. In part (a) of Figure 161, spherical waves emerging from a pinhole interfere with plane waves from the same original laser source. The interference between the plane waves and the spherical waves forms circular fringes of

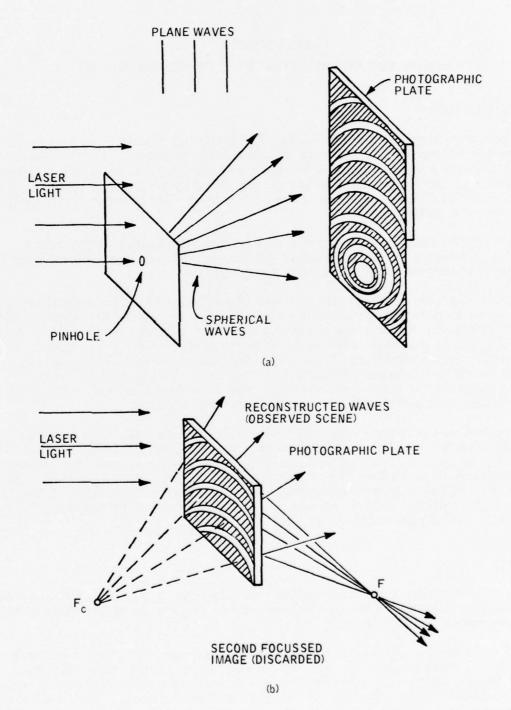


Figure 161. A Hologram as a Zone Plate

constructive and destructive interference. These fringes are recorded as light and dark zones in the photographic plate. This recording of the interference pattern between the plane wave and the spherical wave forms a hologram, a simple one, but still a hologram. It is also similar to a Fresnel zone plate.

When the photographic plate is developed and illuminated with laser light, as shown in part (b) of Figure 161, a real image and a virtual image of the original object are produced, in accordance with the principles of holography. Since the original image was simple, a point, the reconstructed images are both points. The real image will be a converging bundle of rays which focus to a point image, located at the focal point F. The real image is not of particular interest for this application. The virtual image will be a bundle of spherical waves which diverge from the position of the original pinhole. The virtual image is located at the conjugate focal point  ${\bf F_c}$ . The focal length of this system is equal to the distance from the pinhole to the photographic plate in the original recording.

These arguments show that this simple hologram will affect the beam of laser light exactly as a lens would. A negative lens would produce spherically diverging rays, and a positive lens would produce converging rays which would focus to a point.

These considerations are not a rigorous proof, but rather a simple discussion meant to show that holographic zone plates possess the properties of both negative and positive lenses.

There are stringent requirements on the projection system. The hologram must provide high visibility against a background of sunlight on clouds. This means that the brightness of the image must be at least 15,000 ft-L. An orange reticle color provides the best contrast against blue sky and white clouds. The image must be collimated at optical infinity to provide proper aiming of the helmet sight. There must be no undesired reconstruction or interaction with other light sources and no reflections. Vision through the visor with the hologram encoded on it should be undistorted, with high visor transmittance. The hologram should be stable, particularly in humid environments.

To meet these requirements, one must use a volume hologram. Volume holograms are those in which the thickness of the hologram is larger than the spacing between the fringes which form the hologram. Fringes are formed through the thickness of the recording medium, and the entire volume of material is operative in producing the hologram.

Volume holograms can operate in reflection, can be highly transparent (because they operate on a phase principle rather than an amplitude principle), and also provide high efficiency. All these characteristics are desirable in producing hololenses with the required properties.

Of particular importance, in the theory of production of volume holograms and the properties of the images reconstructed from them, are the conditions on angular orientation of the various beams involved in the holographic recording. The amplitude  $\mu$  of the reconstructed image is given by:

$$\mu = \frac{C \sec \psi \operatorname{sinc} \left\{ \left( \frac{kL}{2\cos \psi} \right) \left[ \pm \cos \left( \psi - \theta_{r} \right) \pm \cos \left( \psi - \theta_{s} \right) + \cos \left( \psi - \theta_{i} \right) - 1 \right] \right\}}{\left[ \pm \sin \left( \psi - \theta_{r} \right) \pm \sin \left( \psi - \theta_{s} \right) - \sin \left( \psi - \theta_{i} \right) \right]}$$
(1)

where C is a constant,  $k=2\pi/\lambda$ , with  $\lambda$  the wavelength used both for recording and reconstruction, sinc  $\alpha=\sin\alpha/\alpha$ ,  $\theta_i$  is the angle of the reconstructing beam,  $\theta_r$  is the angle of the reference beam,  $\theta_s$  is the angle of the signal beam from the object, and  $\psi$  is the angle of the reconstructed image. The angles are measured as shown in Figure 162. It is important to note that these angles are defined within the recording medium and will be different from the angles observed outside the medium, because of the operation of Snell's law. In Equation (1), the upper sign represents a real image and the lower sign represents a virtual image.

The diffracted wave is maximized when the argument of Equation (1) is 0. Thus, one is led to the following condition:

$$\pm \cos(\theta_{\mathbf{r}} - \psi) \pm \cos(\theta_{\mathbf{s}} - \psi) + \cos(\theta_{\mathbf{i}} - \psi) - 1 = 0$$
 (2)

This equation essentially represents four vectors that sum to zero. The vectors are of equal length when the same wavelength is used for recording and reconstruction.

Several combinations of angles satisfy Equation (2). Of particular interest is the combination:

$$\theta_i = \theta_r$$
,  $\psi = \theta_s$ 

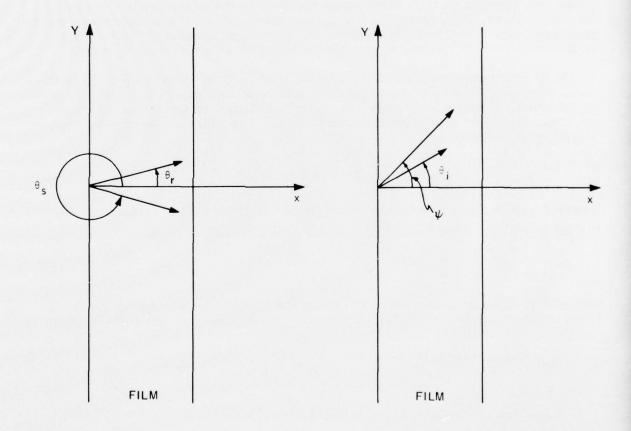


Figure 162. Definition of Angles  $\theta_{\rm S}$ ,  $\theta_{\rm r}$ ,  $\theta_{\rm i}$  and  $\psi$ 

This represents a virtual image, formed when the reconstructing beam is incident along the same direction as the reference beam. The virtual image will be formed in the same position as the original object. This situation is illustrated in Figure 163. Figure 163 shows a recording by a plane wave and a spherical wave from a point source. The two waves are incident on opposite sides of the recording medium. This feature of having the two waves incident from opposite sides will form interference fringes throughout the volume of the material. This shall be considered in more detail later. Figure 163 also shows reconstruction by a plane wave incident in the same direction as the reference wave. The image is reconstructed in reflection as spherical waves apparently diverging from the position of the original point source. This behavior shows why the hologram can be considered equivalent to a lens.

It is instructive to consider the pattern of fringes formed by a plane wave and a diverging spherical wave incident on opposite sides of a volume recording medium as shown in Figure 163a. In this figure, the medium is shown bisecting the angle  $\theta$  between the two beams. The plane wave may be represented by the equation:

$$A e^{i\vec{k}\cdot\vec{r}} = A e^{-k\sin(\theta/2)x + ik\cos(\theta/2)y}$$
(3)

where A is the amplitude of the wave, which is independent of position and  $r = (x^2 + y^2)^{1/2}$ . The spherical wave is given by the equation:

$$\frac{\mathbf{B}}{\mathbf{r}} \mathbf{e}^{i\vec{\mathbf{k}} \cdot \vec{\mathbf{r}}} = \frac{\mathbf{B}}{\mathbf{r}} \mathbf{e}^{i\mathbf{k}\mathbf{r}}$$
 (4)

where B is the amplitude. The origin of the coordinate system is the point from which the spherical wave diverges. The intensity of the light is given by

$$\left|A e^{-ik\sin(\theta/2)x + ik\cos(\theta/2)y} + \frac{B}{r} e^{ikr}\right|^{2} = A^{2} + \frac{B^{2}}{r^{2}} + \frac{2AB}{r} \cos\left[k(-\sin(\theta/2)x + \cos(\theta/2)y - r)\right]$$
(5)

The formation of a fringe will occur at the maxima of this oscillating function; i.e., at positions such that

$$-\sin(\theta/2)x + \cos(\theta/2)y - r / N\lambda$$
 (6)

where N is a large integer. The positions of the fringes have been calculated for the case where  $\theta$  = 30 deg and the origin of the spherical waves lies 2.6794 cm to the left of the left edge of the recording film. For this case, the interaction of the centers of the two wavefronts is near y = 10 cm. The results

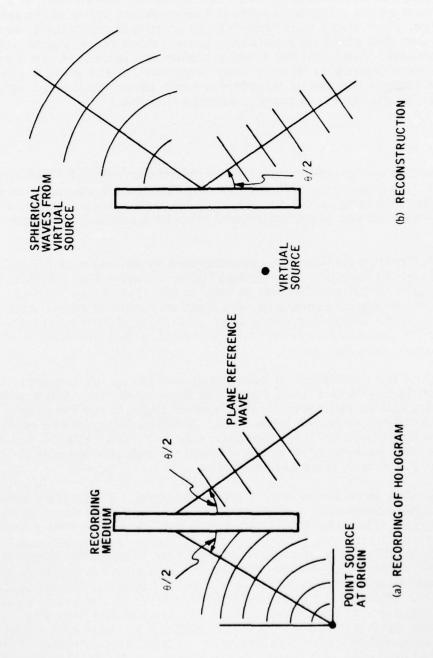


Figure 163. Formation of Virtual Image of Point Source

are plotted in Figure 164, which shows the fringe patterns throughout the thickness of a piece of film assumed to be 14  $\mu$  thick, in the vicinity of y = 10 cm. The numbers on the fringes indicate the appropriate value of the integer N for each fringe. There are approximately 10 fringes through the thickness of the film, so that this could be considered to be a thick three-dimensional holographic material. Note that the x and y scales in Figure 164 are not the same, but that the x dimension is very much expanded. This gives a graphic portrayal of the fringes formed by interference of a plane wave and a spherical wave in a three-dimensional holographic storage medium.

## **APPARATUS**

To perform this holographic work, a new interferometrically stabilized bench and a new holographic system was set up. The bench was a granite slab, 22 in. wide, 6 ft long, and 9 in. thick. This was mounted on tiers of concrete blocks with layers of carpeting and vibralock padding to reduce vibration.

The interferometric stability was investigated by setting up a Michelson interferometer and photographing the fringe patterns formed by a helium-neon laser. Photographs of extended duration were taken, lasting as long as 10 minutes. For the longer exposures, the light was attenuated by neutral density filters to avoid saturation of the film. The fringe pattern remained sharp, even for the longest exposures. This indicates that the granite slab has good interferometric stability.

A bench layout for production of holograms was set up on this granite slab. A diagram is shown in Figure 165. A helium-neon laser for production of bleached holograms in photographic film and an argon laser for production of dichromated gelatin holograms were used. A rifle telescope was employed as a beam expander to enlarge the beam diameter to 7 mm. The beamsplitter was a Jodan variable beamsplitter which allowed the relative amount of light in the signal and reference beams to be varied.

The two mirrors were supported by gimbal mounts. Two micrometer drives provided independent orthogonal rotation of each mount about vertical and horizontal axes. The reference beam proceeded directly to the recording medium. The signal beam was focused by a 2-in. focal length lens. A 25- $\mu$  diameter pinhole in electroformed nickel was located in the focal plane of the lens and provided a spherically diverging beam. The signal beam thus originated from a point source. The pinhole was mounted on a three-axis micropositioner. It was adjusted in the directions transverse to the beam until maximum light intensity was obtained through the pinhole and then was adjusted in the direction parallel to the beam until the Fresnel zones disappeared and a reasonably uniform distribution of light was obtained. This provides the most sensitive adjustment of the pinhole in the focal plane of the lens.

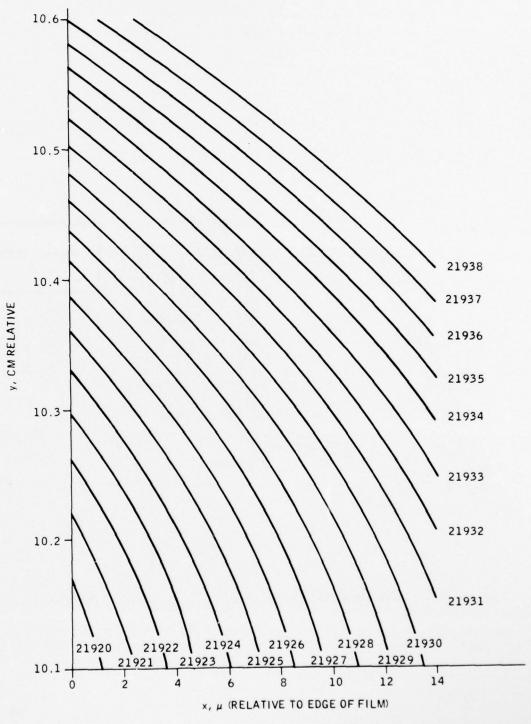


Figure 164. Fringes in Film of Volume Holographic Recording Medium. The point origin is at y = 0 and x = -2.6794 cm. Numbers on the fringes indicate the order of the fringe N, defined in the text.

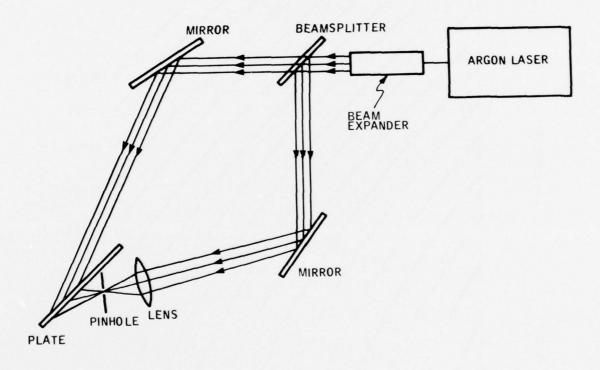


Figure 165. Experimental Arrangement for Hologram Production

The recording medium was mounted in a specially designed plate holder which allowed translation of the recording medium between exposures, so that a number of exposures could be made on a single film. The angle between the film plane and the reference beam was 20 deg, and the angle between the film plane and the signal beam was 30 deg. The film plane could be translated by a micrometer drive perpendicular to the plane of the film. This provided sensitive adjustment of the path difference between the two beams. The path difference was adjusted to be much less than 1 cm. This difference in path between the signal and reference beams has little effect, either for the helium-neon laser or for the argon laser.

If the laser operates in more than one longitudinal mode and if the paths traveled by the reference beam and the signal beam are not of equal length, the visibility of the fringe in the hologram will decrease. To determine criteria for matching the path lengths, the effect of path inequality for the lasers used was evaluated.

The number of axial modes in the helium-neon laser was measured, using a Fabry-Perot interferometer. In the Fabry-Perot interferometer, the fringe pattern forms concentric circular rings. If the laser operates in more than one longitudinal mode, the ring pattern will have substructure. Each ring is split into a number of components corresponding to the number of axial modes in the laser output. By observing the fine structure in the Fabry-Perot interferometer, it was determined that the Spectra-Physics Model 120 heliumneon laser operated in three longitudinal modes.

For the argon laser, the spectral width of the argon line is 3500 MHz, and the mode spacing for the 100-cm cavity is 150 MHz. Therefore, one might have as many as 20 longitudinal modes present. This is probably an upper limit, because modes near the edge of the fluorescent line have low gain.

For the case of a laser operating in three axial modes, the frings modulation is given by

$$M = \frac{2 \cos\left(\frac{\pi D}{d}\right) + 1}{3} \tag{7}$$

and for a laser operating in 20 axial modes, it is given by

$$M = \frac{1}{10} \left[ \sum_{n=1}^{10} \cos \left[ \frac{(2n-1)\pi D}{2d} \right] \right]$$
 (8)

In these equations, d is the length of the laser cavity and D is the difference in path length between the two beams. The modulation of an interference pattern is defined as

$$M = \frac{I_{\text{max}} - I_{\text{min}}}{I_{\text{max}} + I_{\text{min}}}$$
(9)

where  $I_{max}$  and  $I_{min}$  are the intensities at the maxima and minima of the pattern. For D = 0, the modulation will be unity and the fringe visibility will be optimum. For D  $\neq$  0, the contrast in the fringes will decrease according to Equations (7) or (8). These equations have been evaluated for the lasers. The modulation as a function of path length difference is shown in Figure 166. For the helium-neon laser, the fringe visibility is seriously decreased only when the path difference exceeds several centimeters. For the argon laser, matching of the path lengths is more important than for the helium-neon, but is still not extremely critical. Matching of the path lengths to within 2 cm is reasonable and would allow modulation in excess of 0.94. Since the estimate of 20 modes in the argon laser is almost certainly an over-estimate, the path length matching is less critical than these results would indicate.

The conclusion is that tolerance of the matching of the optical path between object and reference beams is of the order of 2 cm, a value which is easily attainable with the experimental apparatus.

#### RESULTS

Volume phase holograms were produced using two different types of material -- bleached 649-F photographic film and dichromated gelatin. Both types were used to project images of a reticle pattern.

## Production of Holograms in 649-F Film

Holograms have been prepared using 649-F photographic film in a reversal bleach process. The reversal bleach system is a method originally developed by Kodak for production of phase holograms with high diffraction efficiency. This system eliminates most of the flare light usually found around the image in holograms bleached by other processes. The reversal bleach process operates by suppressing the low spatial frequencies that are characteristics of the speckle pattern and retaining the desired holographic interference pattern which is of higher spatial frequency. The reversal bleach process accomplishes this by forming a relief image whose thickness variations tend to cancel the variation of index of refraction. The relief images occur primarily for spatial frequencies below about 200 lines/mm and therefore do not cancel out the high spatial frequencies used to record the holographic pattern. The procedure used is tabulated in Table XIII. The exact procedure and times

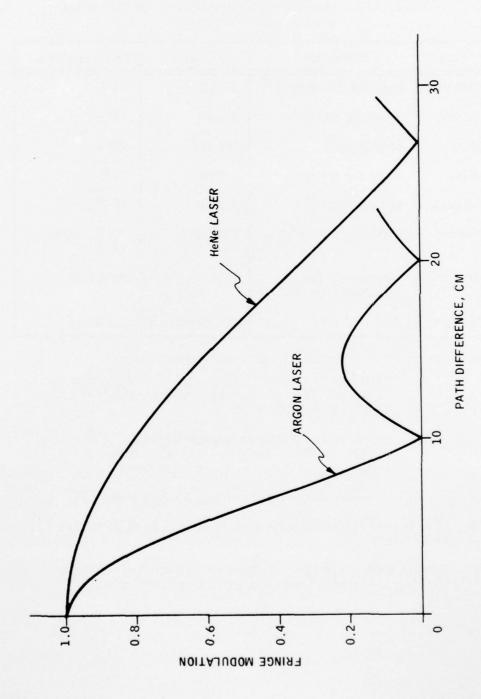


Figure 166. Fringe Modulation as a Function of Path Difference Between Reference and Object Beams

Table XIII. Development Procedure for Reversal Bleach of 649-F Plates

Step	Chemical	Time	Temperature
Develop	Special developerA	5 m in	74°F
Rinse	Running water	2 min	74°F
Stop	Stop bath <sup>B</sup>	30 sec	74°F
Rinse	Running water	2 min	74°F
Bleach	Bleach bath <sup>C</sup>	2 min	74°F
Wash	Running water	10 min	74°F - then 78°F
Dry	Methanol, then isopropyl alcohol	Dip	Ambient
Hang	Air	As required	Ambient

- A. Special developer is made from two solutions:
  - Solution 1: 8 gm sodium sulfite, 40 gm pyrocatechol, 100 gm sodium sulfate, dissolved in water to make 1 liter.
  - Solution 2: 20 gm sodium hydroxide, 100 gm sodium sulfate dissolved in water to make 1 liter.

These two solutions are mixed just before use.

- B. Stop bath: 18 milliliters glacial acetic acid in 1 liter of water.
- C. Bleach bath: 9.5 gm potassium dichromate, 12 milliliters concentrated sulfuric acid in 1 liter of water.

are not extremely critical, with the possible exception of the final drying by dipping in alcohol. This step seems to be necessary to keep the plate from developing water spots. However, the final alcohol dip appears to produce a whitish appearance in the plate which seems to be associated with increased scattering losses. This point was not investigated thoroughly enough to arrive at definite conclusions.

The effect of exposure conditions was investigated. Figure 167 shows the efficiency (defined as the amount of light in the virtual reconstructed image divided by the light incident in the reconstructing beam) as a function of the total energy used to make the hologram. The energy was varied by varying the time of exposure. The results in Figure 167 were obtained at a constant balance ratio of 3.3 to 1. (Balance ratio is defined as the ratio of the intensity in the reference beam to the intensity in the signal beam.) The results in Figure 167 indicate a maximum efficiency near 3 millijoules/cm<sup>2</sup>.

Figure 168 shows the efficiency as a function of the balance ratio. This is for a constant exposure of 2.6 millijoules/cm². A straight line fit by the least squares method to the experimental data points is also included. The balance ratio was varied by rotating the variable beamsplitter. The other conditions of exposure were held constant. For most holographic purposes, the efficiency is usually maximum at a balance ratio around 5. The present data are consistent with efficiency decreasing for ratios above 2. The peak of the curve over the range of balance ratios shown in this appendix were not defined. Probably as one approached smaller values of the balance ratio, the efficiency would decrease.

For each of Figures 167 and 168, the data were obtained on a single piece of film, which was moved in the film holder between exposures. Consequently, each figure refers to a separate constant set of processing conditions. Comparison of the two figures shows that the effect of processing variables can influence the absolute value of the efficiency. Although reasonably good holograms can be produced over a range of processing conditions, not enough work was done to define the optimum conditions for processing the film.

In addition, the values of the efficiency are low, reaching a maximum around 1% in Figure 168. This is in contrast to the claims of Kodak which indicate that efficiencies up to 40% are possible with the reversal bleach process. Presumably the difference lies in optimization of the processing of the film.

The effect of changing the direction of the reconstructing beam on the virtual image formed by the hologram was also investigated. For these measurements, the developed plate containing the hologram was rotated about a vertical axis through the center of the hologram. As the plate was rotated, the reconstructing beam was incident at different angles. A photomultiplier tube wasused to measure the light intensity at the virtual image. For each orientation of the plate, the photomultiplier was moved so as to

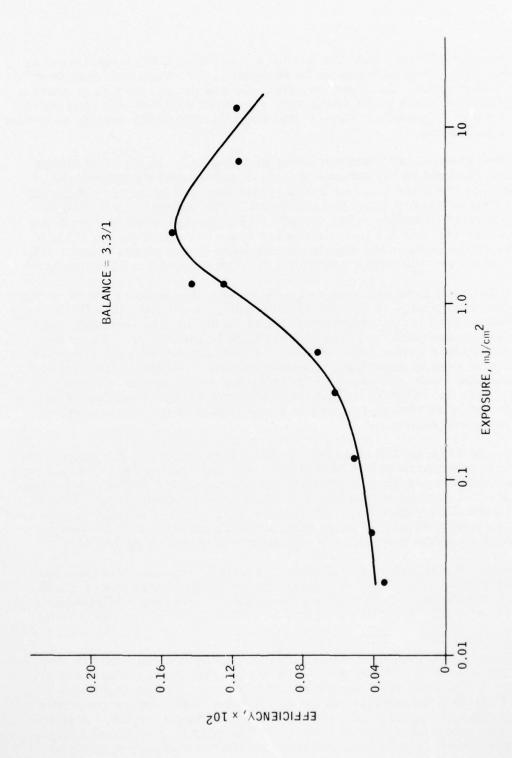


Figure 167. Efficiency as a Function of Exposure for Constant Balance Ratio

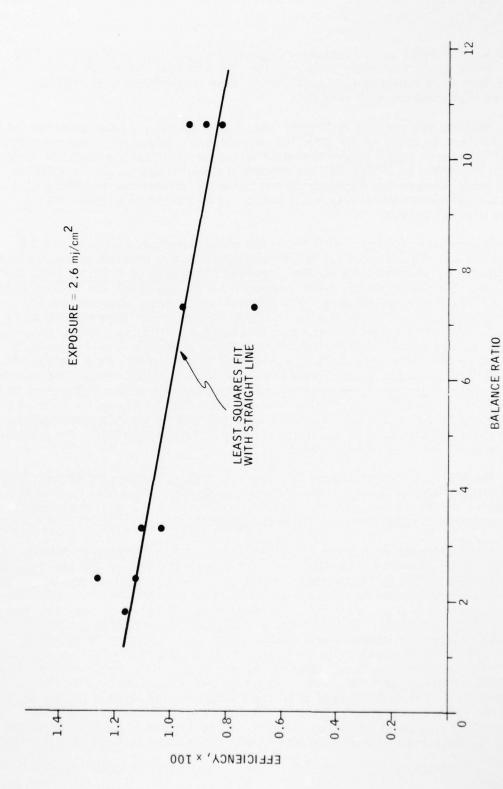


Figure 168. Efficiency as a Function of Balance Ratio for Constant Exposure

intercept all the light in the virtual image at that particular position. The reading of the photomultiplier combination depended on the exact positioning. For each measurement the photomultiplier was moved until a maximum reading at that position was obtained.

The results are plotted in Figure 169. The ordinate is the relative intensity normalized to unity at the position of maximum intensity. The abscissa is the difference in angle of the reconstructing beam from the angle at which maximum intensity is obtained. As expected from Equation (2), maximum intensity occurs when the reconstructing beam is incident on the plate at the same angle as the original reference beam. The points in Figure 169 are the experimental values.

The solid lines in Figure 169 show the theoretical intensity of the diffracted wave as a function of the incidence angle of the readout wave, as calculated using Equation (1), using the appropriate values of  $\theta_i$  and  $\theta_s$  for the experiment. This method has been accepted as standard for the orientation sensitivity of volume holograms. Equation (1), however, depends on an approximation that is a critical step in the analysis. The approximation is that significant contributions to the amplitude of the diffracted wave are produced only by elemental diffracting centers lying along the line through the point at which the diffracted field is calculated and normal to the diffracted waves. Use of this approximation makes the mathematical treatment reasonably tractable. Without it, calculation of the amplitude of the diffracted field would be extremely difficult. Much of the theory that has been developed about image formation in volume holograms implicitly relies on this assumption. However, the validity of this assumption is not certain and there are possibly situations in which it is not applicable.

The theoretical curves shown in Figure 169 show rapid oscillatory structure in the intensity of the diffracted wave, along with a general decrease in amplitude as the angle of the reconstructing beam moves away from the original angle of incidence of the reference beam.

The experimental data show considerable scatter, which presumably is at least partially due to the oscillatory structure indicated by the theoretical curve. However, the full structure contained in the calculated curves is not shown. This is probably due to two factors. The first is that the emulsion undoubtedly distorts somewhat during processing. This would tend to smooth out oscillatory structure. Also, the finite angular spread of the reconstructing beam and the finite acceptance angle of the detector will have an effect of averaging over some angular range and decreasing the amount of oscillatory structure that can be observed. There are some definite oscillatory components to the intensity as a function of angle of the reconstructing wave. It is easily seen by eye that the image will grow brighter and darker as the angle is changed. The experimental point at 10 deg is a good example of this behavior. The image is definitely brighter when viewed at angles of reconstruction slightly less than 10 deg or slightly more than 10 deg. Scatter in

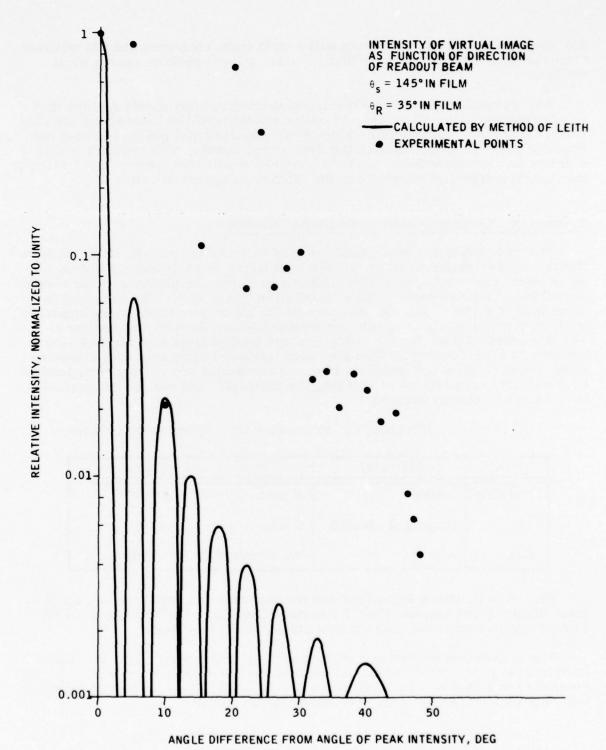


Figure 169. Effect of Changing Direction of Readout Beam on Intensity of Virtual Image

the observed experimental points will result from considerations of whether the point was taken at an angle that lay near a local peak or near a local minimum.

The general trend of the experimental observations shows a slope that is comparable to the slope defined by the envelope of the theoretical oscillations. However, the absolute value of the experimental points is about one order of magnitude higher than the theoretical curve. The reason for this discrepancy is now known. It could possibly result from partial saturation of the detector signal at values near the maximum observed value.

### Production of Holograms in Dichromated Gelatin

The process began with gelatin coated on 2 x 2 in. plates, obtained from Kodak. These plates were sensitized by soaking in an aqueous solution of potassium dichromate for 5 min. After exposure, the plates were processed according to a procedure which is typified in Table XIV. The material is developed in water. The temperature of the water was found to be important, with improved results at water temperature below ambient temperature. The final step of plunging the hologram into heated isopropyl alcohol also appears to be necessary. This step also leads to holograms with a whitish milky appearance which scatters light. The results are critically dependent on the exact procedure of processing the material, and not all the variables have been completely defined.

Table XIV. Development Procedure for Dichromated Gelatin

Step	Material	Time	Temperature
Develop	Water	5 min	54°F
Fix	Isopropyl alcohol	5 min	80°F
Dry	Air	As required	Ambient

As a result, there was considerable variation in the holograms made from dichromated gelatin. The holograms were not reproducible even for different plates exposed under nominally identical conditions.

The diffraction efficiency obtained with dichromated gelatin was not particularly high. The highest values obtained were of the order of 10%, as compared to a theoretical maximum value of 100%. The amount of scattered light varied erratically from one hologram to another.

The drying stage is crucial to production of good holograms in dichromated gelatin. The humidity of the air in which the hologram is dried after washing is isopropyl alcohol is important. The production of holograms of high efficiency is accomplished by literally tearing apart the gelatin during a rapid removal of water by the isopropyl. If the humidity during the drying stage is too high, the voids produced by the tearing will be wiped out and the hologram will have low efficiency. At lower humidity, the gelatin tends to crystallize. The final drying stage is probably the most important part of producing a good hologram using dichromated gelatin. Future work shall investigate the influence of this step systematically.

### Reconstruction and Reticle Projection

When the holograms are illuminated by light in the direction of the original reference beam, both a virtual image and a real image in reflected light are produced. The virtual image is a diverging spherical wave visible as a point of light at an apparent distance behind the hologram equal to the distance of the pinhole from the film. The real image is a beam of light which converges to a point (also at a distance from the film equal to the distance of the pinhole). The situation is sketched in Figure 170. The virtual image is that predicted by Equation (2). The presence of the real image is not predicted by the theory discussed above. It apparently arises because of reflection of the reconstructing beam from the air-film interface, so that essentially an additional reconstructing beam passes through the material at a different angle. This image could be eliminated by liquid immersion of the plate during reconstruction, or by processing the plate so that the efficiency of the virtual image would approach 100%.

In addition, there are real and virtual images produced in transmission. These are not predicted by the simple theory of volume holograms. They are probably the result of interference by beams reflected off the back surface of the hologram during the production process. Light is reflected from the interface of the plate with air and essentially forms a beam traveling in the opposite direction from the original beam. Interference of these wavefronts produces fringes which lead to the holographic images in transmitted light. These images could be eliminated by liquid immersion of the film during production of the hologram.

The holograms have been employed to project images of reticles. For this application, the reticle generator (which consists of a small light bulb with a mask of concentric circles) is placed at the position of the original source, namely the pinhole. The diverging beam of light from the reticle generator interacts with the hologram to produce a reflected plane wave.

This yields an image of the reticle which is apparently at infinity, and which may be viewed by the relaxed eye. The color of the image depends on the angle of observation. As one moves his head, one may observe the color of the image to change. A photograph of this image is shown in Figure 171.

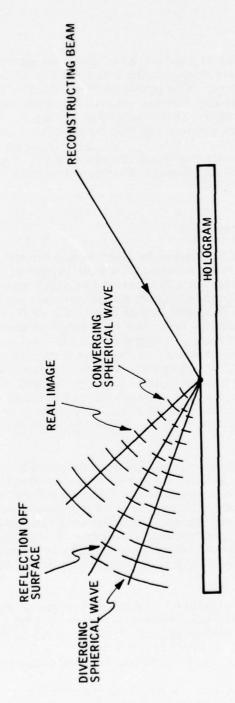


Figure 170. Illustration of Images Observed in Reconstruction

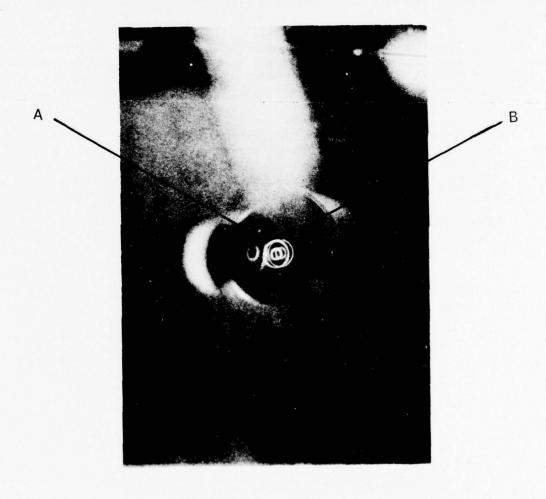


Figure 171. Photograph of Virtual Image of Reticle A. Pattern B is due to direct reflection from surface of plate.

The virtual image of the reticle (which consists of two concentric circles) is marked A in Figure 171. The pattern marked B is due to direct reflection of light from the reticle generator off the interface between the film and air. This pattern is double because of reflections off both front and back surfaces. This reflected image is not focused at infinity, whereas the virtual holographic image is.

To get a satisfactory photograph, it was necessary to place the camera close to the hololens. This is the reason that the virtual image and the light directly reflected from the reticle generator overlap. At greater distances the virtual image can be viewed by eye without interference from the reflected light.

The virtual image appears larger than the original reticle. This is probably due to expansion of the gelatin during processing. There are a number of imperfections in the virtual image, including apparent change in size as the viewing angle is changed, uneven illumination, and lack of perfect roundness. Advances in processing techniques should improve the results.

# APPENDIX II RELAY LENS DESIGN DATA

Table XV of this appendix lists the following relay lens data: radii (R1 and R2), center lens thickness (T), clear apertures (CA1 and CA2), glass types, and parameters. This design was the result of the following procedures to ensure the best possible performance:

- 1) Initial design to establish type of glass and optical layout.

  Design uses lens element radii consistent with Herron test plate list.
- 2) Rerun design with actual glass melt data to establish lens thickness.
- 3) Rerun design with actual lens thickness to establish spacer lengths.

Figure 172 shows the layout and ray trace of the relay optics and Tables XVI, XVII, and XVIII list the design MTF.

Optical fabrication tolerances are as follows:

Surface Quality: ±3 rings of power ) over the clear 1 ring of astigmatism ) aperture

Thickness Tolerance: ±0.003 on singlets (elements 2, 3, 8, and 9 of model data)

±0.002 for total thickness of doublets after cementing (elements 4-5 and 6-7)

Centering within  $\pm 0.001$  of optical axis.

The test plates should be made within 0.1 percent of the specified radius. The actual values were then used in the respace computation.

Scratch and Dig: 80-50 (mirror and lenses)

Spacings Tolerance: ±0.001

Table XV. Relay Lens Recomputation for Glass Melt Data, Test Plates, Radii and Lens Thicknesses

0.65X F/2.5 ELEMENT	R1	R2	Т	CA1	CA2	GLASS
1	INF	INF	0.0790	0.7458	0.7358	QUARTZ
6	3 5384	3 5384	1.2000	0.5098	0.5048	MI.AFN2
,			0.0196			
က	0.7542	1NF	0.1050	0.4885	0.4612	MLAFN2
4	0 4356	-0.8692	0.2093*	0.4117	0,2799	MLAFN2
2	-0.8692	0.2479	0.0490	0,2799	0.2095	MSF56
			APERTURE STOP	0.2077	077	
9	-0.2479	0.8692	0, 1970	0.3199	0, 5059	MSF10
7	0.8692	-0.4356	0.1730*	0.5059	0.5516	MLAFN2
8	INF	-0.8692	0.0050	0.6522	0.6804	MLAFN2
6	0.8692	INF	0.0186 0.1240	0. 7272	0, 7166	MLAFN2
	DEFOCUSSING	SING =	0.5494 O0.0014 (DEP	ARTURE FRO	OM PARAXI	AL FOCUS FOR
			BES	T IMAGING -	SUBTRAC	BEST IMAGING SUBTRACT 0. 0014 FROM
IMAGE	INF		0. 5494)		0.4900	
*INCLUDES 0.901 IN. EXTRA FOR CEMENTING.	001 IN. EXT	RA FOR CEN	IENTING.			
NOTE - POSITI	VE RADIUS	INDICATES 'INDICATES	- POSITIVE RADIUS INDICATES THE CENTER OF CURVATURE IS TO THE RIGHT NEGATIVE RADIUS INDICATES THE CENTER OF CURVATURE IS TO THE LEFT	RVATURE IS JRVATURE IS	то тие во 3 то тие L	GHT EFT
PARAMETERS						
EFL			_	= 10.0890		
FFL	= -0.2142		DIAMETER	- 0. 5287		
F/NO	-: 0			= 1,9905		
FINITE F/NO	000		٠	2.7484		
OBJ DIST IMAGE DIST TOTAL TRACK	= 0.0429 = 0.5480 = 3.0790		DISTANCE			
	7.7001					

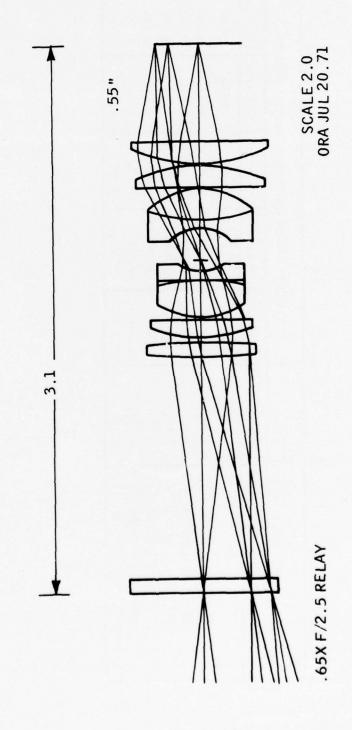


Figure 172. Layout and Ray Trace of Relay Optics

Table XVI. Predicted MTF -- Relay Lens

		Field Position = 0.00 Y Max. (0.00 degree) Relative Illumination = 100.0 percent Distortion = 0.00 percent	0.00 Y Max. ation = 100.0 0 percent	(0.00 degree) percent			
		Wavelength		Weight			
		550.0 nm 525.0 nm 500.0 nm	E E E	10 20 10			
	THEORETICAL DIFFRACTION LIMIT	CAL N LIMIT	FOCUS	FOCUS POSITION (INCHES) PREDICTED MTF	NCHES) P	REDICTED N	ITF
LINES/ MIM	UNOBSCURED	OBSCURED	-0.00060	-0.00040	-0.00020	-0.00000	0.00020
		RAD	RAD	RAD	RAD	RAD	RAD
	0,999	0.999	0.999	0.999	0.999	0.999	0.999
25	0.958	0.958	0.929	0.941	0.947	0.947	0.942
90	0.917	0.916	0.810	0.851	0.873	0.877	0.862
75	0.875	0.875	0.662	0,740	0.787	0.798	0.776
100	0.833	0.834	0.506	0.621	0, 693	0.717	0.692
125	0.792	0.793	0.364	0.504	0.601	0, 639	0,618

Table XVII. Predicted MTF -- Relay Lens

Table XVIII. Predicted MTF -- Relay Lens

LINES/MM	THEORETICAL DIFFRACTION LIMIT UNOBSCURED OBSCU 2. 50 RAD 0. 959 0. 959	TICAL ON LIMIT OBSCURED RAD TA 0.999 0.96	TA TA O 0 0 0 0 0 0 0 0 0 0 0 0 0 0 0 0 0 0	ad Position = tive Illumina ortion = -1.0 Waveleng 550.0 n 525.0 n 500.0 n 500.0 n RAD T/2 0.999 0.999 0.902 0.902	Field Position = 1.00 Y Max. (9.23 degrees)  Relative Illumination = 84.2 percent Distortion = -1.00 percent  Wavelength 550.0 nm 525.0 nm 20 500.0 nm 10 FOCUS POSITION (ING 10 10 10 10 10 10 10 10 10 10 10 10 10	Y Max. (9.22) "cent Weight  Weight  10 20 10 20 -0.00040  -0.00040  0.999 0.999 0.999	Weight 10 20 10 20 10 . 00040 . TAN TAN 6. 0.938	-0.00020 RAD TA 0.999 0.9 0.931 0.853 0.8	S) PR 020 TAN 0.999 0.938	#4.2 percent  #4.2 percent  Weight  10  20  10  20  10  20  10  20  10  20  10  20  10  20  10  20  10  20  10  20  10  20  10  20  10  20  10  20  10  20  10  20  10  20  10  20  2	MTF 0000 TAN 0.999 0.934	0.00020 RAD T 0.999 0. 0.939 0.	120 TAN 0, 999 0, 927 0, 831
50	0.917	0, 883	0.851	0.691	0, 762	0, 023	0.788	0.789	0. 792	0.797	0.774	0.771	0. 736
100	0. 833 0. 792	0.844	0.802	0.624	0.676 0.596	0, 696	0,716	0, 736	0, 724	0. 733	0.701	0, 680	0, 651

## APPENDIX III

VIDEO VISOR PROJECTION FINAL REPORT HELMET MOUNTED DISPLAY DESIGN IRV/ABEL HONEYWELL RADIATION CENTER

### OPTICAL DESIGN

### Background

The previous approaches to the helmet mounted display optical design have been based on the use of a plane combiner and refractive optics to relay the display image to the eye while viewing an external scene. The combiner is located as close to the eye as comfortable. Immediately after the bending of the optical axis from the eye to the display, refractive elements are located to relay the image. The closer the eye lens (element closest to the eye) to the combiner, the smaller the lens. Consequently, the dominant factors in the size of the lens are the effective distance between lens and eye, and the field of view.

The exit pupil of the system is located generally at the eye or at the lens closest to it. In the first case, the exit pupil is formed as in the normal telescope. Every point within the pupil views the entire field of view. In the second case, the view is the same as presented with a framed window seen through by a distant eye. It is also the view presented by a reflex sight. The advantage of this design is that a greater eye freedom is available for the same eye lens size, but its location varies with field angle; on-axis it is centrally located, whereas at the edge of the field it is displaced laterally. To gain advantage of the larger eye freedom for all fields of view, the head must be free to shift relative to the combiner. While such freedom exists in a panel-mounted system, it is absent in a helmet mounted system. Consequently, an exit pupil formed at the eye is the maximum which can be used while presenting the entire field of view. An advantage to the exit pupil located at the eye lens is that the pupil is so large (equal to eye lens diameter) that the proper positioning of the helmet relative to the display is facilitated. However, a sufficiently large eye freedom area is provided presently in the other case so that the helmet positioning is made rather easily anyway. In both cases the eye lens is the same size, but with the exit pupil formed at the eye, some of the relay lenses are smaller.

The major objection to the plane combiner is the size of the system for large fields of view. The approach adopted for the AHRA is intended to provide a lighter and better balanced helmet mounted system for larger fields of view while attaining a relatively high display quality. Essentially, optical power is introduced into the combiner, which serves also as the visor. By reflecting the light twice from the visor, the extra optical components required to relay from the display (or its fiber optics extension) are relatively small. The two reflections serve not only to reduce the size of the auxiliary optics,

but also to locate them favorably and to produce the required image quality. In effect, the visor-combiner translates the "window" to the display from a distant point to the eye.

### Double-Bounce Parabolic Combiner

Incorporating optical power into the combiner introduces aberrations which are generally difficult to remove. The difficulty lies in the necessity of either tilting or displacing the axis of the combiner from the zero sightline of the eye. In the case of the tilted axis, off-axis aberrations are introduced which are not readily corrected for by a centered optical system. Furthermore, an asymmetry in the aberration as a function of field angle is also introduced. In the case of a displaced optical axis, the system effectively works at an extremely low f-number, which is also difficult to correct.

The Double-Bounce Parabolic Combiner system incorporates optical power in the combiner (visor), which is a parabolic reflector having an optical axis displaced from the zero sightline of the eye. As a result, the parabolic reflector works at a very low f-number (approximately 0.63), but by virtue of an arrangement providing for two symmetrically disposed reflections, a high degree of image definition is produced.

The Double-Bounce Parabolic Combiner system is an arrangement equivalent to two confocal parabolic reflectors. Such a design provides correction for spherical aberration, coma, and astigmatism. Field curvature introduced by the parabolic reflector is compensated for in the lens which transfers the display light to the combiner. Due to the necessity of locating the exit pupil far off axis, the image formed by the parabolic reflector is distorted anamorphically. Thus the image formation, while sharp, is nonlinear. This nonlinearity is, however, readily compensated for in the CRT beam deflection.

### Description of the System

The CRT image is relayed to the input end of a fiber optics bundle. At the exit end, the light emerges from the fiber optics bundle and is then collimated by a lens. The light is reflected by a plane mirror to the parabolic visor, focused at a plane mirror, and then reflected to the parabolic visor. Once again the inner surface of the parabolic visor reflects the radiation, this time collimating and directing it to the eye.

The parameters of the optical system are as follows:

- 1) Field of view -- square -- 20 deg diagonal
- Exit pupil -- 0.4 inch diameter

- 3) Distance eye sight line to parabolic axis -- 1.5 inches
- 4) Focal length parabolic surface -- 2.0 inches
- 5) Fiber optics image diagonal -- 0.49 inch
- 6) Eye distance (from vertex of combining surface) -- 2.75 inches

Due to the spatial constraints imposed by the head size, it is necessary to introduce a plane folding mirror to bend the light from the collimating lens to the visor. The position of the folding mirror is quite restricted. It cannot be too close to the visor or it will interfere with light reflected from it. In addition, if set back from the visor, it interferes with the collimating lens. The optimum position for the folding mirror puts the entrance pupil outside of the collimating lens. In this way, light from the fiber optics is fed to the visor without obscuration.

The external location of the aperture stop of the collimating lens is not ideal from an image correction standpoint. Generally, for wide angle systems, it is most effective to locate the aperture stop within the basic configuration. The effect of the external location shows up in residual astigmatism, which is the limiting aberration. As a result, it is the collimating lens, rather than the theoretically perfect parabolic combiner, which limits the optical resolution.

Nevertheless, the overall optical resolution satisfies the requirements and this existing limitation points to the potential for wider fields of view with the Double-Bounce Parabolic Visor system under more compatible conditions for the collimating lens, rather than any fundamental limitation of the parabolic visor itself.

The collimating lens is designed with undercorrected field curvature to compensate for the overcorrection inherent in the parabolic reflector. Two reflections from the visor doubles the effect. Since the normal field curvature from a positive lens is undercorrected, the requirement for a positive field element facilitates the attainment of overall field curvature correction.

Not only must the visor reflect the display with good image quality, but also transmit the external scene without distortion, optical power, or loss of resolution. It turns out that with the outer surface having the identical shape as the inner, the requirements for these characteristics of the image are satisfied. Furthermore, if the outer surface is parabolic, but with a slightly longer focal length, the transmitted image quality, linearity, and uniformity of negligible optical power over the field of view is improved. For all practical purposes, it is like viewing through a flat window.

### Design Data

The design of the collimating lens (Figure 173) was made to conform to the location of the entrance pupil, the available space to the fiber optics bundle, and the requirement for field curvature compensation of the parabolic visor. With these restructions it was designed separately, then combined with parabolic visor and optimized for overall performance.

The required diameters of the collimating lens were obtained by tracing rays from a 0.4-inch exit pupil (eye location) over the specified field of view. Since no physical stop was placed at the entrance pupil, the actual exit pupil became larger. However, at the prescribed eye position, no greater than 0.4 inch of eye freedom area was made available for the entire field of view.

The system has been evaluated in terms of point spread energy distribution, MTF, and linearity resulting from a large number of ray traces from the eye to the fiber optics bundle. The field points of MTF evaluation are shown in Figure 174 and the values given in Table XIX. The MTF data is based on an eye pupil size of 0.25 inch which represents accommodation to a low light level. At an optical frequency of 850 line pairs/inch, corresponding to a horizontal resolution of 500 line pairs, the diffraction-limited MTF is 0.83 (Figure 175). It can be noted that this value is obtained in the system about the center of the field of view. At the extremities of the field of view, the MTF drops to a value of approximately 0.61. As stated previously, the reason for this lies in the residual astigmatism of the collimating lens rather than in the parabolic visor. For the most part, the eye pupil will be less than 0.25 inch (probably one-half of this value); consequently the system will be working at even lower, but uniform, values of MTF due to the diffraction of the eye itself.

Due to the displacement of the eye pupil from the optical axis of the parabolic combiner, the image is distorted, i.e., the beam angles in are not linear with the beam angles out. The distortion is not rotationally symmetric; hence, it cannot be corrected by a rotationally-symmetric collimating lens. However, the correction is readily made in the CRT deflection circuits. The distortion evaluated at points defined in Figure 176 are given in Table XX.

Table XXI summarizes the effect of transmission through the visor in terms of focusing distance and distortion (line-of-sight error) for the case of the outer surface being parabolic, but with a slightly longer focal length than the inner.

# System Potential

The Double-Bounce Parabolic Visor HMD appears to be the most promising for the extension of the field of view with high image quality along with compact and balanced construction. As noted previously, satisfactory image quality is available with the visor. By arranging the system so that

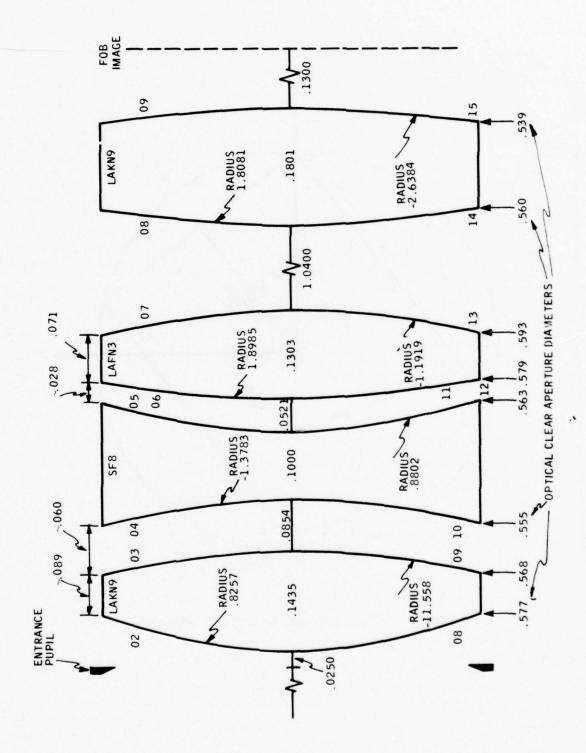


Figure 173. AHRA HMD Lens to GEM

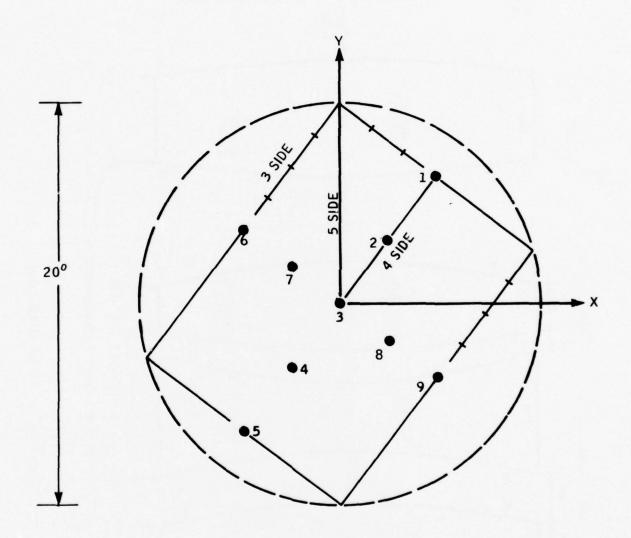


Figure 174. Field Points of MTF Evaluation

Table XIX. AHRA HMD Linked (Refocusing of Eye for All Points)

MTF Summary

Point No.	Focus Shift	Wave O	otic MTF
Point No.	(in.)	SAG	TAN
1	+0.00075	0.58	0.58
2	-0.00025	0.79	0.78
3	-0.00050	0.83	0.83
4	+0.00025	0.80	0.77
5	+0.00350	0.63	0.59
6	+0.00050	0.69	0.75
7	-0.00025	0.80	0.81
8	-0.00025	0.80	0.81
9	+0.00050	0.72	0.73

Note: Modulus values all taken @ 850 line pairs/inch (1700 TV lines/inch).

the collimating lens field stop lies within, the required overall image quality can be achieved. This is particularly the case if the parabolic visor axis lies above the eye and the larger extension of the field is horizontal. With different systems for each eye, perhaps two parabolic visors blended into one between the eyes would be effective. In both systems, a fiber optics bundle would be located above the eye.

While it is difficult to define the extent of field coverage achievable, it seems appropriate to strive for 30 degrees and perhaps a 30 x 40 degree field with the larger extension in the horizontal direction.

### Recommended Steps

The following steps are recommended to develop a system with a larger field of view:

- Design a vertically oriented 30-degree Double-Bounce Parabolic Visor system
- 2) Investigate the feasibility of a blended parabolic visor
- 3) Build a breadboard model of a complete system

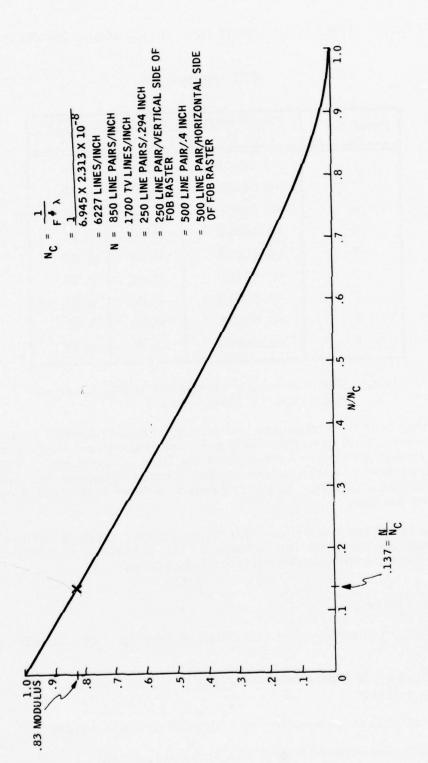


Figure 175. Response of an Aberration Free System

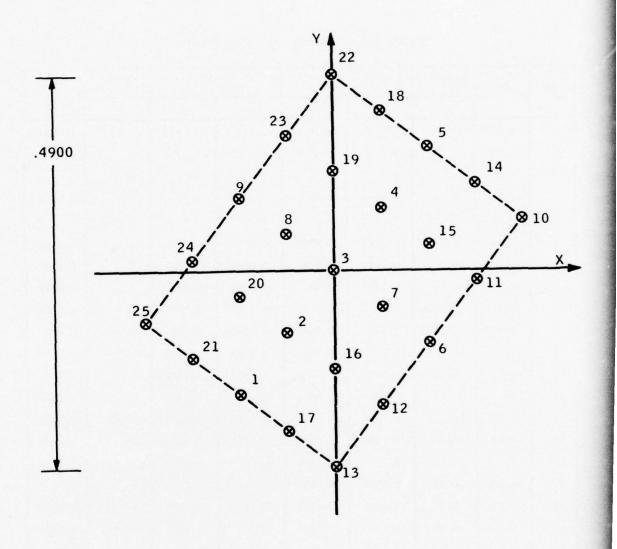


Figure 176. Ideal Distortion Free Grid @ FOB

Table XX. Distortion Evaluation

Point	Fraction Def. @	al Field Eye	Ideal I Positi		Actual Posit		Linear Di @ FO	
No.	x	у	х	у	x	y	x	у
1	+0.48	+0. 64	-0.1176	-0.1568	-0.1177	-0.1378	-0.0001	0.0190
2	+0.24	+0.32	-0.0588	-0.0784	-0.0588	-0.0734	0	0.0050
3	0	0	0	0	0	0	0	0
4	-0.24	-0.32	0.0588	0.0784	0.0588	0.0838	0	0.0054
5	-0.48	-0.64	0.1176	0.1568	0.1177	0.1794	0.0001	0.0226
6	-0.48	+0.36	0.1176	-0.0882	0.1176	-0.0771	0	0.0111
7	-0.24	+0,18	0.0588	-0.0441	0.0588	-0.0412	0	0.0029
8	+0.24	-0.18	-0.0588	0.0441	-0.0588	0.0471	0	0.0030
9	+0.48	-0.36	-0.1176	0.0882	-0.1176	0.1004	0	0.0122
10	-0.96	-0.28	0.2352	0.0686	0.2355	0.1021	0.0003	0.0335
11	-0.72	+0.04	0.1764	-0.0098	0.1765	0.0069	0.0001	0.0167
12	-0.24	+0.68	0.0588	-0.1666	0.0588	-0.1513	0	0.0153
13	0	+1.00	0	-0.2450	0	-0.2168	0	0.0282
14	-0.72	-0.46	0.1764	0.1127	0.1766	0.1378	0.0002	0.0251
15	-0.48	-0.14	0.1176	0.0343	0.1176	0.0425	0	0.0082
16	0	+0.50	0	-0.1225	0	-0.1149	0	0.0076
17	+0.24	+0.82	-0.0588	-0.2009	-0,0588	-0.1798	0	0.0211
18	-0.24	-0.82	0.0588	0.2009	0.0588	0.2273	0	0.0264
19	0	-0.50	0	0.1225	0	0.1311	0	0.0086
20	+0.48	+0.14	-0.1176	-0.0343	-0.1176	-0.0264	0	0.0079
21	+0.72	+0.46	-0.1764	-0.1127	-0.1865	-0.0906	-0.0001	0.0221
22	0	-1.00	0	0.2450	0	0.2820	0	0.0370
23	+0.24	-0.68	-0,0588	0.1666	-0.0588	C. 1850	0	0.0184
24	+0.72	-0.04	-0.1764	0.0093	-0.1765	0.0267	-0.0001	0.0178
25	+0.96	+0,28	-0.2352	-0.0686	-0.2355	-0.0376	-0.0003	0.0310

Table XXI. AHRA HMD Through Parabolic Visor

			DATA S	DATA SUMMARY		
CASE A	Inside Visc Outside Vi Visor Vert	Inside Visor Surface (Adj Outside Visor Surface: Visor Vertex Thickenss:	Inside Visor Surface (Adj. to eye): Outside Visor Surface: Visor Vertex Thickenss: 0.1 inch		Parabolic-Radius 4.0 inches Parabolic-Radius 4.0 inches	hes
	Direction of Sight	of Sight	Line-of-Sight Error	ght Error	Optical Power F	Optical Power Focusing Distance
	Y-Axis (deg)	X-Axis (deg)	Y-Axis (mrad)	X-Axis (mrad)	Y-Axis (ft)	X-Axis (ft)
	+10	0	-0.368	0.0	+68	+75
(on-axis)	0	0	+1.438	0.0	+104	+87
	-10	0	+2.607	0.0	+398	+116
CASE B	Inside Vise Outside Vi Visor Vert	Inside Visor Surface (Adj Outside Visor Surface: Visor Vertex Thickness:	Inside Visor Surface (Adj. to eye); Outside Visor Surface; Visor Vertex Thickness; 0.1 inch		Parabolic-Radius 4.0 inches Parabolic-Radius 4.03 inches	ches
	Direction of Sight	of Sight	Line-of-Si	Line-of-Sight Error	Optical Power Focusing Distance	cusing Distance
	Y-Axis (deg)	X-Axis (deg)	Y-Axis (mrad)	X-Axis (mrad)	Y-Axis (ft)	X-Axis (ft)
	+10	0	-1.428	0.0	+868	+955
	0	0	+0.093	0.0	- 9549	-1194
(on-axis)	-10	0	+1.143	0.0	-273	-1194
	0	10	-0.007	-1.389	-1061	-796
	0	-10	-0.007	+1.389	-1061	-796

# $\begin{array}{c} \text{APPENDIX IV} \\ \text{DEVELOPMENT OF A HELMET MOUNTED} \\ \text{VISOR DISPLAY} \end{array}$

PRECEDING PAGE BLANK NOT FILMED

# APPENDIX IV DEVELOPMENT OF A HELMET-MOUNTED VISOR DISPLAY

### FOREWORD

This appendix is a paper prepared by P.D. Pratt, Honeywell Systems and Research Center, and given by Capt. D. F. Kocian, Wright-Patterson AFB, at the Symposium on Visually-Coupled Systems Development and Application on 9 November 1972 at Brooks Air Force Base, Texas. As published here, this appendix (paper) provides a digest of Honeywell's final report on the Mod 6 Helmet-Mounted Visor Display. Included in the paper are development reports more recent than those available when the first approval copy of the final report was prepared (July 1972). In reviewing the approval copy, Capt. Kocian made several technical observations which should be included in the report. These additions appear in this appendix.

### DEVELOPMENT OF A HELMET-MOUNTED VISOR DISPLAY

by

Dean F. Kocian, Capt, USAF
Aerospace Medical Research Laboratory
Aerospace Medical Division
Air Force Systems Command
Wright-Patterons AFB, Ohio

Patrick D. Pratt
Senior Principal System Analyst
Honeywell Inc.
Minneapolis, Minnesota

(This paper was prepared by P.D. Pratt and given by Capt. D.F. Kocian on 9 November 1972 at the Symposium on Visually Coupled Systems Development and Application at Brooks Air Force Base, Texas.)

#### ABSTRACT

This paper describes the research and development involved in the evolution of a helmet display technique that utilizes the helmet visor as the last optical component of the display system and which may be suitable for integration into high-performance tactical aircraft. It is a well known fact that one of the aircrew member's most important problems in tactical aircraft is obtaining sufficient information to adequately perform his mission requirements. In order to accomplish the flight control, navigation, reconnaissance, and weapon delivery tasks he is required to perform, he must have a satisfactory view of the external environment and displayed information from aircraft systems. To date, neither tactical aircraft cockpit/canopy design nor panel mounted display have been tailored to the perceptual capabilities and requirements of the operator to provide this view. The development of a helmet-mounted visor display was, therefore, an attempt to provide the airborne operator with a display which successfully met the known requirements for a satisfactory airborne display such as field-of-view, resolution, display magnification, and contrast against backgrounds of high ambient brightness, while not significantly impairing the operator's outside view or degrading his total performance during flight. This paper will first describe the problems and design constraints that were imposed during the development of the visor display as a result of experience with hardware that was then available and flight testing completed up to this period of time. The paper will then proceed to discuss the design concept study employed to determine the particular technique to be used for providing a visor display and the engineering and fabrication problems associated in building the prototype visor display delivered to Aerospace Medical Research Laboratory during February of 1972.

# CONTENTS

	Page
INTRODUCTION	1
TECHNICAL DISCUSSION	2
Design Concept Study Tradeoff Analysis	2 4
Parabolic Visor Projection Approach	6
Reticle Projection Breadboard	6
Video Projection Breadboard	6
Hololens Projection Approach	10
Breadboard Evaluation	10
Reticle Projection Design	10
Parabolic Visor Development	15
Video Projection Design	17

## ILLUSTRATIONS

Figure		Page
1	Sidemount Helmet Mounted Display	3
2	Breadboard of Reticle Visor Project	8
3	Video Display Breadboard	9
4	Ray Trace of Parabolic Visor Reticle Projection	13
5	Reticle Generator, 1.5 FL Paraboloid	14
6	HMS Assembly	16
7	Layout of Visor Projection Display	18
8	First Order Ray Trace, Video Projection	21
9	Ray Interference with Two Central Mirror Design and Parabolic Distortion	23
10	Parabolic Distortion and Skewed Exit Pupil	24
11	Correction of Parabolic Distortion	25
12	First Computer Design with Principal Plane Inside Collimator Lens Assembly	27
13	Second Computer Design with Principal Plane Outside Collimation Lens Assembly	28
14	Video Display Configuration	32
15	Developmental Helmet Mounted Display Prototype Delivered to AMRL in February 1972	33
16	Image of Retina Resolution Chart on CRT	34
17	Image of Retina Resolution Chart from CRT Through Relay Optics, FOB, and Collimation Lens	35
18	NAVAIR VR HMU	37
19	Model 7A Concept	39
20	Preliminary Advanced Design Artist's Concept	40
21	Advanced Concept Prototype A	42
22	Advanced Concept Prototype B	43
23	IHMS/D Advanced Concept Prototype B	44

# TABLES

Table		Page
1	Visor Reticle Projection Design Goals	4
2	Visor Video Display Design Goals	5
3	Rejected Approaches to Visor Projection	5
4	Advantages of Parabolic Visor Reticle Projection	7
5	Advantages of Parabolic Visor for Video Projection Technique	7
6	Visor Video Display Design Constraints	11
7	Reticle Projection Design Tradeoff Parameters	12
8	Tradeoff Parameters for Video Projection Design	19
9	Display Design Optimization by Ray Trace	20
10	Video Display Design Tradeoffs	29
11	Video Display Design Constraints	29
12	Video Display Critical Design Areas	30
13	Performance MOD 6 Video Visor Projection	31
14	MK 1 Mod I 20 Degree Field of View HMD	38

#### INTRODUCTION

The high-performance aircraft in the Air Force inventory and the equipment enboard these aircraft have been designed to execute and complete a number of complex and hazardous missions. The Air Force aviator of today, flying high-performance aircraft, is responsible for ensuring the completion of these particular missions. At present, the equipment and mission related tasks are such that the decision-making capability of the human operator is required. To exercise this decisionmaking capability in an effective manner, especially during the short time intervals of some tasks such as weapon delivery, the human must have the requisite information presented to him in an adequate format and at the same time must be able to implement his decisions. This requires that the airborne operator be correctly integrated with the systems he must use and that the design philozophy applied for accomplishing this integration reflect the limitations and peculiarities of the human operator in a flight environment. The utilization of Visually Coupled Systems (VCS) is one approach for accomplishing this integration.

VCS contain basically two major subsystems. The first comprises equipment that provides for the implementation of his decisions or the control functions. This consists of techniques using head position, eye position, or a combination of the two to command the driven system (sensor, weapon, powered vehicle, etc.) The second comprises equipment that provides information presentation. The general approach has been to employ some type of Helmet-Mounted Display to provide a feedback function presenting imagery derived from the driven system or addition flight control/weapon status parameters as commanded by the operator. The control portion of VCS (using head position sensing only), although not developed to its full potential, has been refined to a degree that operational use in high-performance aircraft has been a reality for several years. The development of helmet mounted displays while satisfactory for some limited applications still must overcome the man/display human factors problems that have limited their applications.

A helmet mounted display (HMD), as the name implies, is an electromechanical device mounted on the helmet which allows the operator to view TV-type information from the weapons, sensors or flight instruments he is using. A major consideration in the design philosophy of HMDs is that it must overcome the limitations of current panel mounted displays concerning contrast rendition, and display size, and in the case of Heads Up Displays (HUD) limited field of view. One distinct advantage of the HMD is that it can be used with an angular pickoff (head position) measurement device which measures the observer's line of sight. In essence, this forms a VCS and allows the observer to see the imagery of the scene from a day-or-night imaging sensor in the direction that he moves his head and provides him with a true

kinetic sense of where the imagery is relative to the aircraft. The most serious problem which most HMDs have is that to some degree they interfere with the observer's normal binocular vision. To maintain display contrast rendition in high ambient brightness conditions it is often necessary to occlude part of the airborne operator's field of view or reduce light transmission to the observer's eye. In some cases the HMD optics may also occlude part of the operator's peripheral vision depriving him of essential motion cues. It was felt that the most innocuous method of presenting display information on the helmet would be to have no other optical elements in front of the observer's eye except the helmet visor which was normally in place anyway.

### TECHNICAL DISCUSSION

One of the better early HMD design approaches was based upon the use of a flat combiner and refractive optics (Figure 1). The refractive optics contained in the display body, project collimated light from a one-inch CRT towards the flat combiner in front of the eye. The two major objections to the flat combiner are: (1) the size of the system for large fields of view and, (2) the requirement for an optical element (flat combiner) between the pilot's eye and the visor that limits the use of eye glasses. The approach required by AHRA program is essentially to introduce optical power into the combiner which also serves as the visor. Therefore, not only will the size of the optical system be reduced, but the extra optical component (flat combiner) is eliminated.

It was also felt that pilot acceptance would be most favorable if a projection scheme of this type were developed. Based upon these considerations this program was undertaken to explore and develop technology which would permit display presentation on the helmet visor.

### DESIGN CONCEPT STUDY

The AHRA program started a design concept study to explore various techniques for projecting reticle and video information on the visor, as a part of the optical system. These techniques were the geometrical optical methods such as a parabolic, spherical, or elliptical visor; the holographic technique coated or embossed on the visor; and a polaroid diffraction element inserted in the visor.

The design concept study was divided into four main areas. (1) a technological study was made of present techniques and component state of the art, (2) methodology was developed to determine the criteria for complex tradeoff analysis and establishment of design goals, (3) design concepts were studied for the various types of visor projection



Figure 1. Sidemount Helmet Mounted Display

techniques, and (4) a tradeoff analysis was conducted on each design approach developed during the design concept study.

The results of detailed studies of the various design approaches for reticle and video projection were evaluated against the requirements summarized in Table 1 and Table 2 for the reticle and video projection techniques.

Table 1. Visor Reticle Projection Design Goals

Reticle generator	Mounted within helmet-visor envelope
Alignment to sensors	<±2.5 degrees
	Not sensitive to mechanical flexure or humidity
Exit pupil	20 mm
Image	Infinity collimation
	Orange color
	20 percent contrast against 20,000 ft-L background
	Visible against low brightness background
	Uniform illumination
	Sharp
	Adjustable intensity
	No distortion or undesired reconstruction or reflections
Vision	±120 degrees with no distortion
Weight	<15 oz
Visor	60 to 70 percent transmittance
Ghost image brightness	Minimum 120:1 ratio of primary to ghost image

### TRADEOFF ANALYSIS

The results of this evaluation and additional tradeoff analysis eliminated the hologram, polaroid diffraction element, spherical visor, double-ellipsoid visor, and single reflective, off-axis parabolic visor from further consideration (see Table 3). Although the phase volume holographic technique has a good deal of promise, it was not developed enough for program use. The relief hologram embossed on a visor was rejected on the basis of its low diffraction efficiency and consequent low imagery brightness. The polaroid diffraction element, which

Table 2. Visor Video Display Design Goals

Horizontal resolution	500 TV lines at 50 percent output response with 750 TV lines at 50 percent response input from CRT
Grey scale	Eight shades
Contrast	20 percent contrast ratio against 10,000 ft-L
Brightness uniformity	3 percent image uniformity with 1 percent CRT uniformity
FOV	20 degree minimum
Exit pupil	10 mm at surface of eye
Focus	18 inches to infinity
Linearity	3 percent
Weight	Less than 20 ounces

Table 3. Rejected Approaches to Visor Projection

Technique		Disadvantages
•	Phase volume hologram coated on visor	Under development and not available
	Relief hologram embossed on visor	Low Diffraction efficiency
9	Polaroid diffraction element inserted in visor	Fixed pattern and not visible under low ambient light levels
•	Double spherical visor	Large optics required for complex optical correction
•	Double ellipsoid visor	Complex optical correction and difficult shape to fabricate
•	Single off-axis parabolic visor	Complex optical correction for off axis aberrations

would be inserted in a visor, was eliminated from further consideration due to its fixed pattern and lack of visibility under low ambient background lighting levels. Furthermore, the spherical, ellipsoid, and off-axis parabolic visor projection techniques were all rejected on the basis of large optics required for complex optical corrections.

## PARABOLIC VISOR PROJECTION APPROACH

The single-bounce parabolic and the double-bounce parabolic approaches were the remaining candidates for the reticle and video visor projection techniques. Tables 4 and 5 summarize the advantages of the parabolic visor for both reticle and video projection. The primary advantage of the parabolic approach is that optical correction for optical aberrations are not required for either reticle or video visor projection. Another important advantage of the parabolic visor is its reasonable approximation to the standard Air Force helmet visor.

The elmination of optical correction allowed early breadboard demonstrations of parabolic visor projection techniques with off-the-shelf refractive optics and parabolic mirrors to verify the conclusions of the design concept study and tradeoff analysis.

### RETICLE PROJECTION BREADBOARD

The reticle projection breadboard shown in Figure 2 permitted design feasibility to be determined on the basis of image quality, resolution, collimated imagery, and uniform illumination of both the exit pupil and reticle pattern. It also allowed the measurement of the exit pupil and evaluation of reticle imagery for distortion, image quality, and surface finish of the paraboloid. Furthermore, the performance of the parabolic design could be evaluated for visibility of ghost imagery and contrast of the primary image against a bright background. Although the paraboloid used in the breadboard did show evidences of waviness, line splitting, and distortion, the demonstration of the concept of reticle projection was considered to be satisfactory.

## VIDEO PROJECTION BREADBOARD

The objectives of the breadboard, shown in Figure 3, were to demonstrate the feasibility and image quality of the symmetrical parabolic visor video projection technique. The breadboard consisted of a resolution test pattern to simulate the source of imagery, a collimation lens to project collimated light on a parabolic plastic section and a single central mirror to reflect light back to the paraboloid all mounted on a special optical bench.

Table 4. Advantages of Parabolic Visor Reticle Projection

- No optical correction required for 3 degree FOV reticle projection
- Collimated imagery across FOV
- Techniques exist for fabrication of parabolic visor with acceptable surface quality
- No chromatic aberration
- Symmetrical visor for ease of mounting on helmet
- Close approximation to shape of standard visor

## Table 5. Advantages of Parabolic Visor for Video Projection Technique

- Symmetrical visor for ease of mounting on helmet
- Imagery relayed into pilot's vision
- Self correction of spherical aberration, coma and astigmatism
- Compact design
- High image quality over wide field of view
- Small lightweight optics

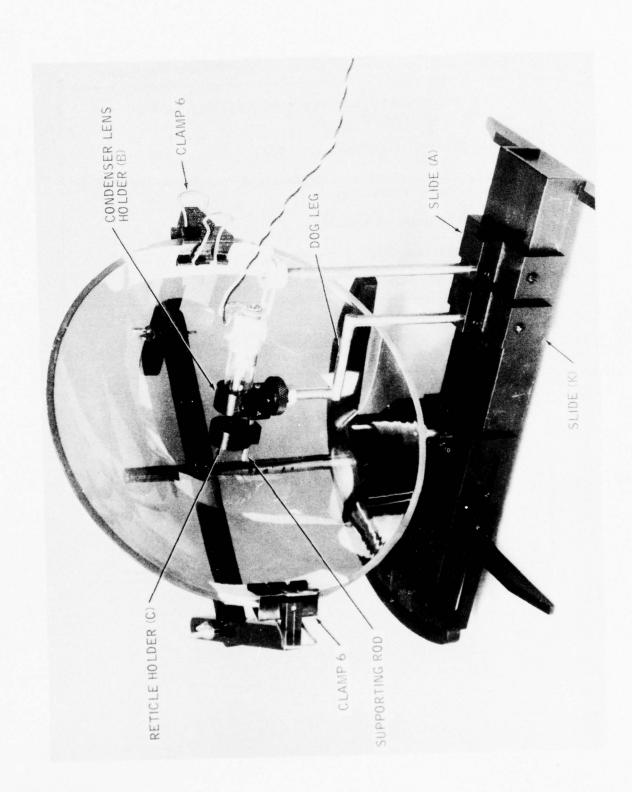


Figure 2. Breadboard of Reticle Visor Project

Figure 3. Video Display Breadboard

Since the symmetrical parabolic approach is self-correcting, the requirements on the collimation lens are not severe and an off-the-shelf camera lens was used. The first evaluation of the symmetrical approach was with a paraboloid of poor quality. However, the resolution target was positioned such that an image appeared with good resolution and feasibility of the symmetrical parabolic approach was demonstrated.

#### HOLOLENS PROJECTION APPROACH

Two holo lenses were fabricated by Honeywell and Naval Weapons Center for use in breadboard demonstrations. The best hololens was fabricated by Naval Weapons Center, but the sharpest image was not formed at infinity since zero horizontal and vertical parallax occurred at two distances. Also, both real and virtual images with several orders were formed as well as the directly reflected image. Both hololenses had fuzzy images and were not satisfactory for the AHRA program.

#### BREADBOARD EVALUATION

After the breadboards of the most promising techniques had been completed and evaluated, it was found that the parabolic visor at the present state of technology was the superior design approach. Since this approach might possibly be developed for operational use in high-performance aircraft the complexity of the engineering design decisions was increased. Table 6 includes additional major areas for consideration for the video display -- minimum acceptable performance factors could be established based upon only the limited laboratory and flight experience that had been gathered on HMD up to this time. Many of the constraints included in Table 6 applied to the requirements for visor reticle projection.

#### RETICLE PROJECTION DESIGN

The reticle design tradeoff, summarized in Table 7 started with the parabolic visor ray trace shown in Figure 4. This ray trace shows the off-axis focal plane of the paraboloid to lie almost entirely upon the plane of the reticle mask which generates the virtual image of the reticle projected into the pilot's vision by the visor. Therefore, this ray trace shows the reason for the excellent image quality observed with the reticle generator breadboard, i.e., reticle mask lies in the off-axis focal plane of the paraboloid.

Several design iterations were required for the visor tracks and retractable reticle before the final design shown in Figure 5 was completed.

Table 6. Visor Video Display Design Constraints

#### A. Optical Constraints

- 1. Proper combination of reflective/anti-reflective coatings.
- 2. Minimum see-through distortion
- 3. Maximize visor transmittance

#### B. Human Factor

- 1. Crash Safety
- 2. Maintain rigidity of helmet for ejection
- 3. Binocular rivalry, vertigo, display luminance
- 4. Helmet weight and center-of-gravity
- 5. Air relief to prevent pressure differential upon ejection.
- 6. Pilot safety from electrical energy in the CRT and quick disconnect provision
- 7. Light and noise seal of helmet
- 8. Must permit glasses to be worn
- 9. Instrument visibility, night vision, and no undesirable reconstructions from the display surface
- 10. No loss of peripheral vision

#### C. Physical Constraints of Tactical Aircraft

- 1. Helmet envelope
- 2. Position of CRT
- 3. Hardware compatibility with other aircraft systems
- 4. Mesh of parabolic visor with oxygen mask

#### D. Technology Development

- 1. Advanced fiber-optic-bundle (flattened)
- 2. CRT brightness versus resolution
- 3. Visor material and coatings (resistance to solvents/stability of plastics)
- 4. Visor fabrication to an aspheric shape
- 5. Limitations in test equipment and techniques
- 6. Off-axis projection using aspheric surfaces for mirrors/ elimination of double bounce technique for parabola
- 7. Helmet design

#### E. The Real World (Reliability - Maintainability - Cost)

- 1. Minimum cost for visor fabrication
- 2. Simple alignment of helmet optical system
- 3. Reoperatability of optical components
- 4. Rugged helmet unit

Table 7. Reticle Projection Design Tradeoff Parameters

Exit Pupil (area)	Increase filament area and source power
Image Brightness and Contrast	Increase source power and shorten lamp life
Orange Color	Increase source power and shorten lamp life or lose brightness
Image Collimation Across FOV and Exit Pupil	May require optical correction for parabolic and does require correction for spherical visor
Reduce Ghost Image	Increase reflectance of inside visor surface, decrease visor transmittance and reduce reflectance of visor outside surface
Uniform Reticle Illumination	Brightness reduction due to diffuser or increased length due to fiber optic bundle
Reduce Helmet Envelope	Shorten effective focal length, (decrease visor radius) and increase distortion
Increase Lamp Life	Reduce image brightness and contrast Use fiber optic diffuser rather than diffuser plate Increase visor reflectance Remove color filter
Reduce Heat Generation	Remote lamp location, heat sink or reduce lamp brightness and image visibility

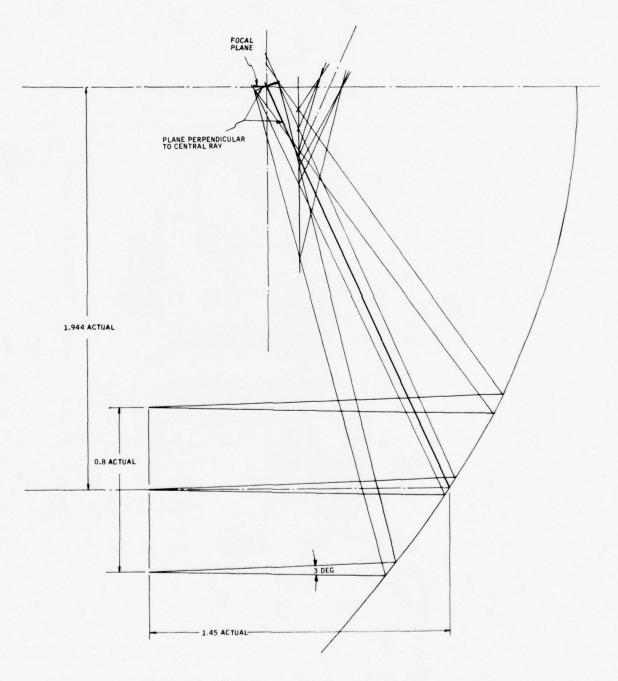


Figure 4. Ray Trace of Parabolic Visor Reticle Projection

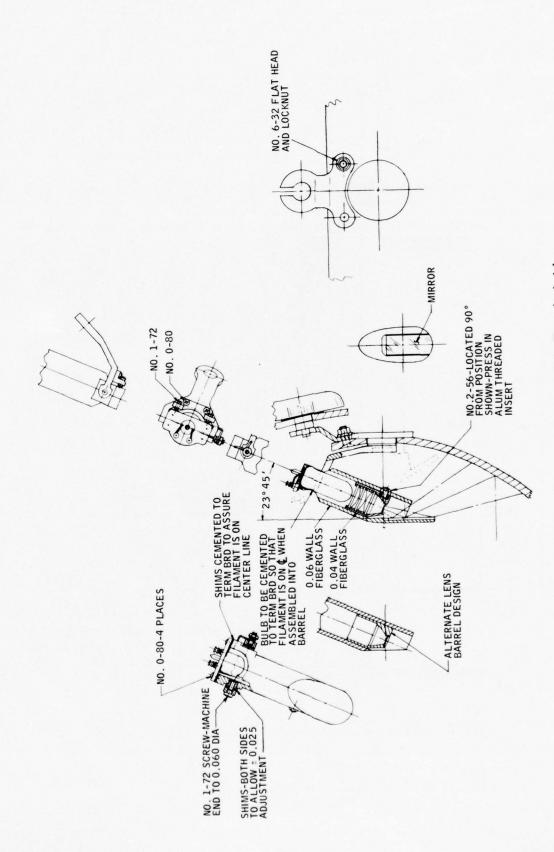


Figure 5. Reticle Generator, 1.5 FL Paraboloid

Design constraint of visibility against a high background brightness, uniform reticle pattern illumination and a large exit pupil required the development of a special tungsten lamp design and an adjustable condenser projection system to illuminate the reticle pattern. Alignment and collimation constraints dictated that the reticle generator must be adjustable in three axes but still allow retraction under the visor and visor cover. Boresight repeatability required a special visor bearing track with small clearances that would be able to slide without binding.

The design requirement for a ratio of 120:1 between the primary and ghost image of the reticle required the development of dielectric coatings for 30 percent reflectance on the inside surface and a 0.5 percent reflectance on the outside surface of the visor of the prototype shown in Figure 6. These coatings had to be durable and withstand the usual humidity requirements. Approximately 150 trial depositions were required over a period of five months to develop the reflective and anti-reflective coatings required for the plastic visor.

#### PARABOLIC VISOR DEVELOPMENT

The one critical area, common to both reticle and video display visor projection techniques, was the development of a plastic parabolic visor. Seventeen different approaches were considered over a period of a year and a half for fabricating plastic paraboloids and four approaches were considered for the fabrication of parabolic molds. The techniques that showed the greatest promise were compression molding, injection molding, aspheric blade generation, and fine cut and polishing of pre-molded parabolic blanks. The last technique was that selected for the AHRA program on the basis of time and cost for fewer than 10 units.

The first step of the parabolic fabrication procedure was to generate a true parabolic cam required for the inside of the parabolic visor. This cam was then used to cut an aluminum male mold for vacuum forming acrylic blanks. These blanks were then annealed and potted into female molds which were also machined from the original cam. The potted parabolic section was then rough machined to the approximate parabolic shape and delivered to Goeger Optical Company of Chicago for final cutting and polishing to a parabolic shape. The paraboloids were then referenced and cut to the proper visor shape.

However, the paraboloids were not perfect and the image quality, seethrough distortion, prismatic deviation, and boresight stability are areas requiring improvement by development of better technique for parabolic shell fabrication. The prismatic effects require the proper matching of the outside surface of the visor shell to its inside surface. Analysis has shown that if the focal length of the outside surface paraboloid is somewhat larger than the inside paraboloid, then the



Figure 6. HMS Assembly

prismatic effect can be effectively eliminated. This requires that the outside surface be finished in addition to the inside surface.

Another design problem to be investigated is the elimination of undesired ghost that can be seen when the helmet mounted assembly is tested in bright sunlight. Images of eye brows and highly reflective eye glass rims (which are close to the focal point of the paraboloid) are then visible. This suggested that visor transmittance was not optimum. Additional reduction in visor transmittance may be needed.

#### VIDEO PROJECTION DESIGN

The basic design problem for video projection on a curved visor is that a real image must be formed in the vicinity of the center of the forehead at the focal point of the visor combiner. Obviously, the cathode ray tube itself cannot be located at this position and some form of relay optics must be used. The AHRA design approach was to use a relay lens and a fiber optics to transfer imagery from the CRT mounted at the back of the helmet as shown in Figure 7. This design approach relays the CRT imagery around the helmet above and to one side of the forehead. The collimation optics and the concave partially reflecting visor are used to form a real image of the display at the focal point of the visor combiner near the center of the forehead. The decision to mount the CRT remotely, at the back of the helmet, is a result of a tradeoff for the lowest center of gravity at the expense of the requirement for relay optics and a fiber optic bundle to convey the imagery to the pront of the helmet.

The double reflecting parabolic combiner display employs a symmetrical arrangement of the parabolic combiner and parabolic mirror about central plane mirror located at the focal point of the paraboloid and normal to its axis. This symmetry is extended to the location of the eye and the collimation optics on either side of the central mirror. The display image is free from coma because of the double (comacompensating) deflection at the paraboloid. Astigmatism is minimized by locating the collimation lens and the eye near the paraboloid's entering and exiting off-axis focal points, respectively.

To implement this design, it is necessary to satisfactorily locate and space the parabolic visor and other optical components. Twenty-five design iterations and layouts were required before an optical computer design could be executed. These design iterations required that each change in the optical approach be traded off against mechanical constraints for helmet mounting. The tradeoff parameters shown in Table 8 were optimized as shown in Table 9 by first order ray tracing.

The early design iterations correctly located the fiber optic bundle and two mirrors on either side of the collimation lens as shown in Figure 8. However, the first-order ray tracing assumed a symmetrical ray

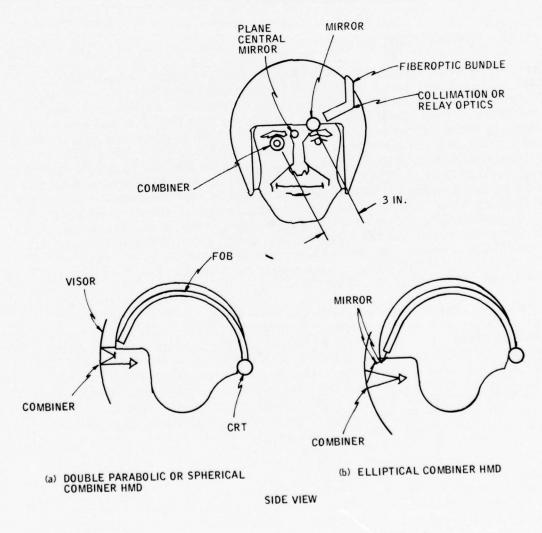


Figure 7. Layout of Visor Projection Display

Table 8. Tradeoff Parameters for Video Projection Design

#### Parameter to Vary

- Distance between visor optical axis and observer line of sight
- Angle between vertical plane containing the line of sight (LOS) and the plane containing the LOS and optical axis of the visor
- Location and alignment of FOB
- 6 Mirror locations, separations, and angles
- Optical elements locations and dimensions
- Angle of vision obscuration by mirrors
- Location of real image and extreme optical rays between optical components
- Locations of exit pupil and aperture stop (entrance pupil)
- Sections of helmet required to be removed
- Active areas and focal length of paraboloid
- Cross sectional view of plane containing the observer line of sight and visor axis
- Front view showing eye location and optical element location

Table 9. Display Design Optimization by Ray Trace

Table 9. Display Desi	ıgn	Optimization by Ray 11ace	
To Optimize the Following			
• Field of view	-	20 degrees as design goal	
• Exit pupil	-	0.4 in (10 mm) design goal	
<ul> <li>Forehead clearance</li> </ul>	-	0.25 in. minimum	
<ul><li>Upward vision</li></ul>	-	40 degrees without obscuration	
• Visor mounting	-	Clearance for collimation optics, FOB, and mirrors between visor and helmet	
<ul> <li>Inclination angle of optical axis</li> </ul>	-	> 30 degrees for minimum inter- ference with visor tracks	
Optics mounting	-	Optical components must be mounted between visor and helmet shell with minimum removal of helmet shell	
Visor retraction	-	Components below brim of helmet must retract with visor	
By Ray Tracing Between the Following			

- Aperture stop

- Focal surfaces

- FOB

Center of eye rotation - Curved mirror

• Eye pupil

CombinerCentral mirror

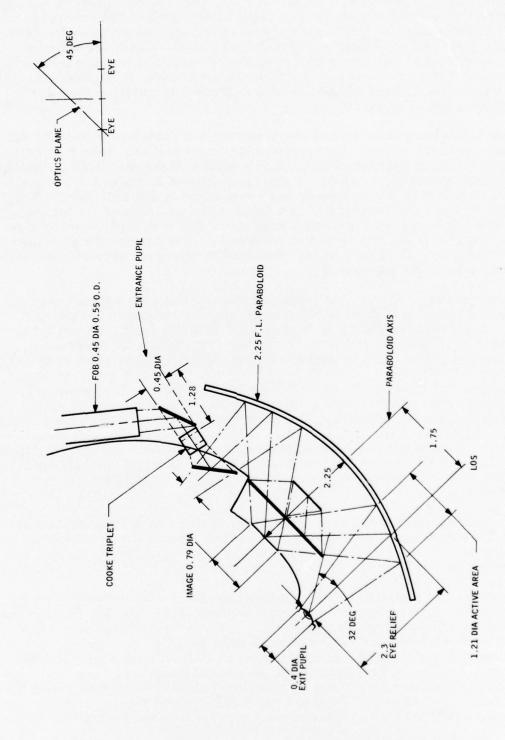


Figure 8. First Order Ray Trace, Video Projection

trace from the top to the bottom half of the paraboloid. This symmetrical ray trace incorrectly showed that two central mirrors could be used and indicated that the exit pupil to be equal to the entrance pupil of the paraboloid or the exit pupil of the triplett collimation lens. At this point of the design tradeoff, several optical design computer runs were made. Rigorous ray tracings showed that the ray trace pattern was not symmetrical about the optical axis due to parabolic distortion (see Figure 9) and that the exit pupil is smaller than the entrance pupil (Figure 10).

These ray traces show that the two central mirror approach could not be used because of ray interference (Figure 9) and that a single central mirror must be positioned at the focal point of the paraboloid. Another important result of the rigorous ray trace shown in Figure 9 is the effect of parabolic distortion on the rays entering the exit pupil. For example, the rays leaving the exit pupil make an angle of 10 degrees with the horizontal and the same rays enter the exit pupil from angles of 11.5 and 8.5 degrees with the horizontal. This produces an image distortion along the plane which contains the observer line of sight and optical axis of the paraboloid.

These rigorous ray tracings revealed more. Not only is the image distorted by the double reflection at the parabolic visor, but the exit pupil is skewed, as shown in Figure 10. The exit pupil, identified by points 1'', 2' and 3', is the image formed by the double paraboloid and central mirror of the entrance pupil, identified by points 1, 2 and 3. The preliminary first-order calculations indicated that the size of the exit pupil would be approximately equal to that of the entrance pupil, i.e., 0.4 inch, which is the diameter of the clear aperture of the collimator-optics. However, the diameter of the exit pupil depends on the direction of the line of sight. When looking 10 degrees away from the axis of the paraboloid, the exit pupil measures nearly 0.5 inch; when looking 10 degrees toward that axis, it measures only 0.3 inch; for the boresight direction the exit pupil has the expected diameter of 0.4 inch.

One advantage of the skewed exit pupil is that it has a constant height over the entire distance between the vertical planes D and E (see Figure 10). If the exit pupil were not skewed, then its size would decrease on either side of the optimum eye location.

To correct for image distortion created by the double reflecting parabolic visor, it is necessary to distort the ray trace passing through the entrance pupil as shown in Figure 11. It can be seen that for rays A and B each entering the exit pupil at a field angle of 10 degrees, these rays must leave the skewed entrance pupil at field angles of 9 and 11 degrees, respectively. Therefore, this represents a  $\pm 10$ -percent distortion correction which must be provided to the rays as they leave the collimation optics at the entrance pupil of the paraboloid. This correction was provided by a second-order correction in the horizontal and

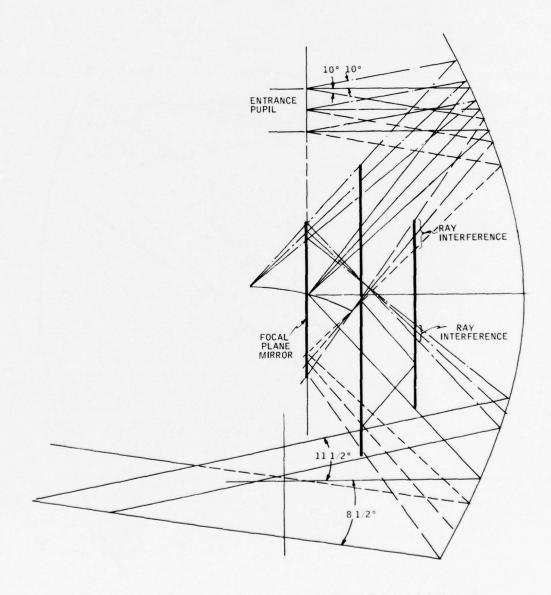


Figure 9. Ray Interference with Two Central Mirror Design and Parabolic Distortion

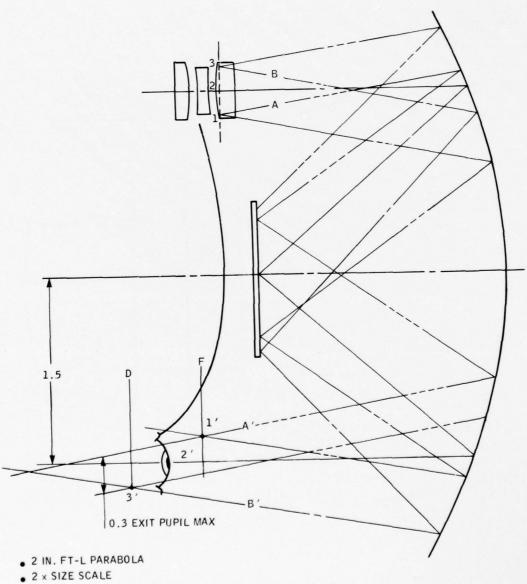


Figure 10. Parabolic Distortion and Skewed Exit Pupil

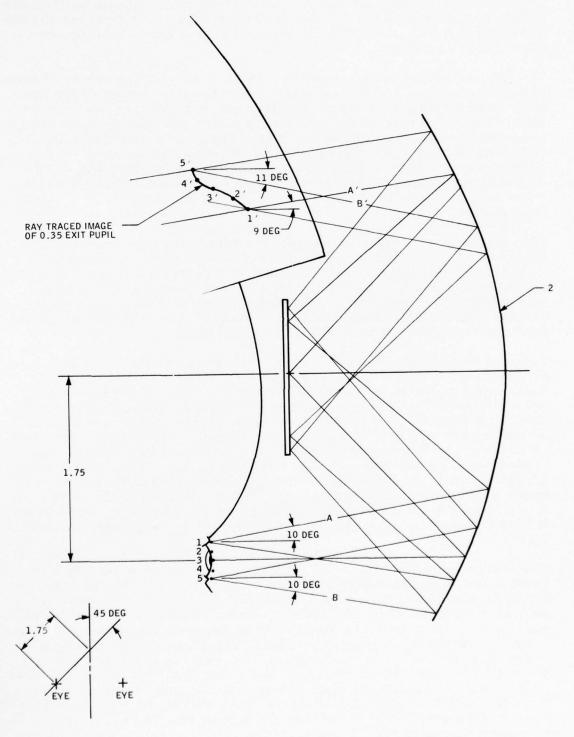


Figure 11. Correction of Parabolic Distortion

vertical sweeps of the cathode ray tube electronics. At this point in the design it also became evident that the boresight mirror (between the top of the paraboloid and the collimation optics) also was a limiting constraint to the exit pupil.

The first computer design shown in Figure 12 locates the principal plane at the entrance pupil of the paraboloid near the first vertex of the last element of the collimation optics. However, the primary design constraint on the location of the collimation optics and the boresight mirror is noninterference with any of the rays. This design positioned the first lens element too close to the upper ray trace at the top of the paraboloid and only a 0.3-inch exit pupil could be obtained with a 20-degree field of view. One tradeoff of this design is that the exit pupil could be increased, but only at the expense of reducing the 20-degree field of view.

This problem was solved by locating the principal plane outside of the last element of the collimation lens assembly as shown in Figure 13. This arrangement shows that a 0.4 inch exit pupil for upward vision can be obtained with a 0.5-inch diameter entrance pupil and this design was used for the final optical computer design for the video display. The horizontal line of sight has an exit pupil of approximately 0.5 inch; for downward vision it is approximately 0.6 inch.

Table 10 summarizes the video display design tradeoffs. The exit pupil is limited by the diameter of the collimation lens since the exit pupil is the image of the entrance pupil of the lens. If the diameter of the collimation lens is too large then it will not fit under the visor. Another design tradeoff is the system resolution which is now limited by the number of fibers in the fiber optic bundle. The resolution could be improved by increasing the bundle diameter, but this enlarges the helmet envelope and increases the difficulty of fitting it under the visor. Another limitation to the diameter of the fiber optic bundle is the focal length of the triplet collimation lens. The larger the bundle, the longer the focal length for a given field angle coverage, and the more difficult it is to fit lens assembly and fiber optic bundle on the helmet under the visor.

The design constraints imposed on the helmet mounted assembly are summarized with their design impacts in Table 11. Time and cost limitations required the use of a modified visor cover and a standard central visor knob which increased the helmet envelope. Time and cost also limited the amount of effort available for developing a faired visor shape to replace the flat side extenders, which were eventually used. Safety dictated the use of a fiberglass CRT/relay lens housing for protection against corona discharge and a double hinged central mirror support for cash safety. Either eye operation required the use of a flexible round fiber optic bundle rather than a flattened rigid fiber optic bundle which would have minimized the helmet envelope. Either eye operation also required a large central mirror, reversible CRT mount,

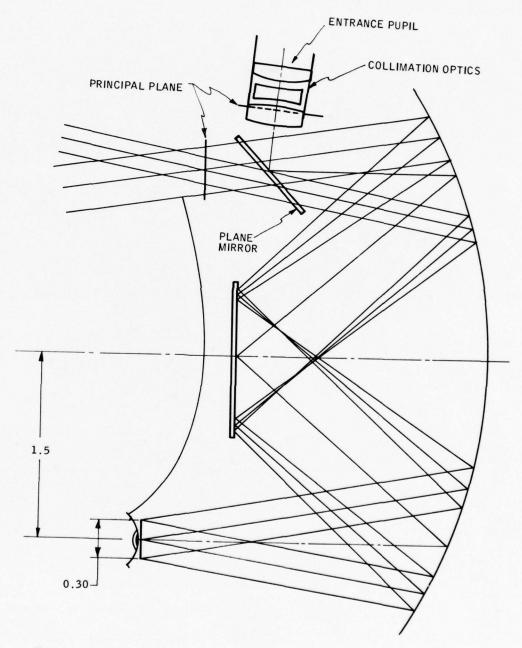


Figure 12. First Computer Design with Principal Plane Inside Collimator Lens Assembly

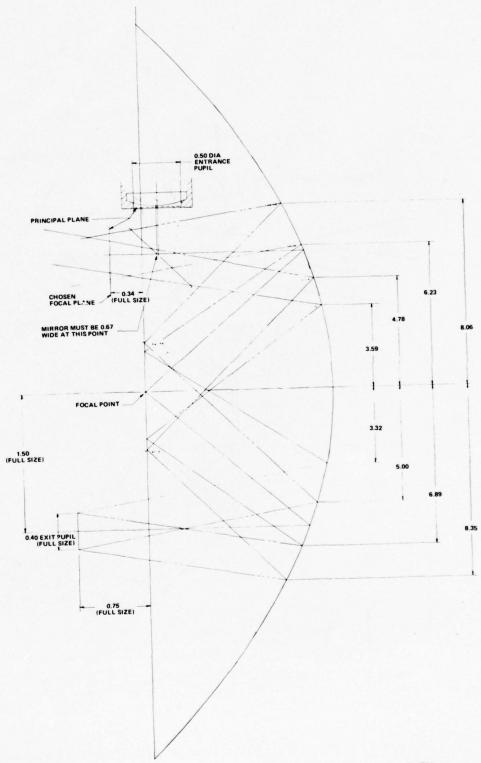


Figure 13. Second Computer Design with Principal Plane Outside Collimation Lens Assembly

Table 10. Video Display Design Tradeoffs

Parameter	Tradeoff
Product of field of view and exit pupil, i.e., 20 degrees x 0.4 inch	Interference with ray trace by collimation lens and folding mirror
Exit pupil	Diameter of collimation lens that will fit under visor
Resolution	Diameter of fiber optic bundle to fit under visor and limitation of focal length and diameter of triplet collimation lens for lay- out on helmet under visor.

Table 11. Video Display Design Constraints

Design Constraint	Impact on Design
Time and cost	Used visor cover and central visor knob which increased helmet envelope
Cost and time	Machined visor rather than develop- ing molding techniques
Safety against corona discharge	Fiberglass CRT/relay lens housing
Either eye operation and cost	Utilized round flexible FOB rather than flattened rigid FOB to reduce helmet envelope
	Required a larger central mirror than for single eye operation
Cost and time	Used flat side visor extenders rather than wrap around visor
Low c. g. and minimum envelope	Used FOB for remote CRT location

two collimation lens mount brackets and two helmet cut out areas for the collimation lens assembly. Therefore, the requirement for either eye operation resulted in a design that dictated the use of the fiber optic bundle for remote location of CRT, addition piece parts and fabrication.

The critical design areas of the video display are summarized in Table 12. The development of better techniques for fabricating the parabolic visor is the greatest need here. System performance is summarized in Table 13.

The final prototype design is shown in Figure 14. A photograph of this prototype is shown in Figure 15

Table 12. Video Display Critical Design Areas

Parabolic visor	Difficult to fabricate
Central mirror	Double-hinged to prevent injury to pilot
Boresight	Small visor track tolerance required: careful alignment of central mirror, visor and collimation lens
Undesired reflections	Need to develop advanced visor coatings
Parabolic distortion	Required CRT deflection correction
Image quality	Surface finish of paraboloid needs to be improved
See-through distortion	Uniform and uncontrolled visor thickness is needed
Reduction of brightness	Light attenuation by fiber optic bundle, four mirrors, and double parabolic reflection required high reflective mirrors
White out	Upper portion of visor must be opaque to prevent direct reflection of the light off the central mirror into observer's vision

Table 13. Performance MOD 6 Video Visor Projection

FOV: 20 deg

Exit Pupil: 0.4 to 0.6 inch

Grey Scale: 7 to 8

MTF of Collimation Optics:

- Center of FOV 0.83 at 850 line pairs/inch

- 0.4 of FOV 0.78 at 850 line pairs/inch

- 0.8 of FOV 0.58 at 850 line pairs/inch

Limiting Resolution:

- CRT: 300 TV lines

- CRT and FOB: 300 TV lines

Figures 16 and 17 show the image of the retina resolution chart as formed on the CRT and then relayed through the relay lens, fiber optic bundle, and collimation lens. Although the limiting resolution of 300 TV lines is not degraded by the fiber bundle the defects of the bundle are clearly visible. It is also evident that the multifiber structure limits the static photographic resolution while the dynamic resolution would be improved with direct viewing of moving imagery.

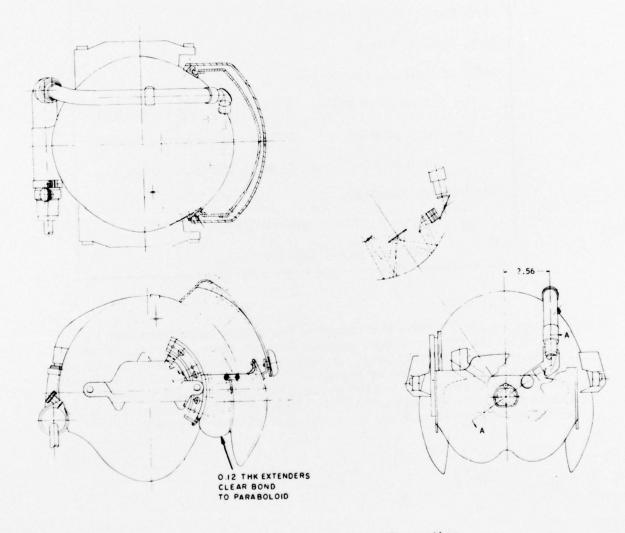


Figure 14. Video Display Configuration

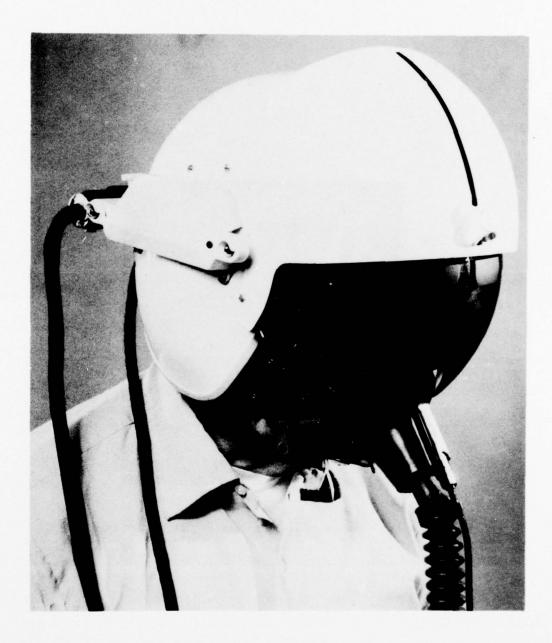


Figure 15. Developmental Helmet Mounted Display Prototype Delivered to AMRL in February 1972

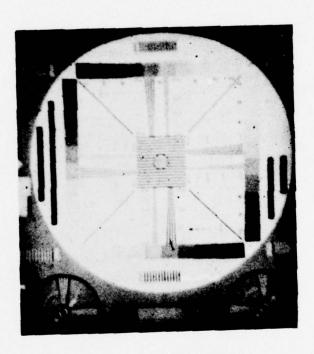


Figure 16. Image of Retina Resolution Chart on CRT

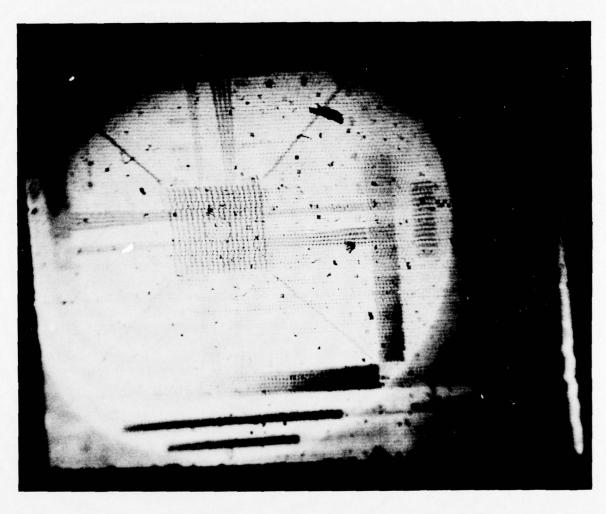


Figure 17. Image of Retina Resolution Chart From CRT Through Relay Optics, FOB, and Collimation Lens

The basic reticle projection design developed during the AHRA program was used as an interim design concept for developing a VTAS visor reticle helmet mounted unit for the Navy. The design objectives were for a compact, lightweight, and streamlined helmet mounted assembly. The visor was fabricated by vacuum drawing heated flat acrylic stock sheet into a female mold. This vacuum forming method was chosen because it leaves the inside surface of the visor blank untouched thus retaining the original fine polished surface (of the sheet stock). Therefore, the criticality of polishing the inside surface of the visor is eliminated since no specific optical character need be maintained. However, the inside surface will not be a true paraboloid and some decollimation of the imagery may be experienced which is not critical for reticle visor projections. Moreover, this method does not have complete control over the thickness of the plastic shell, so it may not satisfy the requirements for prismatic deviation.

However, Honeywell has now developed an improved visor forming technique. In this process, acrylic stock sheet is vacuum formed over a polished male mold, resulting in an excellent concave surface finish as well as preserving the original finish on the convex surface. The visors formed by this improved process can be installed in the interim NAVAIR VRHMU shown in Figure 18.

Funding has been provided by the Air Force for the procurement of operational Integrated Helmet Mounted Sight/Displays. The first unit, the Mark I Mod I, will be a mechanical redesign of the AHRA Model 6 with particular emphasis on improvement of size, weight, and balance. The optical components and performance will be essentially the same as Model 6. The next unit will be the Advanced Concept Prototype which will further improve the appearance, weight and balance of the helmet and provide for improvement of the optics of the display. The helmet mounted display and sight functions will be integrated into a single optical system mounted on the helmet.

The advantages of the Mark I Mod I helmet mounted visor display are summarized in Table 14. Reductions in weight and envelope are obtained through the use of the new VRHMU sensor bars, a flattened fiber optic bundle design, elimination of the visor cover, and a lower pivot point of the visor. See-through distortion and prismatic deviation are controlled by a wrap-around visor design and improved visor fabrication techniques. A baffle blocks stray light between the helmet and the top of the visor. The vertical and lateral position of the exit pupil is adjustable to fit the observer's eye position; this is done by providing vertical and lateral adjustments to the visor position. The artist's concept of this model is shown in Figure 19.

The Preliminary Advanced Design HMD, shown as an artist's concept in Figure 20, integrates the sight sensor bars with the Helmet Mounted Display and uses a three point suspension for attaching this assembly to a standard Air Force helmet. The intent of this design approach is to eliminate any boresight shift due to relative motion between the HMD



Figure 18. NAVAIR VR HMU

Table 14. MK 1 Mod I 20 Degree Field of View HMD

## Reduction in Weight, Vertical Clearance and Envelope

- VRHMU type sensor bars
- Flattened fiber optic bundle
- No visor cover
- Lower visor pivot point

# Reduction of See-Through Distortion and Prismatic Deviation

- Wrap around visor
- Improved visor fabrication technique for control of visor profile and improved surface figure

#### Miscellaneous

- Stray light baffle
- e Adjustable visor for adjustment of exit pupil position
- Trichroic inside reflective coating on visor only to eliminate undesired reflections

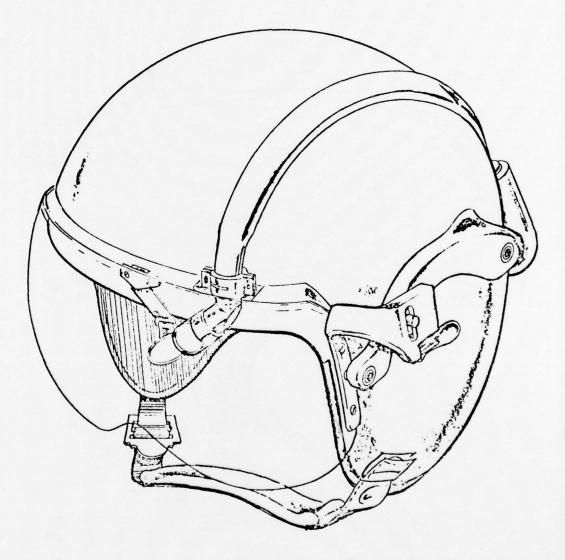


Figure 19. Model 7A Concept

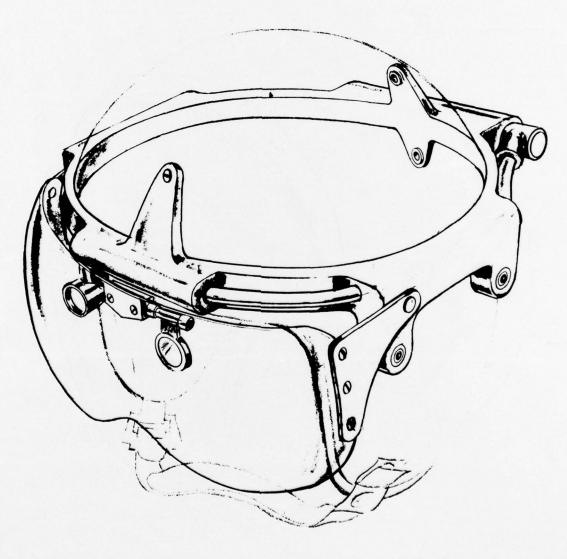


Figure 20. Preliminary Advanced Design Artist's Concept

and the sensor bars caused by flexure of the helmet. Rapid installation of the helmet mounted unit on a customized helmet is an additional advantage.

The Advanced Concept refers to the optical design of that part of the HMD which begins with the collimation optics and includes the boresight mirror, the central mirror and the paraboloidal visor. This Advanced Concept can be implemented in either of two configurations -- A: with the CRT mounted at the back of the helmet and using a fiber optic -- B: mounted on the side of the helmet without a fiber optic bundle. The Advanced Concept Prototype A is shown as a sketch in Figure 21. The design of the Advanced Concept Prototype B is shown in Figure 22; this shows the installation of the optical components of the system. The sketch of the Advanced Concept Prototype B is shown in Figure 23.

The Advanced Concept design approach elevates the boresight direction and the center of the display field of view eleven degrees with respect to the axis of the paraboloidal visor. This was done to raise the central mirror above the upward periferal limit of the visual field of the pilot and it also has the advantage of minimizing the size of the central mirror. Furthermore, elevating the central mirror allows the upper portions of the visor to be opaque without obscuring upward vision of the pilot. Roll stabilization has been accommodated by suitably enlarging the lateral dimension of the central mirror. This design provides an enlarged exit pupil; it has been increased from 0.4 inch to 0.6 inch diameter.

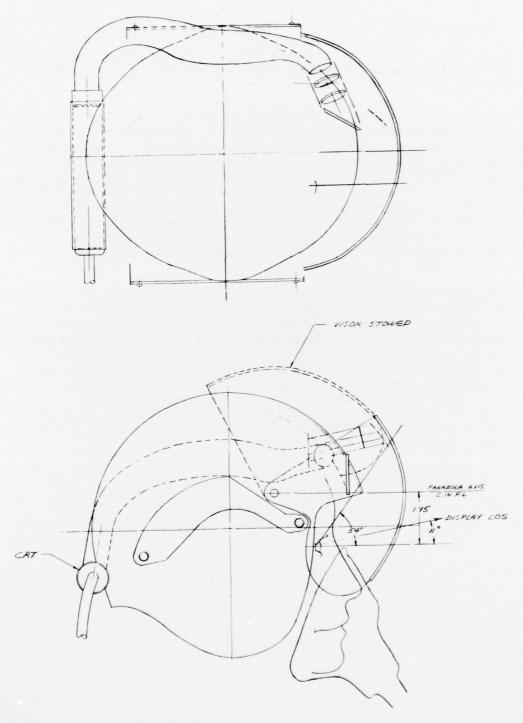


Figure 21. Advanced Concept Prototype A

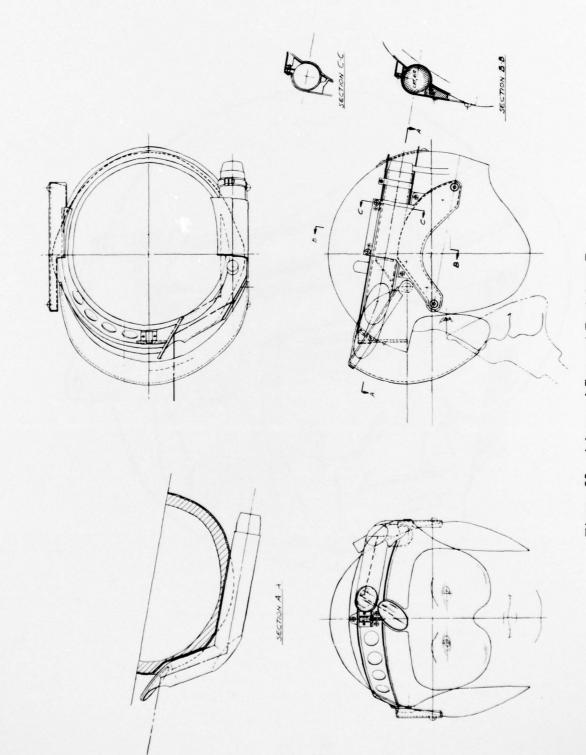


Figure 22. Advanced Concept Prototype B



Figure 23. IHMS/D Advanced Concept Prototype B